The role of VIP in neuro-immune modulation of hippocampal neurogenesis

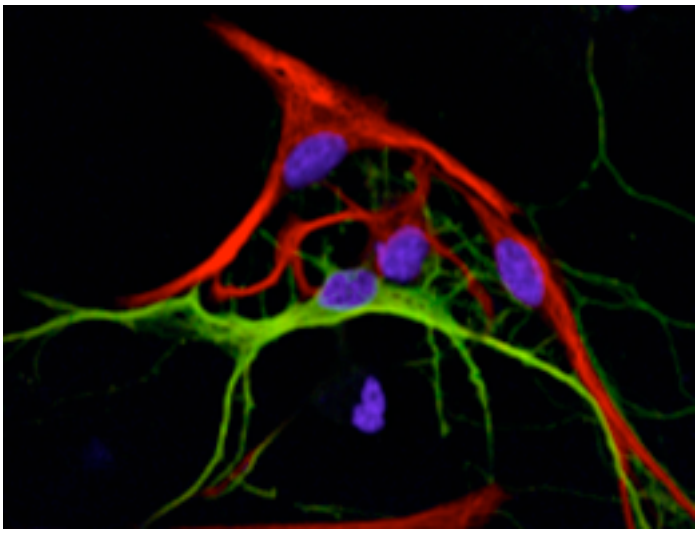

A Thesis for the Degree of Doctor of Philosophy

March 2014

Damla Khan

Supervisors
Professor William P Gray
Professor Stephen B Dunnett

CARDIFF UNIVERSITY
PRIFYSGOL CAERDYDD

DECLARATION

This work has not been submitted in substance for any other degree or award at this or any other university or place of learning, nor is being submitted concurrently in candidature for any degree or other award.

Signed …… (candidate) Date……..

STATEMENT 1

This thesis is being submitted in partial fulfillment of the requirements for the degree of ……(insert MCh, MD, MPhil, PhD etc, as appropriate)

Signed …… (candidate) Date ……

STATEMENT 2

This thesis is the result of my own independent work/investigation, except where otherwise stated.
Other sources are acknowledged by explicit references. The views expressed are my own.

Signed …… (candidate) Date ……..

STATEMENT 3

I hereby give consent for my thesis, if accepted, to be available for photocopying and for inter-library loan, and for the title and summary to be made available to outside organisations.

Signed …… (candidate) Date ……

STATEMENT 4: PREVIOUSLY APPROVED BAR ON ACCESS

I hereby give consent for my thesis, if accepted, to be available for photocopying and for inter-library loans **after expiry of a bar on access previously approved by the Academic Standards & Quality Committee.**

Signed …… (candidate) Date ……

“Every man can, if he so desires, be the sculptor of his own brain”

~ Santiago Ramón y Cajal

Abstract

Hippocampal neurogenesis occurs within the subgranular zone of the dentate gyrus and is important for learning and memory. Neurogenesis is impaired in many pathological conditions; an observation that may account for learning and memory deficits in patients suffering from these conditions. Studies on immune-deficient mice show reduced hippocampal neurogenesis and associated learning and memory impairments in mice devoid of $CD4^+$ T lymphocytes.

Neuropeptides are potential candidates for mediating neuro-immune interactions. Vasoactive Intestinal Peptide (VIP) is a neuropeptide, released by firing interneurons from the stem cell niche, that modulates hippocampal neurogenesis via VPAC1/2 receptors. VIP receptors are also present on T lymphocytes.

Microglia are innate immune cells that regulate hippocampal neurogenesis. They are ideally placed to communicate with T lymphocytes that normally reside outwith the brain parenchyma. Given the nescience underlying T lymphocyte regulation of hippocampal neurogenesis, we sought to investigate the hypothesis that VIP modulates T lymphocytes to release cytokines to regulate hippocampal neurogenesis via interaction with microglia.

We have shown that T lymphocytes supernatant increases the proliferation of hippocampal nestin-expressing cells. This effect is further enhanced under VIP treatment via VPAC1 receptor subtype. Examining possible cytokine involvement, we found that IL-4 mediates proliferation. Using Mac-1-SAP to deplete resident microglia, we demonstrated that supernatant acts primarily via microglia to increase supernatant effects. T lymphocytes induce microglia to upregulate cytokines and mediators such as IL-10 and BDNF. Phenotyping showed an additional neurogenic effect under VIP treated supernatant.

Our results show VPAC1 receptor subtype expressed by $CD4^+$ T lymphocytes mediates VIP proliferative effects on hippocampal precursor cells via IL-4 cytokine release. Microglia are key for mediating this effect via release of mediators. The findings of this study implicate a novel mechanism for VPAC1 $CD4^+$ T lymphocyte

receptor as a neuro-immune mediator of hippocampal neurogenesis, and from a therapeutic perspective, shows that the effect can be pharmacologically manipulated.

Acknowledgments

To my greatest teachers, my parents, who have supported my passion for learning with the most inspirational love. I dedicate this to you. Thank you for your constant encouragement. To my siblings, Mohsin and Romana, who have encouraged me to follow my dreams and achieve my goals. You paved a path for your younger sister, led by example.

A special thank you to Laura Westacott, Craig Stevenson, Yateen Patel, Claris Diaz, Emma Yhnell, Ludivine Breger, Mariah Lelos, Emma Owens, Madeha Khan, Zubeyde Bayram-Weston, Ngoc-Nga Vinh, Amy Evans, Vicky Roberton, Nawardee Chompoo, Kate Shires, Harri Davidson, Simon Brookes, Ed Torres, Pete Watson, Awen Gallimore, Emily Colbeck, Catherine Naseriyan.

To my sisters Ruebia Asif, Ambrin Zubair, Zahra Al-Kindy and Sanam Parvaiz, thank you for your love, support and creating fantastic memories that I will always hold dear. The distance only made our friendship stronger.

Lastly, I would like to thank my supervisors Professor Liam Gray, Professor Stephen Dunnett and Dr Malik Zaben without whose guidance and support this work would never have come to fruition.

The road was not straight but the journey was an adventure.

Table of contents

List of figures

List of Tables

Abbreviations

ANOVA = Analysis of variance
APC = Antigen presenting cells
BAF = BRG1- or HRBM- associated factors
BDNF = brain derived neurotrophic factor
BrdU = 5-bromo-2-deoxyuridine
cAMP = cyclic adenosine monophosphate
CD28 = cluster of differentiation 28
CNS = central nervous system
CSF = cerebrospinal fluid
CTL-4 = cytotoxic T-lymphocyte antigen 4
DAPI = 4'6-diamidino-2-phenylindole
DCX = doublecortin
EAE = experimental autoimmune encephalomyelitis
FACS = fluorescence activated cell sorting
FGF-1 = fibroblast growth factor-1
GABA = gamma-aminobutyric acid
GFAP = glial fibrillary acidic protein
IFN-ϒ = interferon gamma
IGF1 = insulin-like growth factor 1
IL-4,-10,-13 = interleukin-4,-10,-13
LPS = lipopolysaccharides
MHC = major histocompatibility complex
NBA = neurobasal A
NeuN = neuronal nuclei
NGF = nerve growth factor
NMDA = N-methyl-D-aspartate
NPY = neuropeptide Y
n.s. = non significant
PAC1 = PACAP receptor 1
Pax6 = paired box 6
PBS = phosphate buffered saline
PFA = paraformaldehyde
PI = propidium iodide
Prox1 = prospero homeobox 1
RBC = red blood cells
RPMI = Roswell Park Memorial Institute
SGZ = subgranular zone
SVZ = subventricular zone
TCR = T cell receptor
TLE = temporal lobe epilepsy
TNF = tumour necrosis factor
TuJ1 = neuron-specific class IIIβ-tubulin
VEGF = vascular endothelial growth factor
VIP = vasoactive intestinal peptide
VPAC1 = vasoactive intestinal peptide /PACAP receptor 1
VPAC2 = vasoactive intestinal peptide /PACAP receptor 2

Chapter 1

Introduction

1. Introduction

1.1: Neurogenesis: A brief history

> *"Once development has ended, the founts of growth and regeneration of the axons and dendrites dries up irrevocably. In the adult centres, the nerve paths are something fixed and immutable: everything may die, nothing may be regenerated. It is for the science of the future to change, if possible, this harsh decree."*
>
> - Ramon y Cajal

The last 60 years has birthed a paradigm shift, revolutionizing our understanding of neurogenesis. Pioneering neuroscientist Ramon y Cajal's (1913) doctrine on the nervous system's inability to regenerate after birth was widely accepted and it took several decades before a body of work was able to refute his theory, giving prominence to the concept of adult neurogenesis. Numerous studies documented as early as 1898 showed preliminary evidence for adult neurogenesis, however limited study tools at the time hindered research in to the field (Levi, 1898; Allen, 1912). In the 1960s, Altman and Das (1965) were the first to demonstrate the generation of newly dividing cells within the dentate gyrus of the mammalian hippocampus using autoradiography. However challenging Cajal's decree did not prove fruitful and indeed it took a further 20 - 30 years before this idea gained momentum. Even after Goldman and Nottebohm (1983) published their seminal paper on adult songbirds – revealing neuronal replacement and functional integration – resistance continued on a broad scale. It was, in fact, a combination of *in vitro* generation of neurons and glia from the adult rodent brain (Reynolds and Weiss, 1992) and the subsequent identification of neural progenitor cells in the human dentate gyrus (Eriksson et al., 1998) that truly marked a turning point in moving the scientific community towards accepting this change in dogma. At last, neural stem cells were able to provide a viable conceptual basis underlying adult neurogenesis.

Our understanding of neurogenesis has transpired over most of the last century to be defined today as the generation of neurons, from neural progenitors cells, throughout adulthood within defined microenvironments (niches) (Riquelme et al.,

2008). In mammals, these microenvironments are restricted to the subventricular zone of the lateral ventricles and the subgranular zone of the hippocampal dentate gyrus (Kaplan and Hinds, 1977, Eriksson et al., 1998, Gage et al., 1995, Richards et al., 1992). Newly synthesised neurons are able to migrate, differentiate and mature to become functionally integrated within the neural network (van Praag et al., 1999, Jessberger and Kempermann, 2003, Ge et al., 2006).

1.2: Hippocampal neurogenesis

Hippocampal neurogenesis is important for learning and memory, with impaired hippocampal neurogenesis associated with pathological states such as epilepsy, ischaemia and depression (Parent et al., 1997, Hattiangady et al., 2004, Liu et al., 1998, Tsai et al., 2013, Malberg et al., 2000, Perera et al., 2007, Gray and Sundstrom, 1998). A combination of intrinsic factors and external cues regulate hippocampal neurogenesis within a specialized stem cell niche. These multifactorial influences are involved in a dynamic process of neurogenic regulation, highlighting that the niche cannot be thought of in isolation as an anatomically distinct area. Rather, it is a "functional entity" influenced by the highly organized niche structure itself and factors such as environmental cues (exercise, enriched environments) and systemic regulation, to name but a few (Russo et al., 2011).

1.2.1: Hippocampal neurogenesis: a role in learning and memory

Learning and memory is associated with hippocampal neurogenesis (Kempermann and Gage, 2002). The acquisition and retention of memories is a complex process, which may be explained by fine pattern separation whereby the dentate gyrus can separate information into distinct memories. Cortical inputs are received by dentate granule cells from the entorhinal cortex. In particular, immature granule cells are ideal for maintaining and transmitting inputs, given their increased intrinsic excitability and sparse connectivity with CA3 pyramidal cells (Amaral et al., 1990, Esposito et al., 2005, Ge et al., 2007). The accuracy of memory encoding is dependent on fine pattern separation, with lesions of the dentate gyrus impairing pattern separation-dependent memory (Gilbert et al., 2001, Gilbert et al., 1998, Hunsaker and Kesner, 2008). Clelland and colleagues (2009) have shown the importance of newborn neurons for normal pattern separation function in the

dentate gyrus using two behavioural assays. They used a spatial navigation radial arm task and a spatial, non-navigable task. Ablating neurogenesis impaired performance when stimuli were presented with little spatial separation but not when widely separated. This supports the role of neurogenesis in other studies, where learning hippocampal-dependent tasks not only increases survival of newly generated neurons in the dentate gyrus, it also induces a more persistent memory and in turn correlates to an increase in the number of cells in the hippocampus (Gould et al., 1999, Sisti et al., 2007). The dentate gyrus, the stem cell niche and the factors the modulating it are therefore critical to our understanding of the relationship between neurogenesis and cognition. This subject area is therefore of paramount importance in addressing pathological conditions.

1.2.2: Neural stem cells and the stem cell niche

Neural stem cells are defined as cells derived from the nervous system that 1) have the potential to self renew through symmetrical division and 2) are able to give rise to the major cell types of the brain (neurons, astrocytes, oligodendrocytes) (Gage, 2000). Neural stem cells are present within the subgranular zone, with the stem cell niche residing at the interface between the granule cell layer and hilus region of the dentate gyrus (Abrous et al., 2005). The subgranular zone is exclusively concentrated around blood vessels and comprises of endothelial cells, astrocytes, microglia, local interneurons and factors such as hormones that are delivered by the blood stream (Cameron and Gould, 1994, Palmer et al., 2000, Riquelme et al., 2008).

Astrocytes are key components within the niche that provide support to other cell types by secreting local signals (cytokines, growth factors) and modulating adult neurogenesis (Song et al., 2002, Ashton et al., 2012, Barkho et al., 2006). *In vitro* studies have shown that astrocytes co-cultured with neural stem cells increase proliferation and neuronal fate commitment of these cells (Song et al., 2002). A specific population of cells loosely classified as astrocytes, but what we regard as neural progenitor/stem cells, are responsible for giving rise to differentiated progeny (Seri et al., 2001). These astrocytes are characterized by the stem cell marker nestin and the astrocytic marker glial fibrillary acidic protein (GFAP). These quiescent neural progenitor (Type I) cells are an early precursor population that

share morphological and antigenic features with radial glial cells (Fukuda et al., 2003). These Type I cells divide asymmetrically to produce a morphologically distinct transiently amplifying neural progenitor (Type II) cell population ($Nestin^{+}GFAP^{-}$). Following a series of symmetrical divisions, these cells become post-mitotic Type 1 neuroblasts which mature into Type 2 neuroblasts and immature neurons **(Figure 1).** These newly formed neurons migrate a short distance to the granule cell before differentiating into granule neurons and becoming integrated into the functional hippocampal circuit, with mossy fibres extending towards the CA3 region (van Praag et al., 2002, Carlen et al., 2002, Doetsch, 2003). Indeed, it is of importance to note that neural stem cells are present throughout different regions of the mammalian brain outwith the two neurogenic regions (SGZ and SVZ). These areas include the forebrain, spinal cord, corpus callosum, cerebral cortex (Weiss et al., 1996, Seri et al., 2006, Reznikov, 1991, Gage et al., 1995, Gage, 2000). However, neural stem cells within these regions remain in a quiescent state (Gage, 2000); a factor determined by the niche and intrinsic cues.

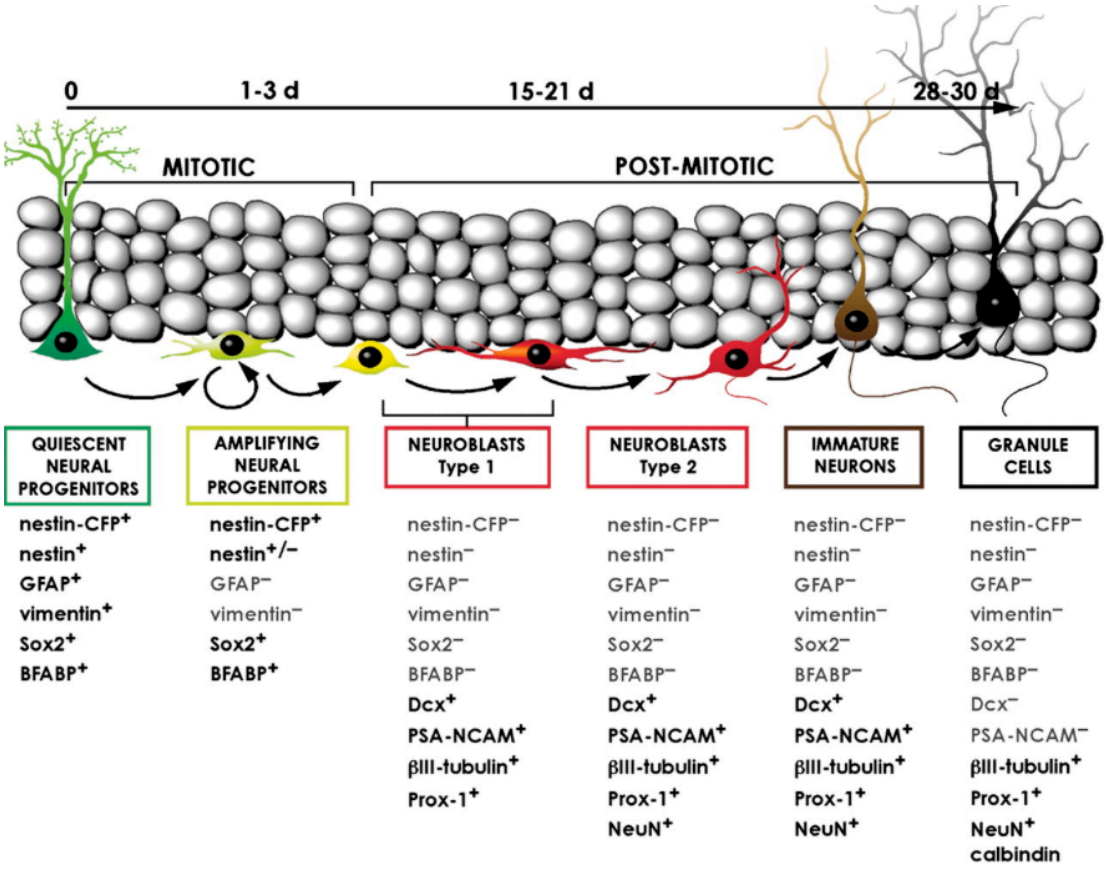

Figure 1: Neuronal differentiation in the dentate gyrus. Quiescent neural progenitor (Type I) cells generate a population of transiently amplifying neural progenitor (Type II) cells through asymmetrical divisions. After several rounds of symmetrical divisions, Type II cells exit the cell cycle within 1-3 days and become post-mitotic Type 1 neuroblasts. Within the next 15-21 days, these Type I neuroblasts mature into Type 2 neuroblasts and then immature neurons. These neurons have apical processes, basal axons and soma located in the granule cell layer. After another 1-15 days, immature neurons acquire the characteristics of mature granule neurons, developing extensive branching, long axonal processes that form the mossy fiber (taken from (Encinas et al., 2006)).

1.2.3: A role for interneurons in modulation of neurogenesis

Local networks are increasingly implicated in modulating activity, with a key role for local interneurons in excitation-neurogenesis coupling. Although there is diverse heterogeneity amongst hippocampal dentate gyrus interneurons, most are GABAergic and therefore the role of GABA has been studied extensively (Maccaferri and Lacaille, 2003). New born neurons respond to extracellular GABA, stimulating differentiation and migration (Conover and Notti, 2007). Dentate gyrus progenitor cells in mice lacking the $GABA_A$ receptor subunit α (responsible for tonic GABA input) have decreased proliferation (Mihalek et al., 1999; Rudolph and Antkowiak, 2004). These mice also have impaired cell migration (Mihalek et al., 1999). Mature dentate granule cells respond to GABA and receive GABAergic inputs, which causes depolarization and subsequent increased Ca^{2+} levels (Deisseroth et al., 2004).

Increased Ca^{2+} stimulated NeuroD expression, a transcriptional factor required for neuronal survival and maturation (Kobayashi and Buckmaster, 2003, Deisseroth et al., 2004). Other studies have shown that $GABA_A$ receptor antagonists shorten dendrites and decrease spine density, while GABA receptor agonist administration increases dendrite length (Sun et al., 2009, Ge et al., 2006). Other neurotransmitters with an important role include glutamate, which decreases cell proliferation in the hippocampus. Conversely the use of an NMDA antagonist enhances proliferation (Mackowiak et al., 2009).

Neuropeptides are co-localized with classical neurotransmitters, particularly GABAergic interneurons in the hippocampus, and are released under specific firing conditions. The role of neuropeptides released by interneurons ha been extensively studied. Neuropeptide Y (NPY) is proliferative for postnatal hippocampal precursor cells acting via the Y1 receptor subtype, which subsequently activates the Erk1/2 pathway (Howell et al., 2003). Adult NPY knock-out mice have significantly reduced cell proliferation and immature neurons (Howell et al., 2005). Galanin is another neuropeptide and is involved in cognition. It is co-localized with serotonergic/noradrenergic projection neurons in the dentate gyrus and mediates proliferative and trophic effects on postnatal hippocampal precursor and neuroblast via GalR2/3 receptors (Abbosh et al., 2011). The neuropeptide vasoactive intestinal peptide (VIP) is trophic for hippocampal precursor cells and drives fate determination via its VPAC2 and VPAC1 receptors, respectively (Zaben et al., 2009). This was confirmed *in vivo* using adult VIP knock-out mice, which has significantly reduced numbers of precursor cells (Zaben et al., 2009). Both NPY and VIP are released by GABAergic interneurons in the dentate gyrus. These studies stress the importance of neurotransmitters in the regulation of hippocampal neurogenesis.

1.2.4: Intrinsic regulation

Intrinsic factors are expressed by neural stem cells and dictate their fate. The list of intrinsic factors are extensive and discussed in depth in a review by Hseih (2012). The transcriptional factor Sox2 regulates stem cell self-renewal and is expressed by neural precursor cells in the subgranular zone (Lefebvre et al., 2007, Komitova and Eriksson, 2004, Sun et al., 2007, Lugert et al., 2010, Favaro et al., 2009). Deletion of

Sox2 in adult subgranular zone neural stem cells results in a decrease in the number of immature neurons and granule cells (Favaro et al., 2009). Notch signalling is believed to control Sox2 expression (Ehm et al., 2010).

Pax6 is another noteworthy intrinsic factor regulating cell proliferation and maintaining the stem cell pool (Maekawa et al., 2005). During development, Pax6 mediates self-renewal via β-catenin signalling (Gan et al., 2014). In adults, Pax6 directly interacts with the Brg1-containing BAF complex in neural progenitor cells to maintain self-renewal. Deletion of Brg1 or Pax6 results in fate determination

Similarly, cell fate is determined by a multitude of factors including the transcriptional factor NeuroD1. Fewer immature granule cells are found following the conditional deletion of NeuroD1, which supports the findings that NeuroD1 is critical for neuronal precursor cell differentiation and survival (Gao et al., 2009). Wnt/β-catenin signalling controls NeuroD1 transcription (Kuwabara et al., 2009). The granule neuronal marker prospero-related homeobox gene Prox1, expressed by immature and mature neurons, is required for neuronal survival and maturation (Jessberger et al., 2008, Lavado et al., 2010, Karalay et al., 2011). Studies have shown that conditional deletion of Prox1 in neural stem cells reduces the number of granule cells (Lavado et al., 2010). Interestingly, the Prox1 gene is also controlled by Wnt/β-catenin signalling (Karalay et al., 2011). In addition to these intrinsic cues, extrinsic factors play an essential role in neurogenic regulation.

1.2.5: Environmental cues

One of the well established modulators of hippocampal neurogenesis are external cues: environmental enrichment and exercise. The concept of environmental enrichment dates back to the 1960s and has since been recognized as a setting to enhance brain stimulation, increasing net hippocampal neurogenesis and improves spatial learning in rodents (van Praag et al., 1999, Nilsson et al., 1999, Rosenzweig, 1966). Environmental enrichment comprises larger housing conditions and objects for physical exertion (e.g. running wheel), whilst facilitating greater social interaction (Sztainberg and Chen, 2010).

Kempermann and colleagues (1997) were the first to show a link between environmental enrichment and neurogenesis. Mice housed in enriched environments had an increased number of new neurons survive compared to control mice. Mice in enriched environments also exhibited faster learning in the Morris water maze paradigm, where mice are trained to find a hidden platform (Morris et al., 1982). This suggests new neurons contribute to enhanced cognition. Though it has been shown that water maze performance improves in "enriched" mice despite ablation of neurogenesis, these tasks were not specific to dentate gyrus-specific learning (Meshi et al., 2006, McHugh et al., 2007). Voluntary exercise on a running wheel alone also enhances survival of newly born neurons in the dentate gyrus (van Praag et al., 1999). Taken together, current research indicates a role for environmental-induced hippocampal neurogenesis in mediating cognition.

1.2.6: Systemic modulation of hippocampal neurogenesis

Given the close proximity of the subgranular zone to blood vessels, interaction between the stem cell niche and the systemic niche is not surprising. Factors delivered from the blood stream can therefore potentially modulate hippocampal neurogenesis. In a study published in 2007, magnetic resonance imaging was used to generate cerebral blood volume maps of exercising mice (Pereira et al., 2007). This study showed that an increase in exercise was accompanied by an increase in cerebral blood volume of the dentate gyrus; this positively correlated to increased neurogenesis. Another cleverly designed experimental model, heterochronic parabiosis, has further demonstrated the significance of the systemic system in the modulation of neurogenesis (Villeda et al., 2011). This experimental design involved coupling the blood stream of two animals – one aged and one young – and showed decreased neurogenesis and cognitive decline in young animals exposed to "aged blood". Further to this, "rejuvenation" with blood from young animals increased neurogenesis. These experiments are keeping in line with the concept of aging, whereby studies suggest that age-associated decline in hippocampal proliferation is a result of changing levels of circulating hormones, which are indeed important in neurogenic regulation; it has been shown that while adrenal steroids decrease production of new neurons, adrenalectomy increases cell proliferation and generation of neurons and glia in the dentate gyrus (Cameron and McKay, 1998,

Cameron and Gould, 1994, Montaron et al., 1999). These studies suggest potent effects of systemic circulation and is an intriguing prospect for immune signalling in neurogenic modulation; a factor fast-emerging as a key player.

1.3: Immune regulation of neurogenesis

Immune regulation of the central nervous system is a dynamic and complex area of research still in its infancy. We now appreciate the CNS is not an "immune-privileged" site mutually exclusive of immunological function (Shrestha et al., 2013). Rather, there is a complex and delicate relationship between the two systems under both physiological and pathological states (Karman et al., 2004, Butovsky et al., 2006). Conventionally, the concept of neuro-immune regulation has been dominated by the belief that the immune system is a responsive system that adheres to an organized response following infection. Although this is true, the immune system is also heavily involved in brain homeostatic regulation and indeed neurogenesis (Ziv et al., 2006, Wolf et al., 2009). Our understanding of this subject area has altered dramatically in the last decade and is paving the way for new insights into neurogenic regulation (Moalem et al., 1999, Shechter et al., 2009, Ziv et al., 2006). Whilst immune cells are being appreciated as effectors of CNS maintenance and repair, a novel role for distinct populations of innate immune cells, particularly microglia, are being identified outwith the parameters of immune regulation; this extends to a complex relationship with components of the adaptive immune system, in particular T lymphocytes (Ziv et al., 2006, Ginhoux et al., 2010, Derecki et al., 2010).

1.3.1: Innate vs. adaptive immunity

There are two types of immunity: innate and adaptive. Components of innate "non-specific" immunity, as the name suggests, target all foreign antigens and include macrophages, dendritic cells and microglia. On the contrary, adaptive immunity is antigen specific and includes T and B lymphocytes. The origin of these cell types is illustrated in **Figure 2.**

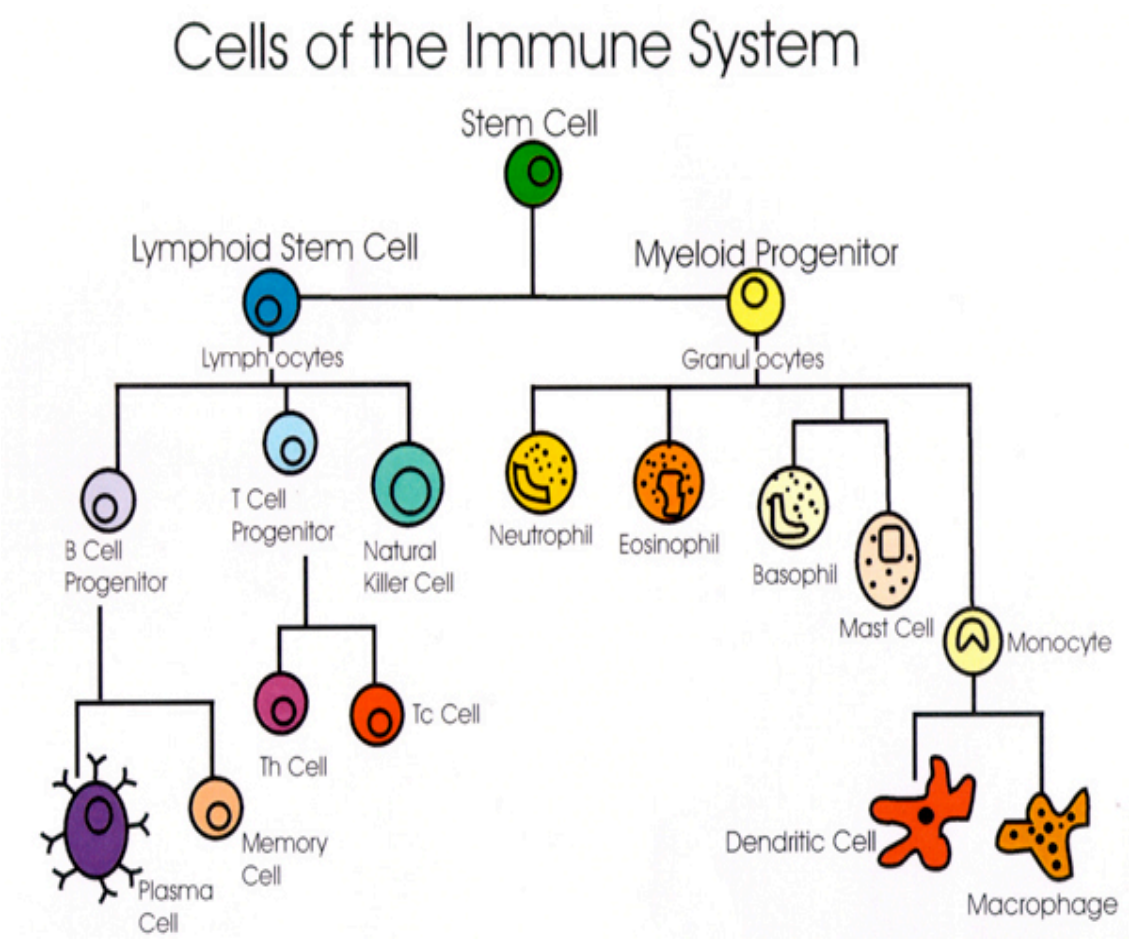

Figure 2: Cells of the immune system. Stem cells divide into two distinct groups that give rise to precursor cells of innate (myeloid progenitor) and adaptive (lymphoid stem cell) immunity. These cells further differentiate into specific cell types (Taken from Online Textbook of Bacteriology, Todar).

1.3.2: Microglia: innate immune cells

Microglia, innate immune cells that comprise approximately 15% of the brain cell population, are primarily involved in maintaining homeostatic regulation. These cells are found in high densities in the hippocampus (Lawson et al., 1990). Microglial activity primarily involves tissue surveillance and appropriate phagocytic action. Microglia are also antigen-presenting cells and have the capacity to produce a variety of cytokines and chemokines (Aloisi et al., 2000, Ladeby et al., 2005). Recently, fate map analysis has shown that microglia are derived from myeloid progenitor cells (Ginhoux et al., 2010).

Under physiological conditions, microglia have a quiescent phenotype characterised by ramified processes (Ladeby et al., 2005). These microglia become "activated"

following a brain insult that changes their phenotype; cells have enlarged cell bodies and withdrawn processes. Microglial populations are divided into two primary subsets, M1 and M2, however other subsets do exist (M2a, M2b, M2c) (Kigerl et al., 2009, Chhor et al., 2013). These subpopulations are categorized on the premise of cytokine production. Cytokines are a diverse group of proteins that act as chemical messengers between cells (Kronfol and Remick, 2000). M1 "classical" subsets are regarded as pro-inflammatory and associated with interferon gamma (IFNγ) production while M2 "alternative" microglia are of an anti-inflammatory nature and associated with interleukin-4 (IL-4) production. However, there is some controversy surrounding this classification due to overlaps in some cytokines between M1 and M2 phenotypes, which was highlighted at the Venusberg meeting in 2013. It was suggested that a simple M1/M2 classification cannot necessarily distinguish a "good" cell from a "bad" cell.

Historically, microglia are regarded as detrimental to neurogenesis. Indeed, microglia activated by the bacterial endotoxin lipopolysaccharide (LPS) decrease the survival of hippocampal progenitor cells (Cacci et al., 2005). Systemic LPS injection also activates microglia in the hippocampus and is associated with decreased neurogenesis (Ekdahl et al., 2003). However, this conventional thinking is fast changing as microglia exhibit beneficial effects (Ekdahl et al., 2009, Ziv et al., 2006). It is postulated that the environment and duration, nature and intensity of microglia-activating stimuli contribute to the beneficial or detrimental function (Ajmone-Cat et al., 2003, Schwartz et al., 2006). This is also said to be the reason why cells cannot be classified purely as M1/M2 cells; there is a complexity to microglia that is dictated by environment. For instance, contrary to short-term LPS exposure, chronic LPS exposure to microglia progressively inhibits pro-inflammatory secretion (Ajmone-Cat et al., 2003). In their capacity as beneficial immune cells, microglia regulate basal neurogenesis levels. Blocking microglia using the anti-inflammatory agent minocycline decreases proliferation of newly generated neurons (Ziv et al., 2006). Furthermore, hippocampal microglia exposed to enriched environments express the neuroprotective factor IGF-1 (Ziv et al., 2006). IL-4-activated microglia are also shown to increase the number of newly generated neurons (Butovsky et al., 2006).

It is clear that microglia play a key role in both immune and homeostatic regulation. The exact nature of the relationship between microglia and neurons remains unclear. However, microglial involvement reinforces the importance of innate immunity in modulating neurogenesis.

1.3.3: Adaptive immunity

Immune cell entry into the brain is tightly regulated to prevent adverse events. Immune cells are able to traverse the CNS during inflammatory states in an attempt to minimize the damage (Moalem et al., 1999, Shechter et al., 2009). T lymphocytes and other components of the adaptive immune system are therefore subject to the regulatory mechanisms that specify which cells are able to enter the CNS. Indeed, this explains why T lymphocytes are essentially absent from the brain parenchyma under physiological conditions (Wolf et al., 2009, Ziv et al., 2006). However, FACS analysis of cerebrospinal fluid, which is produced within the choroid plexus and occupies the subarachnoid space and ventricular system, shows a subpopulation of T lymphocytes called $CD4^+$ T lymphocytes that express the cell adhesion molecule P-selectin; this suggests a possible mechanism by which T lymphocytes could be recruited to the brain parenchyma via P-selectin interactions (Kivisakk et al., 2003). However, the jury is still out on how T lymphocytes enter the brain. In fact, this remains one of the most challenging areas of study in neuroimmunology.

1.3.4: Classification of T lymphocytes

T lymphocytes originate from lymphoid cells in the bone marrow and migrate to the thymus where they differentiate and then proliferate. These T lymphocytes go through a series of changes distinguished by changes in surface proteins. T lymphocytes are eventually subdivided into two distinct populations: cytotoxic T lymphocytes that express the surface marker $CD8^+$ and helper T lymphocytes that express the $CD4^+$ marker (Zhu and Paul, 2008). Cytotoxic $CD8^+$ T lymphocytes, as their name suggests, are involved in the destruction of infected cells whilst $CD4^+$ T lymphocytes mediate immune response via cytokine release. $CD4^+$ T lymphocytes are further subdivided primarily into two distinct groups, Th1 and Th2, however other subgroups do exist (e.g. Th17, Treg) (Zhu and Paul, 2008). These $CD4^+$ T

lymphocytes are categorized based on the production of signature cytokines. The Th1 phenotype is conventionally regarded as pro-inflammatory and associated with the production of IFNγ, interleukin-2 (IL-2) and tumour necrosis factor alpha (TNFα) (Zhu and Paul, 2008, Mosmann et al., 1986). These cytokines activate immune response against macrophages, whilst Th2 phenotypes are associated with anti-inflammatory activities and the secretion of IL-4, -10, -13 (Mosmann et al., 1986, Zhu and Paul, 2008). Although these cytokines are associated with pro- or anti- inflammatory activity, they play a role in non-immune regulation of neurogenesis (Vallieres et al., 2002, Song and Wang, 2011). Of note here is that various cell types, including microglia and astrocytes, locally produce cytokines in the brain (Freidin et al., 1992, Krady et al., 2005). Although cytokines are usually produced in response to certain stimuli such as infection, studies suggest there is constant low-level cytokine expression within blood vessels in the brain (Licinio et al., 1998). Also of importance is that cytokines cannot transcend the blood-brain barrier under physiological conditions. Cytokines can enter the brain via 2 mechanisms:

1. passive transport from circumventricular regions lacking a blood-brain barrier
2. carrier-mediated transportation across the blood-brain barrier

Similarly, T lymphocytes cannot traverse the blood-brain barrier under physiological conditions.

1.3.5: T lymphocyte entry into the brain

Paul Ehlrich's work during the late 19th Century was the first in demonstrating that the CNS was an anatomically distinct region. Later, it would be recognized that the inability of the water-soluble dye he injected into peripheral circulation to stain all organs except the brain was due to the restrictive nature of the blood-brain barrier. It is well established that blood-brain barrier breakdown manifests in an influx of immune mediators entering the brain, including T lymphocytes (Lightman and Greenwood, 1992, Gronberg et al., 2013). Mounting evidence implicates T lymphocytes in modulating hippocampal neurogenesis under physiological

conditions but few T lymphocytes are found within the brain parenchyma. Therefore, what remains perplexing is the ability of T lymphocytes to modulate neurogenesis if, indeed, they do not infiltrate the brain.

There is much evidence to support this notion of "long-distance" action, whereby T lymphocytes are not present within the brain. Rather, they are situated in close proximity to elicit their neurogenic effects (Wolf et al., 2009, Derecki et al., 2010, Zhu and Paul, 2008). In a mouse model of Alzheimer's disease, cognitively impaired mice showed significant improvement in memory tasks following T cell infusion of Aβ-specific Th2 cells (Cao et al., 2009). Analysis of brain sections showed some $CD3^+$ (a T lymphocyte specific marker) cells (3-10 cells) in a few brain sections but not all. Ziv and colleagues (2006) also showed a few sections with some $CD3^+$ staining when investigating T lymphocyte modulation of hippocampal neurogenesis. Again, these cells were very few in number. This supports findings that suggest some constant trafficking of T lymphocytes in to the brain in low numbers (Kivisakk et al., 2003). However, even if T lymphocytes manage to traverse the blood-brain barrier or indeed traffic through areas where the blood-brain barrier is absent, it seems highly unlikely that such a small number of cells are able to elicit the effects that have been observed in studies of T lymphocyte regulation of neurogenesis under physiological conditions. Rather, the question to address is where could these T lymphocytes reside?

Blood capillaries reside deep within the brain supplying the brain parenchyma and could be a potential route of T lymphocyte entry. There is a significant population of T lymphocytes and myeloid cells (from which they originate) within the meningeal spaces surrounding the brain parenchyma. Derecki and colleagues (2010) showed increased accumulation of $CD4^+$ T lymphocytes in the meningeal spaces in wild type mice following Morris water maze training. The choroid plexus is another region from which $CD4^+$ T lymphocytes could modulate neurogenesis. Approximately 80% of human CSF cellular composition constitutes $CD4^+$ T lymphocytes (Ransohoff et al., 2003, Svenningsson et al., 1995). It is therefore possible that CSF is a potential reservoir from which T lymphocytes could migrate into meningeal spaces - specifically the subarachnoid space though which CSF flows - ideally positioning

them to interact with the brain. Homing studies support this concept, showing systemically injected T lymphocytes preferentially localize within the leptomeningeal (pia and arachnoid mater) compartment within two hours due to P-selectin interactions (Carrithers et al., 2000). These studies show a preference of T lymphocytes for meningeal spaces and provide a potential area of activity for communication with the brain. However, it is evident that the mechanisms underlying T lymphocyte modulation of neurogenesis remains poorly understood. Regardless, their role in neuromodulation is compelling and therefore understanding the mechanisms is central to studying this area.

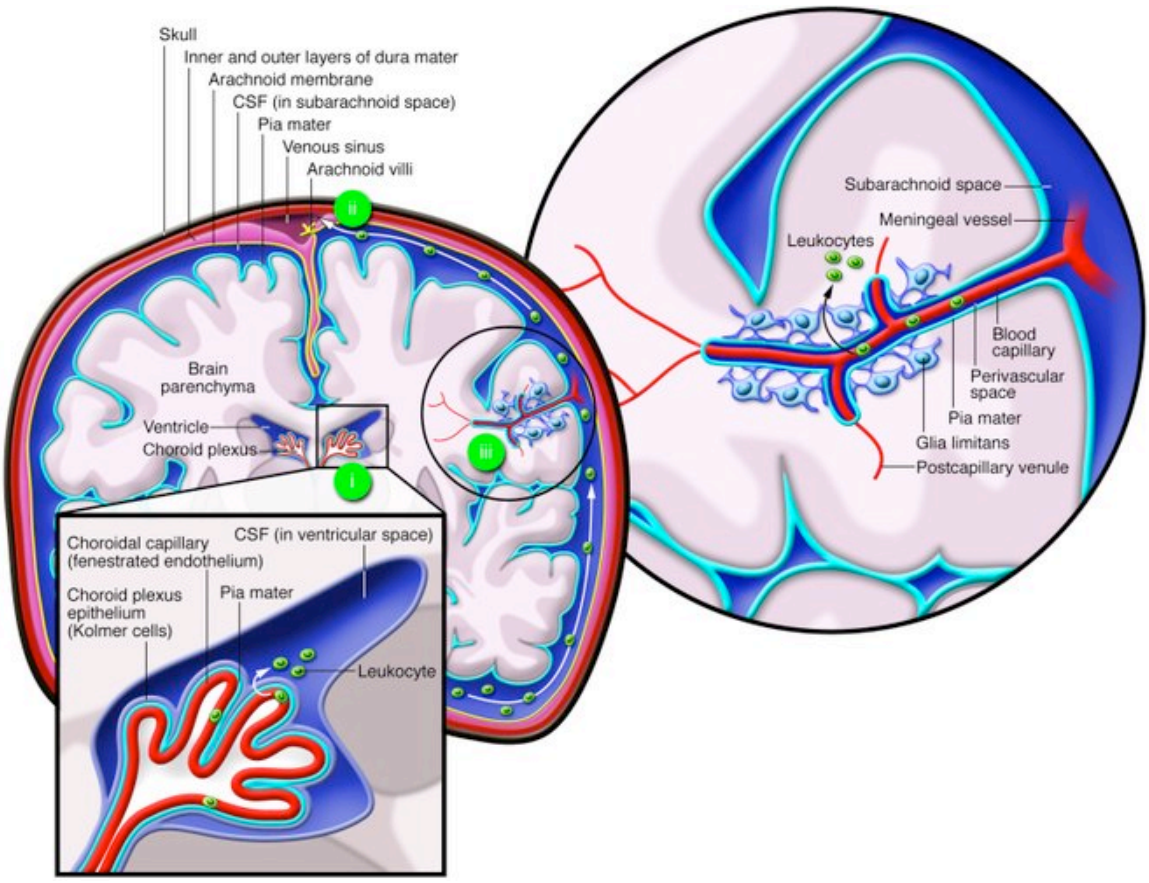

Figure 3: Structure of brain and routes of leukocyte entry. The brain membranes (dura, arachnoid and pia mater) lie underneath the skull and enclose the brain parenchyma. Leukocytes/lymphocytes can enter via the choroid plexus which flows through the subarachnoid space and exits through the venous sinus. They can also enter through blood since the main arterial branches divide into capillaries that terminate within the brain (Taken from Wilson et al., 2010).

1.3.6: T lymphocytes: a role in neuromodulation

Immune-deficient mice have impaired hippocampal neurogenesis. Ziv and colleagues' (2006) seminal paper observed reduced proliferation of newly generated neurons in immune-deficient mice devoid of T and B cells compared to wild types. Environmental enrichment could not enhance hippocampal neurogenesis in these mice whilst replenishment with T lymphocytes recognizing CNS-specific antigens did. When investigating nude mice devoid specifically of T lymphocytes, proliferation and neuronal differentiation was reduced (Ziv et al., 2006). Again, this effect was rescued by intravenous injection of T lymphocytes. Other studies showed impairment of cognitive function in models of general immune deficiency, with a role for T lymphocytes (Brynskikh et al., 2008, Kipnis et al., 2004). However these studies did not identify a correlation to hippocampal neurogenesis. It was, in fact, Wolf and colleagues (2009) that confirmed the role of T lymphocytes in mediating the change in neurogenesis reported by Ziv et al. (2006); however replenishment was in contrast to previous work as Wolf et al. (2009) used non-CNS specific T lymphocytes. Wolf et al. (2009) also investigated cognitive performance and showed impaired learning. In an attempt to further elucidate this mechanism, Derecki et al. (2010) reported increased accumulation of IL-4 producing $CD4^+$ T lymphocytes in the meninges. Furthermore, IL-4 knockout mice exhibit cognitive defects. These studies are supportive of each other and suggest a beneficial role for T lymphocytes in regulating hippocampal neurogenesis. However, one key question remains unanswered: how do T lymphocytes communicate with the hippocampal stem cell niche? Neuropeptides present themselves as potentially ideal candidates for this role.

1.4: Vasoactive Intestinal Peptide: a role in neuromodulation

1.4.1: VIP: receptors and distribution

Vasoactive Intestinal Peptide (VIP) is a neuropeptide that, as the name suggests, was originally identified as a vasodilator in the gut by Said and Mutt over 40 years ago (Said and Mutt, 1970). However, we have now come to appreciate its role as a neuropeptide with potent immunomodulatory effects (Bryant et al., 1976). It is, in fact, one of the most extensively studied neuropeptides. The primary structure of this 28 amino acid peptide is conserved across most mammalians and it is

structurally related to secretin and glucagon (Said and Mutt, 1970, Said and Mutt, 1972). VIP is widely distributed across the central/peripheral nervous systems and the central/peripheral lymphoid organs (Said and Rosenberg, 1976, Larsson et al., 1976). In the brain, VIP is widely distributed, particularly by interneurons within the dentate gyrus of the hippocampus (Acsady et al., 1996). VIP nerve endings are present within lymph organs, including the spleen where they are found amongst T lymphocytes (Bellinger et al., 1996, Moody et al., 2003). Indeed, these VIP-nerve terminals provide a direct link between the CNS and immune system.

VIP acts via its three G-protein coupled seven transmembrane receptors, VPAC1, VPAC2 and PAC1. VIP binds to VPAC1 and VPAC2 receptors with high affinity but has a 1000-fold lower affinity to PAC1 (DiCicco-Bloom, 1996). VPAC1 mouse and rat receptors share an 83% homology with human receptors, whilst VPAC2 rat receptors share an 87% homology (Moody et al., 2003). Expression of all their receptors varies during development. Whilst all three receptors are highly expressed during embryonic development, neuropithelial VPAC1 and PAC1 expression is downregulated during postnatal period (Basille et al., 2000). However, PAC1 postnatal expression levels remain controversial (Basille et al., 2000, Shioda et al., 2006). In adult rats, all three receptors are shown to have high expression, particularly in the dentate gyrus of the hippocampus (Moody et al., 2003, Sheward et al., 1995).

1.4.2: VIP: a role in the CNS

VIP has pleiotropic effects in the CNS, from regulating synaptic transmission to circadian rhythms (Scharf et al., 2008). VIP mediates neurotrophic and neuroprotective effects on the CNS via the release of cytokines and growth factors (Brenneman et al., 2003, Brenneman et al., 1998, Servoss et al., 2001). These include BDNF and IGF-1, which are pro-neurogenic mediators that enhance neuron survival (Reichenstein et al., 2008, Bondy and Cheng, 2004, Servoss et al., 2001).

VIP is important for neurogenesis from embryonic development through to adulthood. Blocking VIP receptors during embryonic development increases cell death in the neocortex of mice, results in reduced brain size and reduced cell DNA

content (Zupan et al., 2000, Gressens et al., 1994). VIP also modulates postnatal hippocampal neurogenesis and acts via VPAC2 receptors to alter proliferating precursor fate choice. It expands the pool of symmetrically dividing dentate gyrus neural precursor cells, as well as having independent VPAC2 mediated trophic effects (Zaben et al., 2009). VIP also acts on VPAC1 receptors to direct these cells towards a neuronal fate. *In vivo* models using VPAC2 knockout mice further substantiate these findings (Zaben et al., 2009).

In addition to modulating hippocampal neurogenesis, VIP modulates learning and memory. There is a dual role for VIP in the CNS. Both administration of VIP and inhibition impairs spatial memory (Itoh et al., 1994, Glowa et al., 1992). When administered to pregnant mice, these antagonists result in cognitive deficits in off-spring (Hill et al., 2007). Interestingly, in mouse models of Alzheimer's disease, VIP agonists provide protection against impaired spatial learning (Gozes et al., 1996, Gozes et al., 1999).

1.4.3: A role for VIP and T lymphocytes in immunomodulation

T lymphocytes express the VIP receptors VPAC1 and PAC1 constitutively, whilst VPAC2 expression is differentially regulated (Delgado et al., 1999b, Delgado and Ganea, 2001b). It is therefore not surprising that VIP plays an important role in the modulation of T lymphocytes, favouring a Th2 phenotype and VPAC2 responses (Delgado et al., 2004). The reason for a bias towards Th2 over Th1 is not fully known.

Naïve $CD4^+$ T lymphocytes require activation by antigen presenting cells such as microglia to induce cytokine production. Two signals are delivered by antigen presenting cells: 1) binding of the antigenic peptide/MHC class II complex with the T cell receptor 2) binding of co-stimulatory molecules on antigen presenting cells. These co-stimulatory molecules include B7.1 and B7.2, which interact with counter-receptors CD28 and CTL-4 on T lymphocytes (June et al., 1994). VIP down-regulates their expression without affecting MHC class II expression in LPS-stimulated bone marrow derived dendritic cells (Ganea et al., 2003). This is similar to the effects of VIP on macrophages and suggests a potential mechanism by which VIP favours a Th2 phenotype and its anti-inflammatory role.

A number of cytokines have been identified in the relationship between VIP and T lymphocytes. IL-12 is a key mediator of the Th1/Th2 balance. VIP inhibits IL-12, a cytokine whose suboptimal doses favour a Th2 phenotype (Xin and Sriram, 1998, Delgado et al., 1999b). VIP promotes Th2 cell proliferation and survival (not Th1) (Delgado et al., 2002). *In vitro* studies have shown that the Th2 cytokines IL-4 and IL-5 are produced by macrophages following treatment with VIP, while Th1 cytokines IFN-γ and IL-2 were inhibited (Delgado et al., 1999a). Inhibition of IL-2 production is mediated by VPAC1 and VPAC2 receptors via induction of intracellular cAMP (Wang et al., 1999). This is supported *in vivo* where VIP administration in immunized mice reduces the number of IFN-γ-producing cells, while increasing the number of IL-4-producing cells (Delgado et al., 1999a). VIP treatment of macrophages also favours Th2 production and Th1 inhibition in $CD4^+$ T lymphocytes (Delgado et al., 1999a). Also, VIP pushes the T lymphocyte subset ratio in favour of a protective Th2 phenotype associated with anti-inflammatory production in non-obese diabetic mice (Jimeno et al., 2010). VIP promotes Th2 differentiation and subsequent IL-4 production on established Th2 cell lines(Voice et al., 2001). In fact, the relationship between VIP and IL-4 is of a complex nature. Antigen-stimulated Th2 cells secrete VIP, which then favour Th2 differentiation and survival, followed by further IL-4 production. However, IL-4 inhibits VIP production whilst reducing VPAC2 expression on Th2 cells, not Th1 (Voice et al., 2001, Delgado et al., 2002, Delgado and Ganea, 2001a, Metwali et al., 2000, Metwali et al., 2002).

In its regulation of T lymphocytes, VIP activates a number of transcriptional factors. VIP induces the Th2 transcriptional factor JunB in stimulated T lymphocytes (Delgado and Ganea, 2000, Wang et al., 2000). It also upregulates the transcriptional factor c-Maf which is essential for IL-4 expression (Voice et al., 2003). Given the mounting evidence implicating VIP in T lymphocyte mediation, it is plausible that VIP can play a key role in modulating neuro-immune interactions.

1.5: Neurogenesis in pathological states

It is important to understand the implications of impaired hippocampal neurogenesis. This is observed in pathological states including epilepsy, mood

disorders, stress and ischaemia.

i) Epilepsy

Temporal lobe epilepsy is characterized by recurrent seizures and cognitive impairment (Murphy, 2013) Animal models of epilepsy have demonstrated increased cell proliferation in the hippocampal dentate gyrus following acute seizures produced by pilocarpine, kindling or kainate treatment (Parent et al., 1997, Bengzon et al., 1997, Gray and Sundstrom, 1998). This increase in neurogenesis returns to baseline within 2 months after the initial seizure (Jessberger et al., 2007). A significant proportion of the newly generated dentate granule cells exhibit abnormal morphological features in the form of basal dendrites, which have immature synapses (Shapiro et al., 2005). These persist for prolonged periods and could therefore be involved in the development of chronic epilepsy (Shapiro and Ribak, 2006). The underlying mechanisms in increasing cell genesis remain to be fully determined but it is postulated that mitogenic factors released by dying cells or reactive microglia could account for the increase in neural stem cells. These include nerve growth factor (NGF), brain-derived neurotrophic factor (BDNF), fibroblast growth factor-1 (FGF-1) and vascular endothelial growth factor (VEGF) **(Figure 4)** (Gomez-Pinilla et al., 1995, Shetty et al., 2003, Croll et al., 2004, Shetty et al., 2004). There is also the involvement of neurotransmitters such as neuropeptide Y, which regulates physiological neurogenesis in the dentate gyrus in a neuroproliferative manner (Howell et al., 2003). Interestingly, NPY is essential for seizure-induced proliferation as demonstrated in studies with NPY knock-out mice; there is a significant reduction in seizure induced dentate gyrus proliferation (Howell et al., 2007). Increase in cell number is also observed in the hippocampus of children with temporal lobe epilepsy (Blumcke et al., 2001). Interestingly, while acute seizures induce an increase in cell proliferation, chronic epilepsy (characterized by significant spontaneous seizures) reduces hippocampal neurogenesis by 64-81% (Parent et al., 1998, Hattiangady et al., 2004). Furthermore, there is impaired differentiation of neural stem cells (Blumcke et al., 2001).

In addition to impaired hippocampal neurogenesis, both animal models and patients of temporal lobe epilepsy exhibit cognitive impairments (Howard et al.,

2010, Barkas et al., 2012, Inostroza et al., 2011, Cardoso et al., 2011). Indeed, treatment with antiepileptic and antidepressant drugs can block seizure-induced neurogenesis in rodents and reverse impairment in patients with temporal lobe epilepsy, restoring some learning and memory deficits (Jessberger et al., 2007, Barkas et al., 2012). Since temporal lobe epilepsy combines deficits in hippocampal neurogenesis and learning and memory, this pathological state emphasises the importance for studying hippocampal neurogenesis.

Indeed, emerging literature implicates a role for inflammation as both a causative agent of pathology as well as a consequence of the disease. Pro-inflammatory molecules and activated microglia have been identified in the hippocampus of patients with temporal lobe epilepsy (Crespel et al., 2002, Aronica et al., 2007, Ravizza et al., 2008, van Gassen et al., 2008). Pro-inflammatory cytokine (IL-1β, TNF and IL-6) induction is triggered within 2 hours of status epilepticus, predominantly by microglia and astrocytes (De Simoni et al., 2000, Vezzani and Granata, 2005). A pathological cascade ensues, activating the complement system and up-regulating chemokine production and receptor expression. Increased chemokine expression by neurons and glia are suggested to direct leukocytes to the brain (Fabene et al., 2008). This is in line with studies that show the presence of T lymphocytes in epileptic tissue from humans and TLE models (Fabene et al., 2008, Ravizza et al., 2008). Tissue from humans and TLE models have identified activated astrocytes and microglia expressing inflammatory mediators (Ravizza et al., 2008, Crespel et al., 2002, Dube et al., 2010). Therefore, there is strong evidence for the immune system in chronic TLE, which may account for the associated learning and memory deficits in pathological neurogenesis.

ii) Mood disorders

Hippocampal neurogenesis is implicated in depression**.** Patients with depression have reduced hippocampal volume (Small et al., 2011, Fotuhi et al., 2012). Adult-generated hippocampal neurons are required to regulate mood and also to ensure the effectiveness of antidepressant treatment (Petrik et al., 2012, Santarelli et al., 2003). Treatment with antidepressant drugs enhances cell proliferation in the dentate gyrus and reduces stress levels, which is a predisposing factor of depression

(Santarelli et al., 2003, Encinas et al., 2006) (Malberg et al., 2000, Czeh et al., 2001). In keeping with the concept of antidepressant effectiveness, ablation of hippocampal neurogenesis in mice does in fact impair antidepressant efficacy (Santarelli et al., 2003). However, of note here is that ablation of neurogenesis in animal models does not always cause depressive-like symptoms, nor does stress always decrease neurogenesis (Jayatissa et al., 2010, Lagace et al., 2010). Eisch and Petrik (2012) propose the *neurogenic interconnectome* model with the idea that a multitude of factors reflecting the delicate balance of neurogenic regulation may come in to play here. This involves different regions of the brain, the diverse functions of the hippocampus and the involvement of the stem cell niche itself. It is clear that the pathophysiology of depression remains undetermined. Whether hippocampal dysfunction and altered stress response is a predisposing factor rather than a causative agent in depression remains unclear. Understanding the factors regulating hippocampal neurogenesis and the stem cell niche can provide effective strategies for antidepressant drug treatments.

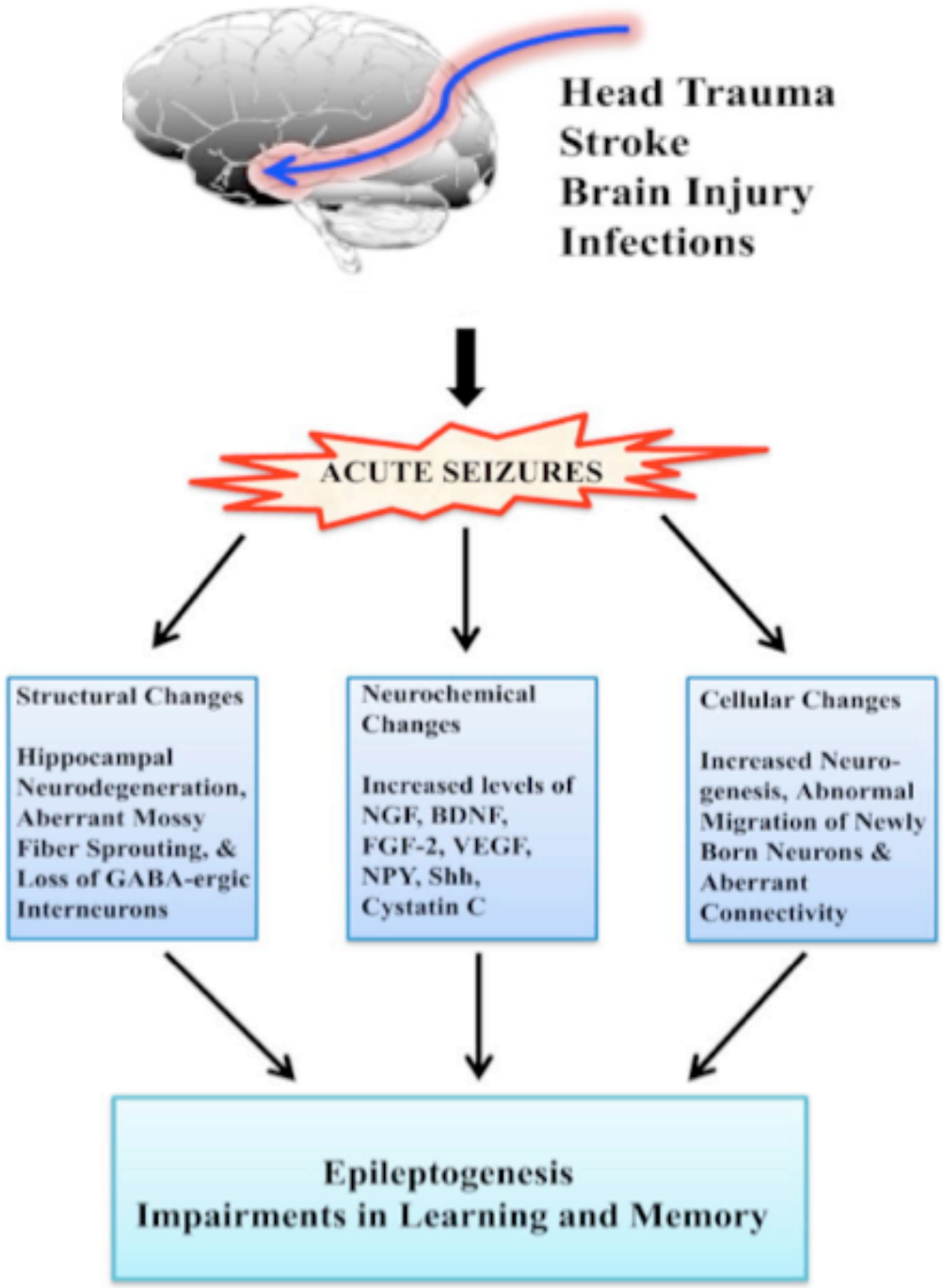

Figure 4: Changes following acute seizures. Changes include structural, neurochemical and cellular changes. These are primarily observed in the hippocampus (Taken from Kuruba et al., 2009).

iii) Brain ischaemia

Global and focal (stroke) ischaemia increase hippocampal neurogenesis. Following global ischaemia, there is an increase in the proliferation of neural progenitor cells, with almost all of the newly generated progenitors in the dentate gyrus adopting a neuronal phenotype (Liu et al., 1998, Kee et al., 2001). Neurons are able to extend

their dendrites to the molecular layer of the dentate gyrus, thereby establishing synapses with other neurons (Tanaka et al., 2004). There is also increased neurogenesis in the subgranular zone of the dentate gyrus following focal ischaemia (Jin et al., 2001). Again, cognitive impairments are associated with ischaemic insults (Hattori et al., 2000). Increasing hippocampal neurogenesis could potentially repair cognitive impairments and restore hippocampal neurogenesis. (Nunn and Hodges, 1994).

1.6: Using animal models to investigate human neurogenesis

Using rodent models to understand human neurogenesis has proven highly controversial. Does the magnitude of hippocampal neurogenesis in rodents reflect that in humans? Is this level of neurogenesis in the human brain at a level that has functional significance? Are the study tools used for rodents applicable for human studies?

Until recently, the seminal paper by Eriksson et al. (1998) was the only study to show adult neurogenesis within the human brain using the unambiguous cell proliferation marker BrdU. However, given the high risk of mutations associated with BrdU, this compound has since been banned and subsequent studies have not been able to utilize this key marker. As such, the quantification of neuronal generation and dynamics of hippocampal neurogenesis remained elusive. More recently, advances have been made to address these points. Knoth and colleagues (2010) used doublecortin (DCX), a marker of immature neurons in the rodent dentate gyrus, to determine its viability as an alternative marker to measure neurogenesis in humans. In agreement with studies in rodents, there was a decline in neurogenesis as demonstrated with the reduction in the number of DCX^+ cells with age. This 10-fold decrease from puberty to adulthood is comparable to rodent studies. Cell staining showed DCX^+ cells co-expressed maturation markers such as NeuN; providing strong evidence of cell differentiation and maturation. However the proportion of proliferating cells and mature cells was not quantified. More recently, Spalding et al. (2013) have provided compelling evidence to support the original findings of Eriksson and colleagues (Eriksson et al., 1998). Having previously used carbon dating to investigate neurogenesis in the SVZ (Bergmann et

al., 2012), they applied the same methodology to investigate adult human hippocampal neurogenesis and its dynamics. They quantified the total number of neurons added daily to the hippocampus (1400) and calculated this as a 1.75% turnover within the renewing fraction. The rate in adult humans was comparable to that observed in adult rodents. In further agreement with rodent studies, there is a decline in neurogenesis with age, however it is at a steadier rate than the dramatic decline observed between the young and adult stage in rodents (4 fold vs. 10 fold, respectively). These studies suggest a functional significance for neurogenesis in humans and, as with rodent studies, could potentially reveal the importance for new neurons in cognition. Therefore our study has the potential to be used for translational research of human neuroimmunomodulation.

1.5: Research aims and hypothesis

The immune system and central nervous system are intertwined, with the regulation of hippocampal neurogenesis focal to its relationship. Microglia and T lymphocytes are important components in the regulation of hippocampal neurogenesis with a potential role for neuropeptides in relaying signals from the stem cell niche to these cells. The exact mechanism by which these cell types can communicate remains largely undetermined. We have therefore sought to investigate the role of VIP as a mediator of neuroimmune interactions in the modulation of hippocampal neurogenesis. With the presence of VIP receptors on T lymphocytes and the correlation between T lymphocytes and neurogenesis, we postulate that VIP acts on T lymphocytes to regulate hippocampal neurogenesis via release of cytokines. Of note here is VIP's ability to cross the blood-brain barrier (Dogrukol-Ak et al., 2003). Furthermore, given the importance of microglia, we suggest a key role for these cells in this paradigm. Understanding and defining the factors and mechanisms regulating the stem cell niche is crucial to hippocampal neurogenesis. Restoring impaired neurogenesis can potentially restore cognitive impairments in patients of epilepsy and mood disorders. In addition, it opens the possibility to recapitulate the stem cell microenvironment in non-neurogenic areas to allow neurogenesis and repair damaged regions following brain insult. This area of regenerative medicine holds much promise.

Chapter 2

Methods

2. Methods

2.1: Generation of primary rat hippocampal neuronal cultures

Dentate granule cells are born during development and migrate from the dentate notch (adjacent to the SVZ) to the nascent dentate gyrus, laying down the foundation of the dentate granule cell layer (hilus, SGZ) (Nowakowski and Rakic, 1979, Altman and Bayer, 1990b). More than half of the granule cell layer, where hippocampal neurogenesis occurs, forms during the postnatal period (Namba et al., 2005, Namba et al., 2007). During the first week of postnatal development, there is a significantly large production of granule neurons (Altman and Bayer, 1990a). After a systematic process of organization, precursor cells are found within the SGZ where they divide at the region between the granule cell layer and the hilus. This process of granule cell production occurs from postnatal day 5-7 throughout adulthood (Li and Pleasure, 2007). Given that the dentate gyrus is established during the postnatal period, coupled with the fact that there is significantly less anoxia in the postnatal brain and therefore can withstand the process of cell culturing (Wheal, 1991), is the reason we elected to utilise postnatal rat hippocampal cultures to investigate our research questions. All animal work was performed in accordance to the United Kingdom Animal (Scientific Procedures) Act 1986. Every effort was made to minimise the number of animals used and their suffering. Primary rat hippocampal neuronal cultures were generated following a multi-step procedure of hippocampal dissection, cell release and dissociation and then cell plating.

2.1.1: Hippocampal dissection

For each experiment, 6-10 Sprague Dawley rats aged post-natal day 7-10 were sacrificed by atlanto-axial dislocation (Schedule I) followed by quick decapitation. The brains were removed and placed into a petri dish. The hippocampi were dissected under sterile conditions and placed into Gey's balanced salt solution (Sigma, U.K.) supplemented with 4.5mg/mL glucose **(Figure 5)**. The hippocampi were then transferred onto a sterile melinex strip on the stage of a MacIlwain tissue chopper. Transverse sections of 400μM thickness were cut and the chopped tissue was immediately transferred to a petri dish containing 4ml of Gey's solution.

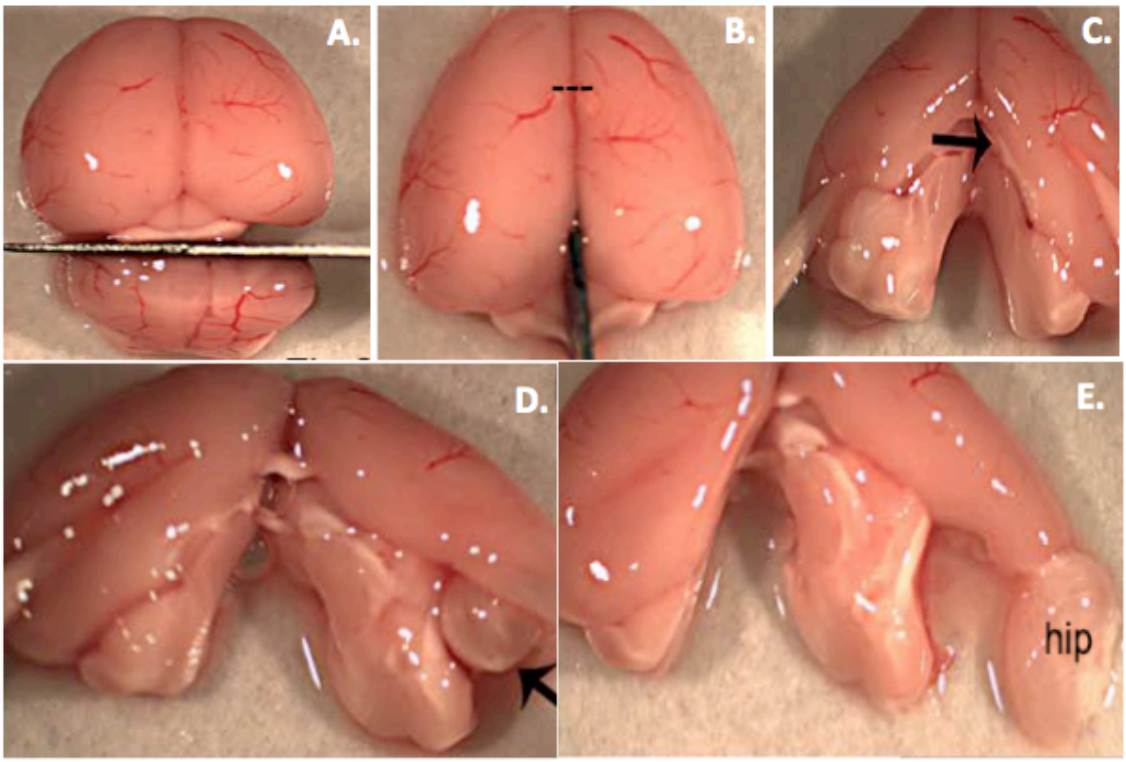

Figure 5: Dissection of hippocampus. The brain was removed from the skull and placed dorsal side up. **A.** The cerebellum was removed using a scalpel blade. **B.** A second cut was made sagittaly down the midline. **C.** The two halves of the brain were gently separated. **D & E** One side of the brain was held steady using a flat brush while the other brush was placed inside the hippocampal groove to roll out the hippocampus. These steps were repeated for the other half of the brain (images taken from Kalifa, 2008).

2.1.2: Cell release and dissociation

Gey's solution was aspirated and replaced with pre-warmed papain solution filter sterilized through a 0.2µM filter (0.22µM pore, Millipore) for 30 minutes at 37ºC to facilitate digestion of connective tissue. Papain (22.0 U/mg, Sigma) was prepared at a concentration of 2mg/mL in Neurobasal A (Invitrogen) supplemented with 2% B-27 (Invitrogen) and 0.5mM glutamine (Sigma). Papain solution was aspirated after 30 minutes and replaced with 4mL of NBA/B-27/glutamine and triturated to initiate cell release. The top two layers of cell suspension were transferred on top of an Optiprep gradient and a further 2mL were added to cell suspension, triturated and all 4mL were transferred on top of the gradient. This enabled partial purification of cells from debris by centrifugation for 15 minutes at room temperature at 1900 rpm. The two-step density Optiprep gradient was prepared by making two 2mL solutions of Optiprep (Axa-shields). The 10% solution was carefully placed on top of the 20% solution. Following centrifugation, the fraction containing cells was collected using a pipette and diluted in 2mL NBA/B-27/glutamine and centrifuged for 5 minutes at room temperature at 1100 rpm.

Supernatant was aspirated and cells were re-suspended in NBA/B-27/glutamine (1mL per animal used).

2.1.3: Cell plating

Live (Trypan blue excluding) cells were counted in a haemocytometer and cell suspension was then diluted in pre-warmed NBA/B-27/glutamine to yield 100, 000 cells/mL for plating. Cells were plated at 500µL per well at the above density directly onto poly-L-lysine pre-coated cover slips in 24 well plates. 250µL of 50µg/mL poly-L-lysine (Sigma) was applied for an hour, aspirated and washed with pre-warmed NBA/B-27/glutamine to remove excess poly-L-lysine. At 2 hours post-plating, medium was aspirated to remove any non-adherent cells and washed once with pre-warmed NBA/B-27/glutamine to remove residual debris. Medium was then replaced with fresh pre-warmed medium supplemented with antibiotic/antimycotic (Penicillin/Streptomycin and Fungizone). Conditions were added as per experimental requirements. Cultures were maintained at 5%CO_2/9% O2/37ºC incubator conditions. For cultures longer than 3 days, two thirds medium was replaced every 3 days.

2.2: Using a $CD4^+$ isolation kit to extract $CD4^+$ T lymphocytes from adult mice

The use of $CD4^+$ T lymphocyte cell cultures is an established study paradigm (Palmer et al., 1978; Rouabhia et al., 1992). To determine the effects of T lymphocytes supernatant on hippocampal cultures, we generated $CD4^+$ T lymphocytes cultures following a multi-step protocol using a specifically designed mouse $CD4^+$ isolation kit (Cedarlane Laboratories, Figure 2.2). According to the manufacturer, this isolation kit eliminates more than 95% of B cells and $CD8^+$ cells from lymphocyte preparations, which result in enriched mouse $CD4^+$ T cells in column eluent (Cedarlane Laboratories). However, using immunohistochemical analysis we have found our cultures have a purity of approximately 70% *(Chapter 3)*. The cultures were generated in standard culture medium (NBA/B27/Glutamine) which we have previously tested in the lab as a viable alternative to standard serum based RPMI media (see Appendix I). This ensures hippocampal cultures are not exposed to mitogens from the RPMI media which trigger neuronal differentiation. T lymphocytes cultures were generated for 24 hours and then the supernatant was

collected and stored at -20ºC until required for treatment on hippocampal cultures.

2.2.1: Spleen extraction and erythrocyte lysis

All animal work was performed in accordance to the United Kingdom Animal (Scientific Procedures) Act 1986. Every effort was made to minimise the number of animals used and their suffering. For each experiment, 4 eight week old C57/BL6 mice were sacrificed by atlanto-axial dislocation followed by quick decapitation (Schedule I). The spleens were extracted under sterile conditions and placed in phosphate buffered saline (PBS). Each spleen was placed in a 100µM cell strainer (BD Biosciences, USA) with 1ml of fresh PBS and minced using the end of a 10mL syringe plunger. The sieved mixture was triturated and put in a 15mL falcon tube and diluted in 10mL of PBS. The cell solution was centrifuged for 6 minutes at room temperature at 1300 rpm. Supernatant was discarded and the erythrocytes were lysed by trituration in 5ml of 5x lysis buffer (Cedarlane). The solution was centrifuged for 6 minutes at room temperature at 1300rpm.

2.2.2: Column activation

One column was used per 2 spleens. The cap and cotton wool were removed and the bottom of the column was snapped off to attach a stopcock. The column was washed with 10mL PBS and immediately followed by the addition of the total volume of the reconstituted column reagent (Cedarlane). This was allowed to run through the column bed and then the stopcock was immediately closed. The column reagent was left at room temperature for a minimum of 30 minutes.

2.2.3: Addition of antibodies

Supernatant was removed from the centrifuged splenocytes and re-suspended in 1mL PBS. Two sets of centrifuged splenocyte solutions were combined and the total volume of cell reagent (Cedarlane, Canada) was added to the solution. The solution was vortexed and cell suspension was adjusted to 7mL with PBS and incubated at 4ºC for 30 minutes. The solution was then further diluted in PBS to give a total volume of 10mL and centrifuged for 6 minutes at room temperature at 1300 rpm.

2.2.4: Cell sample loading and elution

The column was washed with 10mL PBS and immediately followed by the addition of splenocytes which were collected in a sterile petri dish and then transferred to a 15mL falcon tube. Cells were centrifuged for 6 minutes at room temperature at 1300rpm. Supernatant was discarded and the cell pellet was re-suspended in 1mL pre-warmed NBA/B-27/glutamine supplemented with 1% antibiotic/antimycotic. Viable cells were determined as per section 2.1.3 to yield 1, 000, 000 cells/mL. Cells were plated at 500µL per well in a 24 well plate pre-coated with poly-L-lysine. Conditions were added as per experimental requirements. 1µg/mL of anti-CD3 was used for activation of T lymphocytes. Cultures were maintained for 24 hours at 5% CO_2/9% O_2/37ºC incubator conditions, after which supernatant was collected in falcon tubes and kept at -20ºC until required.

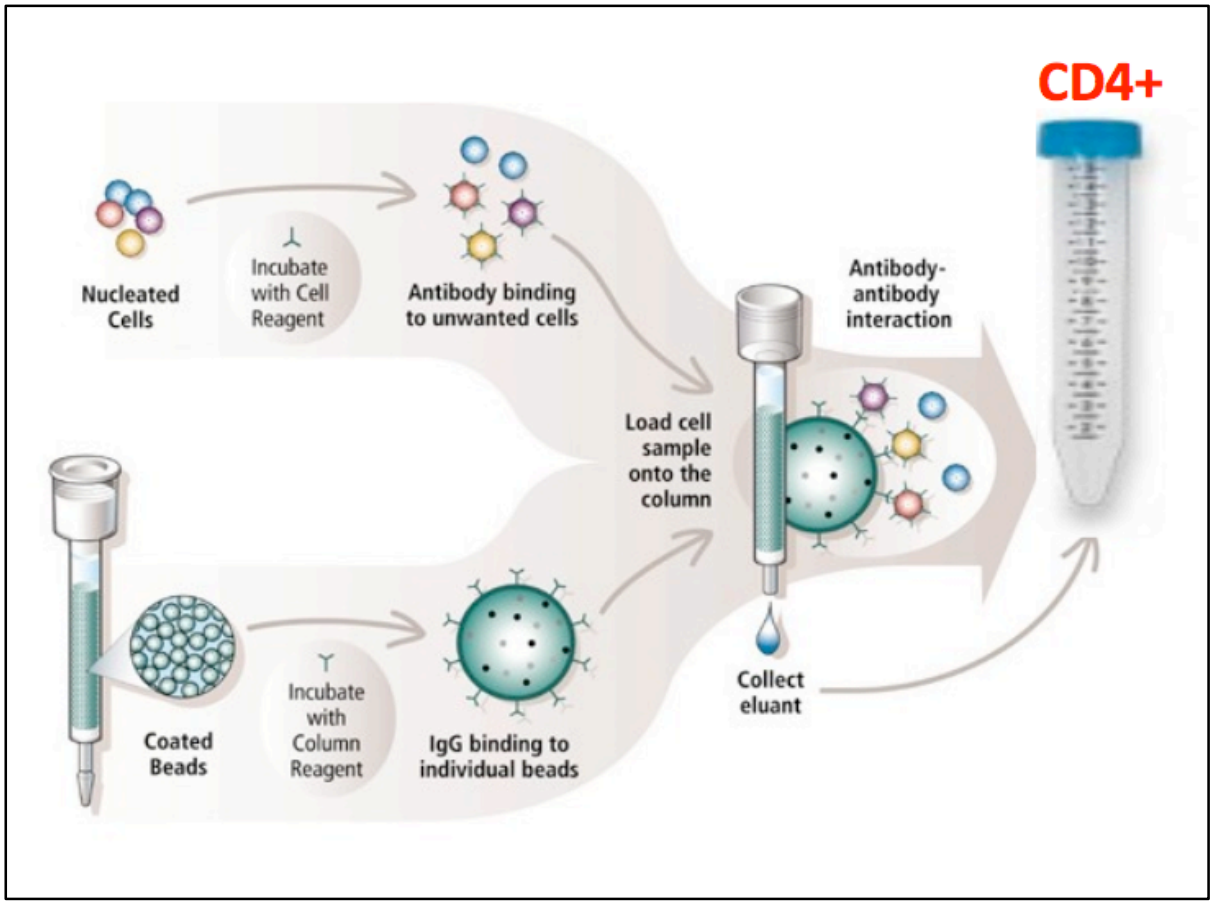

Figure 6: CD4⁺ isolation kit. Schematic taken from Cedarlane Laboratories manual.

2.3: Generating pure CD4⁺ T lymphocytes cultures by flow cytometry

Flow cytometry is an established technique that allows cell populations to be sorted into distinct groups using specific markers to identify them (Ibrahim et al. 2007).

Cells in a stream of fluid are passed through the flow cytometer in single file and lasers are fired on to them. Light signals emitted from cells are collected and correlated to specific parameters defined by the user including protein expression, gene expression and cell morphology. Depending on the specifications outlined, individual cells can be diverted from the fluid stream to be collected as a viable specific population with a purity approaching 100%. To generate a pure $CD4^+$ T lymphocytes culture independent to the $CD4^+$ isolation kit, flow cytometry was applied. Three spleens from adult C57/BL6 mice were used per experiment to generate a pure $CD4^+$ T lymphocytes population, a splenocytes population without $CD4^+$ T lymphocytes and a population containing all splenocytes.

2.3.1: Preparation of single cell suspensions from tissues

Spleen tissue was homogenised in a multiwell plate using the back of a 10mL syringe plunger and forced through a 70μM cell strainer (BD Biosciences). Homogenised tissue was resuspended in 1mL standard culture medium and centrifuged at 1300 rpm for 5 minutes at room temperature. Spleen cell pellets were subjected to lysis of red blood cells by re-suspending in 5mL of RBC lysis buffer (BioLegend) for 90 seconds at room temperature. Cells were then washed in standard pre-warmed culture medium and transferred to a 15mL falcon tube via a 70μM cell strainer. Cells were plated out into a 96 well round bottom plate for antibody staining.

2.3.2: Antibodies and cell staining

96 well plates were centrifuged at 1500 rpm for 3 minutes at room temperature and washed twice with PBS. Anti-mouse antibodies for flow cytometric analysis are described in Table 1. The correct dilutions of the antibodies to give efficient staining were established by titration of the antibodies by various members of a lab group well versed with flow cytometry. A fixable dead cell staining kit (LIVE/DEAD Aqua, Invitrogen) was used prior to antibody staining to eliminate dead cells from flow cytometric analysis. The kit is based on a reaction between a fluorescent reactive dye with cellular amines. Intense fluorescent staining occurs when the reactive dye enters compromised membranes of dead cells and reacts with free amines inside the cell and also on its surface. Live cells only allow the dye to react with amines on

the cell surface and therefore they produce a relatively dull fluorescence stain. Therefore 3µl of diluted (1:10 in PBS) LIVE/DEAD aqua was added directly to cell pellet and left at room temperature for 15 minutes in the dark. Cells were washed twice with FACS buffer.

Fc receptors are glycoproteins found on blood cells (B cells, tissue macrophages) that have high affinity for Fc regions of monomeric IgG and therefore can cause non-specific binding and high background staining. To minimise this, Fc receptors were blocked for 10 minutes at 4°C in the dark using anti-CD16/32 antibodies (eBiosciences) diluted to 5µg/mL. For staining of surface markers, 25µL of diluted (in FACS buffer) antibody (CD3, CD4; *Table 1*) were added to the cells and incubated for 10 minutes at 4°C in the dark. To remove unbound antibodies, cells were washed twice in FACS buffer. Cells were re-suspended in 200µL FACS buffer and transferred to FACS tubes for flow cytometric analysis.

2.3.3: Flow cytometry analysis and gating strategy

For flow cytometric analysis, samples were acquired using a FACS Aria III cell sorter (BD Biosciences) and were analysed using BD FACSDiva 7.0 software (BD Biosciences). For analysis of each sample the same gating strategy was adopted **(Figures 7-9)**. Firstly, the lymphocyte population was gated based on typical lymphocyte forward scatter and side scatter patterns. Then dead cells were gated out to avoid non-specific antibody binding using live/dead aqua. Cells with compromised membranes stain readily with live/dead aqua and have higher fluorescence intensity compared to cells with intact membranes. The $CD4^+$ and $CD3^+$ T cell populations were gated from the live lymphocyte population based on fluorescent intensity levels from CD4 and CD3 specific antibody staining. Relative proportions of $CD4^+$ cells were determined as 1:4 with respect to total population.

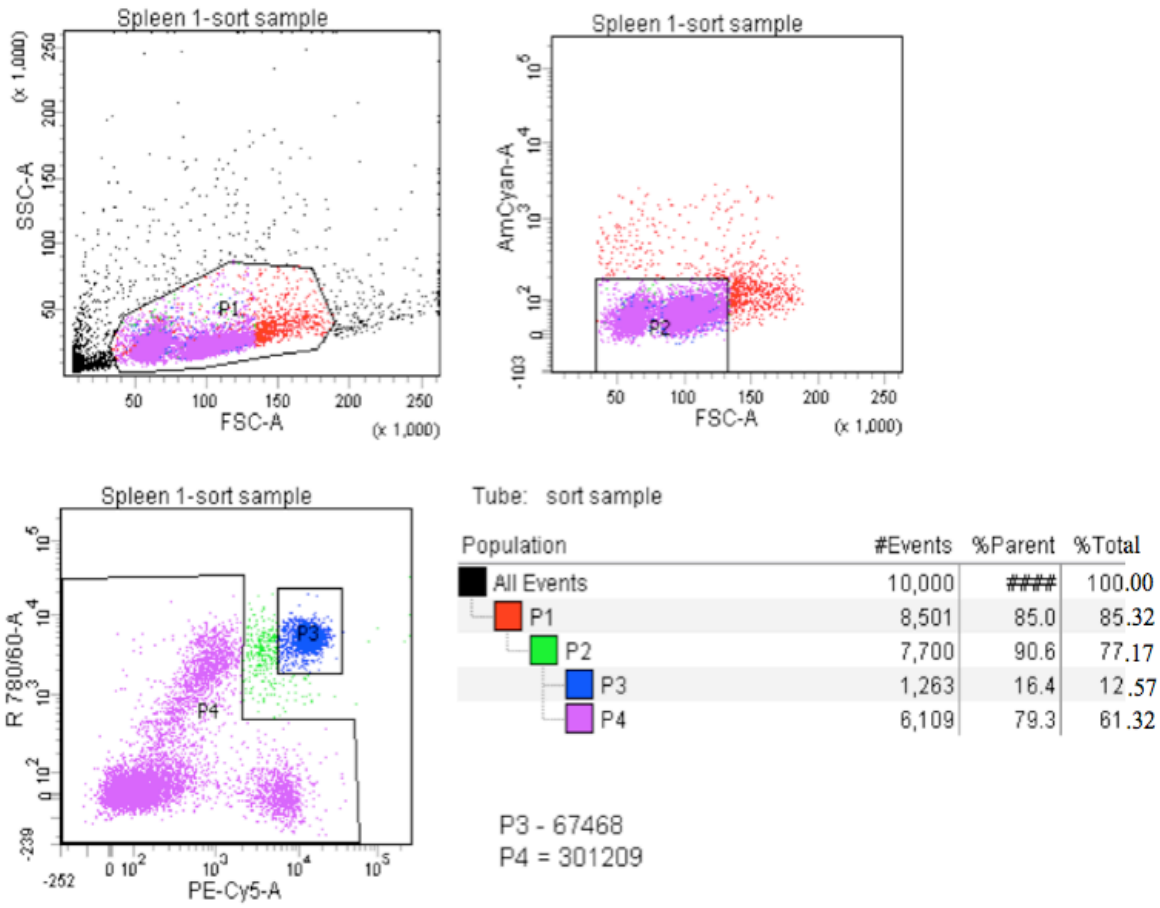

Figure 7: Spleen sort 1. Samples were acquired using a FACS Aria III cell sorter and were analysed using BD FACSDiva 7.0 software. For analysis of each sample the same gating strategy was adopted. Firstly, the lymphocyte population was gated based on typical lymphocyte forward scatter (FSC-A) and side scatter (SSC-A) patterns. Dead cells were gated out to avoid non-specific antibody binding using live/dead aqua. The $CD4^+$ and $CD3^+$ T cell populations were gated from the live lymphocyte population based on fluorescent intensity levels from CD4 and CD3 specific antibody staining. P1 = all cells, P2 = live cells P3 = $CD3^+CD4^+$, P4 = $CD3^-CD4^-$, $CD3^+CD4^-$, $CD3^-CD4^+$

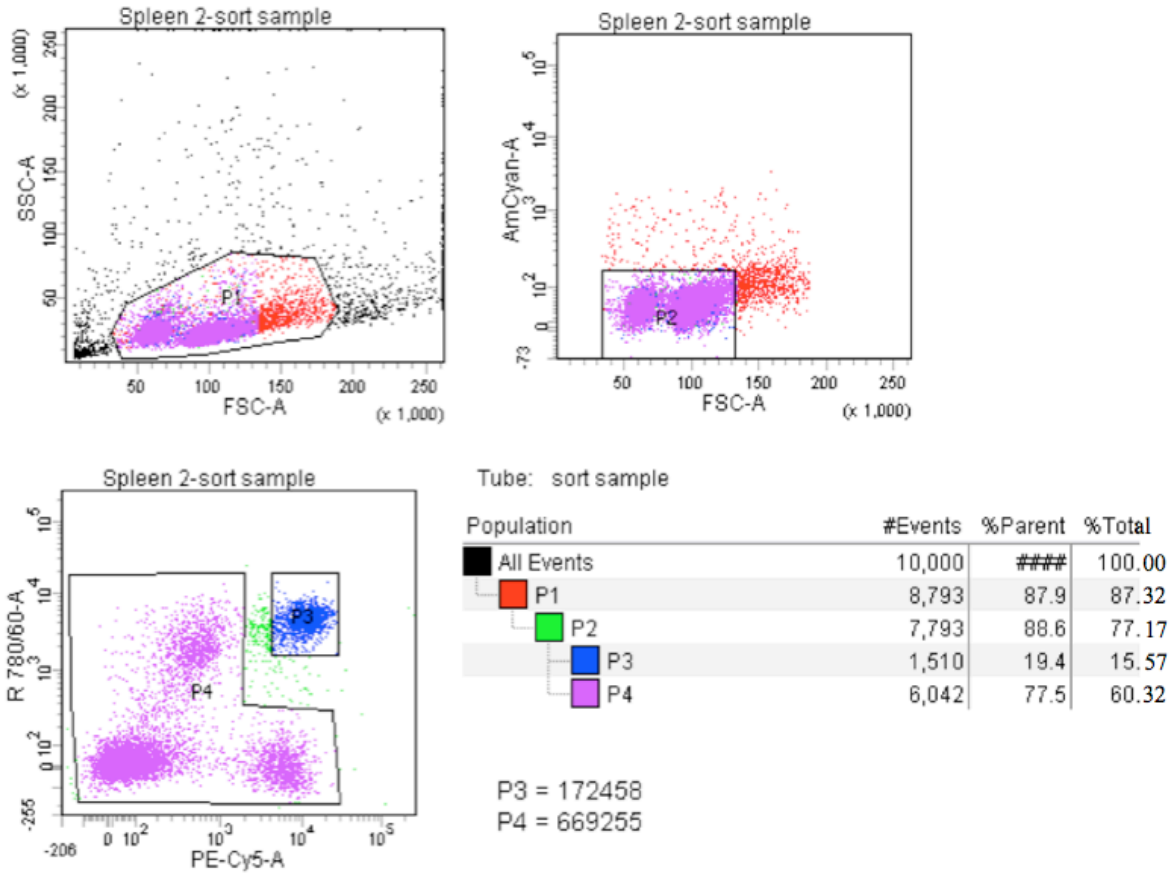

Figure 8: Spleen sort 2. Samples were acquired using a FACS Aria III cell sorter and were analysed using BD FACSDiva 7.0 software. For analysis of each sample the same gating strategy was adopted. Firstly, the lymphocyte population was gated based on typical lymphocyte forward scatter (FSC-A) and side scatter (SSC-A) patterns. Dead cells were gated out to avoid non-specific antibody binding using live/dead aqua. The $CD4^+$ and $CD3^+$ T cell populations were gated from the live lymphocyte population based on fluorescent intensity levels from CD4 and CD3 specific antibody staining. P1 = all cells, P2 = live cells P3 = $CD3^+CD4^+$, P4 = $CD3^-CD4^-$, $CD3^+CD4^-$, $CD3^-CD4^+$

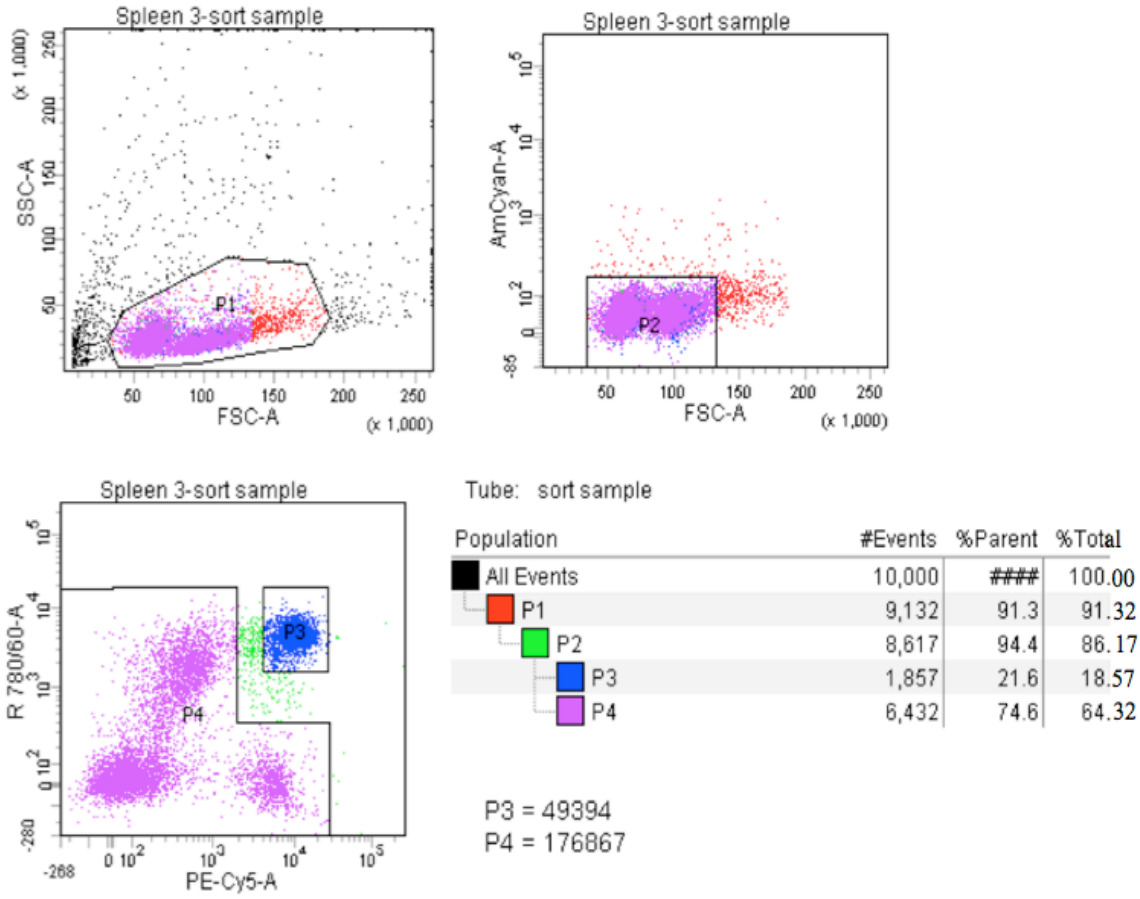

Figure 9: Spleen sort 3. Samples were acquired using a FACS Aria III cell sorter and were analysed using BD FACSDiva 7.0 software. For analysis of each sample the same gating strategy was adopted. Firstly, the lymphocyte population was gated based on typical lymphocyte forward scatter (FSC-A) and side scatter (SSC-A) patterns. Dead cells were gated out to avoid non-specific antibody binding using live/dead aqua. The $CD4^+$ and $CD3^+$ T cell populations were gated from the live lymphocyte population based on fluorescent intensity levels from CD4 and CD3 specific antibody staining. P1 = all cells, P2 = live cells P3 = $CD3^+CD4^+$, P4 = $CD3^-CD4^-$, $CD3^+CD4^-$, $CD3^-CD4^+$

2.3.4: Sample collection and cultures

Cells were collected in two tubes, one with $CD4^+$ T lymphocytes and the other with all cell populations. Another sample was comprised of all cell types based on a 1:4 ratio of $CD4^+$ T lymphocytes to all other cell types as calculated from BD FACSDiva software analysis. Cells were treated with experimental conditions and maintained for 24 hours at 5%CO_2/9%O_2/37ºC incubator conditions. Supernatant was collected in falcon tubes and kept at -20ºC until required.

2.4: Studying cell proliferation

2.4.1: Using BrdU incorporation to study cell proliferation

Using 5-bromo-2-deoxyuridine (BrdU) to study cell proliferation is an established method (Miller & Nowakowski, 1988; van Praag et al., 1999). This thymidine analogue is incorporated into cells during the S-phase of the cell cycle and therefore used to specifically label dividing cells (Taupin, 2007). The cell cycle of neural progenitor cells is 12-14 hours and the S-phase equates to one third or half of this period (Nowakowski & Hayes, 2000). Hippocampal cultures were generated as detailed in section 2.1 for 3DIV under standard control conditions. Culture medium was removed from cultures and replaced with experimental conditions and a final concentration of 20μM BrdU for the terminal 6 hours before fixation. Cells were fixed in 4% paraformaldehyde (PFA) for 30 minutes at 4ºC. Experimental conditions were added at the same time as BrdU to study proliferative effects of the factors being investigated in one cell cycle; the aim was to exclude trophic effects and greatly reduce the risk of secondary mediators from having an effect. After fixation, cells were washed twice with PBS and processed for expression of BrdU and counterstained with the nuclear cell marker 4'6-diamidino-2-phenylindole (DAPI) as detailed below in section 2.8. The total number of DAPI positive and BrdU positive cells were counted to determine the mitotic index, which is calculated as the total number of BrdU positive cells over the total number of $DAPI^+$ cells. This is indicative of the total number of cells transitioning from the S phase to the G2 phase of the cell cycle **(Figure 10)**.

2.4.2: Determining the labelling index and growth fraction

Using Ki-67 to study cell kinetics is an established method (Kee et al., 2002, Mandyam et al., 2007). Ki-67 is an endogenous proliferative marker expressed by cells during the active phases of the cell cycle (G1, G2, M phase) and used to determine the labelling index or growth fraction. The labelling index is calculated as the number of Ki-67 expressing cells incorporating BrdU over the total number of Ki-67 positive cells. The growth fraction is calculated as the number of cycling precursors (Ki-67 positive cells) over the total number of DAPI positive cells. This allows us to determine whether proliferative effects are due to speeding of the cell cycle (labelling index) or recruitment of quiescent cells (growth fraction). Primary

rat hippocampal cultures were generated under standard control conditions for 3DIV as detailed in section 2.1. At 3DIV, culture medium was removed from cultures and replaced with experimental conditions and a final concentration of 20μM BrdU for the terminal 6 hours before fixation in 4% PFA. After fixation, cells were washed with PBS and stained for BrdU incorporation and Ki-67 expression as detailed in section 2.8.

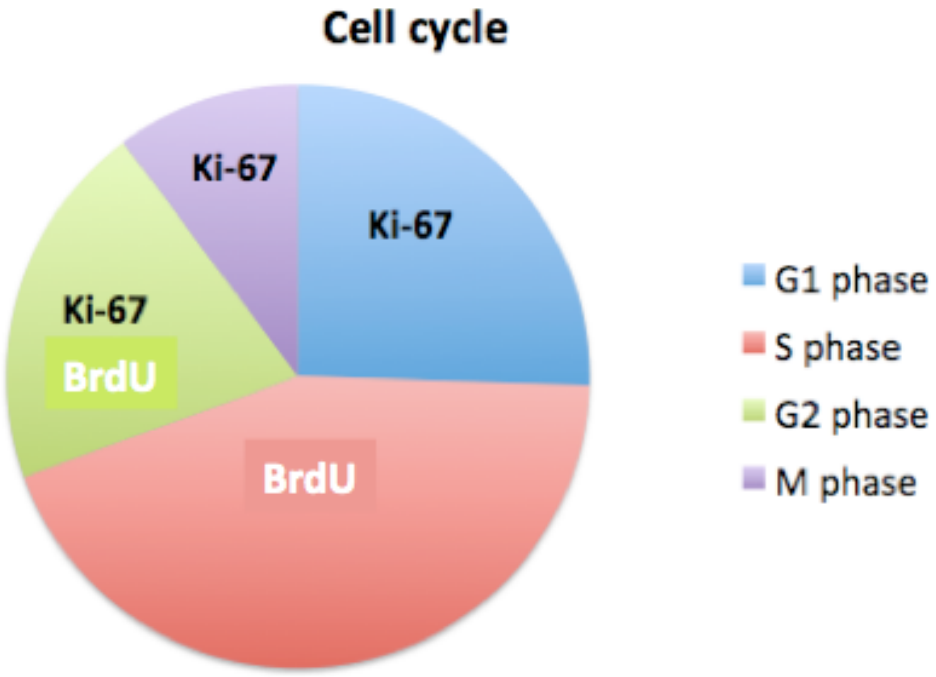

Figure 10: Expression of proliferative markers during the cell cycle. BrdU is expressed by cells transitioning from the S (synthesis) to G2 (growth) phase. Ki-67 is expressed during the G2, G1 and M (mitosis) phase. There is overlap in the G2 phase.

2.5: Pharmacological manipulation to investigate mediation of proliferative effects

2.5.1: Examining VPAC1 mediating proliferation

Investigating expression of VIP receptors in T lymphocyte cultures in the lab has shown VPAC1 and PAC1 mRNA expression before and after CD3 activation; VPAC2 is not expressed (see Appendix II). A VPAC1 receptor agonist [Lys15, Arg16, Leu27]-VIP (1-7) - GRF (8-27) (Phoenix Pharmaceuticals, Inc.) and a VPAC1 receptor antagonist [Ac-His1, D-Phe2, Lys15, Arg16, Leu27]-VIP (1-7)-GRF (8-27) (Phoenix Pharmaceuticals, INC.) were used to investigate VIP receptor mediation of T

lymphocytes. Primary rat hippocampal cultures were generated as detailed in *section 2.2* under standard control conditions for 3DIV. Culture medium was removed from cultures and experimental conditions and a final concentration of 20μM BrdU were added for the terminal 6 hours before fixation in 4% PFA. Experimental conditions for T lymphocytes supernatant were added when T lymphocytes were plated as detailed in *section 2.2.* To investigate VPAC1 mediation using the VPAC1 antagonist, 1μM VPAC1 antagonist and 1μM VPAC1 antagonist with 30nM VIP was added to T lymphocytes. Similarly for VPAC1 mediation using a VPAC1 agonist, 1μM VPAC1 agonist was added to T lymphocytes. Therefore, experimental conditions for investigating the effect of VPAC1 antagonist on hippocampal cultures were standard control conditions, 5% supernatant, 30nM VIP added directly to hippocampal cultures, 5% supernatant pre-treated with VIP, 1μM VPAC1 antagonist added directly to hippocampal cultures, 5% supernatant pre-treated with 1μM VPAC1 antagonist and 5% supernatant pre-treated with VPAC1 antagonist and 30nM VIP. Similarly for investigating the effect of VPAC1 agonist on hippocampal cultures, experimental conditions were standard control conditions, 5% supernatant, 30nM VIP added directly to hippocampal cultures, 5% supernatant pre-treated with VIP, 1μM VPAC1 agonist added directly to cultures and 5% supernatant pre-treated with 1μM VPAC1 agonist. After fixation in 4% PFA, cells were immunostained as described below in *section 2.8.*

2.5.2: Examining IL-4 mediation of T lymphocytes supernatant

Candidate cytokines have been investigated in T lymphocytes cultures following activation and under treatment with VIP (see Appendix II). Given the role of IL-4 in T lymphocyte mediated effects and its importance as a Th2 effector cytokine, IL-4 mRNA expression has been investigated as detailed in section 2.9. To further investigate the role of IL-4 in mediating T lymphocytes effect on hippocampal cells, IL-4 antagonists were used. To investigate the role of mouse IL-4 (released by T cells), a mouse-specific anti-IL-4 antibody was used. Similarly, in a separate set of experiments, the role of rat IL-4 (released by resident microglia and other cells) was investigated using a rat-specific anti-IL-4 antibody. Primary rat hippocampal cultures were generated under standard control conditions for 3DIV as detailed in *section 2.1*. At 3DIV, culture medium was replaced with experimental conditions, a

final concentration of 20μM BrdU and 10μg/mL mouse or rat anti-IL-4 antibody (Huang et al., 2007; Sigma) for the terminal 6 hours before fixation in 4% PFA. Experimental conditions were standard control conditions, 5% supernatant, 30nM VIP added directly to hippocampal cultures, 5% supernatant pre-treated with VIP, standard control conditions with 10μg/mL anti-IL-4, 5% supernatant with 10μg/mL anti-IL-4, 30nM VIP added directly to hippocampal cultures with 10μg/mL anti-IL-4 and 5% supernatant pre-treated with VIP with 10μg/mL anti-IL-4. Cells were then immunostained as described in *section 2.8.*

2.6: Investigating cell death in cultures

Using the highly polar cell death marker propidium iodide (PI, Invitrogen) to quantify cell death is an established method (Brana et al, 2002, Eguchi et al., 1997). Used in conjunction with the nuclear cell marker DAPI (Sigma), cell death was quantified in cultures using a protocol previously established and validated in the lab. PI is a fluorescent dye that enters dead or dying cells with leaky membranes and binds to the nucleic acid of the cytoplasm and nucleus, where it fluoresces (Lecoeur, 2002). DAPI is a non-polar dye that binds to double-stranded DNA of all (live and dead) cells and therefore gives total cell numbers. Rat hippocampal cultures were grown under experimental conditions for 5DIV. At 5DIV, culture medium was replaced with fresh pre-warmed culture medium containing PI (5μg/ml) and DAPI (20μg/ml) for 40 minutes at 37ºC. The medium was removed and replaced with fresh NBA/B-27/glutamine and imaged live for quantification of cell death. Cell death was determined as the total number of PI^+ cells over the total number of $DAPI^+$ cells.

2.7: Investigating the role of microglia in cultures

To investigate the role of microglia, two approaches were utilised. One involved depletion of microglia and the other involved studying pure microglial cultures. Both these techniques have been previously verified and validated in our lab.

2.7.1: Depletion of microglia from hippocampal cultures

Microglia represent approximately 15% of the total cell population in the brain and are present in high densities in the hippocampus (Lawson et al., 1990). To deplete

microglial cells from hippocampal cultures, rat-Mac-1-SAP (Advanced Targetting Systems) was used. The Mac-1-SAP antibody specifically binds to CD11b receptors on microglia; the antibody is conjugated to the ribosome-inactivating protein saporin. Once the antibody binds to microglia, saporin is internalized and breaks away from the antibody, inactivating the ribosome. This in turn leads to protein inhibition and ultimately kills microglia. Primary rat hippocampal cultures were generated as detailed in *section 2.1* and grown under standard control conditions for 2DIV. At 2DIV, culture medium was removed and 100µg/mL Mac-1-SAP (in pre-warmed standard culture medium) was added to cultures for 24 hours. For control conditions, cultures were replaced with fresh culture medium. After 24 hours, medium was removed from both Mac-1-SAP containing cultures and control cultures and washed with fresh pre-warmed culture medium before treatment with experimental conditions and 20µM BrdU. These were added for the terminal 6 hours before fixation in 4% PFA. Cells were then immunostained as detailed in *section 2.8.*

2.7.2: Generation of pure microglia cultures

Pure microglial cultures (>95%) were generated from rat hippocampal tissue. This protocol was adapted in our lab by Dr Robert Nunan from the original protocol for microglial isolation by Guilian and Baker (2006). Primary rat hippocampal cultures were generated as detailed in section 2.1. Cells were plated 1mL/well in poly-L-lysine pre-coated 6 well plates at a density of 500, 000 cells/mL. Cultures were maintained for 7DIV without medium change in standard culture medium (NBA/B-27/glutamine/antibiotic) supplemented with 10% fetal bovine serum (FBS). At 7DIV, cells were placed on a plate shaker for 10 minutes at 1200 rpm at 37ºC. This is a modification to the method previously described by Guilian and Baker; their methods were either a shake at 37ºC for 15 hours at 180 rpm or alternatively a "cold shake" for 30 minutes at 4ºC. The modified method has the distinct advantage of being less time consuming whilst generating high purity cultures. Furthermore, these microglia are isolated from the hippocampus, which has only been described by a few groups (Ren et al., 1999; Frank et al., 2006; de Haas et al., 2007; Choi et al., 2008). Following "shaking", plates were subjected to several hard taps and swirling to dislodge weakly attached cells (microglia) into the medium. Cell suspensions

from several wells were pooled together in a 15mL falcon tube. Viable cells were counted in a haemocytometer using trypan blue. Cells were plated 1mL/well in uncoated 6 well plates at a density of 100, 000 cells/mL. After 1 hour, cultures were washed with fresh pre-warmed culture medium to remove FBS and weakly attached cells. Cells were then treated with experimental conditions for specific time frames as detailed in Chapter 5.

2.8: Immunohistochemistry

Following fixation in 4% PFA for 30 minutes at 4ºC, cells were washed three times with PBS to completely remove it.

2.8.1: BrdU detection

To detect BrdU, cells were incubated in 250µL/well 2M hydrochloric acid (HCl;, Fisher Scientific) for 30mins in a 37ºC water bath. This unfolds double stranded DNA and allows antibodies to attach to the BrdU. Cells were washed three times with PBS to remove residual HCl. Primary antibodies were then added.

2.8.2: Addition of primary antibodies

Non-specific binding sites were blocked with 250µL/well of 5% donkey blocking serum (DBS, Sigma) in 0.1% Triton-X (Sigma) in PBS (PBS-T) for 30 minutes at room temperature. Blocking solution was replaced with 250µL/well primary antibodies diluted in blocking solution overnight at 4ºC (see Table 1 for antibodies and dilutions)

2.8.3: Addition of secondary antibodies

Cells were washed three times with PBS and incubated with 250µL/well secondary antibodies (see *Table 1* for antibodies and dilutions) diluted in 0.1% PBS-T for 2 hours at room temperature in the dark. Cells were washed three times with PBS and then counterstained with 250µL/well of 5µg/mL DAPI diluted in ddH_2O for 6 minutes at room temperature in the dark. Cells were then washed three times with PBS to remove residual DAPI. For each experiment, negative controls (absence of primary antibodies) were used to exclude non-specific secondary antibody binding. Cover slips were then mounted on slides and sealed with clear nail varnish and

stored at 4ºC until imaged. A mounting solution comprising 50% glycerol and 50% PBS was used.

Table 1: List of antibodies and dilutions

Antibody	Manufacturer	Dilution	Function
Rat anti-BrdU	AbD serotec	1:200	Binds to BrdU incorporated into single stranded DNA. Used to measure cell proliferation.
mouse anti-rat nestin	BD Biosciences	1:200	Nestin is an intermediate filament expressed by dividing neuroepithelial stem cells and transient radial glial cells in the developing rat CNS.
rabbit anti-TuJ1	Cambridge Biosciences	1:500	Class III β-tubulin is expressed by neurons in the CNS and PNS. It is used as a neural stem cell marker
rabbit anti-Prox1	Abcam	1:500	Prox1 is a protein-coding gene expressed during embryonic development and adult neurogenesis. It is used as a dentate specific granule cell marker.
Ki-67	DAKO	1:500	Ki-67 antigen is a larger nuclear protein expressed during the active phases of the cell cycle. It is used to determine the growth fraction and labelling index.
CD4 APC-efluor 780	eBiosciences	1:100	CD4 is a cell surface receptor expressed by a subpopulation of mature T lymphocytes.
CD3 PeCy5	BD Pharmingen	1:50	CD3ε is a chain of the CD3/TCR complex found on all mature T lymphocytes.
donkey anti-mouse Alexa Fluor 555	Invitrogen	1:1000	Alexa Fluor 555 is labeled with a bright, photostable, orange-fluorescent. It is used to detect mouse primary antibodies.
donkey anti-rat Alexa Fluor 488	Invitrogen	1:1000	Alexa Fluor 488 is labeled with a bright, photostable, green-fluorescent dye. It is used to detect rat primary antibodies.
donkey anti-rabbit Alexa Fluor 555	Invitrogen	1:1000	Alexa Fluor 555 is labeled with a bright, photostable, orange-fluorescent. It is used to detect rabbit primary antibodies.
donkey anti-rabbit Alexa Fluor 488	Invitrogen	1:1000	Alexa Fluor 488 is labeled with a bright, photostable, green-fluorescent dye. It is used to detect rabbit primary antibodies.
anti-CD4	Sigma	1:500	CD4 is a cell surface glycoprotein expressed by a subset of mature T lymphocytes

2.9: Real-time PCR analysis

To investigate mRNA expression, cDNA was generated from samples. At the specified time points, cells were collected in 1mL TRIzol (Invitrogen) to isolate high quality RNA, DNA and proteins from cells (Chomczynski, 1993). RNA was isolated and converted to cDNA following a multistep protocol. cDNA samples were used for quantitative PCR analysis.

2.9.1: Phase separation and RNA isolation

After homogenizing the sample in 1mL TRIzol, 200µL of chloroform was added and the tube was vigorously shaken by hand for 15 seconds. After incubating for 2-3 minutes at room temperature, each sample was centrifuged at 12000 rpm for 15 minutes at 4ºC. The sample separated into three layers, with RNA almost exclusively present in the upper aqueous phase. The aqueous phase was removed and transferred into a fresh tube. 500µL of 100% isopropanol was added to the aqueous phase and incubated at room temperature for 10 minutes. Samples were then centrifuged at 12000 rpm for 10 minutes at 4ºC. Supernatant was removed and the pellet was washed with 1mL of 75% ethanol. The samples were vortexed and then centrifuged at 75000 rpm for 5 minutes at 4ºC. Supernatant was removed and the RNA pellet was left to air dry for 10 minutes. 30µL of RNAse free water was added to each sample and incubated on a heat block set at 55ºC for 10 minutes.

2.9.2: DNAse treatment

DNAse treatment removes genomic DNA contamination. The protocol was followed according to the manufacturer's instructions (PrimerDesign Ltd). 3µL of 10x Precision DNAse reaction buffer and 1µL of Precision DNAse enzyme was added to each sample. Samples were incubated for 10 minutes at 30ºC (DNAse treatment) and then for 5 minutes at 55ºC (DNase inactivation).

2.9.3: Reverse transcription

After quantifying the amount of RNA per sample (ng/µL) using a NanoDrop ND-1000 UV-Vis Spectrophotometer (as detailed below in section 2.9.4 for cDNA quantification), RNA was transcribed into cDNA using a reverse transcription kit (PrimerDesign Ltd). For each RNA sample, 1µg of RNA template was added with 1µL RT primer and RNAse/DNAse-free water to make a final volume of 10µL in a 200µL thin-walled PCR tube. Each sample was placed in a heat block set to 65ºC for 5 minutes and then immediately cooled in an ice water bath. After this annealing step, 10µL of the mix was added to each sample on ice to extend RNA templates into complementary DNA strands (cDNA). Samples were then placed on a heat block for 20 minutes at 55ºC. The reaction was heat inactivated by incubation at 75ºC for 15 minutes.

Table 2: Components of PCR reaction tube

Components of PCR reaction tube	Volume per sample
2X Precision MasterMix	10µL
Reconstituted primer	1µL
RNAse/DNAse free water	4µL
cDNA template (25ng/µL)	5µL
TOTAL VOLUME	**20µL**

2.9.4: Determining cDNA concentration and purity

All cDNA samples, concentration and purity were determined using a NanoDrop ND-1000 UV-Vis Spectrophotometer. Distilled water was used as a buffer to blank the cycle. 1.5µL of cDNA sample was loaded and measured in ng/µL. Standard 260nm:280nm spectrophotometric analysis was used to determine the purity of cDNA by calculating the A260/A280 ration. A ratio greater than 1.50 is indicative of good quality cDNA.

2.9.5: Quantitative real-time PCR

Quantitative real-time PCR was conducted on single-stranded cDNA using a one-step PCR kit designed by PrimerDesign Ltd, Southampton. A rat-specific or mouse-specific real-time PCR assay with SYBR green was used depending on the species sample. PCR reactions were performed in a real-time thermocycler (Rotar-Gene 6000, Corbett Robotics Ltd) according to the manufacturer's instructions for 50 cycles. All primers were designed by PrimerDesign Ltd (see Table 3) and provided in a lyophilised form to be reconstituted in 600µL RNAse free water.

PCR reaction tubes comprise of the reconstituted primer, Primer Design 2X Precision MasterMix with SYBRgreen and RNAse/DNAse free water. 2ng/µL of cDNA was added to the mix to be reverse transcribed. The volumes are detailed in Table 2. PrimerDesign 2X MasterMix comprises of 2X reaction buffer, 0.025 U/µL Taq polymerase, 5mM MgCl2 and dNTP mix (200µM of each dNTP). The PCR reaction amplification conditions were programmed according to the manufacturer's instructions as detailed in Table 4.

Table 3: Primers and their sequences

Primer	Sequence	Position	Tm	Product length
Chi3l3	CCTGGGTCTCGTGGAAGC (forward) GCAGTGAGAAGCAGCCTTG (reverse)	424 545	57.1 56.9	122
Nos2	CACCACCCTCCTTGTTCAAC (forward) CAATCCACAACTCGCTCCAA (reverse)	2431 2562	56.7 56.5	132
IL-10	CTGGACAACATACTGCTGACA (forward) GGCATCACTTCTACCAGGTAAA (reverse)	182 288	56.2 56.3	107
TNF	GCTCCCTCTCATCAGTTCCA (forward) CTCCTCTGCTTGGTGGTTTG (reverse)	345 453	56.8 56.8	109
IL-4	AGCAACGAAGAACACCACAG (forward) GCAGCTCCATGAGAACACTAG (reverse)	258 382	56.7 56.7	125
BDNF	ATTACCTGGATGCCGCAAAC (forward) TGACCCACTCGCTAATACTGT (reverse)	1010 1111	56.9 56.8	102
GAPDH (rat)	CACTGAGCATCTCCCTCACA (forward) AGAGGGTGCAGCGAACTTTA (reverse)		59.4 57.3	110
GAPDH (mouse)	ATGACATCAAGAAGGTGGT (forward) CATACCAGGAAATGAGCTT (reverse)	832 990	60 59.7	1296

Table 4: PCR reaction amplification conditions

Process	Time	Temperature
enzyme activation	10 minutes	95°C
denaturation	15 seconds	95°C
data collection	60 seconds	60°C

2.9.6: Data collection and analysis

Since SYBR green binds to double-stranded DNA and fluoresces, the amount of cDNA being amplified by specific primers can be quantified. This data was used to determine the amount of cDNA amplified by the genes of interest and the house-keeping gene GAPDH. Following automatic normalization of data by Rotar Gene software (version 2.1.0), a threshold at which fluorescence data was analyzed was set. This is the level at which the rate of amplification is greatest during the exponential phase. The Ct values (threshold cycle), defined as the number of cycles for each sample to attain the threshold level (and thus equates to the abundance of cDNA target present), were collected and the comparative Ct (2[-Delta Delta C(t)] or [2-ΔΔCt]) method was used to analyse raw data; this compares Ct values of the sample against a calibrator. ΔCt value was calculated as the average Ct value of the

gene of interest minus the average Ct value for the housekeeping gene. Therefore the ΔΔCt value was calculated as the ΔCt value of the control minus the ΔCt value of the sample of interest. These values were calculated as absolute values of the level of comparative expression based on the equation:

$$\text{Comparative Expression Level} = 2^{-\Delta\Delta Ct}$$

Data was then analysed for statistical significance using a statistical analysis software programme called prism (GraphPad Inc.).

2.10: Imaging and statistical analysis

Images were taken on a DM RBE microscope (Leica Microsystems Limited) at 20x magnification. Six systemically randomized fields per well were taken using the Leica Application Suite image-capturing system version 3.8.0. **(Figure 9)** Data was averaged per well and expressed in cells/mm^2 or as a percentage, based on a sample of 4 wells per condition per experiment. All experiments were repeated a minimum of three times to give a value of n = 12. This is an established method that has been validated for cell counting (Howell et al., 2003; Howell et al., 2005; Zaben et al., 2009). One experiment consisted of hippocampi from 6-10 animals, pooled and prepared as described in section 2.1. Graph Pad prism data analysis software (GraphPad Inc.) was used to plot data points. For statistical comparisons, One Sample *t*-Test, Student's t test or a one way analysis of variance (ANOVA) with Bonferroni correction for multiple comparisons were used ($p < 0.05$ considered significant). One Sample *t*-Test was used to test the mean value of distribution within a single sample. Student's t test was used when comparing the mean of two sample groups and a single variable. A one way ANOVA was used to compare the mean of three or more independent sample groups and a single variable. Bonferroni correction for multiple comparisons was used with the one way ANOVA to adjust *P* values and controls for false positives.

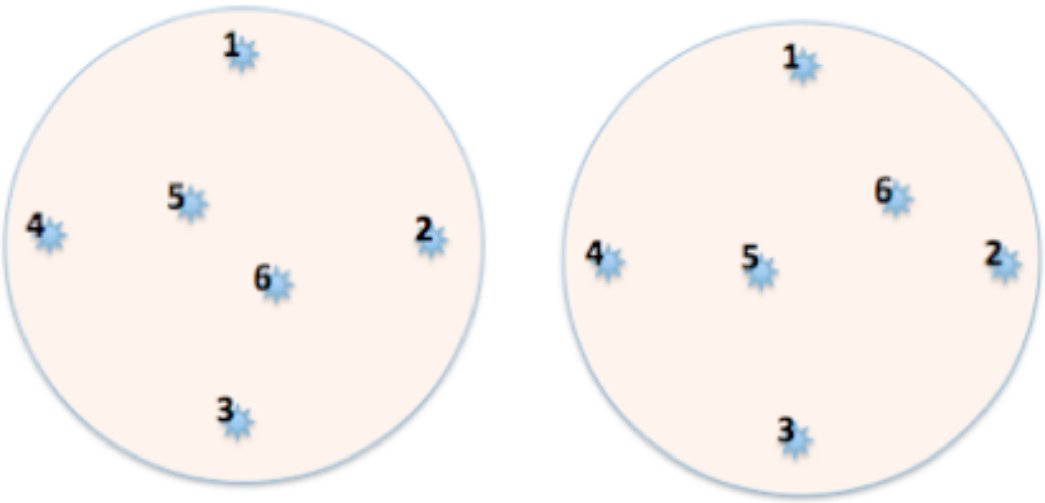

Figure 11: Cell counting in the well. Examples of cell counting in the well. 6 images were taken per well. Images 1-4 were taken in a clockwise manner and images 5 and 6 were taken anywhere at random in the centre of the well.

Chapter 3

Activated $CD4^+$ T lymphocytes supernatant increases proliferation of hippocampal progenitor cells

3.1 Introduction

3.1.1: Introduction

Restricted immune cell entry into the CNS, courtesy of the blood-brain barrier, has primarily been the driving force behind prescribing the term "immune-privileged" to describe the brain. This term is rather misleading, suggesting the brain is impervious to immune regulation; in fact the brain is an immune specialized organ that combines cross-talks between innate and adaptive components of immunity to regulate CNS homeostasis in a distinct fashion (Ziv et al., 2006, Ekdahl et al., 2003, Wolf et al., 2009, Derecki et al., 2010). Signalling molecules such as cytokines, chemokines and growth factors are central to homeostatic regulation and although their role is well documented in inflammatory response following injury or disease, their contribution under physiological conditions remains to be defined.

3.1.2: Immune regulation of the neurogenic niche

Conventionally, immune regulation of the CNS was associated with detrimental effects on neurogenesis (Ekdahl et al., 2003, Monje et al., 2003). In this capacity, immune cells such as macrophages and lymphocytes are recruited to the CNS to execute their immune functions. However, mounting research suggests a beneficial role for immune cells in the regulation of neurogenesis under physiological conditions (Kipnis et al., 2004, Wolf et al., 2009, Butovsky et al., 2006, Ziv et al., 2006). In this respect, there is a delicate balance between the innate and adaptive components of the immune system.

The neurogenic niche represents a functionally distinct region of the brain permissive for neuronal development. This dynamic microenvironment is influenced by an array of factors including the immune system. In addition to the innate components of immunity such as microglia and TLRs, it is becoming apparent that adaptive immune regulation of neurogenesis is crucial, with T lymphocytes as key players (Bsibsi et al., 2002, Ziv et al., 2006, Wolf et al., 2009). Although largely absent from the brain parenchyma under physiological conditions, T lymphocytes are positioned within close proximity to the brain parenchyma and indeed the subgranular zone niche where hippocampal neurogenesis occurs. In fact, the subgranular zone is approximately 100μM from the ventricle walls; it is within the

choroid plexus of the lateral ventricles that T lymphocytes are found in abundance (Ziv et al., 2006, McMenamin et al., 2003). Mice devoid of T lymphocytes have impaired neurogenesis, which is restored partially upon T lymphocytes replenishment from wild types (Sartori et al., 1997, Ziv et al., 2006). Interestingly, this is specific to $CD4^+$ T lymphocytes (Wolf et al., 2009). Further still, these T lymphocytes do not act independent of other components involved in immunity. Rather, evidence supports the need for an intact immune system for homeostatic maintenance of neurogenesis, whereby innate cells such as microglia must be present for T lymphocytes to exhibit their neurogenic regulatory function (Ziv et al., 2006).

3.1.3: T lymphocyte entry into the CNS

There is much controversy surrounding the route of T lymphocyte entry into the CNS under physiological conditions. There is evidence for some constant T lymphocyte trafficking in low numbers into the brain parenchyma and of interest are the high numbers of T lymphocytes in the cerebrospinal fluid (CSF), a protective fluid which flows within the subarachnoid space of the meningeal layers that cover the brain (Kivisakk et al., 2003). The cellular composition of CSF of a healthy human individual comprises some 150, 000 cells, of which 80% are $CD4^+$ memory T lymphocytes (Ransohoff et al., 2003, Svenningsson et al., 1995). From the point of immune surveillance, it is likely that these cells could traverse the CSF-blood barrier in a steady, tightly controlled manner, albeit in low numbers. In the context of T lymphocyte modulation of hippocampal neurogenesis, these CSF T lymphocytes could be responsible for increased proliferation of neural progenitor cells within the hippocampal stem cell niche, either through direct contact with the stem cell niche or from close proximity including the meningeal spaces (Ziv et al., 2006, Wolf et al., 2009). Direct interaction could also potentially include systemically delivered T lymphocytes via blood vessels in the subgranular zone. Regardless of the source and route of T lymphocytes entry, it is established that they must be in an "activated" state to elicit their effects. This "activation" is a result of T lymphocyte-antigen interaction. In their capacity as "activated" cells, T lymphocytes are able to release effector mediators (Flamand et al., 1990, Baran et al., 2001). In contrast, "naïve" T lymphocytes that have not received a signal, circulate without having the capacity to

release notable levels of cytokines until activated by a signal. These signals are delivered by antigen presenting cells. This signal is the result of binding of the antigenic peptide/MHC class II complex with the T cell receptor and binding of co-stimulatory molecules on antigen presenting cells. These co-stimulatory molecules include B7.1 and B7.2, which interact with counter-receptors CD28 and CTL-4 on T lymphocytes (June et al., 1994).

3.1.4: Activated T lymphocytes traverse the CNS

T lymphocyte entry into the CNS remains unclear. Recent studies using experimental autoimmune encephalomyelitis (EAE) models have shown that systemically injected encephalitogenic T lymphocytes preferentially enter leptomeningeal spaces; that is the arachnoid and pia mater of the meninges (Carrithers et al., 2000, Bartholomaus et al., 2009). These T lymphocytes are also found within the choroid plexus parenchyma and given that CSF, which is produced in the choroid plexus, runs within the space between the arachnoid and pia mater suggests a strong link for T lymphocyte modulation and regulation from this region (Carrithers et al., 2000). Activated T lymphocytes are restricted to immune-surveillance in the leptomeningeal space until triggered by a specific antigen (Bartholomaus et al., 2009). Indeed, it is only activated T lymphocytes that are equipped with the necessary molecular components that enable trafficking to the CNS (Engelhardt and Coisne, 2011). *In vivo* activation of naïve T lymphocytes occurs when an antigen presenting cell (APC) presents an antigen to the T cell receptor on the T lymphocyte; this binding to the T cell receptor works in conjunction with the transmembrane protein CD3 to convert the binding into intracellular signals (Alberts et al., 2002). Similarly, T lymphocytes can be activated *in vitro* by the addition of an anti-CD3 antibody, which mimics T lymphocyte stimulation (Tsoukas et al., 1985).

3.1.5: Aims and overview

The aim of the work described in this chapter was to generate a novel culture paradigm to investigate the effect of $CD4^+$ T lymphocytes supernatant on primary hippocampal cultures. The aim was to establish a valid culture paradigm to determine whether $CD4^+$ T lymphocytes must be in an activated state to elicit an

effect on hippocampal cultures. Specifically, we wanted to investigate the effects of supernatant on hippocampal proliferation of cell-specific phenotypes, cell survival and differentiation.

3.2 Methods

The spleen is the largest secondary lymphoid organ in the body. It contains approximately a quarter of all lymphocytes and is responsible for initiating immune responses to blood-borne antigens (Kuper et al., 2002; Nolte et al., 2002; Balogh et al., 2004). In rodents, the spleen reaches peak development at puberty (Losco, 1992). Splenocytes is a vague term used to describe all spleen cells, including red and white blood cells. Typically, an adult mouse spleen consists of 1x10^8 white blood cells (50-60% B cells, 30% T cells, 5% macrophages, and <5% others). To investigate the effect of T lymphocytes on hippocampal cells, 5% supernatant from $CD4^+$ T lymphocytes cultures were added to primary hippocampal cultures. Hippocampal cells were treated with T lymphocytes supernatant from either "naïve" cells that are in an inactive state or "activated" cells that are treated with anti-CD3 to mimic stimulation by antigen presenting cells. Experimental conditions in this chapter are defined as either treatment in standard culture medium (NBA/B-27/Glutamine) or the addition of 5% T lymphocytes supernatant in standard culture medium at the given time point.

3.2.1: Generation of primary rat hippocampal cultures

For each experiment, 6-10 Sprague-Dawley rat pups aged P7-10 were used to generate primary hippocampal cultures as detailed in *section 2.1.* Viable cells were plated at a density of 100, 000 cells/mL directly on to poly-L-lysine coated coverslips in 24-well plates. At 2 hours post-plating, cells were washed to remove residual debris and replenished with fresh NBA/B-27/glutamine medium supplemented with antibiotic/antimycotic. Cells were grown under control or treatment conditions as per experimental requirements (5%CO_2/9%O_2/37°C incubator conditions).

3.2.2: Isolating $CD4^+$ T lymphocytes using a $CD4^+$ isolation kit

For each experiment, 4 spleens were used from adult mice to generate $CD4^+$ T lymphocytes cultures as detailed in *section 2.2.* Following a multi-step protocol as part of a $CD4^+$ isolation kit, viable cells were plated at a density of 1, 000, 000 cells/mL directly on to poly-L-lysine coated 24 well plates. 1µg/mL of anti-CD3 was added at plating to activate cells or left untreated for "naïve" cultures. Cells were

grown in standard culture medium (NBA/B-27/glutamine) supplemented with antibiotic/antimycotic for 24 hours (5%CO_2/9%O_2/37°C incubator conditions) and then supernatant was collected and stored at -20°C until required.

3.2.3 Examining purity of $CD4^+$ T lymphocytes cultures

$CD4^+$ T lymphocytes cultures generated using the $CD4^+$ isolation kit were tested for their purity. Cultures were generated as per *section 2.2.* Cultures were grown for 24 hours in standard culture medium supplemented with antibiotic/antimycotic and then fixed in 4% PFA. Cells were washed with PBS and immunostained for $CD4^+$ and DAPI expression as detailed in *section 2.8*.

3.2.4 Isolating cell populations from the spleen by flow cytometry

3 spleens were used from adult mice to generate three populations of cultures: pure $CD4^+$ T lymphocytes, splenocytes without $CD4^+$ T lymphocytes, splenocytes with $CD4^+$ T lymphocytes. Spleens were collected and stained for flow cytometric sorting following a multi-step protocol as detailed in *section 2.3*. Cells were treated with a fixable dead cell staining kit (LIVE/DEAD Aqua; 1:10 in PBS) to identify dead cells for flow cytometric analysis. The fluorescent reactive dye in the kit enters compromised membranes, reacts with free amides and fluoresces intensely. The dye also reacts with cell surface amines but with much less intensity. Therefore viable cells that do not allow the dye to enter the cell produce a much weaker fluorescence signal. Fc receptors were blocked for 10 minutes at 4°C using 5ug/mL anti-CD16/32 antibodies. Fc receptors are glycoproteins found on blood cells (B cells, tissue macrophages) that have high affinity for Fc regions of monomeric IgG and therefore can cause non-specific binding and high background staining. To minimise this, Fc receptors were blocked. Cells were then stained with antibodies for CD3 and CD4 diluted in FACS buffer. Samples were acquired using a FACS Canto II flow cytometer (BD Biosciences). Each spleen sample was analysed using the same gating strategy *(section 2.3.3)*. Once the samples were collected in standard culture medium supplemented with antibiotic/antimycotic, cells were plated as before *(section 3.2.2)* on 24 well plates for 24 hours (5%CO_2/9%O_2/37°C incubator conditions) under control or treatment conditions. Supernatant was then collected and stored at -20°C until required.

3.2.5: Studying supernatant effect on cell proliferation

The thymidine analogue BrdU is incorporated into cells during the S-phase of the cell cycle and therefore used to specifically label dividing cells (Taupin, 2007). BrdU is used to calculate the mitotic index, which is indicative of the total number of cells transitioning from the S phase to the G2 phase of the cell cycle. The mitotic index is the number of BrdU positive cells with respect to total number of cells (DAPI positive cells). Therefore to measure cell proliferation, a final concentration of 20μM BrdU was added at 3DIV for the terminal 6 hours. Experimental conditions (control or 5% supernatant) were added at the same time point. Cells were then fixed in 4% PFA for 30 minutes at 4°C. Cells were washed with PBS before being processed for BrdU incorporation. Specific cell markers nestin (putative progenitor cell markers), TuJ1 (neuronal marker) and Prox1 (dentate gyrus granule cell neuron marker) were used during processing by immunohistochemistry to investigate proliferation of these cell types. The total numbers and proportions of each specific marker were determined.

3.2.6: Defining supernatant effect on the labelling index and growth fraction

Ki-67 is an endogenous proliferative marker expressed by cells during the active phases of the cell cycle (G1, G2, M phase) and used to determine the labelling index or growth fraction. The labelling index is calculated as the number of Ki-67 expressing cells incorporating BrdU over the total number of Ki-67 positive cells. The growth fraction is calculated as the number of Ki-67 positive cells over the total number of DAPI positive cells. This allows us to determine whether proliferative effects are due to speeding of the cell cycle (labelling index) or recruitment of quiescent cells (growth fraction). Cells were grown under control conditions for 3DIV. Experimental conditions and 20μM BrdU were added for the terminal 6 hours. Cells were then fixed in 4% PFA for 30mins at 4°C. Cells were washed with PBS before being processed for BrdU incorporation and Ki-67 expression to determine the labelling index and growth fraction.

3.2.7: Characterising the effect of $CD4^+$ T lymphocytes supernatant on cell-specific phenotypes

To characterize cell-specific phenotypes, cultures were treated with experimental

conditions over time. In these set of experiments, cells were grown under control conditions for 3DIV and then replaced with treatment conditions for 3 days. At 6DIV cells were fixed in 4% PFA for 30 minutes at 4°C and washed with PBS before being processed for nestin and TuJ1 expression. The total numbers and proportions of each cell marker were determined.

3.2.8: Quantifying cell death in cultures treated with $CD4^+$ T lymphocytes supernatant

In two separate sets of experiments, cells were grown under experimental conditions for either 3DIV or 5DIV. At each given time point, cells were exposed to the cell death marker PI (5µg/ml) and nuclear cell marker DAPI (20µg/ml) for 40 minutes at 37ºC. The medium was then replaced with fresh culture medium (NBA/B-27/glutamine) and imaged live for quantification of cell death. The proportions of non-viable cells (PI^+) in the total cell population ($DAPI^+$) were calculated.

3.2.9: Imaging and statistical analysis

Images were taken on a DM RBE microscope (Leica Microsystems Limited) at 20x magnification. Six systemically randomized fields per well were taken using the Leica Application Suite image-capturing system version 3.8.0. Data was averaged per well and expressed in cells/mm^2 or as a percentage, based on a sample of 4 wells per condition per experiment. All experiments were repeated a minimum of three times. Graph Pad prism data analysis software (GraphPad Inc, San Diego, CA, USA) was used to plot data points. For statistical comparisons Student's t test was used ($p < 0.05$ considered significant). To determine the mean distribution, a One Sample *t*-Test was used.

3.3 Results

3.3.1: CD4+ T lymphocyte kit does not generate pure cultures

Using a CD4+ T lymphocyte isolation kit to isolate CD4+ T lymphocyte cultures is a an established method. According to the manufacturer, this isolation kit eliminates more than 95% of B cells and CD8+ cells from lymphocyte preparations, which result in enriched mouse CD4+ T cells in column eluent (Cedarlane Laboratories). Immunohistochemical analysis was used to quantify the purity of our cultures. The isolation kit was used to generate cultures *(section 2.2)* for 24 hours under standard control conditions. Cells were fixed in 4% PFA and processed for expression of CD4 and DAPI. The total number of cells and the proportion of CD4+ cells were calculated. The proportion of CD4+ cells, with respect to the total number of cells (DAPI+) was 0.71 SE ± 0.02 **(Figure 12 B)**. Therefore our cultures have a purity of approximately 70%.

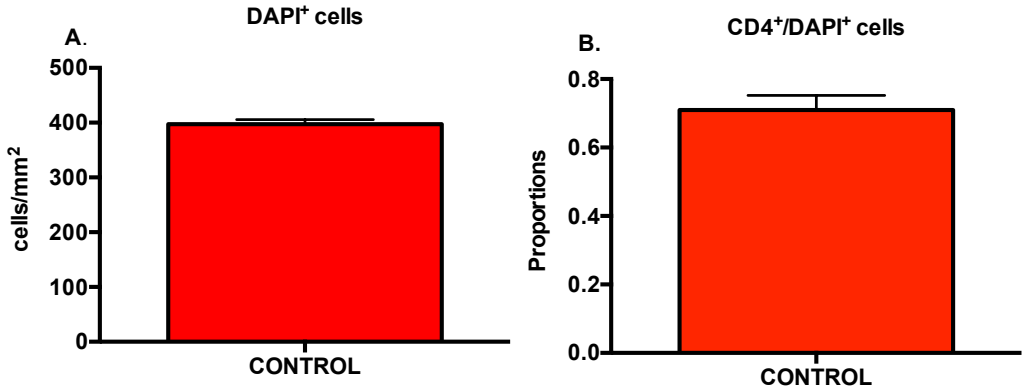

Figure 12: Purity of cultures generated using a CD4+ T lymphocyte isolation kit. CD4+ T lymphocyte isolation kit was used to generate cultures for 24 hours under standard control conditions. Cells were fixed in 4% PFA and processed for expression of CD4+ and DAPI. **A.** Total number of DAPI+ cells **B.** Proportion of CD4+ cells with respect to total cell numbers. Data represents mean ± SE based on a sample that represents 8 wells from two different experiments. A One Sample *t*-Test was used.

3.3.2: Naïve supernatant does not change total cell counts in hippocampal cultures

Despite the high percentage of CD4+ T lymphocytes present within the splenocyte preparation, a supernatant effect on hippocampal cells was not expected as T lymphocytes that are in an inactive "naïve" state generate very little/negligible levels of cytokines, chemokines and growth factors (Baran et al., 2001). To

investigate the effect of supernatant generated from $CD4^+$ T lymphocyte isolation kit on hippocampal cells *in vitro*, hippocampal cultures were generated under control conditions for 3DIV. At 6DIV, cultures were treated with experimental conditions and then fixed in 4% PFA. Cells were processed for expression of the stem cell marker nestin and the immature neuronal marker class III β-tubulin (TuJ1). Cells were counterstained with DAPI to measure total cell numbers. There was no change in the total number of cells between naïve supernatant treated cells and control conditions (137.3 ± 4.38 vs. 139.9 ± 3.85; t(22)=0.46) **(Figure 13 A)**. There was also no change in the proportions of cell specific phenotypes, as observed in the proportions of nestin positive cells (0.35 ± 0.019 vs. 0.35 ± 0.012; t(22)=0.18) **(Figure 13 B)** and TuJ1 positive cells (0.09 ± 0.004 vs. 0.11 ± 0.003; t(22)=1.92) **(Figure 13 C),** with respect to total cell numbers, following treatment with naïve supernatant. Naïve supernatant does not change cell numbers in hippocampal cultures.

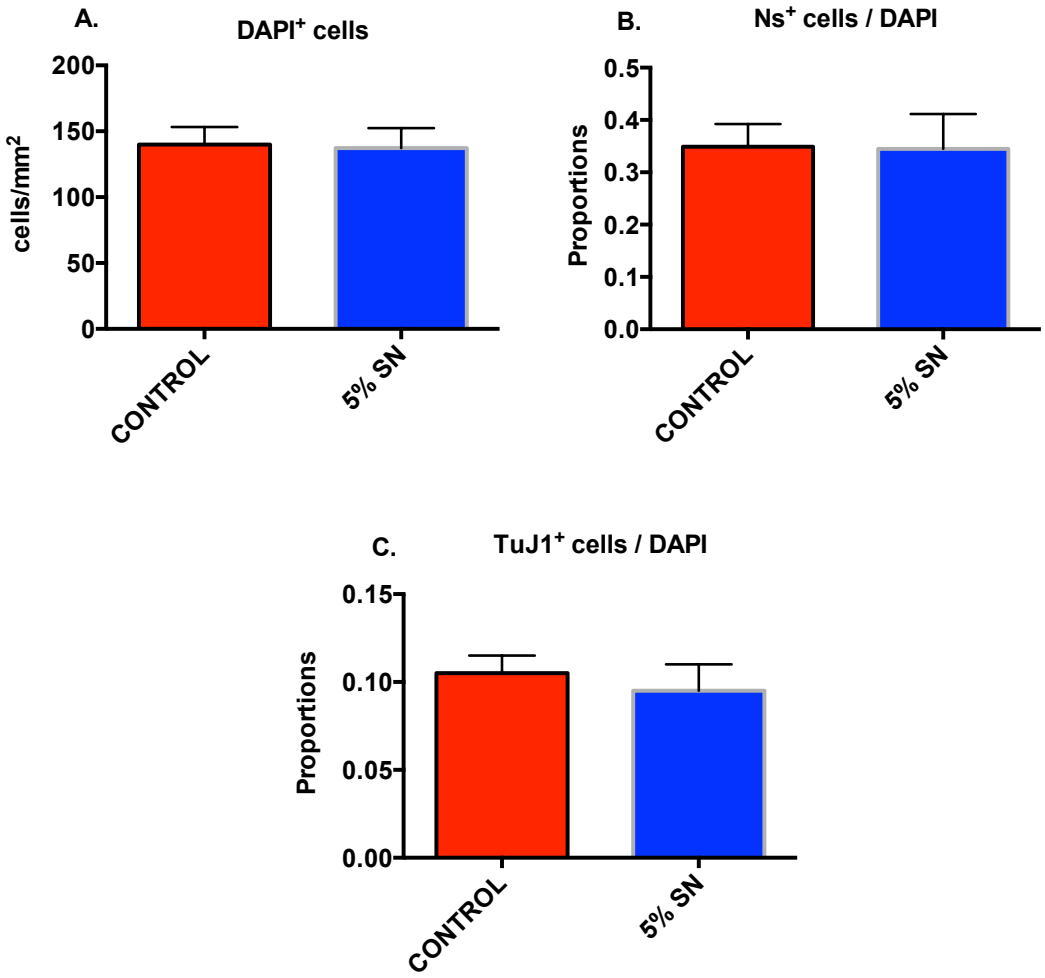

Figure 13: Naïve supernatant does not increase the proportion of cell-specific phenotypes. Hippocampal cells were generated under control conditions for 3DIV and then treated with experimental conditions until 6DIV. Cells were immunostained for nestin and TuJ1 expression. **A.** Total cell counts as measured by the number of DAPI positive cells **B.** Proportion of nestin cells and **C.** TuJ1 cells, with respect to total number of cells. Data represents mean ± SE based on a sample that represents 12 wells per condition from three different experiments. Comparisons between control and treatment is a Student's t-test (*, $p < 0.05$, **, $p < 0.01$, ***, $p < 0.001$)

3.3.3: Activated supernatant increases the total number of hippocampal cells

In vitro, naïve T lymphocytes are activated by treatment with anti-CD3 (Flamand et al., 1990, Li and Kurlander, 2010). This mimics T lymphocyte activation by antigen presenting cells, which gives T lymphocytes the capacity to produce sufficient quantities of inflammatory mediators. To investigate the effect of activated T lymphocytes on hippocampal cultures, cultures generated from the isolation kit were treated with an anti-CD3 compound (Cambridge Biosciences). Hippocampal cultures were generated for 3DIV under control conditions and treated with experimental conditions until 6DIV. Cells were stained with DAPI to measure total

cell counts. There was an increase in total cell counts under treatment with 5% activated supernatant compared to control (167.0 ± 0.97 vs. 138.3 ± 1.09; t(22)=19.66) **(Figure 14)**. These results suggest activated supernatant increases the total number of cells in culture.

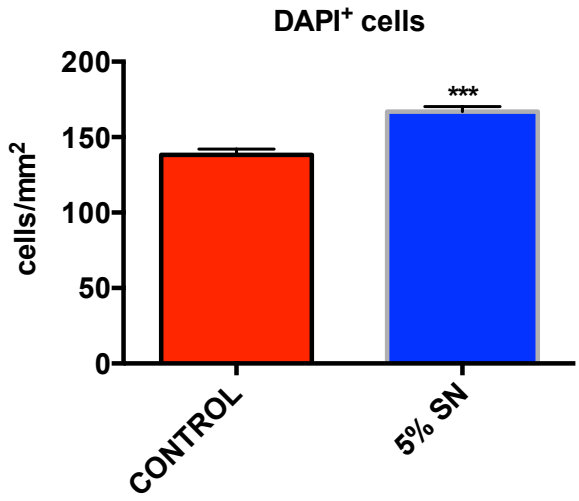

Figure 14: Activated supernatant increases the total number of hippocampal cells. Hippocampal cells were generated under control conditions for 3DIV and then treated with experimental conditions until 6DIV. Cells were stained with DAPI. Total cell counts as measured by the number of DAPI positive cells. Data represents mean ± SE based on a sample that represents 12 wells per condition from three different experiments. Comparisons between control and treatment is a Student's t-test (*, $p < 0.05$, **, $p < 0.01$, ***, $p < 0.001$)

3.3.4: Activated supernatant is not trophic for hippocampal cultures

The increase in total cell numbers is either a trophic or proliferative effect. To determine the effect of activated supernatant on cell survival, cultures were generated for 3DIV under control and experimental conditions. At 3DIV, cultures were exposed to the cell death marker propidium iodide (Lecoeur, 2002) prior to live imaging. DAPI was used to measure total cell numbers. There was an increase in the total number of cells under treatment with 5% supernatant compared to control (157.7 ± 4.38 vs. 137.2 ± 1.151; t(22)=4.51) **(Figure 15 A)**. However, there was no change in the proportion of dead cells with respect to total cell numbers at 3DIV under treatment with 5% supernatant compared to control (0.21 ± 0.005 vs. 0.21 ± 0.004; t(22)=0.5) **(Figure 15 B)**. These results suggest activated supernatant has no effect on cell survival in culture.

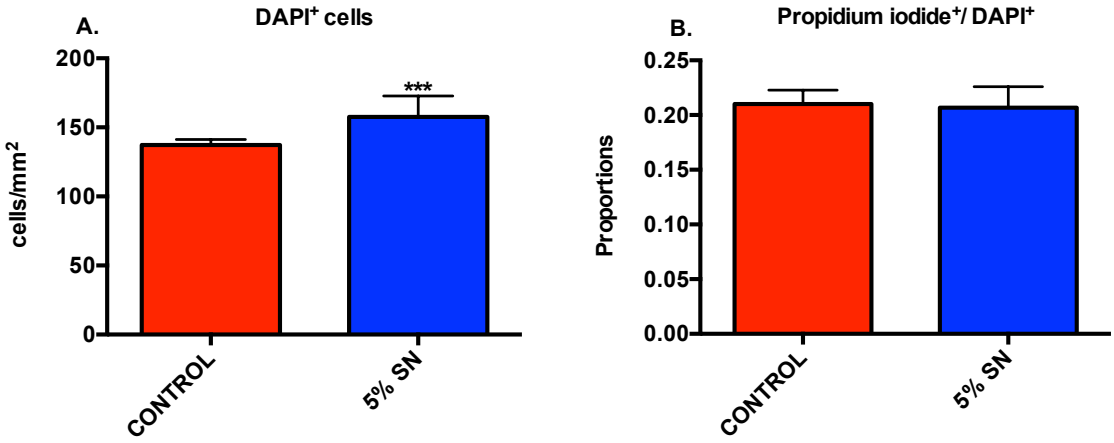

Figure 15: Activated supernatant has no effect on cell survival. Hippocampal cells were generated under control and experimental conditions for 3DIV. At 3DIV cells were exposed to the cell death marker propidium iodide and DAPI. **A.** Total cell counts as measured by the number of DAPI positive cells. **B.** Proportion of propidium iodide positive cells, with respect to total number of cells. Data represents mean ± SE based on a sample that represents 12 wells per condition from three different experiments. Comparisons between control and treatment is a Student's t-test (*, $p < 0.05$, **, $p < 0.01$, ***, $p < 0.001$)

3.3.5: Activated supernatant increases the mitotic index of hippocampal cells

Given the increase in hippocampal cell numbers is not due to a trophic effect of activated supernatant, proliferative effects were investigated. BrdU is proliferative marker used to specifically label dividing cells and calculate the mitotic index (Taupin, 2007). The mitotic index is indicative of the total number of cells transitioning from the S phase to the G2 phase of the cell cycle and calculated as the number of BrdU positive cells with respect to total number of cells (DAPI positive cells). Therefore to measure cell proliferation, hippocampal cell cultures were generated for 3DIV under standard control conditions and pulsed with BrdU for the terminal 6 hours before fixation. Cultures were treated with experimental conditions at the same time as the addition of BrdU. Cells were processed for BrdU incorporation and DAPI expression to calculate the mitotic index ($BrdU^+/DAPI^+$). There was a significant increase in the proportion of BrdU positive cells, with respect to total number of cells, following treatment with 5% activated supernatant compared to control (0.18 ± 0.005 vs. 0.12 ± 0.003; $t(22)=9.55$) **(Figure 16 B)**. There was no change in the total number of cells as measured by the number of DAPI positive cells (129.4 ± 1.22 vs. 128.9 ± 0.91; $t(22)=0.3$) **(Figure 16 A)**. These results show that activated supernatant has a proliferative effect on hippocampal cells.

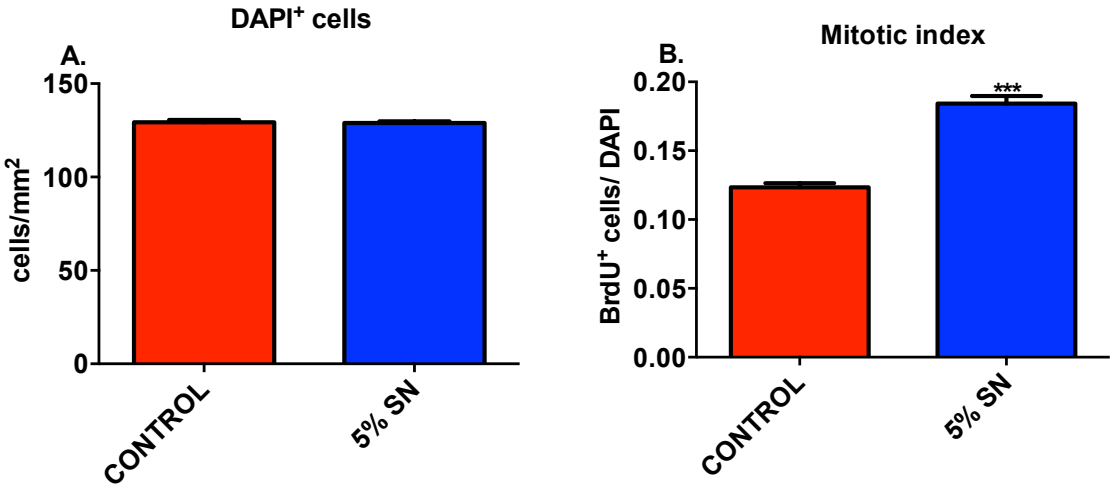

Figure 16: Activated supernatant increases the mitotic index of hippocampal cells. Hippocampal cells were generated under control conditions for 3DIV. BrdU and treatment conditions were added for the terminal 6 hours before fixation. Cells were immunostained for BrdU incorporation. **A.** Total cell counts as measured by the number of DAPI positive cells. **B.** Proportion of BrdU incorporating cells with respect to total number of cells. Data represents mean ± SE based on a sample that represents 12 wells per condition from three different experiments. Comparisons between control and treatment is a Student's t-test (*, $p < 0.05$, **, $p < 0.01$, ***, $p < 0.001$)

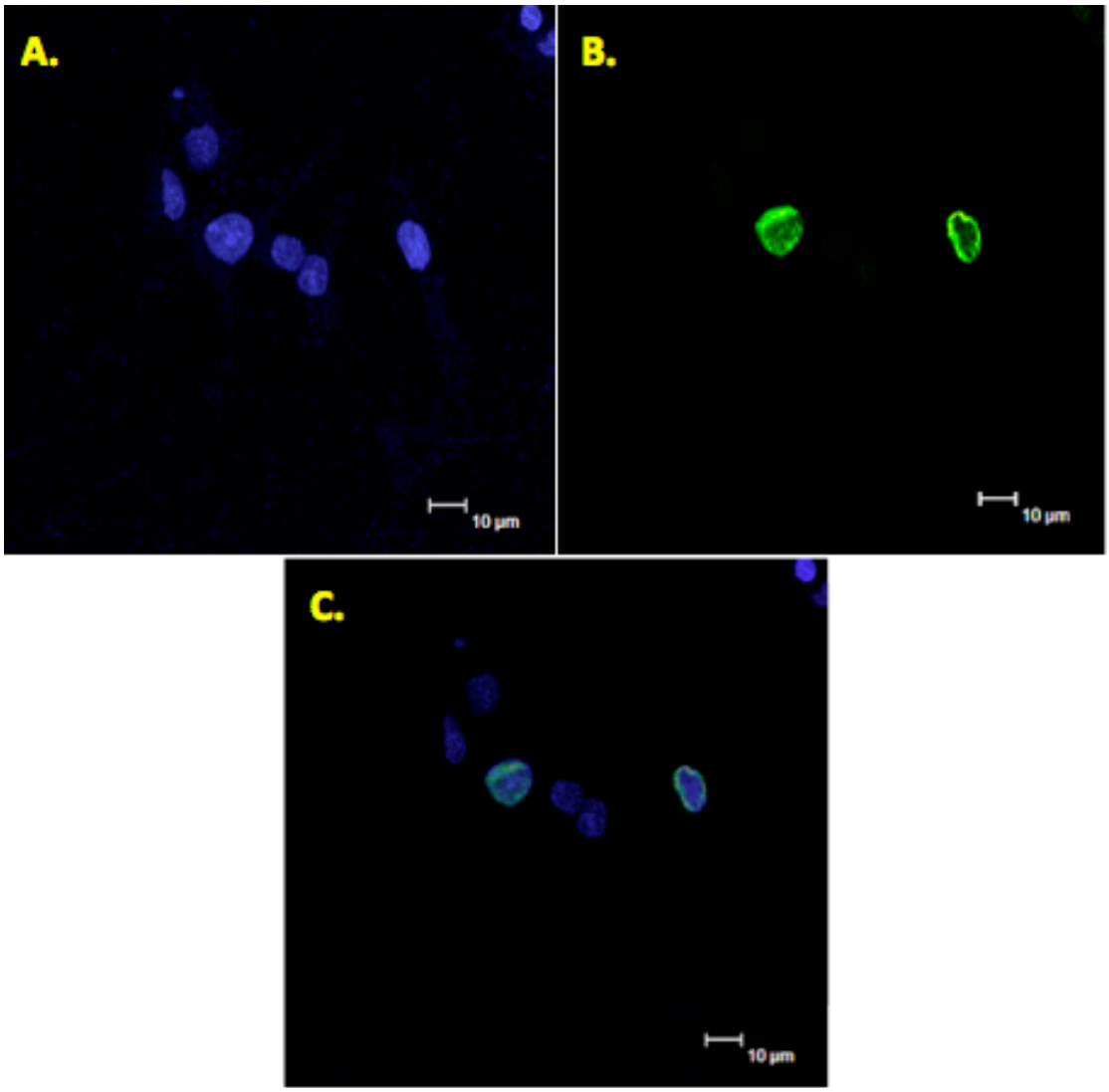

Figure 17: BrdU stained cells. Hippocampal cells were generated under control conditions for 3DIV and then treated with BrdU and treatment conditions for the terminal 6 hours before fixation. Cells were then processed for BrdU and counterstained with DAPI. **A.** DAPI stained cells **B.** BrdU incorporated cells **C.** merged image.

3.3.6: Activated supernatant increases proliferation of nestin-expressing hippocampal cells

Nestin is widely employed as a neural stem cell marker (Kitajima et al., 2005, Ernst and Christie, 2006), with nestin-expressing cells representing the main population of cycling cells in our cultures. The effects on proliferation of this cell subpopulation by activated supernatant was investigated by generating hippocampal cultures for 3DIV and treating them with experimental conditions for the terminal 6 hours before fixation. Cultures were immunostained for BrdU and nestin expression. There was an increase in the number of nestin-expressing cells incorporating BrdU,

with respect to the total population of nestin-expressing cells, following treatment with 5% supernatant compared to control (0.23 ± 0.022 vs. 0.15 ± 0.007; t(22)=3.28) **(Figure 18 B).** There was no change in the total number of nestin-expressing cells, with respect to total cell numbers, between control and treatment with T lymphocytes supernatant (0.35 ± 0.008 vs. 0.34 ± 0.01; t(22)=0.78) **(Figure 18 A)**. These results suggest activated supernatant increases the rate of proliferation of nestin-expressing cells.

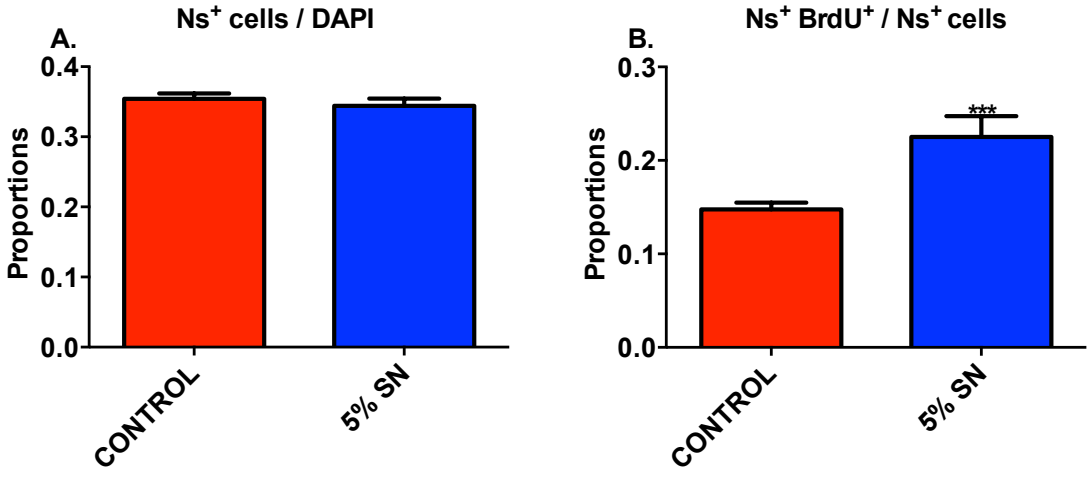

Figure 18: Activated supernatant increases proliferation of nestin-expressing hippocampal cells. Hippocampal cells were generated under control conditions for 3DIV. BrdU and treatment conditions were added for the terminal 6 hours before fixation. Cells were immunostained for BrdU incorporation and nestin expression. **A.** Proportion of nestin positive cells with respect to total cell numbers. **B.** Proportion of nestin-expressing cells incorporating BrdU, with respect to the total number of nestin positive cells. Data represents mean ± SE based on a sample that represents 12 wells per condition from three different experiments. Comparisons between control and treatment is a Student's t-test (*, $p < 0.05$, **, $p < 0.01$, ***, $p < 0.001$)

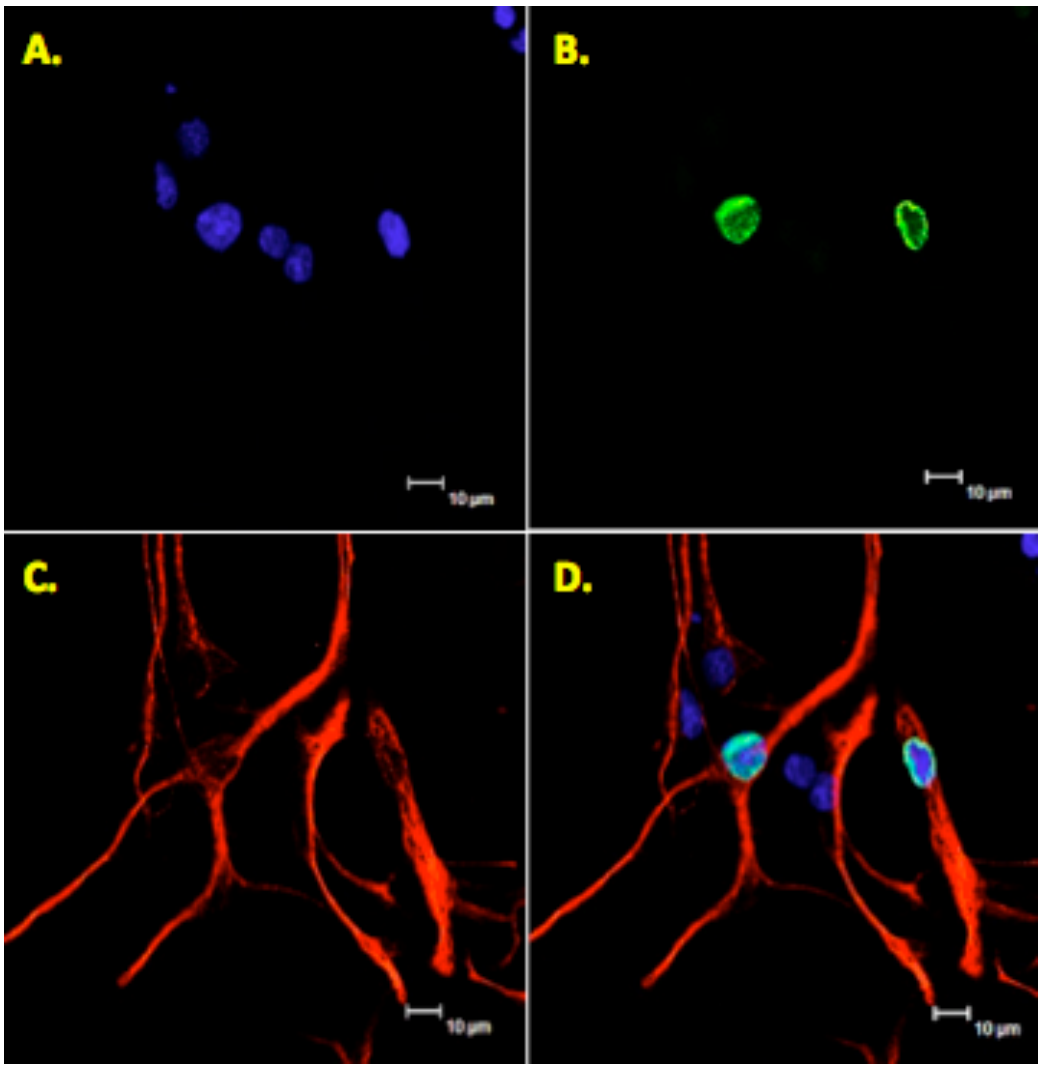

Figure 19: Nestin-expressing cells incorporating BrdU. Hippocampal cells were generated under control conditions for 3DIV and then treated with BrdU and treatment conditions for the terminal 6 hours before fixation. Cells were then processed for nestin, BrdU and counterstained with DAPI. **A.** DAPI stained cells **B.** BrdU incorporated cells **C.** nestin-expressing cells **D.** nestin-expressing cells incorporating BrdU.

3.3.7: Activated supernatant increases proliferation of neuronal class III β-tubulin expressing hippocampal cells

TuJ1 is a marker for immature neurons (Menezes and Luskin, 1994, Gould et al., 2001). To investigate the effect of activated supernatant on the proliferation of this cell subpopulation, cultures were generated under standard control conditions for 3DIV. BrdU and experimental conditions were added for the terminal 6 hours before fixation. Cultures were immunostained for BrdU and TuJ1 expression. There was an increase in the number of TuJ1-expressing cells incorporating BrdU, with respect to the total population of TuJ1-expressing cells, following treatment with 5% activated supernatant compared to control (0.078 ± 0.004 vs. 0.14 ± 0.004; $t(22)=10.38$) **(Figure 20 B).** There was no change in the total number of TuJ1-expressing cells, with respect to total cell numbers, between control and treatment with T

lymphocytes supernatant (0.315 ± 0.01 vs. 0.31 ± 0.01; t(22)=0.46) **(Figure 20 A)**. These results suggest activated supernatant increases the rate of proliferation of TuJ1-expressing hippocampal cells.

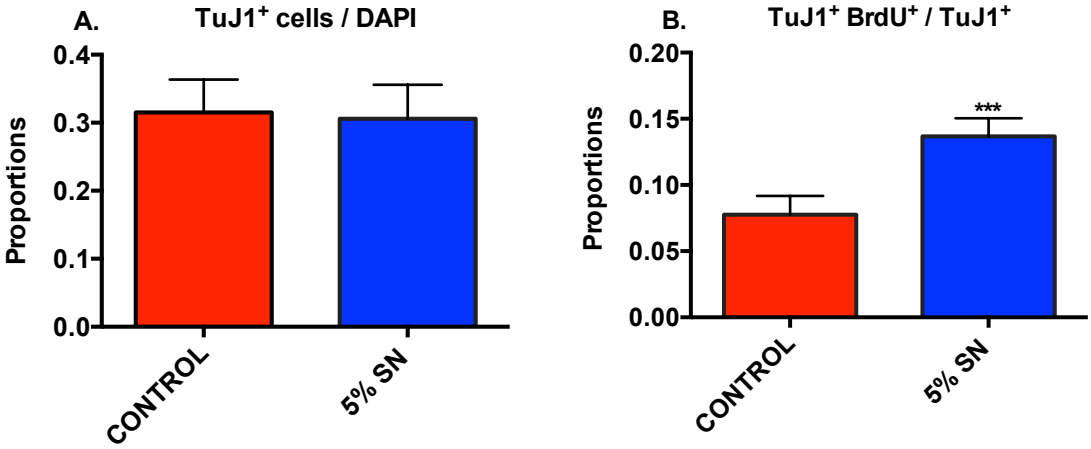

Figure 20: Activated supernatant increases proliferation of neuronal class III β-tubulin expressing hippocampal cells. Hippocampal cells were generated under control conditions for 3DIV. BrdU and treatment conditions were added for the terminal 6 hours before fixation. Cells were immunostained for BrdU incorporation. **A.** Proportion of TuJ1 positive cells with respect to total cell numbers. **B.** Proportion of TuJ1-expressing cells incorporating BrdU, with respect to the total number of nestin positive cells. Data represents mean ± SE based on a sample that represents 12 wells per condition from three different experiments. Comparisons between control and treatment is a Student's t-test (*, $p < 0.05$, **, $p < 0.01$, ***, $p < 0.001$)

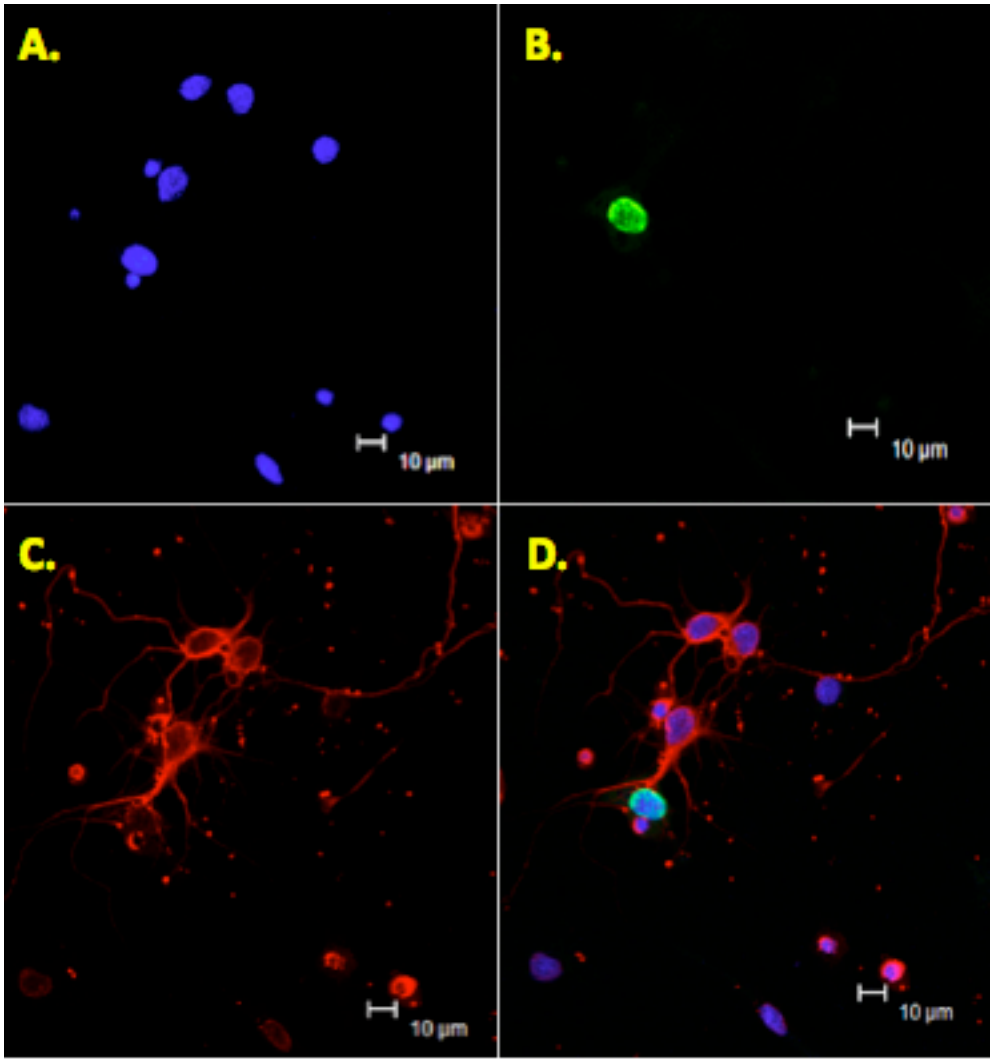

Figure 21: TuJ1-expressing cells incorporating BrdU. Hippocampal cells were generated under control conditions for 3DIV and then treated with BrdU and treatment conditions for the terminal 6 hours before fixation. Cells were then processed for TuJ1, BrdU and counterstained with DAPI. **A.** DAPI stained cells **B.** BrdU incorporated cells **C.** TuJ1-expressing cells **D.** TuJ1-expressing cells incorporating BrdU.

3.3.8: Activated T lymphocytes supernatant does not alter the growth fraction but increases the labelling index of hippocampal cells

To determine whether proliferative effects were due to speeding of the cell cycle (labelling index) or recruitment of quiescent cells (growth fraction), the endogenous proliferative marker Ki-67 was used. Ki-67 is an endogenous proliferative marker expressed by cells during the active phases of the cell cycle. The growth fraction is calculated as the proportion of cycling precursor cells (Ki-67 positive) with respect to the total number of cells (DAPI). When used with BrdU, the labelling index is determined by the proportion of Ki-67 expressing cells incorporating BrdU with respect to Ki-67 positive cells. Cells were generated under standard control

conditions for 3DIV and treated with experimental conditions and BrdU for the terminal 6 hours before fixation. Cultures were immunostained for BrdU and Ki-67 expression. There was no change in the proportion of Ki-67 positive cells, with respect to total cell numbers, under treatment with 5% activated supernatant compared to control (0.79 ± 0.005 vs. 0.79 ± 0.004; t(22)=0.87) **(Figure 22 A)**. However, there was an increase in the proportion of BrdU positive cells, with respect to Ki-67 expressing cells, under treatment with 5% activated supernatant compared to control (0.19 ± 0.003 vs. 0.14 ± 0.003; t(22)=12.31) **(Figure 22 B)**. This increase in the labelling index suggests treatment with 5% activated supernatant increases the speed of the cell cycle rather than recruiting more cells into the cell cycle.

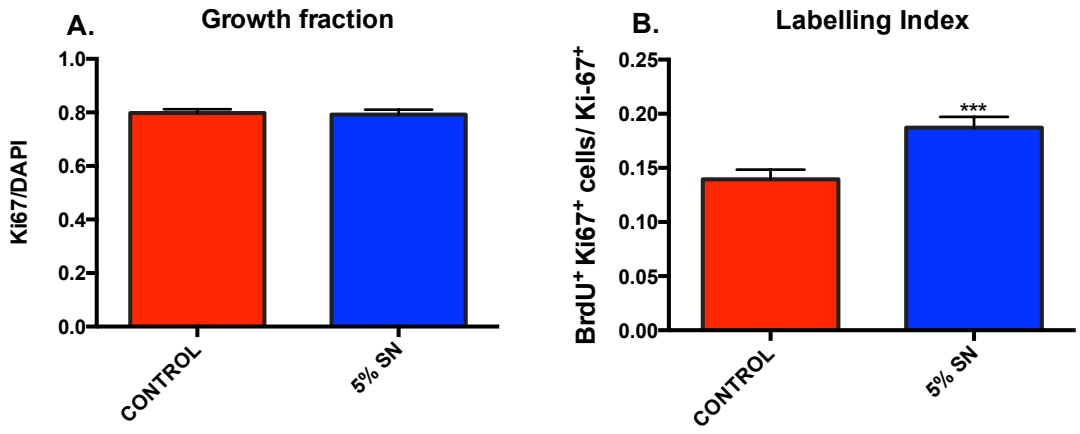

Figure 22: Activated supernatant does not alter the growth fraction but increases the labelling index of hippocampal cells. Hippocampal cells were generated under control conditions for 3DIV. BrdU and treatment conditions were added for the terminal 6 hours before fixation. Cells were immunostained for BrdU incorporation and Ki-67 expression. **A.** Proportion of Ki-67 positive cells with respect to total cell numbers. **B.** Proportion of BrdU incorporating cells, with respect to the total number of Ki-67positive cells. Data represents mean ± SE based on a sample that represents 12 wells per condition from three different experiments. Comparisons between control and treatment is a Student's t-test (*, $p < 0.05$, **, $p < 0.01$, ***, $p < 0.001$)

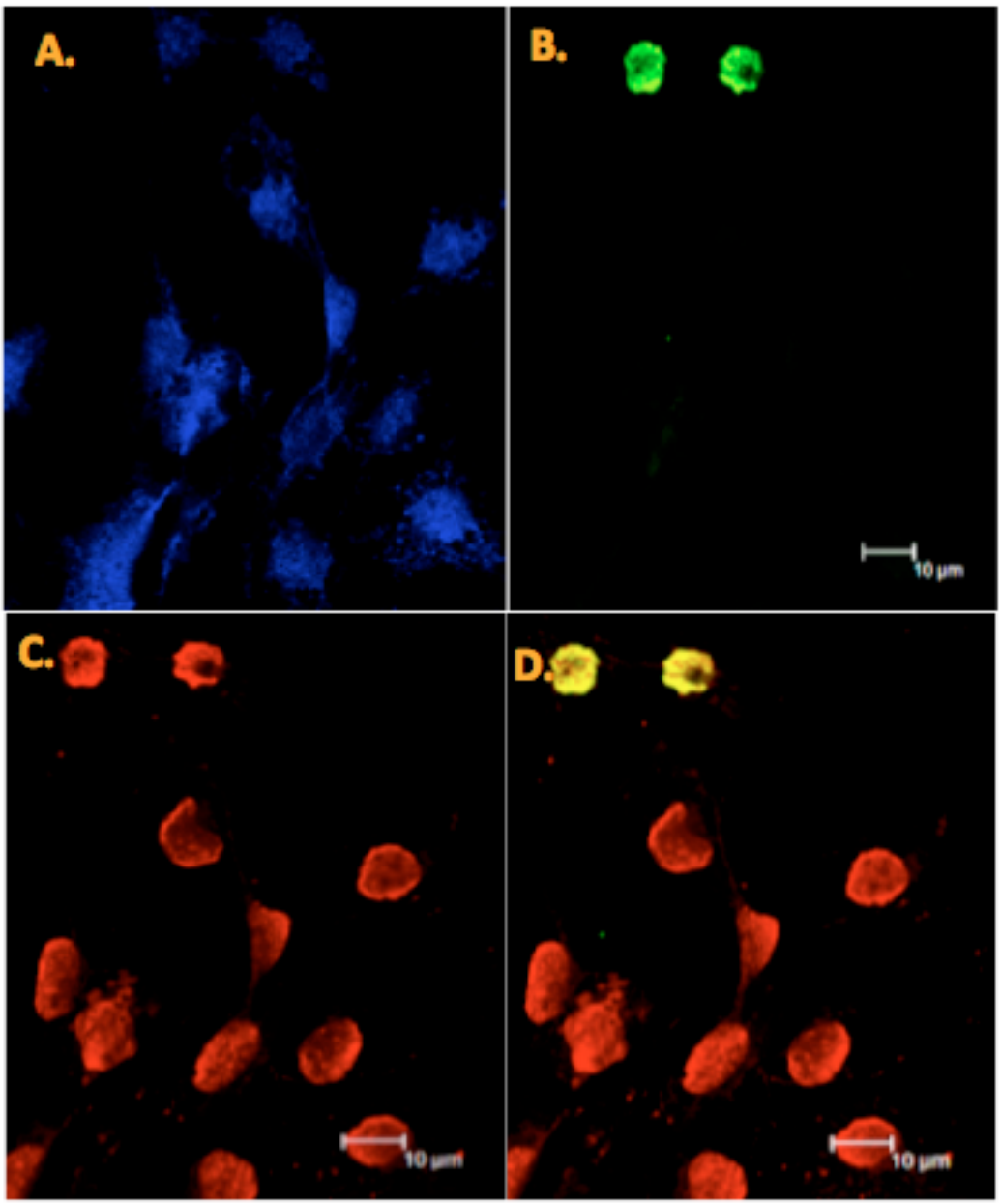

Figure 23: Ki-67-expressing cells incorporating BrdU. Hippocampal cells were generated under control conditions for 3DIV and then treated with BrdU and treatment conditions for the terminal 6 hours before fixation. Cells were then processed for Ki-67, BrdU and counterstained with DAPI. **A.** DAPI stained cells **B.** BrdU incorporated cells **C.** Ki-67-expressing cells **D.** Ki-67-expressing cells incorporating BrdU.

3.3.9: Activated supernatant increases the proportion of cell-specific phenotypes

In a set of experiments, the overall effect of activated supernatant was investigated by generating hippocampal cultures under control conditions for 3DIV and then treating them with experimental conditions until 6DIV. Cultures were fixed and processed for nestin and TuJ1 expression. There was an increase in total cell counts as indicated by DAPI staining under treatment with 5% activated supernatant compared to control (167.0 ± 0.97 vs. 138.3 ± 1.09; t(22)=19.66) **(Figure 24 A)**. There was also an increase in the proportion of nestin-expressing cells with respect to total cell numbers under treatment with 5% activated supernatant compared to control (0.46 ± 0.002 vs. 0.40 ± 0.008; t(22)=7.58) **(Figure 24 D)**. The same trend was observed in the proportion of TuJ1 positive cells with respect to total cell numbers under treatment with 5% activated supernatant compared to control (0.15 ± 0.003 vs. 0.10 ± 0.005; t(22)=6.75) **(Figure 24 F)**. Interestingly, there was also an increase in the proportion of nestin-positive cells expressing TuJ1 following treatment with 5% activated supernatant compared to control (0.09 ± 0.001 vs. 0.05 ± 0.003; t(22)=12.59) **(Figure 24 B)**. These results suggest activated supernatant increases the total number of cells in culture, increasing progenitor cell proliferation and driving progenitor cell progeny towards a neuronal fate.

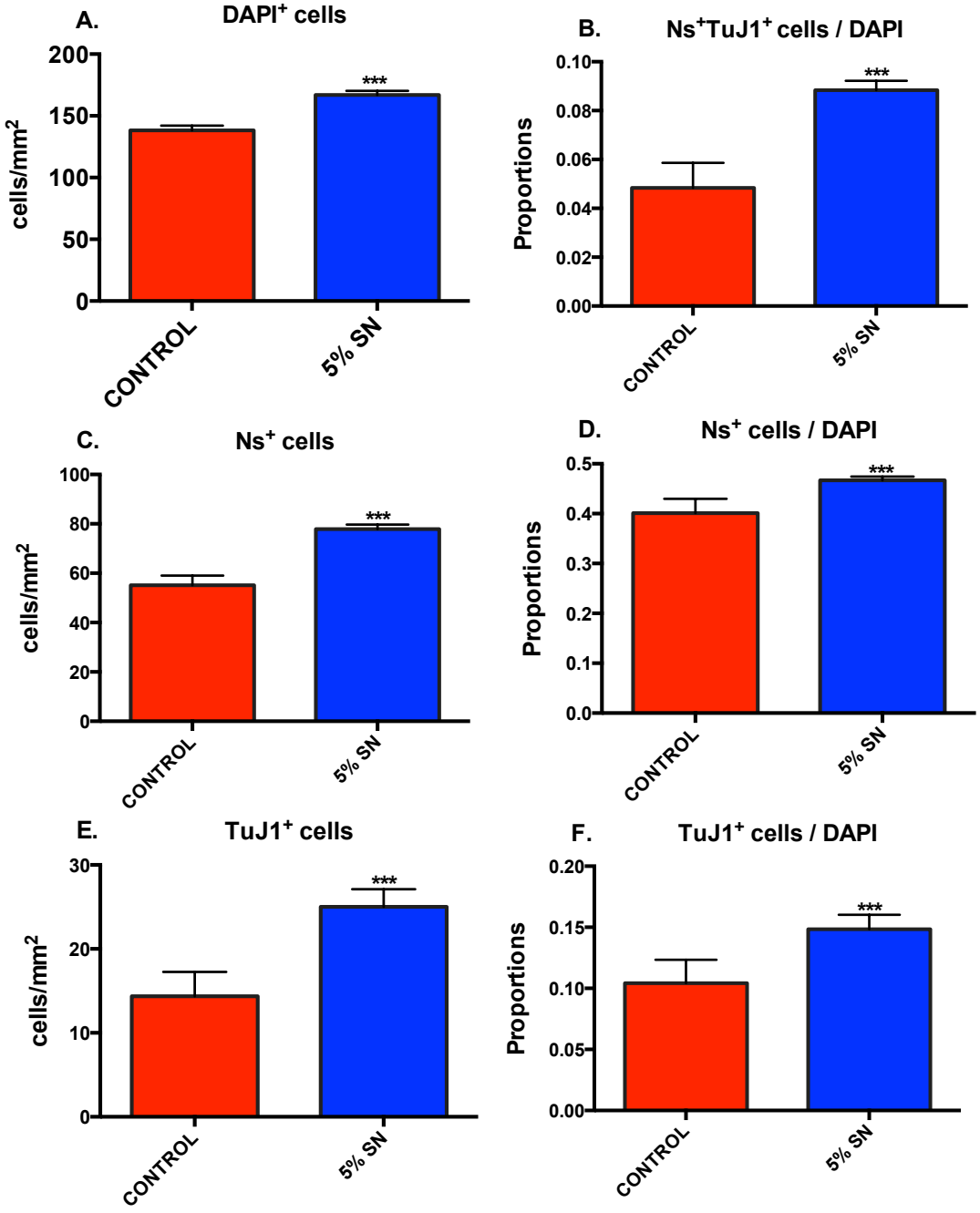

Figure 24: Activated supernatant increases the proportion of cell-specific phenotypes. Hippocampal cells were generated under control conditions for 3DIV and then treated with experimental conditions until 6DIV. Cells were immunostained for nestin and TuJ1 expression. **A.** Total cell counts as measured by the number of DAPI positive cells. **B.** Proportion of nestin cells expressing TuJ1, with respect to total number of cells **C.** Total number of nestin expressing cells **D.** Proportion of nestin cells **E.** Total number of TuJ1 cells and **F.** Proportion of TuJ1 cells. Data represents mean ± SE based on a sample that represents 12 wells per condition from three different experiments. Comparisons between control and treatment is a Student's t-test (*, $p < 0.05$, **, $p < 0.01$, ***, $p < 0.001$)

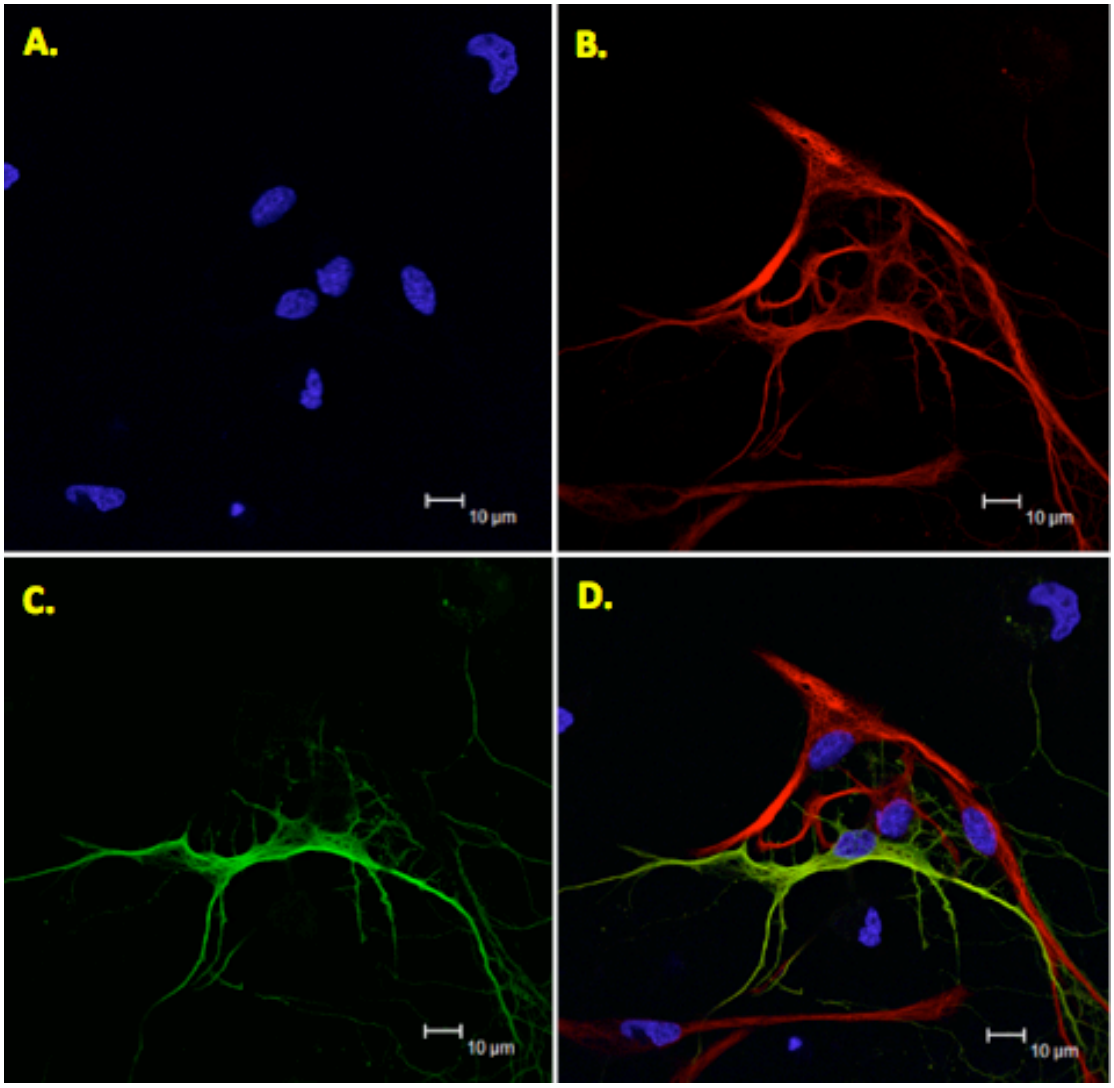

Figure 25: Nestin and TuJ1 co-localized staining. Hippocampal cells were generated under control conditions for 3DIV and then treated with treatment conditions until 6DIV. After fixation, cells were processed for nestin, TuJ1 and counterstained with DAPI. **A.** DAPI stained cells **B.** nestin-expressing cells **C.** TuJ1-expressing cells **D.** merged image.

3.3.10: Activated supernatant increases the proportion of class III β-tubulin positive cells co-expressing Prox1

During hippocampal dissection, there is a risk of contamination of neural progenitor cells from other regions of the brain. To determine whether the increase in the total number of newly generated neurons was specific to progenitors and neurons of the dentate gyrus, the antibody Prox1 was used. Prox1 defines granule cell identity (Iwano et al., 2012) and was therefore used together with TuJ1. Cultures were grown under control conditions for 3DIV and then treated with experimental conditions until 6DIV. Cells were stained for expression of TuJ1 and Prox1. There was a difference in the total DAPI counts, with an increase under treatment with 5% activated supernatant compared to control (164.9 ± 0.45 vs. 138.1 ± 0.39; t(22)=44.80) **(Figure 26 A)**. There was also difference in the total TuJ1 counts, with an increase under treatment compared to control (26.55 ± 0.45 vs. 15.78 ± 0.38; t(22)=18.23) **(Figure 26 C)**. There was also an increase in total Prox1 numbers under treatment compared to control (24.28 ± 0.47 vs. 13.89 ± 0.25; t(22)=19.50) **(Figure 26 E)**. This trend was also observed in the proportion of TuJ1 and Prox1 numbers, with respect to total cell counts, under treatment compared to control (0.16 ± 0.002 vs. 0.11 ± 0.003, t(22)=13.13 df; 0.15 ± 0.003 vs. 0.10 ± 0.002, t(22)=14.49, respectively) **(Figure 26 D & F)**. There was also an increase in the proportion of TuJ1 cells co-expressing Prox1 under treatment compared to control (0.14 ± 0.002 vs. 0.09 ± 0.001; t(22)=26.05) **(Figure 26 B)**. These results suggest that the increase in newly generated neurons under treatment with activated supernatant is specific to those of the dentate gyrus.

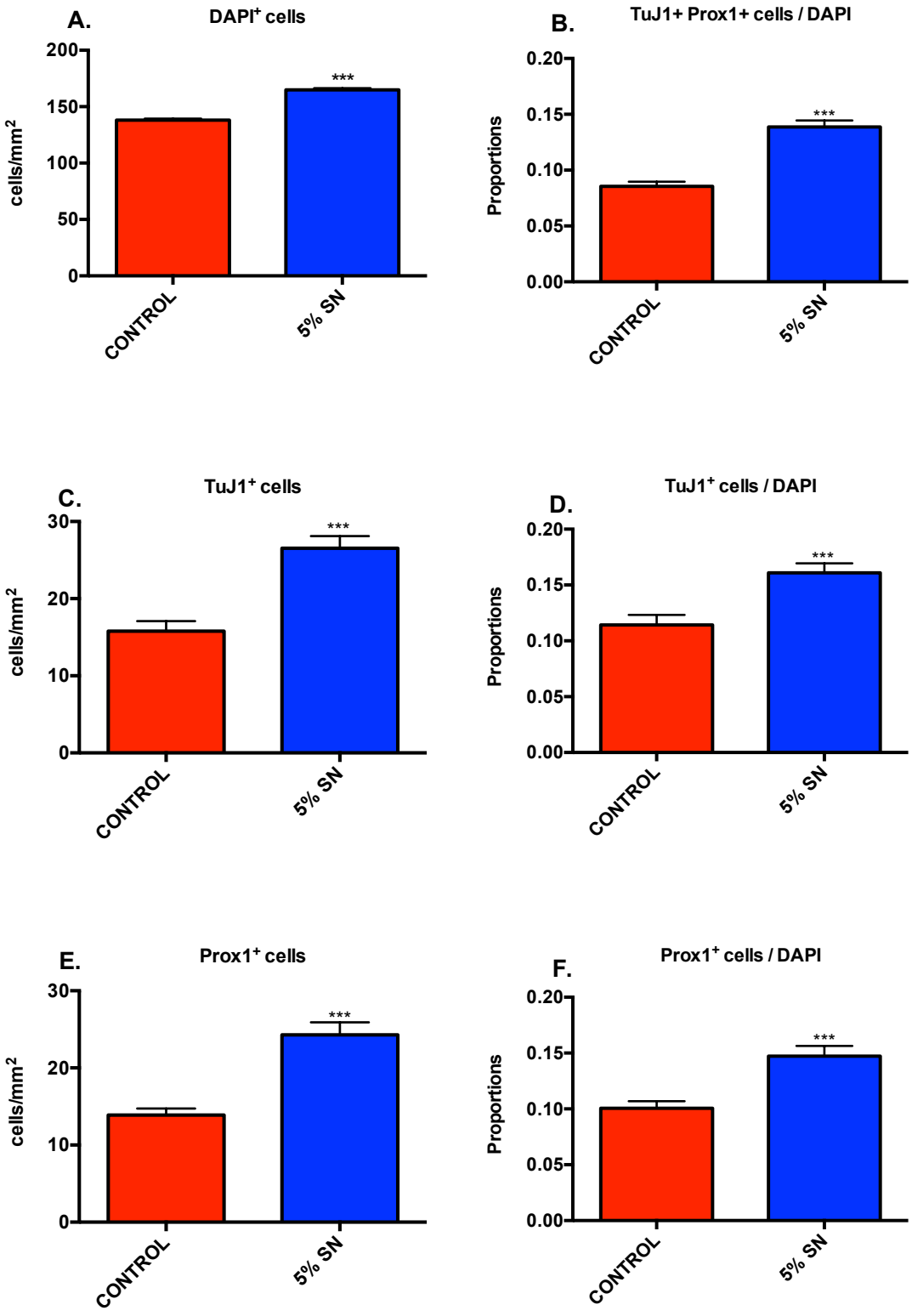

Figure 26: Activated supernatant increases the proportion of class III β-tubulin positive cells co-expressing Prox1. Hippocampal cells were generated under control conditions for 3DIV and then treated with experimental conditions until 6DIV. Cells were immunostained for TuJ1 and Prox1 expression. **A.** Total cell counts as measured by the number of DAPI positive cells. **B.** Proportion of TuJ1 cells expressing Prox1, with respect to total number of cells **C.** Total number of TuJ1 expressing cells **D.** Proportion of TuJ1 cells **E.** Total number of Prox1 cells and **F.** Proportion of Prox1 cells. Data represents mean ± SE based on a sample that represents 12 wells per condition from three different experiments. Comparisons between control and treatment is a Student's t-test (*, $p < 0.05$, **, $p < 0.01$, ***, $p < 0.001$)

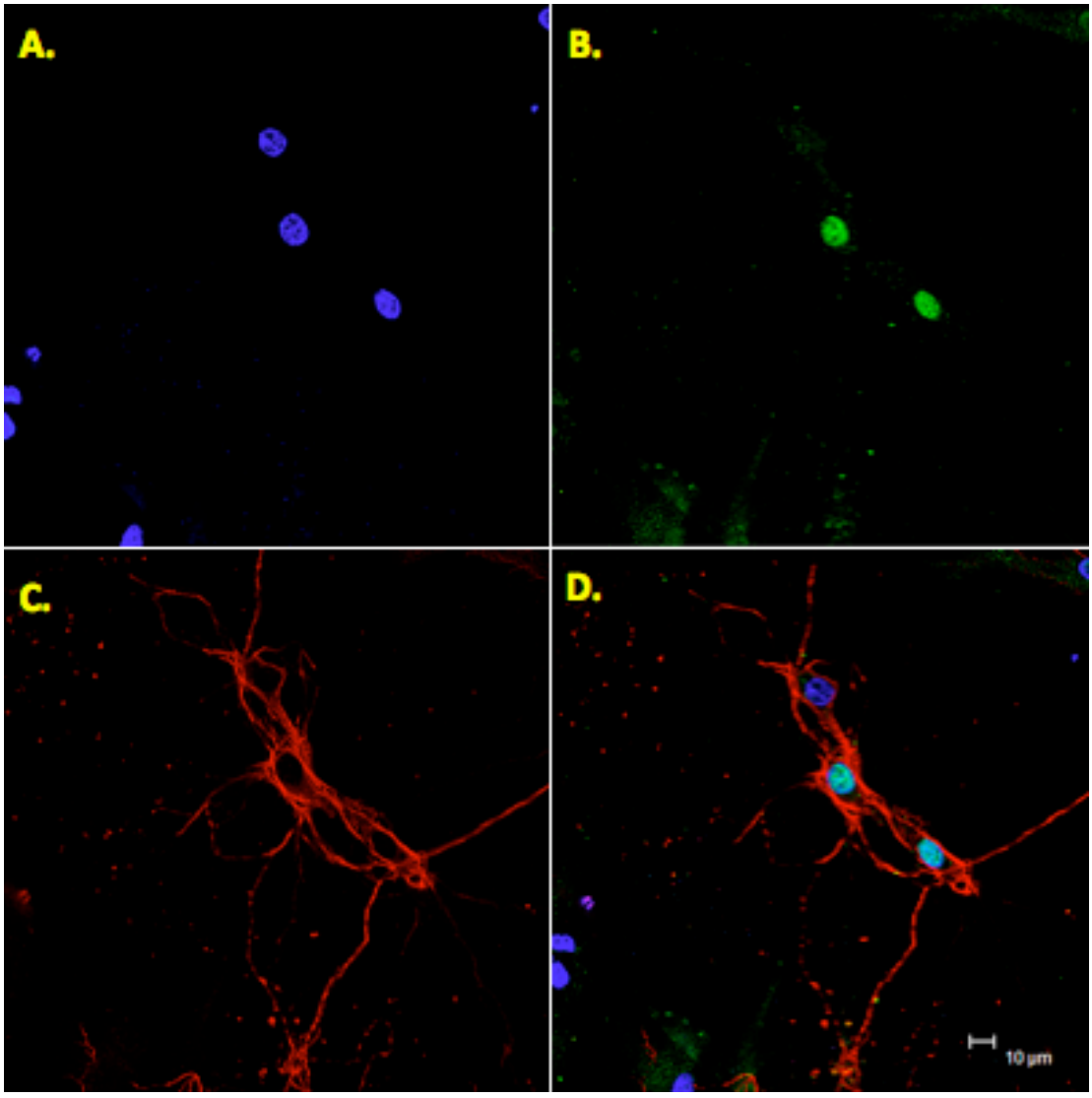

Figure 27: TuJ1 and Prox1 co-localized staining. Hippocampal cells were generated under control conditions for 3DIV and then treated with treatment conditions until 6DIV. After fixation, cells were processed for TuJ1, Prox1 and counterstained with DAPI. **A.** DAPI stained cells **B.** Prox1-expressing cells **C.** TuJ1-expressing cells **D.** merged image.

3.3.11 $CD4^+$ T lymphocytes isolated using flow cytometry confirm their proliferative effect on hippocampal cells

In addition to T lymphocytes, the spleen contains numerous cell types, including B lymphocytes, macrophages, dendritic cells. There is contamination of other cell types in $CD4^+$ cultures generated using the $CD4^+$ isolation kit *(section 3.3.1)*. However, given the effects of supernatant on hippocampal cells is purely by CD3-activated cultures (and not naïve supernatant) suggests the effect is mediated by T

lymphocytes. This is due to the specificity of CD3 for T lymphocytes. To determine whether the observed effects under treatment with 5% activated supernatant was due to activation of $CD4^+$ T lymphocytes, pure $CD4^+$ cultures were generated. Cells were sorted by flow cytometry. Splenic populations were divided into $CD4^+$ cells and splenocytes without $CD4^+$ cells. To determine whether supernatant effects were a direct effect of $CD4^+$ T lymphocytes or a downstream effect on other cell populations present in the cell culture, a mixed population containing all splenocytes was generated. Flow cytomtery software (BDFacs Diva) was used to determine the ratio of $CD4^+$ T lymphocytes to all other splenocytes (1:4). Cells were pooled together from both samples according to this ratio and placed into a fresh tube to produce splenocytes with $CD4^+$ cells. Once sorted using a flow cytometry sorter, the cells were grown for 24 hours under control ("naïve") or activated (anti-CD3 added to cultures) conditions. The supernatant from these cultures were collected and added to hippocampal cultures at 3DIV for the terminal 6 hours before fixation. BrdU was also added during this 6 hour pulse and cells were processed for BrdU and nestin expression. There was a difference in the mitotic index between control and treatment groups ($f(7,88)=0.81$). There was an increase in the mitotic index of hippocampal cultures treated with supernatant from pure $CD4^+$ cultures activated with anti-CD3 compared to control (0.19 ± 0.002 vs. 0.14 ± 0.003; $p < 0.001$) **(Figure 28 A)**. There was also an increase in the mitotic index of activated cultures with all cell populations compared to control (0.19 ± 0.002 vs. 0.14 ± 0.003) **(Figure 28 A).** The magnitude of the effect was comparable to that of treatment of hippocampal cultures with supernatant from pure CD4+ cultures activated with anti-CD3 (0.19 ± 0.002 vs. 0.19 ± 0.002; p = n.s.). There was no change in other treatment conditions compared to control. There was also a difference in the mitotic index between control and treatment groups in the proportion of nestin-expressing cells incorporating BrdU, with respect to the total number of nestin-positive cells, ($f(7,88)=5.7$) **(Figure 28 B)**. The same trend was observed whereby there was an increase under treatment with supernatant from anti-CD3 activated cultures with all cell population and from pure $CD4^+$ cultures compared to control (0.19 ± 0.002 vs. 0.14 ± 0.003; 0.19 ± 0.003 vs 0.14 ± 0.003, respectively) **(Figure 28 B)**. These results confirm activated $CD4^+$ T lymphocytes are directly involved in the modulation of hippocampal neurogenesis.

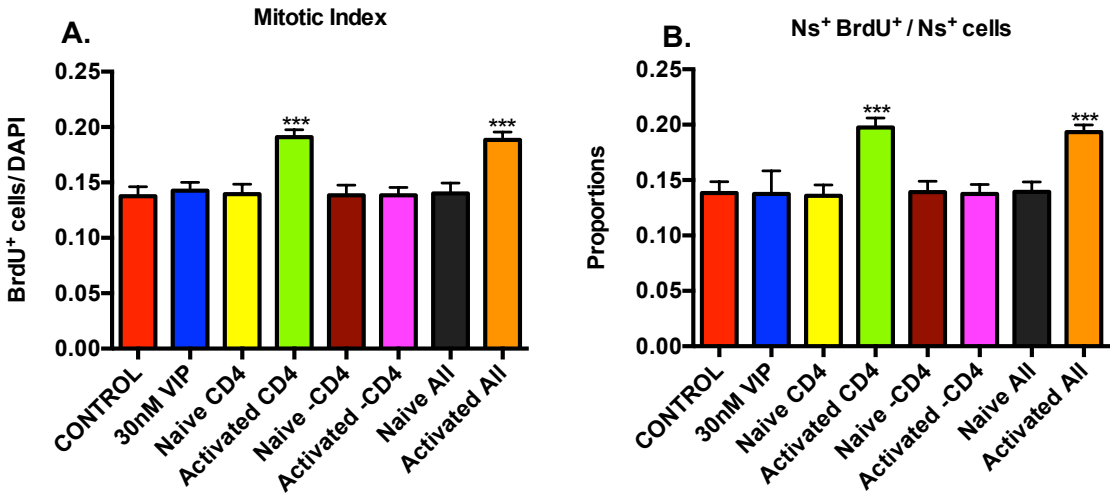

Figure 28: CD4 T lymphocytes isolated using flow cytometry confirm their proliferative effect on hippocampal cells. Cells were sorted using a flow cytometer and grown in culture medium for 24 hours under experimental conditions and the supernatant was collected. Hippocampal cells were generated under control conditions for 3DIV and then treated with 5% supernatant and BrdU for the terminal 6 hours before fixation. Cells were processed for nestin and BrdU expression. **A.** Proportion of BrdU incorporating cells with respect to total cell numbers. **B.** Proportion of nestin-expressing cells incorporating BrdU, with respect to the total number of nestin positive cells. Data represents mean ± SE based on a sample that represents 12 wells per condition from three different experiments. Comparisons between control and treatment is a Student's t-test (*, $p < 0.05$, **, $p < 0.01$, ***, $p < 0.001$)

3.4 Discussion

3.4.1: $CD4^+$ T lymphocytes must be in an activated state to increase hippocampal cell numbers through proliferative mechanisms

$CD4^+$ T lymphocytes supernatant has a proliferative effect on hippocampal cells. *In vivo*, there is strong evidence to suggest T lymphocyte modulation of hippocampal neurogenesis via unknown mechanisms (Wolf et al., 2009, Ziv et al., 2006). In this novel *in vitro* model, hippocampal neuronal cultures generated from (P7-10) Sprague Dawley rats were treated with supernatant derived from adult mice T lymphocytes cultures. It is well established that T lymphocytes are in a resting "naïve" state, in which they do not elicit their immune functions. The activation of T lymphocytes in this study design has demonstrated that $CD4^+$ T lymphocytes activation is a pre-requisite for T lymphocyte modulation of hippocampal neurogenesis.

Consistent with previously published work demonstrating a decrease in systemic $CD4^+$ T cells results in decreased hippocampal neurogenesis (Wolf et al., 2009), the data in this chapter shows $CD4^+$ T lymphocytes modulate hippocampal neurogenesis. Whilst treatment of hippocampal cells with T lymphocytes supernatant from naïve cultures did not change the total number of hippocampal cells - or indeed the population of nestin or TuJ1 expressing cells - T lymphocytes supernatant from cultures activated with anti-CD3 significantly increased the total number of hippocampal cells. Given that naïve supernatant would not be expected to comprise of cytokines released by T lymphocytes, these findings support the notion that activation of $CD4^+$ T lymphocytes triggers the release of cytokines and factors supportive of hippocampal neurogenesis.

There are four possible mechanisms by which activated T lymphocytes supernatant increase hippocampal cell numbers: (i) trophic effects (ii) increased proliferation (iii) recruitment of quiescent cells to divide or (iv) a combination. Initially the trophic effect of supernatant on hippocampal cells was investigated using the cell death marker propidium iodide. There was no difference in cell death under treatment with activated supernatant. Therefore the next mechanism investigated was the proliferative effect of supernatant on hippocampal cells. Using the

established proliferative marker BrdU to determine the number of cells undergoing proliferation during the S phase of the cell cycle (Morstyn et al., 1986), results showed an increase in the number of BrdU labelled cells.

In a set of experiments, the labelling index and growth fraction were determined to further investigate the effect of supernatant on hippocampal cells. Adapted from (Lu et al., 1996) and established in our lab as a protocol for determining cell kinetics, cells were treated with supernatant and stained for BrdU incorporation and Ki-67 expression. The growth fraction, calculated as the total number of Ki-67 positive cells divided by the total number of cells, was not altered under treatment with supernatant. However the labelling index, calculated as the number of BrdU incorporating cells expressing Ki-67 divided by the total number of Ki-67 positive cells, increased under treatment with supernatant. These results suggest that activated T lymphocytes supernatant increases the speed of the cell cycle but does not recruit quiescent cells.

3.4.2: Activated $CD4^+$ T lymphocytes supernatant is proliferative for hippocampal cells and their progeny

To further delineate the proliferative effects of activated T lymphocytes supernatant on hippocampal cells, immunohistochemical analysis was used to determine the effects on major cell phenotypes. The number of BrdU incorporating cells expressing nestin and TuJ1 increased significantly during a 6 hour treatment. This suggests supernatant enhances self-renewal by acting on nestin positive cells, whilst also having a neuroproliferative effect on TuJ1 positive cells. By speeding the cell cycle, as evident from data on labelling index, activated supernatant increases cell proliferation resulting in an overall increase in cell numbers. Treatment with activated supernatant over a 3 day period significantly increases the total number of nestin and TuJ1 positive cells under treatment with activated T lymphocytes supernatant. There was also a proportional increase, with respect to the total cell numbers, of each cell type. This suggests that the increase in total cell numbers by supernatant is attributed to the generation of newly generated neurons by proliferative mechanisms.

During hippocampal dissection, there is a risk of contamination from cells from other regions outwith the hippocampus. To confirm that the proliferative effect on cells was indeed representative of hippocampal dentate gyrus cells, the granule cell marker Prox1 (Iwano et al., 2012) was used in conjunction with TuJ1. Almost all TuJ1 positive cells were Prox1 positive, confirming the granule cell identity of these early neurons.

3.4.3: Activated $CD4^+$ T lymphocytes supernatant as a valid study paradigm to investigate neuro-immune modulation

Establishing a valid study paradigm for investigating neuro-immune modulation was imperative to this study. A $CD4^+$ isolation column kit was used to generate $CD4^+$ cultures from mouse spleen. Although the isolation kit is a fast and efficient technique to generate cultures, it does not produce a >95% purity of $CD4^+$ T lymphocytes. Studies usually report the use of flow cytometry following the use of an isolation kit to ensure >95% purity of cultures. The validation for using the isolation kit alone (without flow cytometry) for this study paradigm was two fold. Firstly, the data on naïve vs. activated T lymphocytes supernatant clearly demonstrated a need for CD3 activation to elicit neurogenic effects on hippocampal cultures. Given the specificity of anti-CD3 for T lymphocytes, this suggests that T lymphocytes are the mediators of the effects under treatment with supernatant. However, it could be argued that the activation of T lymphocytes could trigger a downstream effect on other cell populations within the culture that could potentially release mediators to increase hippocampal neurogenesis. To address this, pure $CD4^+$ cultures were generated using flow cytometry and compared to cultures without $CD4^+$ T lymphocytes and "all" cultures containing all the cell types. Each cell culture group was grown under control conditions or activated with anti-CD3 for 24 hours. The data clearly demonstrated that $CD4^+$ T lymphocytes are responsible for the supernatant effects on hippocampal cells; activated pure $CD4^+$ cultures and activated "all" cultures were the only two supernatant groups that replicated the effect to the same magnitude as observed under treatment with supernatant generated from the $CD4^+$ isolation kit. Activated cultures without $CD4^+$ did not have an effect on hippocampal cells. This data suggests the use of a $CD4^+$ isolation kit is a more productive method for generating $CD4^+$ T lymphocytes

supernatant to study neuro-immune modulation.

Under physiological conditions, T lymphocytes have been suggested to modulate hippocampal neurogenesis without infiltrating the brain (Kipnis et al., 2004, Wolf et al., 2009). Given the restrictive nature of the blood-brain barrier and evidence for T lymphocytes present in the meningeal spaces surrounding the brain (and a lack of evidence for T cells within the brain), this hypothesis seems logical yet remains undetermined. This study paradigm has been designed with this in mind and given the experimental results, it indeed suggests that T lymphocytes do not need to be present in the culture system to mediate their effects. Broadly speaking, this is suggestive of the notion that T lymphocytes do not need to be present in the hippocampal stem cell niche. Rather, the mediators they release must be present in the modulation of hippocampal neurogenesis and this in turn supports the idea for long distance communication between the stem cell niche and the adaptive immune system.

3.4.4: Chapter summary

The results of this chapter have highlighted the significance of T lymphocyte activation in modulating hippocampal neurogenesis in postnatal rat hippocampal cultures. Activated T lymphocytes supernatant acts via a proliferative mechanism, as indicated by studying the population of BrdU incorporating cells, the labelling index and growth fraction. Indeed, T lymphocytes supernatant increases cell proliferation by speeding the cell cycle of hippocampal cells, enhancing nestin, TuJ1 and Prox1 cell populations.

The use of a $CD4^+$ isolation kit to generate $CD4^+$ cultures from mouse spleen has been validated as a viable and more efficient alternative to generating cultures using flow cytometry Furthermore, the data from this chapter has established a novel study paradigm for investigating neuro-immune interactions in an unprecedented fashion, whilst supporting the idea that T lymphocytes do not need to be present for neurogenic regulation.

Chapter 4

Vasoactive Intestinal Peptide enhances activated $CD4^+$ T lymphocytes proliferative effect on hippocampal cells

4.1 Introduction

4.1.1: Introduction

Although originally identified as a vasodilator, VIP is now a well-established neuropeptide (Henning and Sawmiller, 2001). In fact, it is fast transitioning from a neuropeptide to a strong immune modulator. As such, VIP is shown to drive $CD4^+$ (or T helper (Th)) lymphocyte cell differentiation, and indeed is regarded by some as a Th2 cytokine itself (Pozo and Delgado, 2004). VIP is produced by most lymphocytes and also released by firing interneurons under certain high level frequencies (Martinez et al., 1999, Gomariz et al., 1994, Zaben et al., 2009). This biochemical messenger is a strong candidate for neuro-immune interactions that could potentially drive communication between the hippocampal neurogenic niche and immune cells.

4.1.2: VIP in the brain and a role in neurogenesis

VIP and its receptors are expressed throughout the brain (Dietl et al., 1990, Vertongen et al., 1997). VIP is implicated in regulation of synaptic transmission and also learning and memory (Itri and Colwell, 2003, Itoh et al., 1994). Removing VIP-producing cells causes learning deficits whilst VIP agonists have been shown to protect against impaired spatial learning (Gozes et al., 1993, Gozes et al., 1996). Similarly, VIP antagonists impair spatial learning and this has been further investigated in pregnant mice; injecting VIP antagonists into pregnant mice results in cognitive deficits in offspring (Glowa et al., 1992, Hill et al., 2007). VIP also modulates expression and secretion of neurotrophic factors. VIP is also important for neurogenesis and mediates its effects via both VPAC1 and VPAC2 receptors. It acts via VPAC2 receptors and alters proliferating precursor fate choice. In doing this, VIP expands the pool of symmetrically dividing dentate gyrus neural precursor cells, as well as having independent VPAC2 mediated trophic effects (Zaben et al., 2009). Interestingly, VIP acts on VPAC1 receptors to direct these cells towards a neuronal fate. *In vivo* models using VPAC2 knockout mice further substantiate these findings (Zaben et al., 2009). VIP has also been shown to promote hippocampal neuronal differentiation in embryonic cultures (Blondel et al., 2000). In its capacity as a neuromodulator, and also its ability to traverse the blood-brain barrier, VIP has been suggested as a candidate for future therapeutic purposes. Given its role in

neurogenesis and the brain, there is a potential role for VIP in neuro-immune modulation, with a particular focus on VIP's action on T lymphocytes

4.1.3: VIP receptors are present on T lymphocytes

T lymphocytes express all three VIP receptors. Whilst VPAC1 is constitutively expressed, VPAC2 and PAC1 expression is dynamic (Lara-Marquez et al., 2001, Ganea, 1996). Interestingly, VPAC2 expression is only induced in T lymphocytes following T cell receptor stimulation whereby these cells become "activated" (Delgado et al., 1996b). Following antigenic stimulation, $CD4^+$ T lymphocytes differentiate into Th1 and Th2 effector cells, subpopulations of $CD4^+$ T cells that are defined by their specific cytokine profiles (Mosmann et al., 1986). Indeed Th2 cells express significantly high levels of VPAC1 and VPAC2 receptors (Sharma et al., 2006). Delgado and colleagues have shown both a VPAC1 down regulation and VPAC2 upregulation on $CD4^+$ T lymphocytes following T cell activation. Th1/2 differentiation is determined by the antigen presenting cell, the antigen, the host species and of course the cytokine milieu itself (O'Garra, 1998). Our lab has found VPAC1 and PAC1 mRNA expression in our T lymphocytes cultures under naïve and activated conditions, whilst VPAC2 is undetected (see Appendix II).

4.1.4: VIP favours a Th2 phenotype

VIP has been shown to favour a Th2 phenotype (Delgado et al., 1999a, Delgado et al., 2004a, Voice et al., 2001), with *in vitro* studies demonstrating VIP-induced Th2 cytokine production in $CD4^+$ T lymphocytes (Delgado et al., 2004b). This is supported by *in vivo* studies demonstrating increased Th2 (IL-4 producing) cell numbers in immunized mice treated with VIP (Delgado et al., 1999a, Delgado et al., 2004b). Furthermore, studies from transgenic mice over-expressing VPAC2 show that endogenous VIP, which is recognized by $CD4^+$ T lymphocytes, is essential for their Th2 phenotype (Voice et al., 2003). It is of importance to note that in addition to driving a Th2 phenotype, VIP also inhibits Th1 differentiation (Delgado et al., 2004b). This bias towards a Th2 phenotype supports a role for VIP in anti-inflammatory cytokine production and a potentially beneficial role in neuro-immune modulation.

4.1.5: Aims and objectives

Although the relationship between T lymphocytes and VIP, VIP and neurogenesis and T lymphocytes and neurogenesis have all been investigated independently, this relationship has not been studied collectively to incorporate all three components of this neuro-immune paradigm. Given that VIP is able to cross the blood-brain barrier (Dogrukol-Ak et al., 2003), coupled with the fact that there is a lack of evidence for T lymphocytes present within the brain under physiological conditions, suggests that VIP is a potentially viable candidate for modulating cross talks between the brain and adaptive immune system. The aim of this chapter was therefore to establish a novel protocol to investigate the role of VIP in mediating hippocampal neurogenesis via T lymphocyte interactions.

4.2 Methods

VIP is a neuropeptide released by firing interneurons from within the hippocampal stem cell niche and its receptors are expressed on T lymphocytes. To investigate the role of VIP in neuro-immune coupling to modulate hippocampal neurogenesis, activated T lymphocytes were treated with VIP for 24 hours. The use of a physiological concentration of VIP (30nM) was two fold. Firstly, the effects of VIP under physiological conditions was under investigation. Secondly, 30nM VIP does not have proliferative effects on hippocampal cells in the primary rat hippocampal cultures (Zaben et al., 2009). Therefore, 30nM VIP can be used as a control to exclude VIP's direct effect on hippocampal cells. VIP pre-treated T lymphocytes supernatant was added to hippocampal cultures. Experimental conditions in this chapter are defined as treatment under standard control conditions, 5% activated supernatant, 30nM VIP added directly to hippocampal cultures and 30nM VIP pre-treated activated T lymphocytes supernatant. For pharmacological studies, further treatment groups are highlighted in methodological subsections.

4.2.1: Generation of primary rat hippocampal cultures

For each experiment, 6-10 Sprague-Dawley rat pups aged P7-10 were used to generate primary hippocampal cultures as detailed in *section 2.1.* Viable cells were plated at a density of 100, 000 cells/mL directly on to poly-L-lysine coated coverslips in 24-well plates. At 2 hours post-plating, cells were washed to remove residual debris and replenished with fresh NBA/B-27/glutamine medium supplemented with antibiotic/antimycotic. Cells were grown under control or treatment conditions as per experimental requirements (5%CO_2/9%O_2/37°C incubator conditions).

4.2.2: Generation and VIP treatment of cells isolated using the $CD4^+$ T lymphocyte isolation kit

For each experiment, 4 spleens were used from adult mice to generate $CD4^+$ T lymphocytes cultures as detailed in *section 2.2*. Following a multi-step protocol as part of a $CD4^+$ isolation kit, viable cells were plated at a density of 1, 000, 000 cells/mL directly on to poly-L-lysine coated 24 well plates. 1µg/mL of anti-CD3 was added at plating to activate cells. For VIP activation, splenocytes were treated with

30nM VIP at plating simultaneously during the addition of anti-CD3. Cells were grown in standard culture medium (NBA/B-27/glutamine) supplemented with antibiotic/antimycotic for 24 hours (5%CO_2/9%O_2/37°C incubator conditions) and then supernatant was collected and stored at -20°C until required.

4.2.3 Isolating cell populations from the spleen by flow cytometry

3 spleens were used from adult mice to generate three populations of cultures: pure $CD4^+$ T lymphocytes, splenocytes without $CD4^+$ T lymphocytes and splenocytes with $CD4^+$ T lymphocytes. Spleens were collected and stained for flow cytometric sorting following a multi-step protocol as detailed in *section 2.3.* Cells were treated with a fixable dead cell staining kit (LIVE/DEAD Aqua; 1:10 in PBS) to identify dead cells for flow cytometric analysis. The fluorescent reactive dye in the kit enters compromised membranes, reacts with free amides and fluoresces intensely. The dye also reacts with cell surface amines but with much less intensity. Therefore viable cells that do not allow the dye to enter the cell produce a much weaker fluorescence signal. Fc receptors were blocked for 10 minutes at 4°C using 5ug/mL anti-CD16/32 antibodies. Fc receptors are glycoproteins found on blood cells (B cells, tissue macrophages) that have high affinity for Fc regions of monomeric IgG and therefore can cause non-specific binding and high background staining. To minimise this, Fc receptors were blocked Cells were the stained with antibodies for CD3 and CD4 diluted in FACS buffer. Samples were acquired using a FACS Aria III cytometer (BD Biosciences) with BD FACSDiva 7.0 software. Each spleen sample was analysed using the same gating strategy *(section 2.3.3)*. Once the samples were collected in standard culture medium supplemented with antibiotic/antimycotic, cells were plated as before (*section 3.2.2*) on 24 well plates for 24 hours (5%CO_2/9% O_2/37°C incubator conditions) under control or treatment conditions. Within each sorted group, cells were treated under the following conditions: “naïve” untreated, “activated” with anti-CD3, “activated” with anti-CD3 and treated with 30nM VIP. Supernatant was then collected and stored at -20°C until required.

4.2.4: Studying VIP pre-treated supernatant effect on cell proliferation

The thymidine analogue BrdU is incorporated into cells during the S-phase of the cell cycle and therefore used to specifically label dividing cells (Taupin, 2007). BrdU

is used to calculate the mitotic index, which is indicative of the total number of cells transitioning from the S phase to the G2 phase of the cell cycle. The mitotic index is the number of BrdU positive cells with respect to total number of cells (DAPI positive cells). Cell proliferation was investigated by the addition of a final concentration of 20μM BrdU at 3DIV for the terminal 6 hours. The following experimental conditions were added at the same time point: standard control conditions, 5% activated supernatant, 30nM VIP added directly to hippocampal cultures and 30nM VIP pre-treated activated T lymphocytes supernatant. Cells were then fixed in 4% PFA for 30 minutes at 4°C. Cells were washed with PBS before being processed for BrdU incorporation. Specific cell markers nestin (putative progenitor cell markers) and TuJ1 (neuronal marker) were used during processing by immunohistochemistry to investigate proliferation of these cell types. The total numbers and proportions of each specific marker were determined.

4.2.5: Defining VIP pre-treated supernatant effect on the labelling index and growth fraction

Ki-67 is an endogenous proliferative marker expressed by cells during the active phases of the cell cycle (G1, G2, M phase) and used to determine the labelling index or growth fraction. The labelling index is calculated as the number of Ki-67 expressing cells incorporating BrdU over the total number of Ki-67 positive cells. The growth fraction is calculated as the number of Ki-67 positive cells over the total number of DAPI positive cells. This allows us to determine whether proliferative effects are due to speeding of the cell cycle (labelling index) or recruitment of quiescent cells (growth fraction). Cells were grown under control conditions for 3DIV. Experimental conditions and 20μM BrdU were added for the terminal 6 hours. Cells were then fixed in 4% PFA for 30mins at 4°C. Cells were washed with PBS before being processed for BrdU incorporation and Ki-67 expression to determine the labelling index and growth fraction.

4.2.6: Characterising the effect of VIP pre-treated supernatant on cell-specific phenotypes

To characterize cell-specific phenotypes, cultures were treated with experimental conditions over time. In these set of experiments, cells were grown under control

conditions for 3DIV and then replaced with treatment conditions for 3 days. At 6DIV cells were fixed in 4% PFA for 30 minutes at 4°C and washed with PBS before being processed for nestin and TuJ1 expression. The total numbers and proportions of each cell marker were determined.

4.2.7: Studying VIP receptor mediation

To determine the VIP receptor responsible for splenocyte modulation of hippocampal proliferation, a selective VPAC1 receptor agonist [Lys^{15}, Arg^{16}, Leu^{27}]-VIP (1-7) - GRF (8-27) and selective VPAC1 receptor antagonist [Ac-His^{1}, D-Phe^{2}, Lys^{15}, Arg^{16}, Leu^{27}]-VIP (1-7)-GRF (8-27) were used at a concentration of 1μM, which has been previously documented (Gourlet et al., 1997, Pandol et al., 1986, Zaben et al., 2009, Moody et al., 2001, Moody et al., 1993). For VPAC1 agonist experiments, cells were grown under control conditions for 3DIV and treated for the terminal 6 hours before fixation. Treatment conditions were standard control conditions, 5% activated supernatant, 30nM VIP added directly to hippocampal cultures and 30nM VIP pre-treated activated T lymphocytes supernatant standard treatment conditions, 5% T lymphocytes supernatant pre-treated with 1μM VPAC1 agonist, 1μM VPAC1 agonist added directly to hippocampal cultures. For VPAC1 antagonist experiments, cells were grown under control conditions for 3DIV and treated for the terminal 6 hours under standard control conditions, 5% activated supernatant, 30nM VIP added directly to hippocampal cultures and 30nM VIP pre-treated activated T lymphocytes supernatant, 5% T lymphocytes supernatant pre-treated with 1μM VPAC1 antagonist, 5% T lymphocytes supernatant pre-treated with 30nM VIP and 1μM VPAC1 antagonist and 1μM VPAC1 antagonist added directly to hippocampal cultures.

4.2.8: Imaging and statistical analysis

Images were taken on a DM RBE microscope (Leica Microsystems Limited) at 20x magnification. Six systemically randomized fields per well were taken using the Leica Application Suite image-capturing system version 3.8.0. Data was averaged per well and expressed in cells/mm^2 or as a percentage, based on a sample of 4 wells per condition per experiment. All experiments were repeated a minimum of three times. Graph Pad prism data analysis software (GraphPad Inc, San Diego, CA,

USA) was used to plot data points. For statistical comparisons a one-way ANOVA was used with Bonferroni correction for multiple comparisons ($p < 0.05$ considered significant).

4.3 Results

4.3.1: Pre-treatment of splenocytes with VIP further enhances total hippocampal cell numbers

Given the potent neuromodulatory effects of the neuropeptide VIP and the expression of VIP receptors on T cells (Ganea, 1996, Lara-Marquez et al., 2001), the effect of VIP treatment of T lymphocytes in regulating neurogenesis was investigated. Cultures were generated using the isolation kit as previously described (*section 2.2*) and treated with 30nM VIP. Hippocampal cultures were generated under standard control conditions for 3DIV and treated with experimental conditions until 6DIV. Experimental conditions were standard control conditions, 5% activated supernatant, 30nM VIP added directly to hippocampal cultures, 30nM VIP pre-treated activated T lymphocytes supernatant. The addition of 30nM VIP directly into hippocampal cultures accounts for the effects of residual VIP that may be present in VIP pre-treated supernatant. Cells were stained with DAPI to measure total cell counts **(Figure 29)**. There was a difference between control and treatment groups ($f(3,44)=547$). There was an increase in total cell numbers under treatment with 5% supernatant pre-treated with VIP compared to control (201.0 ± 1.87 vs. 138.3 ± 1.09; $p < 0.001$). There was an increase in total cell numbers under treatment with 5% supernatant compared to control (167 ± 0.97 vs. 138.3 ± 1.09; $p < 0.001$). Of note, the increase in total cell numbers was enhanced under treatment with 5% supernatant pre-treated with VIP compared to treatment with 5% supernatant alone (201.0 ± 1.87 vs. 167 ± 0.97; $p < 0.001$). Consistent with previous findings, treatment with 30nM VIP alone did not increase total cell numbers compared to control (137.8 ± 0.9616 vs. 138.3 ± 1.09; p = n.s.). These results suggest VIP has a direct effect on splenocytes that enhances the effect on total hippocampal cell numbers.

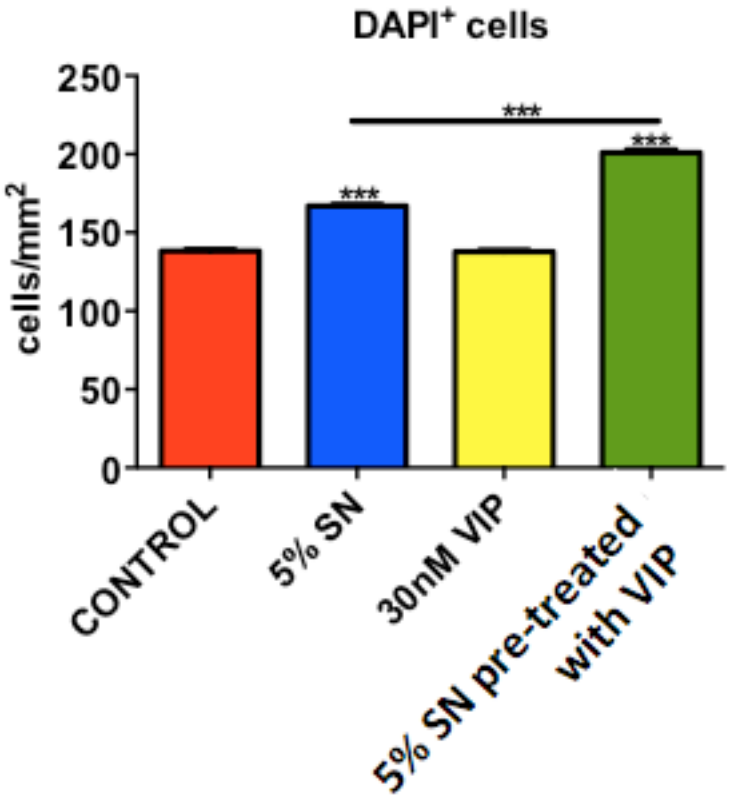

Figure 29: Pre-treatment of splenocytes with VIP further enhances total hippocampal cell numbers. Hippocampal cells were generated under control conditions for 3DIV and then treated with experimental conditions until 6DIV. Cells were stained with DAPI to measure total cell counts. Data represents mean ± SE based on a sample that represents 12 wells per condition from 3 different experiments. Comparisons between control and treatment conditions are a one-way ANOVA with Bonferroni correction for multiple comparisons (*, $p < 0.05$, **, $p < 0.01$, ***, $p < 0.001$)

4.3.2: Pre-treatment of splenocytes with VIP further enhances the mitotic index of hippocampal cells

To determine whether the VIP pre-treated supernatant increase in hippocampal cell numbers was due to proliferative effects, as observed under treatment with activated supernatant alone, the proliferative marker BrdU was used. BrdU specifically label dividing cells and calculate the mitotic index, which is indicative of the total number of cells transitioning from the S phase to the G2 phase of the cell cycle (Taupin, 2007). This is calculated as the number of BrdU positive cells with respect to total number of cells (DAPI positive cells). Hippocampal cultures were generated for 3DIV under standard control conditions. Cells were pulsed with BrdU and treated under standard control conditions, 5% activated supernatant, 30nM VIP added directly to hippocampal cultures, 30nM VIP pre-treated activated T lymphocytes supernatant for the terminal 6 hours before fixation. There was a

difference between control and experimental conditions (f(3, 44)=148). There was a significant increase in the mitotic index following treatment with 5% supernatant pre-treated with VIP compared to control (0.25 ± 0.007 vs. 0.12 ± 0.003, p < 0.001) **(Figure 30 B)**. There was also an increase in the mitotic index following treatment with 5% supernatant alone compared to control (0.18 ± 0.005 vs. 0.12 ± 0.003, p < 0.001). The increase under treatment with 5% supernatant pre-treated with VIP was enhanced compared to treatment with 5% supernatant alone (0.25 ± 0.007 vs. 0.18 ± 0.005, p < 0.001). Consistent with previous findings (Zaben et al., 2009), treatment with 30nM VIP alone did not increase the mitotic index compared to control (0.12 ± 0.004 vs. 0.12 ± 0.003, p = n.s.). There was no change in total cell numbers across experimental conditions (f(3,44)=0.052, p = n.s.) **(Figure 30 A)**. These results suggest VIP enhances the proliferative effect on hippocampal cells.

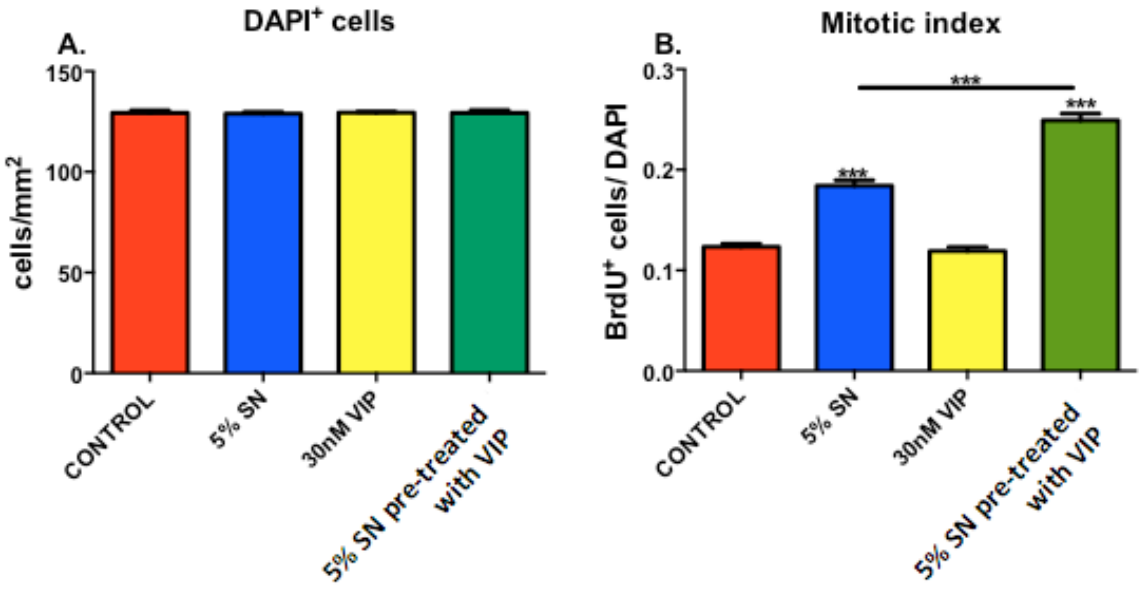

Figure 30: Pre-treatment of splenocytes with VIP further enhances the mitotic index of hippocampal cells. Hippocampal cells were generated under control conditions for 3DIV. BrdU and treatment conditions were added for the terminal 6 hours before fixation. Cells were immunostained for BrdU incorporation. **A.** Total cell counts as measured by the number of DAPI positive cells. **B.** Proportion of BrdU incorporating cells, with respect to total number of cells. Data represents mean ± SE based on a sample that represents 12 wells per condition from 3 different experiments. Comparisons between control and treatment conditions are a one-way ANOVA with Bonferroni correction for multiple comparisons (*, p < 0.05, **, p < 0.01, ***, p < 0.001)

4.3.3: Pre-treatment of splenocytes with VIP further enhances proliferation of nestin-expressing hippocampal cells

The proliferative effect of VIP pre-treated supernatant on nestin-expressing hippocampal cells was investigated. Hippocampal cultures were generated for 3DIV under standard control conditions. Cells were pulsed with BrdU and treated under standard control conditions, 5% activated supernatant, 30nM VIP added directly to hippocampal cultures, 30nM VIP pre-treated activated T lymphocytes supernatant for the terminal 6 hours before fixation. There was a difference between control and experimental groups ($f(3,44)=83$) **(Figure 31 B)**. There was an increase in the proportion of nestin-expressing cells incorporating BrdU, with respect to the total nestin population, following treatment with 5% supernatant pre-treated with VIP compared to control (0.39 ± 0.07 vs. 0.15 ± 0.007, $p < 0.001$) **(Figure 31 B)**. There was also an increase in cultures treated with 5% supernatant alone compared to control (0.23 ± 0.02 vs. 0.15 ± 0.007, $p < 0.001$). The increase in cultures treated with 5% supernatant pre-treated with VIP was enhanced compared to 5% supernatant treatment alone (0.39 ± 0.07 vs. 0.23 ± 0.02, $p < 0.001$). Consistent with previous findings (Zaben et al., 2009), there was no change between VIP treatment of hippocampal cultures and control (0.15 ± 0.005 vs. 0.15 ± 0.007, p = n.s.). There was no change in total nestin cell counts, with respect to total cell numbers, across experimental conditions ($f(3,44)=0.58$, p = n.s.) **(Figure 31 A)**. These results suggest VIP enhances the proliferative effect on nestin-expressing hippocampal cells.

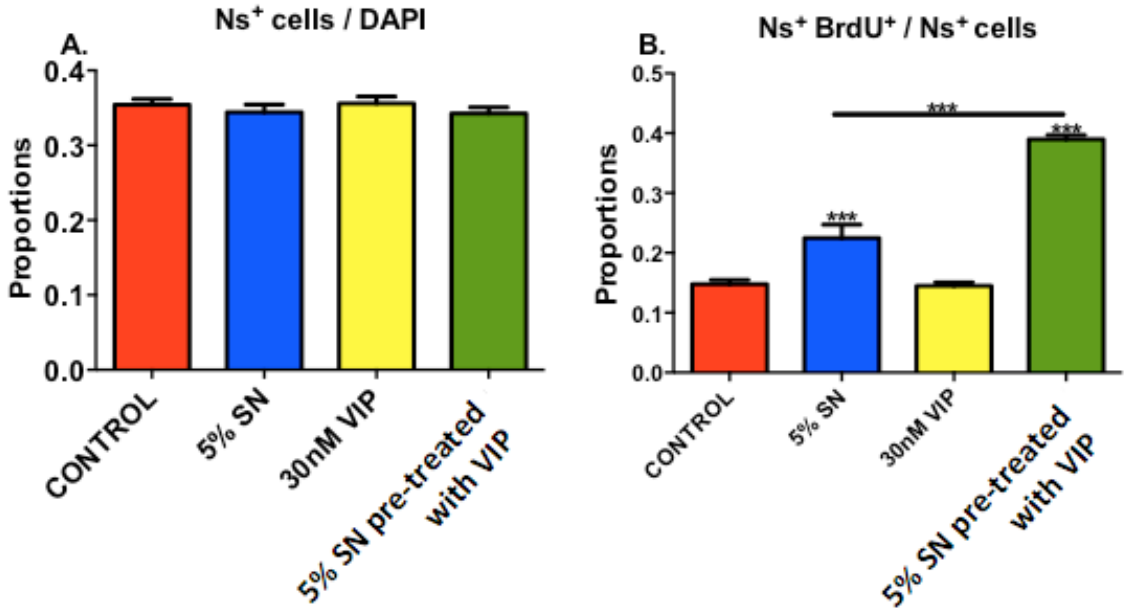

Figure 31: Pre-treatment of splenocytes with VIP further enhances proliferation of nestin-expressing hippocampal cells. Hippocampal cells were generated under control conditions for 3DIV. BrdU and treatment conditions were added for the terminal 6 hours before fixation. Cells were immunostained for BrdU incorporation and nestin expression. **A.** Total number of nestin positive cells with respect to total cell numbers. **B.** Proportion of nestin-expressing cells incorporating BrdU, with respect to total number of nestin positive cells. Data represents mean ± SE based on a sample that represents 12 wells per condition from 3 different experiments. Comparisons between control and treatment conditions are a one-way ANOVA with Bonferroni correction for multiple comparisons (*, $p < 0.05$, **, $p < 0.01$, ***, $p < 0.001$)

4.3.4: Flow cytometry confirms VIP acts on activated CD4+ T lymphocytes to increase proliferation of hippocampal cells

Flow cytometry was used to determine whether the observed effects were due to VIP activity on activated CD4+ T lymphocytes. In Chapter 3, flow cytometry was used to generate pure CD4+ T lymphocytes cultures and subsequently establish that anti-CD3 activated T lymphocytes supernatant is responsible for increased proliferation of nestin-expressing hippocampal cells. Similarly, it was necessary to confirm whether the enhanced proliferative effect of nestin-expressing cells under treatment with 5% supernatant pre-treated with VIP was due to the direct action of CD4+ T lymphocytes. Splenic populations were sorted into three groups using flow cytometry: CD4+ cells, splenocytes without CD4+ cells, splenocytes with CD4+ cells. Flow cytomtery software (BDFacs Diva) was used to determine the ratio of CD4+ T lymphocytes to all other splenocytes (1:4). Cells were pooled together from both samples according to this ratio and placed into a fresh tube to produce splenocytes with CD4+ cells. Within each group, these cells were generated for 24 hours under

the following conditions: “naïve” untreated conditions, “activated” with anti-CD3, “activated” with anti-CD3 and treated with 30nM VIP. Hippocampal cultures were generated for 3DIV and treated with BrdU and experimental conditions for the terminal 6 hours before fixation. Cells were immunostained for Brdu and nestin expression. There was a change in the mitotic index across the experimental groups ($f(10,121)=1.2$) **(Figure 32 A)**. There was an increase in the mitotic index of hippocampal cultures treated with activated $CD4^+$ T lymphocytes supernatant pre-treated with VIP compared to control (0.22 ± 0.005 vs. 0.14 ± 0.003, $p < 0.001$). There was also an increase in the mitotic index of hippocampal cells under treatment with activated $CD4^+$ T lymphocytes supernatant compared to control (0.19 ± 0.002 vs. 0.14 ± 0.003, $p < 0.001$). The effect under treatment with activated $CD4^+$ T lymphocytes supernatant pre-treated with VIP was enhanced compared to activated $CD4^+$ T lymphocytes supernatant alone (0.22 ± 0.005 vs. 0.19 ± 0.002, $p < 0.001$). There was no change in the mitotic index under other treatment conditions.

The same pattern of change was observed in the proportion of BrdU incorporating cells expressing nestin, with respect to the total number of nestin cells ($f(10,121)=3.4$) **(Figure 32 B)**. There was an increase in the proportion under treatment with activated $CD4^+$ T lymphocytes supernatant pre-treated with VIP compared to control (0.23 ± 0.005 vs. 0.14 ± 0.003, $p < 0.001$). There was also an increase in the proportion under treatment with activated $CD4^+$ T lymphocytes supernatant alone compare to control (0.20 ± 0.003 vs. 0.14 ± 0.003, $p < 0.001$). The increase under activated $CD4^+$ T lymphocytes supernatant pre-treated with VIP was enhanced compared to activated $CD4^+$ T lymphocytes supernatant alone (0.23 ± 0.005 vs. 0.20 ± 0.003, $p < 0.001$). There was no change in the mitotic index under other treatment conditions. Taken together, these results suggest VIP acts directly on activated $CD4^+$ T lymphocytes to release mediators that enhance the proliferative effect of activated $CD4^+$ T lymphocytes supernatant.

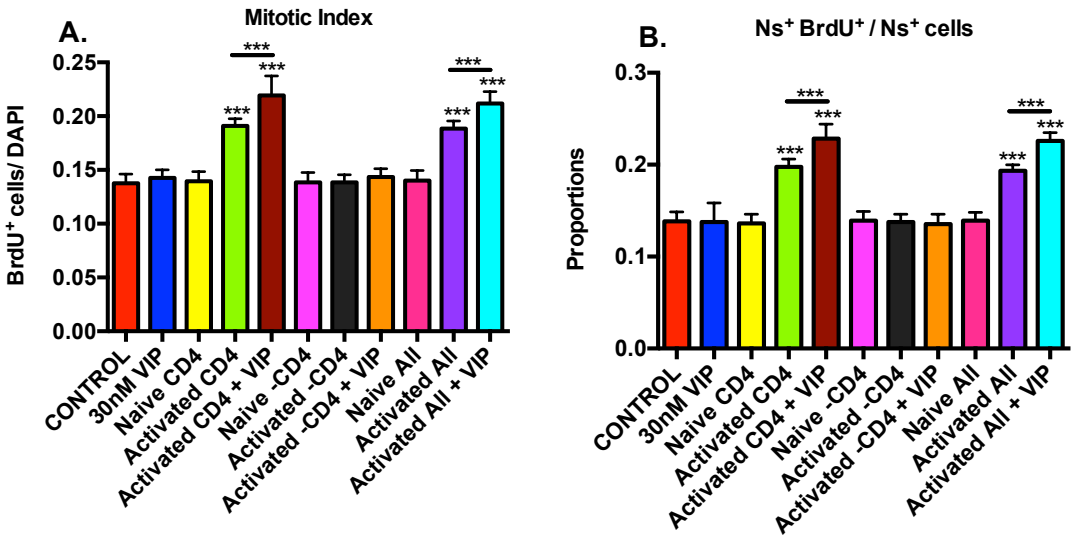

Figure 32: Flow cytometry confirms VIP acts on activated CD4+ T lymphocytes to increase proliferation of hippocampal cells. Hippocampal cells were generated under control conditions for 3DIV. BrdU and treatment conditions were added for the terminal 6 hours before fixation. Cells were immunostained for BrdU incorporation and nestin expression. **A.** Proportion of BrdU incorporating cells, with respect to total cell numbers. **B.** Proportion of nestin-expressing cells incorporating BrdU, with respect to total number of nestin positive cells. Data represents mean ± SE based on a sample that represents 12 wells per condition from 3 different experiments. Comparisons between control and treatment conditions are a one-way ANOVA with Bonferroni correction for multiple comparisons (*, $p < 0.05$, **, $p < 0.01$, ***, $p < 0.001$)

4.3.5: Pre-treatment of splenocytes with VIP further enhances proliferation of neuronal class III β-tubulin expressing hippocampal cells

To investigate the effect of T lymphocytes supernatant pre-treated with VIP on TuJ1-expressing hippocampal cells, hippocampal cultures were generated for 3DIV under standard control conditions. Cells were pulsed with BrdU and treated under standard control conditions, 5% activated supernatant, 30nM VIP added directly to hippocampal cultures, 30nM VIP pre-treated activated T lymphocytes supernatant for the terminal 6 hours before fixation. Cultures were immunostained for BrdU and TuJ1 expression. There was a difference between control and experimental conditions ($f(3,44)=83$). There was an increase in the proportion of TuJ1-expressing cells incorporating BrdU, with respect to the total population of TuJ1-expressing cells, following treatment with 5% T lymphocytes supernatant pre-treated with VIP compared to control (0.16 ± 0.006 vs. 0.078 ± 0.004, $p < 0.001$) **(Figure 33 B)**. There was also an increase in cultures treated with 5% supernatant alone compared to control (0.14 ± 0.004 vs. 0.078 ± 0.004, $p < 0.001$). The increase under treatment with 5% supernatant pre-treated with VIP was enhanced compared to 5%

supernatant treatment alone (0.16 ± 0.006 vs. 0.14 ± 0.004, $p < 0.01$). There was no change between VIP treated hippocampal cultures and control conditions (0.07 ± 0.005 vs. 0.08 ± 0.004, p = n.s.). There was also no change in total TuJ1 counts, with respect to total cell numbers, across experimental conditions ($f(3,44)=0.083$, p = n.s.) **(Figure 33 A)**. These results suggest VIP enhances the proliferative effect on TuJ1-expressing hippocampal cells.

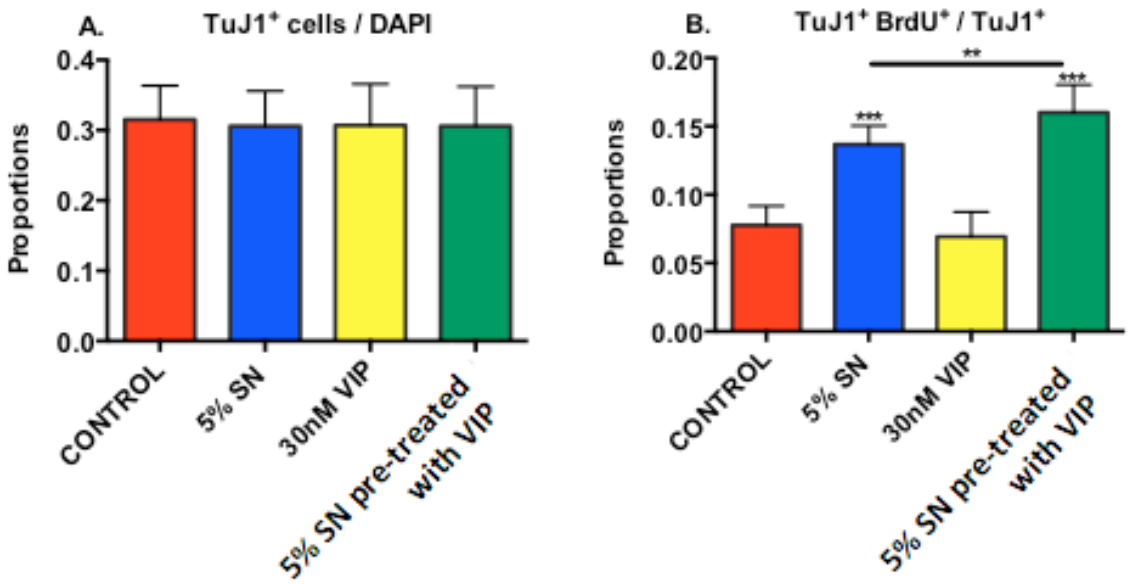

Figure 33: Pre-treatment of splenocytes with VIP further enhances proliferation of neuronal class III β-tubulin expressing hippocampal cells. Hippocampal cells were generated under control conditions for 3DIV. BrdU and treatment conditions were added for the terminal 6 hours before fixation. Cells were immunostained for BrdU incorporation and TuJ1 expression. **A.** Total number of TuJ1 positive cells with respect to total cell numbers. **B.** Proportion of TuJ1-expressing cells incorporating BrdU, with respect to total number of nestin positive cells. Data represents mean ± SE based on a sample that represents 12 wells per condition from 3 different experiments. Comparisons between control and treatment conditions are a one-way ANOVA with Bonferroni correction for multiple comparisons (*, $p < 0.05$, **, $p < 0.01$, ***, $p < 0.001$)

4.3.6: Pre-treatment of splenocytes with VIP further enhances the rate of cell proliferation of hippocampal cells

To determine whether proliferative effects were due to speeding of the cell cycle (labelling index), as observed under treatment with activated supernatant, or recruitment of quiescent cells (growth fraction), the endogenous proliferative marker Ki-67 was used. Ki-67 is expressed by cells during the active phases of the cell cycle and calculated as the proportion of cycling precursor cells (Ki-67 positive) with respect to the total number of cells (DAPI). When used with BrdU, the labelling

index is determined by the proportion of Ki-67 expressing cells incorporating BrdU with respect to Ki-67 positive cells. Hippocampal cells were grown for 3DIV under standard control conditions. Cells were pulsed with BrdU and treated under standard control conditions, 5% activated supernatant, 30nM VIP added directly to hippocampal cultures, 30nM VIP pre-treated activated T lymphocytes supernatant for the terminal 6 hours before fixation. Cells were stained for BrdU and Ki-67 expression to determine the growth fraction and labelling index. There was no change in the growth fraction (Ki-67$^+$/DAPI cells) across experimental conditions ($f(3,44)=0.96$, p = n.s.) **(Figure 34 A)**. However there was a change in the labelling index (BrdU$^+$Ki-67$^+$/Ki-67$^+$) across experimental groups ($f(3,44)=0.30$) **(Figure 34 B)**. There was an increase in the labelling index under treatment with 5% supernatant pre-treated with VIP compared to control (0.22 ± 0.002 vs. 0.14 ± 0.003, $p < 0.001$). There was also an increase under treatment with 5% supernatant compared to control (0.19 ± 0.003 vs. 0.14 ± 0.003, $p < 0.001$). The treatment with 5% supernatant pre-treated with VIP has an enhanced effect compared to treatment with 5% supernatant alone (0.22 ± 0.002 vs. 0.19 ± 0.003, $p < 0.001$). There was no change under treatment with 30nM VIP alone compared to control (0.14 ± 0.002 vs. 0.14 ± 0.003, p = n.s.). These results suggest 5% supernatant pre-treated with VIP enhances the increased rate of cell proliferation.

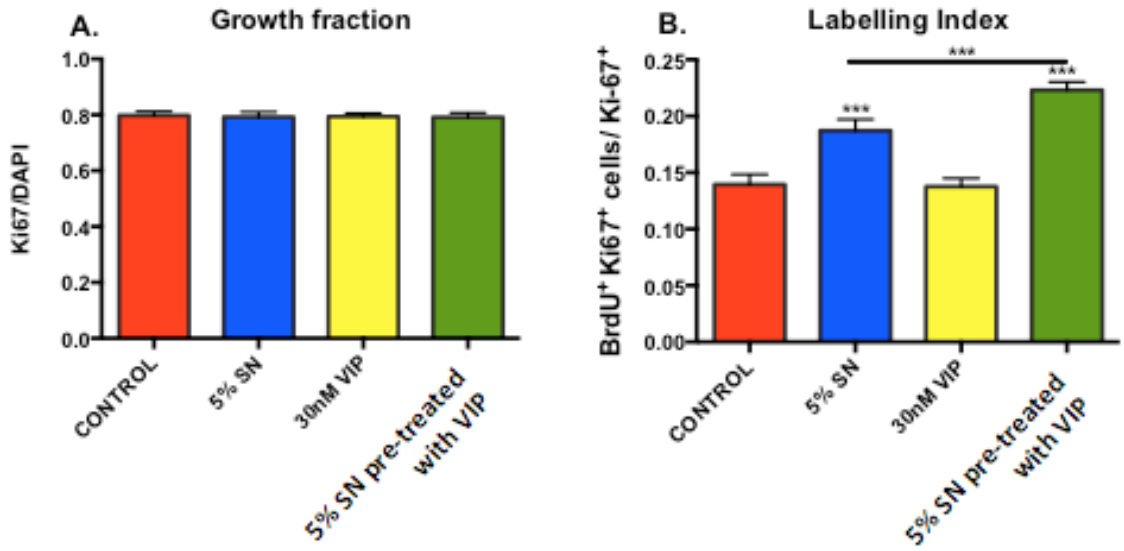

Figure 34: Pre-treatment of splenocytes with VIP enhances the increased rate of cell proliferation. Hippocampal cells were generated under control conditions for 3DIV. BrdU and experimental conditions were added for the terminal 6 hours before fixation.. Cells were immunostained for BrdU incorporation and Ki-67 expression. **A.** Proportion of Ki-67 positive cells with respect to total cell numbers. **B.** Proportion of BrdU incorporating cells, with respect to the total number of Ki-67positive cells. Data represents mean ± SE based on a sample that represents 12 wells per condition from three different experiments. Comparisons between control and treatment conditions are a one-way ANOVA with Bonferroni correction for multiple comparisons (*, $p < 0.05$, **, $p < 0.01$, ***, $p < 0.001$)

4.3.7: Pre-treatment of splenocytes with VIP further enhances neurogenic fate determination

In a set of experiments, the overall effect of T lymphocytes supernatant was investigated. Hippocampal cultures were generated under control conditions for 3DIV. Cells were treated under standard control conditions, 5% activated supernatant, 30nM VIP added directly to hippocampal cultures, 30nM VIP pre-treated activated T lymphocytes supernatant until 6DIV. Cultures were fixed and processed for nestin and TuJ1 expression. There was a difference between control and experimental conditions ($f(3,44)=191$). There was an increase in the proportion of nestin positive cells, with respect to total cell numbers, under treatment with 5% supernatant pre-treated with VIP compared to control (0.63 ± 0.012 vs. 0.40 ± 0.008, $p < 0.001$) **(Figure 35 D)**. There was also an increase under treatment with 5% supernatant alone compared to control (0.47 ± 0.002 vs. 0.40 ± 0.008, $p < 0.001$). The increase under 5% supernatant pre-treated with VIP was enhanced compared to 5% supernatant treatment alone (0.63 ± 0.012 vs. 0.47 ± 0.002, $p < 0.001$). There was no increase under VIP treatment of hippocampal cultures compared to control (0.40 ± 0.005 vs. 0.40 ± 0.008; p = n.s.).

There was a difference between control and experimental conditions in the proportion of TuJ1 positive cells, with respect to total cell numbers ($f(3,44)=89$). The same trend was observed under treatment with 5% supernatant pre-treated with VIP compared to control (0.19 ± 0.005 vs. 0.10 ± 0.005, $p < 0.001$) **(Figure 35 F)**. Again, there was an increase under treatment with 5% supernatant compared to control (0.15 ± 0.003 vs. 0.10 ± 0.005, $p < 0.001$). The increase under treatment with 5% supernatant pre-treated with VIP was enhanced compared to 5% supernatant treatment alone (0.19 ± 0.005 vs. 0.15 ± 0.003, $p < 0.001$). There was no change under VIP treatment of hippocampal cells compared to control (0.096 ± 0.004 vs. 0.10 ± 0.005, p = n.s.).

There was also a difference in the proportion of nestin positive cells expressing TuJ1, with respect to total cell numbers, between control and experimental conditions ($f(3,44)=215$). There was an increase under treatment with 5% supernatant pre-treated with VIP compared to control (0.14 ± 0.004 vs. $0.048 \pm$

0.003, $p < 0.001$) **(Figure 35 B)**. There was also an increase under 5% supernatant treatment alone compared to control (0.088 ± 0.001 vs. 0.048 ± 0.003, $p < 0.001$). The increase under 5% supernatant pre-treated with VIP was enhanced compared to 5% supernatant alone (0.14 ± 0.004 vs. 0.088 ± 0.001, $p < 0.001$). There was no change under VIP treatment of hippocampal cells (0.049 ± 0.002 vs. 0.048 ± 0.003, p = n.s.). Taken together, these results suggest VIP pre-treatment of splenocytes enhances the total number of cells in culture and drives a greater number of progenitor cells towards a neuronal fate.

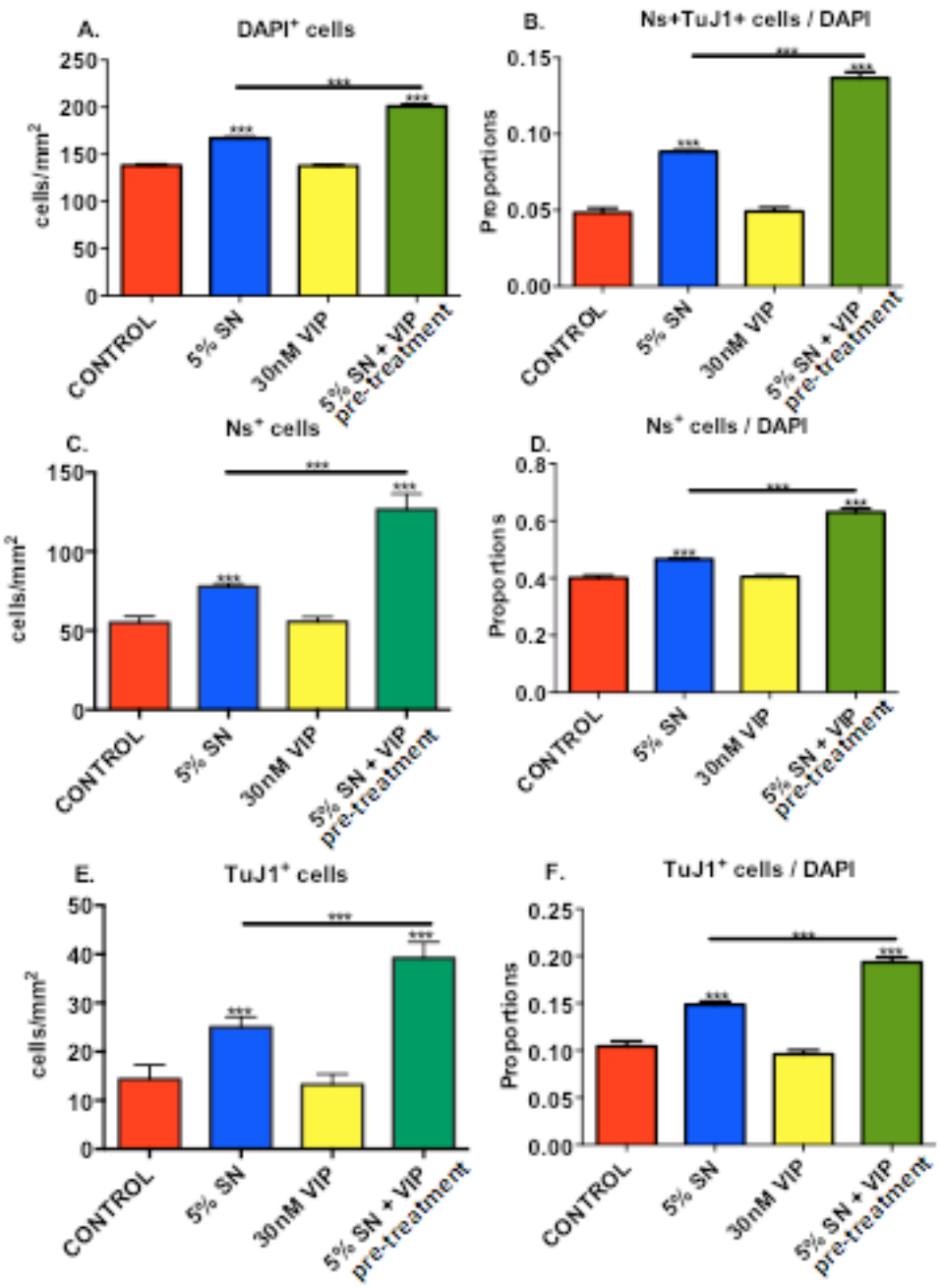

Figure 35: Pre-treatment of splenocytes with VIP further enhances neurogenic fate determination. Hippocampal cells were generated under control conditions for 3DIV and then treated with experimental conditions until 6DIV. Cells were immunostained for nestin and TuJ1 expression. **A.** Total cell counts as measured by the number of DAPI positive cells. **B.** Proportion of nestin cells expressing TuJ1, with respect to total number of cells **C.** Total number of nestin expressing cells **D.** Proportion of nestin cells **E.** Total number of TuJ1 cells and **F.** Proportion of TuJ1 cells. Data represents mean ± SE based on a sample that represents 12 wells per condition from three different experiments. Comparisons between control and treatment conditions are a one-way ANOVA with Bonferroni correction for multiple comparisons (*, $p < 0.05$, **, $p < 0.01$, ***, $p < 0.001$)

4.3.8: Pre-treatment of splenocytes with VIP increases the proportion of class III β-tubulin positive cells co-expressing Prox1

To determine if the TuJ1-expresing (immature neuronal) cells were dentate gyrus specific, the granule cell marker Prox1 was used (Iwano et al., 2012). Postmitotically, Prox1 specifies dentate granule cells and eliminating it causes immature dentate gyrus neurons to loose their granule cell identity and instead differentiate into neurons with CA3 identity (Iwano et al., 2012). Hippocampal cultures were generated under control conditions for 3DIV and then treated with experimental conditions until 6DIV. Cells were fixed and processed for TuJ1 and Prox1 expression. There was an increase in the total cell numbers across experimental conditions ($f(3, 44)=11$) **(Figure 36 A)**. There was an increase in the total cell number under treatment with 5% supernatant pre-treated with VIP compared to control (198.7 ± 1.27 vs. 138.1 ± 0.39, $p < 0.001$). There was also an increase under treatment with 5% supernatant alone compared to control (164.9 ± 0.45 vs.138.1 ± 0.39, $p < 0.001$). The increase under treatment with 5% supernatant pre-treated with VIP was enhanced compared to 5% supernatant alone (198.7 ± 1.27 vs. 164.9 ± 0.45, $p < 0.001$). There was no change under treatment with 30nM VIP alone compared to control (137.4 ± 0.42 vs. 138.1 ± 0.39, p = n.s.).

The same pattern of change across experimental conditions was observed in the number of TuJ1 cells ($f(3,44)=1.4$) **(Figure 36 C)**. There was an increase in TuJ1 numbers under treatment with 5% supernatant pre-treated with VIP compared to control (39.30 ± 0.73 vs. 15.78 ± 0.38, $p < 0.001$). There was also an increase under treatment with 5% supernatant compared to control (26.55 ± 0.45 vs. 15.78 ± 0.38, $p < 0.001$). The increase under treatment with 5% supernatant pre-treated with VIP was enhanced compared to 5% supernatant alone (39.30 ± 0.73 vs. 26.55 ± 0.45, $p < 0.001$). There was no change under treatment with 30nM VIP alone (15.21 ± 0.26 vs. 15.78 ± 0.38, p = n.s).

There was a change in the proportion of TuJ1 positive cells, with respect to total cell numbers, across experimental conditions ($f(3,44)=0.73$) **(Figure 36 D)**. There was an increase in the proportion of TuJ1 positive cells under treatment with 5% supernatant pre-treated with VIP compared to control (0.20 ± 0.004 vs. 0.11 ±

0.003, $p < 0.001$). There was also an increase under treatment with 5% supernatant compared to control (0.16 ± 0.002 vs. 0.11 ± 0.003, $p < 0.001$). The increase under treatment with 5% supernatant pre-treated with VIP was enhanced compared to 5% supernatant alone (0.20 ± 0.004 vs. 0.16 ± 0.002, $p < 0.001$). There was no change under treatment with 30nM VIP alone (0.11 ± 0.002 vs. 0.11 ± 0.003, p = n.s.).

There was an increase in the number of Prox1 positive cells across experimental conditions ($f(3,44)=2.4$) **(Figure 36 E)**. There was an increase under treatment with 5% supernatant pre-treated with VIP compared to control (35.90 ± 0.56 vs. 13.89 ± 0.25, $p < 0.001$). There was also an increase under treatment with 5% supernatant compared to control (24.28 ± 0.47 vs. 13.89 ± 0.25, $p < 0.001$). The increase under treatment with 5% supernatant pre-treated with VIP was enhanced compared to 5% supernatant alone (35.90 ± 0.56 vs. 24.28 ± 0.47, $p < 0.001$). There was no change under treatment with 30nM VIP alone compared to control (12.09 ± 0.25 vs. 13.89 ± 0.25, p = n.s.).

The same pattern of change was observed in the proportion of Prox1 positive cells, with respect to the total cell number, across experimental conditions ($f(3,44)=0.78$) **(Figure 36 F)**. There was an increase in the proportion of Prox1 cells under treatment with 5% supernatant pre-treated with VIP compared to control (0.18 ± 0.003 vs. 0.10 ± 0.002, $p < 0.001$). There was also an increase under treatment with 5% supernatant compared to control (0.15 ± 0.003 vs. 0.10 ± 0.002, $p < 0.001$). The increase under treatment with 5% supernatant pre-treated with VIP was enhanced compared to 5% supernatant alone (0.18 ± 0.003 vs. 0.15 ± 0.003, $p < 0.001$). There was no change under treatment with 30nM VIP alone compared to control (0.09 ± 0.002 vs. 0.10 ± 0.002, p = n.s.).

There was also a change in the proportion of TuJ1 positive cells co-expressing Prox1, with respect to total cell numbers, across experimental conditions ($f(3,44)=1.7$) **(Figure 36 B)**. There was an increase in the proportion under treatment with 5% supernatant pre-treated with VIP compared to control (0.18 ± 0.003 vs. 0.09 ± 0.001, $p < 0.001$). There was also an increase under treatment with

5% supernatant compared to control (0.14 ± 0.002 vs. 0.09 ± 0.001, $p < 0.001$). The increase under 5% supernatant pre-treated with VIP was enhanced compared to 5% supernatant alone (0.18 ± 0.003 vs. 0.14 ± 0.002, $p < 0.001$). There was no change under treatment with 30nM VIP alone compared to control (0.08 ± 0.001 vs. 0.09 ± 0.001, p = n.s.). Taken together, these results suggest treatment with VIP pre-treatment enhances the number and proportion of dentate specific neurons.

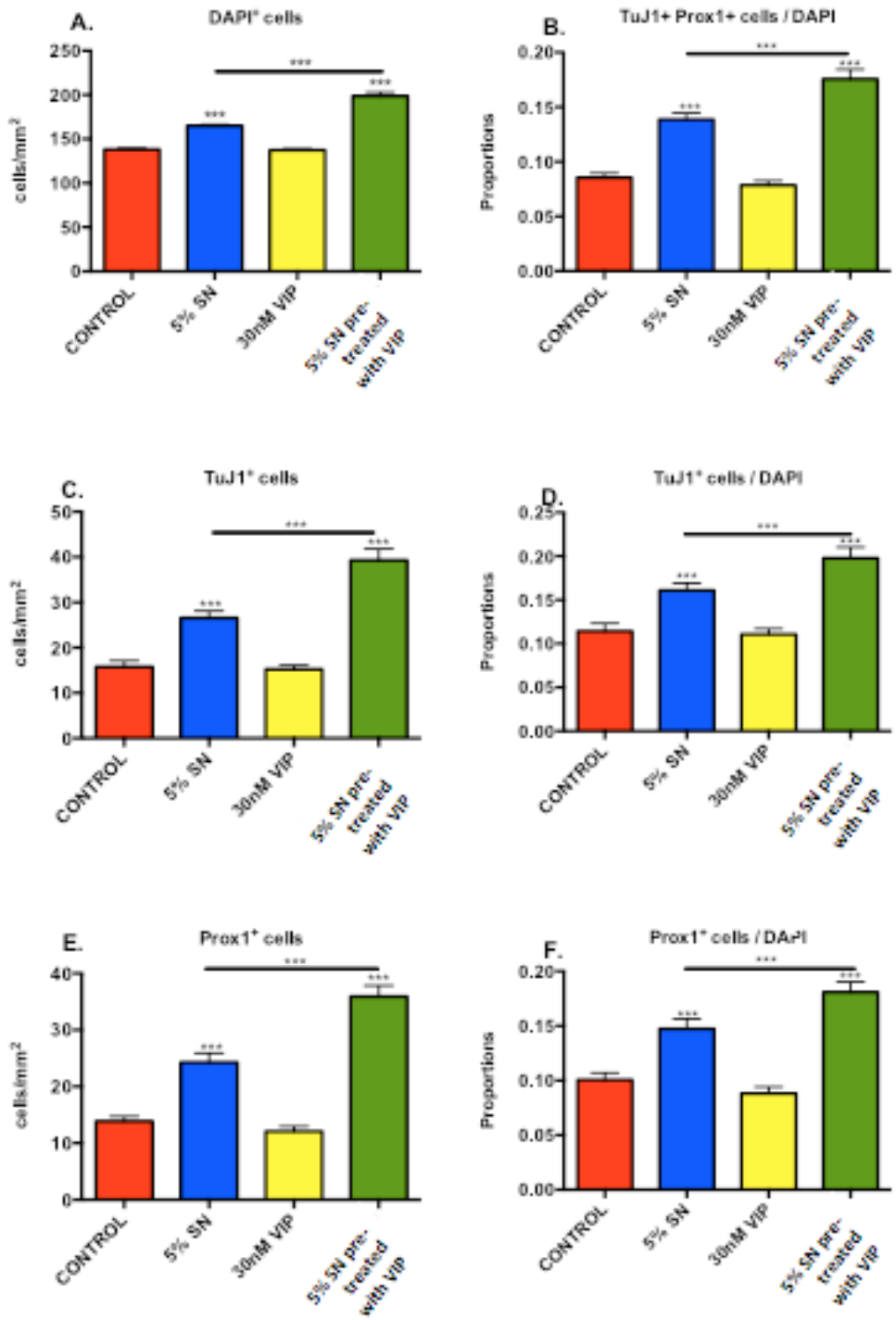

Figure 36: Pre-treatment of splenocytes with VIP increases the proportion of class III β-tubulin positive cells co-expressing Prox1. Hippocampal cells were generated under control conditions for 3DIV and treated with experimental conditions until 6DIV. Cells were fixed and immunostained for TuJ1 and Prox1 expression. **A.** Total cell counts as measured by the number of DAPI positive cells. **B.** Proportion of TuJ1 cells expressing Prox1, with respect to total number of cells **C.** Total number of TuJ1 expressing cells **D.** Proportion of TuJ1 cells **E.** Total number of Prox1 cells and **F.** Proportion of Prox1 cells. Data represents mean ± SE based on a sample that represents 12 wells per condition from 3 different experiments. Comparisons between control and treatment conditions are a one-way ANOVA with Bonferroni correction for multiple comparisons (*, $p < 0.05$, **, $p < 0.01$, ***, $p < 0.001$)

4.3.9: VPAC1 receptor agonist mimics VIP proliferative effects

Given that VPAC1 is constitutively expressed by T lymphocytes (Lara-Marquez et al., 2001), coupled with VPAC1 receptor mRNA expression in our splenocytes cultures (see Appendix II), a VPAC1 receptor agonist was used to investigate its involvement as the receptor subtype mediating VIP proliferative effects. Hippocampal cultures were generated under standard control conditions. BrdU and experimental conditions (as described in *section 4.2.6*) were added for the terminal 6 hours. Cultures were immunostained for BrdU and nestin expression. Consistent with the previous experiments, there was a difference in the mitotic index between control and experimental conditions ($f(5,66)=54$). There was an increase in the mitotic index under treatment with 5% supernatant compared to control (0.19 ± 0.006 vs. 0.14 ± 0.005, $P < 0.001$) **(Figure 37 B)**. Again, this increase was enhanced under treatment with 5% supernatant pre-treated with VIP compared to 5% supernatant treatment alone (0.23 ± 0.006 vs. 0.19 ± 0.006, $p < 0.001$). There was no difference under VIP treatment compared to control (0.13 ± 0.006 vs. 0.14 ± 0.005, p = n.s.). There was an increase in the mitotic index under treatment with 5% supernatant pre-treated with VPAC1 agonist compared to control and 5% supernatant alone, respectively (0.23 ± 0.006 vs. 0.14 ± 0.005, $p < 0.001$; 0.23 ± 0.006 vs. 0.19 ± 0.006, $p < 0.01$). The increase under treatment with 5% supernatant pre-treated with VPAC1 agonist is comparable to that observed under treatment with 5% supernatant pre-treated with VIP (0.23 ± 0.006 vs. 0.23 ± 0.005, p = n.s.). Addition of VPAC1 agonist directly to hippocampal cultures did not increase the mitotic index compared to control (0.13 ± 0.008 vs. 0.14 ± 0.005, p = n.s.). There was no change in total cell numbers across experimental conditions ($f(5,66)=0.16$, p = n.s.) **(Figure 37 A)**. These results suggest VPAC1 receptor mediates VIP proliferative effects.

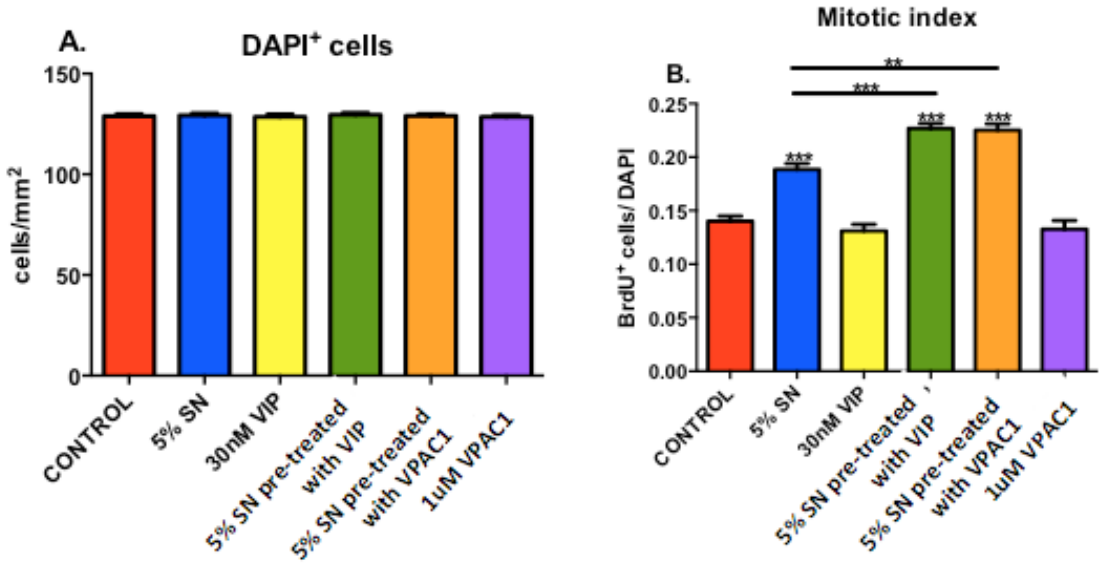

Figure 37: VPAC1 receptor agonist mimics VIP effects on mitotic index of hippocampal cells. Hippocampal cells were generated under control conditions for 3DIV. BrdU and treatment conditions were added for the terminal 6 hours before fixation. Cells were immunostained for BrdU incorporation. **A.** Total cell counts as measured by the number of DAPI positive cells. **B.** Proportion of BrdU positive cells, with respect to total number of cells. Data represents mean ± SE based on a sample that represents 12 wells per condition from 3 different experiments. Comparisons between control and treatment conditions are a one-way ANOVA with Bonferroni correction for multiple comparisons (*, $p < 0.05$, **, $p < 0.01$, ***, $p < 0.001$)

Consistent with the previous experiments, there was a difference in the proportion of the nestin-expressing cells incorporating BrdU between control and experimental conditions ($f(5,66)=93$). There was an increase under treatment with 5% supernatant compared to control (0.25 ± 0.007 vs. 0.14 ± 0.005, $p < 0.001$) **(Figure 38 B)**. This effect was enhanced under treatment with 5% supernatant pre-treated with VIP compared to 5% supernatant treatment alone (0.36 ± 0.02 vs. 0.14 ± 0.005, $p < 0.001$). There was no difference under VIP treatment compared to control (0.13 ± 0.005 vs. 0.14 ± 0.005, p = n.s.). There was an increase under treatment with 5% supernatant pre-treated with VPAC1 agonist compared to control (0.37 ± 0.017 vs. 0.14 ± 0.005, $p < 0.001$), whilst there was no change under treatment with VPAC1 agonist directly to hippocampal cultures (0.14 ± 0.005 vs. 0.14 ± 0.005, p = n.s.). Again, the increase under 5% supernatant pre-treated with VPAC1 was comparable to that under treatment with 5% supernatant pre-treated with VIP (0.37 ± 0.017 vs. 0.36 ± 0.02, p=n.s.). There was no change in total nestin-expressing cell numbers across experimental conditions ($f(5,66)=0.15$, p = n.s.) **(Figure 38 A)**. These results suggest VPAC1 receptor mediates proliferation of nestin-expressing hippocampal cells.

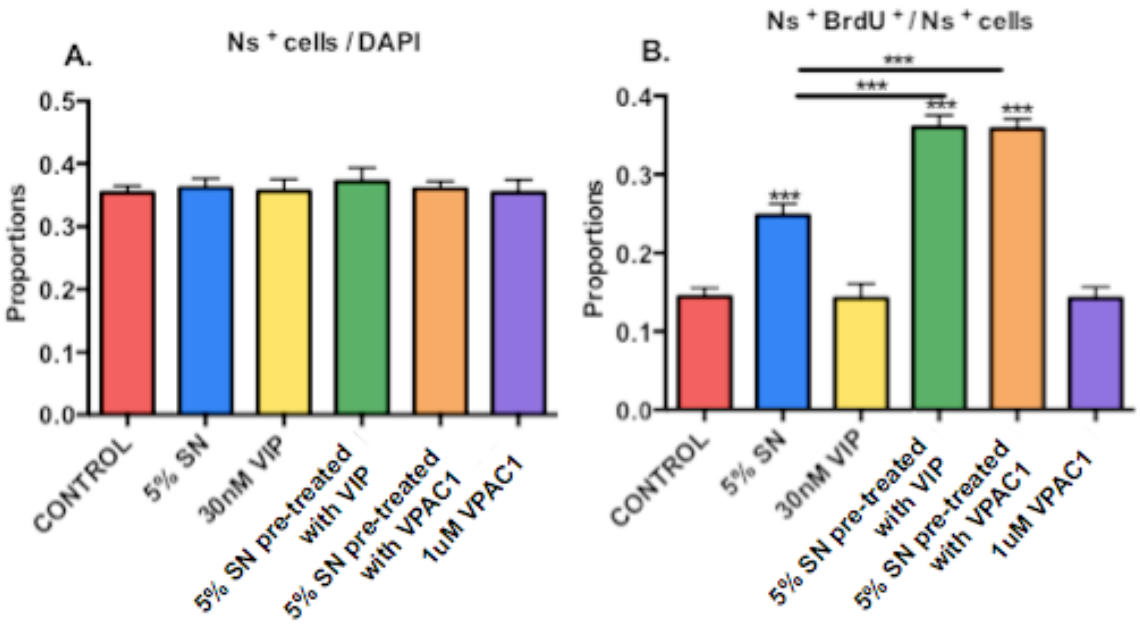

Figure 38: VPAC1 receptor agonist mimics VIP effects on nestin-expressing hippocampal cells. Hippocampal cells were generated under control conditions for 3DIV. BrdU and treatment conditions were added for the terminal 6 hours before fixation. Cells were immunostained for BrdU incorporation and nestin expression. **A.** Total number of nestin cells with respect to total cell numbers. **B.** Proportion of BrdU-incorporating cells expressing nestin, with respect to total number of nestin cells. Data represents mean ± SE based on a sample that represents 12 wells per condition from 3 different experiments. Comparisons between control and treatment conditions are a one-way ANOVA with Bonferroni correction for multiple comparisons (*, $p < 0.05$, **, $p < 0.01$, ***, $p < 0.001$)

4.3.10: VPAC1 receptor antagonist inhibits VIP proliferative effects

To confirm VPAC1 mediates VIP proliferative effects, a VPAC1 antagonist was used. In a set of experiments, cultures were generated for 3DIV under standard control conditions. BrdU and experimental conditions (as described in *section 4.2.6*) were added for the terminal 6 hours. Cultures were immunostained for BrdU and nestin expression. Consistent with the previous experiments, there was a difference in the mitotic index between control and experimental conditions ($f(6,77)=66.58$). There was an increase in the mitotic index under treatment with 5% supernatant compared to control (0.19 ± 0.004 vs. 0.13 ± 0.005, $p < 0.001$) **(Figure 39 B)**. Again, this increase was enhanced under treatment with 5% supernatant pre-treated with VIP compared to 5% supernatant treatment alone (0.24 ± 0.005 vs. 0.19 ± 0.004, $p < 0.001$). There was no difference under VIP treatment compared to control (0.13 ± 0.006 vs. 0.13 ± 0.005, $p < 0.001$)**.** There was a decrease in the mitotic index under treatment with 5% supernatant pre-treated simultaneously with VPAC1 antagonist and VIP compared to 5% supernatant pre-treated with VIP (0.18 ± 0.005 vs. 0.24 ±

0.005, p < 0.001). These levels were reduced to that of treatment with 5% supernatant alone (0.18 ± 0.005 vs. 0.19 ± 0.004) yet still higher than control (0.18 ± 0.005 vs. 0.13 ± 0.005, p < 0.001). There was no difference under treatment with VPAC1 antagonist directly added to cultures compared to control (0.13 ± 0.004 vs. 0.13 ± 0.005, p = n.s.). Addition of 5% supernatant pre-treated with VPAC1 antagonist increased the mitotic index compared to control (0.18 ± 0.003 vs. 0.13 ± 0.005, p < 0.001), at levels comparable to that with treatment under 5% supernatant alone (0.18 ± 0.003 vs. 0.19 ± 0.004, p = n.s.). There was no change in total cell counts across experimental conditions (f(6,77)=0.58, p = n.s.) **(Figure 39 A)**. These results suggest VPAC1 antagonist inhibits VIP's enhanced proliferative effects but does not abolish supernatant effects on cultures.

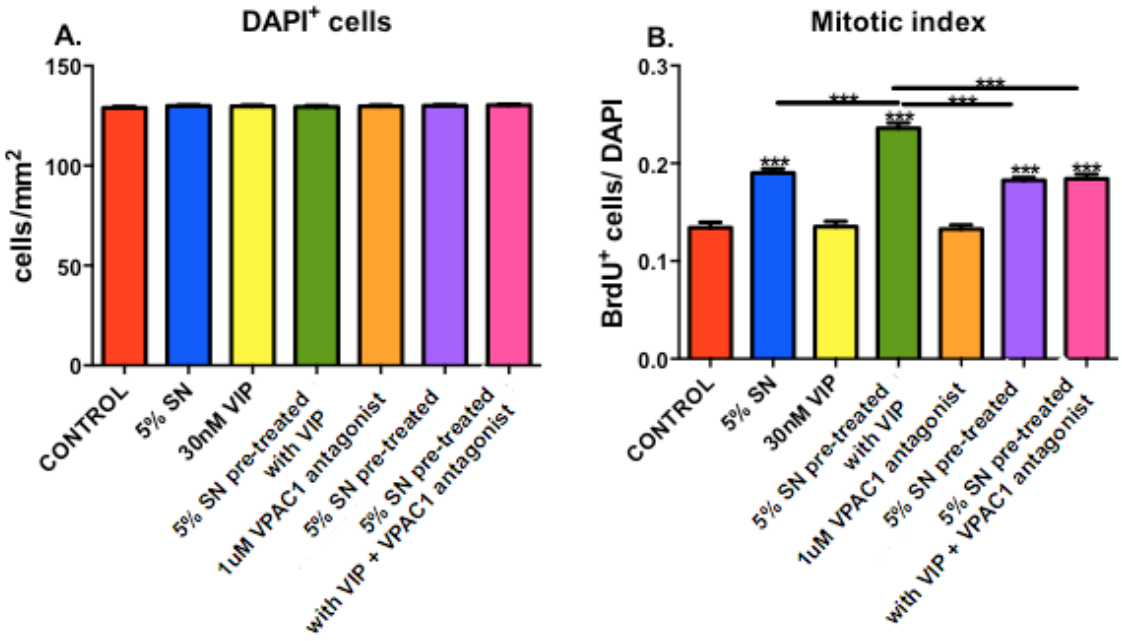

Figure 39: VPAC1 receptor antagonist inhibits VIP effects on mitotic index of hippocampal cells. Hippocampal cells were generated under control conditions for 3DIV. BrdU and treatment conditions were added for the terminal 6 hours before fixation. Cells were immunostained for BrdU incorporation. **A.** Total cell counts as measured by the number of DAPI positive cells. **B.** Proportion of BrdU positive cells, with respect to total number of cells. Data represents mean ± SE based on a sample that represents 12 wells per condition from 3 different experiments. Comparisons between control and treatment conditions are a one-way ANOVA with Bonferroni correction for multiple comparisons (*, p < 0.05, **, p < 0.01, ***, p < 0.001)

Consistent with the previous experiments, there was a difference in the proportion of the nestin-expressing cells incorporating BrdU between control and experimental conditions (f(6,77)=138). There was an increase under treatment with 5%

supernatant compared to control (0.25 ± 0.008 vs. 0.14 ± 0.006, $p < 0.001$) **(Figure 40 B)**. This effect was enhanced under treatment with 5% supernatant pre-treated with VIP compared to 5% supernatant treatment alone (0.34 ± 0.008 vs. 0.25 ± 0.008, $p < 0.001$). There was no difference under VIP treatment compared to control (0.14 ± 0.006 vs. 0.14 ± 0.006, p = n.s). Treatment with 5% supernatant pre-treated simultaneously with VPAC1 antagonist and VIP reduced the proportion compared to 5% supernatant pre-treated with VIP (0.25 ± 0.007 vs. 0.34 ± 0.008, $p < 0.001$). These levels were reduced to that of treatment with 5% supernatant alone (0.25 ± 0.007 vs. 0.25 ± 0.008, p = n.s.) yet still higher than control (0.25 ± 0.007 vs. 0.14 ± 0.006, $p < 0.001$). There was no change under treatment with VPAC1 antagonist directly to cultures compared to control (0.14 ± 0.005 vs. 0.14 ± 0.006, p = n.s.). There was an increase under treatment with 5% supernatant pre-treated with VPAC1 antagonist compared to control (0.26 ± 0.007 vs. 0.14 ± 0.006, $p < 0.001$). There was no change in total nestin-expressing cell numbers, with respect to total cell numbers, across experimental conditions ($f(6,77)=0.50$, p = n.s.) **(Figure 40 A)**. These results suggest VPAC1 antagonist inhibits VIP's enhanced proliferation of nestin-expressing hippocampal cells but does not abolish supernatant effects. Taken together, these results suggest the VPAC1 receptor subtype mediates VIP proliferative effects.

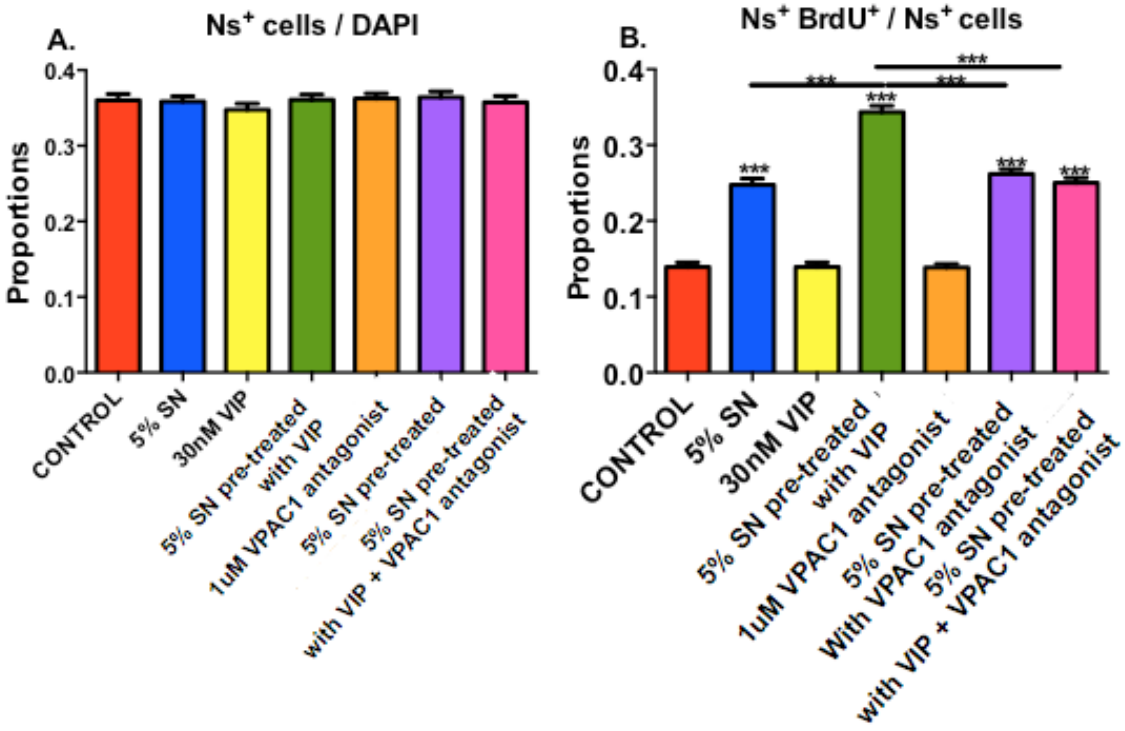

Figure 40: VPAC1 receptor antagonist inhibits VIP effects on nestin-expressing hippocampal cells. Hippocampal cells were generated under control conditions for 3DIV. BrdU and treatment conditions were added for the terminal 6 hours before fixation. Cells were immunostained for BrdU incorporation. **A.** The proportion of nestin positive cells with respect to total cell numbers. **B.** Proportion of nestin positive cells incorporating BrdU, with respect to total number of nestin cells. Data represents mean ± SE based on a sample that represents 12 wells per condition from 3 different experiments. Comparisons between control and treatment conditions are a one-way ANOVA with Bonferroni correction for multiple comparisons (*, $p < 0.05$, **, $p < 0.01$, ***, $p < 0.001$)

4.4 Discussion

4.4.1: VIP acts directly on CD4+ T lymphocytes to enhance the increase of the mitotic index

VIP has pleiotropic effects on cell types depending on the concentration, timing and type of cell involved. Indeed, VIP has been shown to favour a Th2 phenotype whilst inhibiting Th1 cytokines, both *in vitro* and *in vivo* (Delgado et al., 1999a, Delgado et al., 1999b). This is consistent with VIP's established role as an anti-inflammatory agent (Gomariz et al., 2000, Delgado and Ganea, 2000). We examined the role of supernatant from VIP-treated CD4+ T cells on hippocampal cells. There was a significant increase in the proliferation of nestin-expressing hippocampal cells under treatment with supernatant pre-treated with VIP. This effect is greater than that observed under untreated activated supernatant. VIP enhanced the proliferative effect, most likely by skewing T lymphocytes towards a Th2 phenotype. Flow cytometric cell sorting was used to determine the effects of VIP on CD4+ T cells; there was an enhanced proliferative effect on hippocampal cells treated with supernatant from activated CD4+ T lymphocytes treated with VIP. The same was observed under treatment with supernatant from VIP-treated activated cultures containing splenocytes with T lymphocytes. There was no such effect on hippocampal cells treated with supernatant from splenocytes absent of CD4+ T lymphocytes. Furthermore, this effect was only observed in supernatant from activated CD4+ T lymphocytes; supernatant from naïve T lymphocytes treated with VIP did not have an effect on the mitotic index of hippocampal cells. This data shows a direct role of VIP on CD4+ T cells and eliminated its action on other cell types, or indeed a secondary effect of CD4+ T lymphocytes on other cells.

4.4.2: VIP enhances the T lymphocyte proliferative effect on hippocampal cell populations by speeding the cell cycle

Having established that VIP pre-treated CD4+ T lymphocytes supernatant increases the mitotic index, populations of cells within the hippocampal culture were investigated. There was an increase in the proportion of BrdU incorporating cells expressing nestin with respect to total cell numbers. VIP enhanced the increase compared to treatment with activated CD4+ T lymphocytes supernatant not treated with VIP. There was also an enhanced neuroproliferative effect on the number of

BrdU incorporating cells expressing TuJ1 under treatment with supernatant pre-treated with VIP. To determine whether this effect was due to an increase in the recruitment of quiescent cells, or rather increasing the cell cycle speed as observed under treatment with activated supernatant alone, the proliferative markers Ki67 and BrdU were used. The growth fraction (Ki-67/DAPI) was unaltered under treatment with activated supernatant pre-treated with VIP. However, as with activated supernatant, there was an increase in the labelling index (BrdU Ki-67/Ki-67); this effect was enhanced under treatment with supernatant pre-treated with VIP compared to supernatant alone. This data is the first study to demonstrate a proliferative effect of VIP pre-treated $CD4^+$ T lymphocytes supernatant on specific cell populations via an increase in the cell cycle speed.

4.4.3: VIP enhances T lymphocyte mediated neurogenic effects

When treated with activated $CD4^+$ T lymphocytes supernatant over a 3 day period, our data has shown that hippocampal cultures increase net neurogenesis in postnatal (P7-10) rat hippocampal cultures. This is defined as the number of newly generated neurons and is determined using the stem cell marker nestin and immature neuronal marker TuJ1. VIP-treated $CD4^+$ T lymphocytes supernatant enhances this effect, significantly increasing the number of newly generated neurons with respect to the total number of cells in culture. Indeed, the origin of these cells is the dentate gyrus; the neurons (TuJ1 positive cells) were almost completely Prox1 positive. This indicates the cells specifically have granule cell identity (Iwano et al., 2012). This data suggests at physiological concentrations, VIP has the potential to communicate between the stem cell niche and $CD4^+$ T cells to increase hippocampal neurogenesis.

4.4.4: VIP acts via the VPAC1 receptor on $CD4^+$ T lymphocytes

There is differential expression and distribution of VIP receptors across tissues. Studies have shown that while there is constitutive expression of VPAC1 and PAC1 mRNA in T lymphocytes, VPAC2 mRNA expression is induced following activation (Delgado et al., 1996a). This is true of LPS and certain types of activators that are conventionally associated with a Th1 response (Ganea et al., 2003). This shift in VPAC1 to VPAC2 mRNA expression is also observed following activation with anti-

CD3 in conjunction with other stimulatory factors such as PMA (Lara-Marquez et al., 2001). Our data shows VPAC1 and PAC1 mRNA expression continues after anti-CD3 activation, while VPAC2 mRNA remains undetected (see Appendix II). Given that immuo-modulation is predominantly regulated by VPAC1 and VPAC2 receptors (Jiang et al., 1998), VPAC1 mediation was investigated using VPAC1 agonists and antagonists. $CD4^+$ T lymphocytes supernatant pre-treated with the VPAC1 agonist mimicked the proliferative effect of VIP treatment. This suggested the effect was mediated via the VPAC1 receptor. Pre-treatment of T lymphocytes supernatant with VPAC1 antagonist and VIP abolished the proliferative effect, whilst VPAC1 antagonist pretreatment alone did not. These results identify the VPAC1 receptor as the mediator for VIP proliferative effects. This data also demonstrates that anti-CD3 alone does not switch off VPAC1 receptor expression or activate VPAC2 receptor in this culture system.

4.4.5: Chapter summary

The data presented in this chapter has demonstrated a novel mechanism to study the role of neuropeptides in regulating T cell activity on hippocampal cells. VIP acts directly on activated $CD4^+$ T lymphocytes to enhance the proliferative effects observed on hippocampal cells under treatment with activated supernatant alone. This effect is a result of enhancing the cell cycle speed and thereby enhancing the supernatant effect on hippocampal cells. Enhanced proliferation is mediated via the VPAC1 receptor on $CD4^+$ T lymphocytes.

Treating $CD4^+$ T lymphocytes with VIP enhances the supernatant's overall neurogenic effect on hippocampal cells. This effect on fate determination is specific to cells of a granule cell identity. Collectively, this preliminary data suggests a role for VIP as a mediator between the neural stem cell niche and T lymphocytes; this potential mechanism could regulate hippocampal neurogenesis within a physiological setting.

Chapter 5

$CD4^+$ T lymphocytes interact with microglia to modulate hippocampal neurogenesis

5.1:Introduction

5.1.1: Introduction

$CD4^+$ T lymphocytes are broadly subcategorized into two distinct groups: Th1 and Th2. These subgroups are classified based on signature cytokine production; a Th1 cytokine profile is associated with pro-inflammatory cytokines (IFN-γ) while a Th2 cytokine profile is associated with anti-inflammatory cytokines (IL-4) (Zhu and Paul, 2008). Th2 cytokines such as IL-4 are associated with pro-neurogenic effects, though the exact mechanisms remain unknown (Butovsky et al., 2006, Derecki et al., 2010). While T lymphocytes have been shown to regulate hippocampal neurogenesis, a number of cell types are involved in neuro-immune modulation, with a special role for microglia and T lymphocytes (Ziv et al., 2006, Butovsky et al., 2006).

5.1.2: A Th2 cytokine profile is pro-neurogenic: a role for IL-4

VIP promotes Th2 cytokine production and IL-4 is the primary Th2 phenotypic marker (Delgado et al., 2004). Hippocampal IL-4 down-regulation, and concomitant pro-inflammatory IL-1β and IL-6 upregulation, is associated with aging; a functional impairment that can be rescued with IL-4 replenishment (Maher et al., 2005). Very little is known about IL-4 in terms of neurogenesis. Derecki and colleagues (2010) have shown that learning increases accumulation of IL-4-producing T lymphocytes in the meninges. Further to this, IL-4 knock-out mice exhibit severe cognitive defects which can be reversed with wild-type bone marrow or adoptive transfer of IL-4-competent T lymphocytes. Of further interest is the ability of T lymphocytes-generated IL-4 in "programming" microglia to promote neurogenesis (Butovsky et al., 2006, Derecki et al., 2010).

5.1.3: T lymphocytes interact with microglia to regulate hippocampal neurogenesis

Although microglia were conventionally associated with detrimental effects in neurogenic regulation, a beneficial role is fast emerging (Sierra et al., 2010, Nikolakopoulou et al., 2013). The exact mechanism by which T lymphocytes interact with microglia under basal conditions remain poorly understood. The major challenge remains in understanding how T lymphocytes outwith the brain

parenchyma interact with brain microglial cells. As discussed in Chapters 3 and 4, it is possible that T lymphocytes release inflammatory cytokines into the brain; these cytokines could act directly or via intermediary cells such as microglia. These cells are prime candidates, given their role as scavengers of the brain, coupled with their abundance in the brain. Ziv and colleagues (2006) have investigated hippocampal neurogenesis in severe combined immune deficient mice with respect to T lymphocyte involvement and microglial interactions. They reported that immune deficient mice devoid of T and B lymphocytes had reduced proliferation of newly generated neurons which was rescued by intravenous injection of T lymphocytes. Subsequent studies have shown the effect is purely mediated by $CD4^+$ T lymphocytes (Wolf et al., 2009). Ziv and colleagues also found that while environmental enrichment increases proliferation of newly generated neurons, there is also an increase in the proliferation of microglia in the dentate gyrus compared to mice in standard control environments. Furthermore, blocking microglial activity with the use of minocycline decreases proliferation of newly generated neurons (Ziv et al., 2006). These studies suggest a link between T lymphocytes, microglia and neurogenesis; the exact relationship remains to be understood.

5.1.4: Microglia express distinct phenotypes that determine cytokine profiles

Though under debate, microglia are predominantly classed into two subgroups: M1 "classically" activated (pro-inflammatory) or M2 "alternatively" activated (anti-inflammatory) phenotypes. Neuropeptides are potent modulates that can directly affect cytokine secretion of immune cells, including microglia (Levite, 1998). The controversy in classification of microglia stems from the overlapping of certain markers; none-the-less, there are an array of markers for either phenotype (Hickman et al., 2013, Crain et al., 2013). M1 markers include IL-13, TNFα, NOS2 and M2 markers include IL-4, IL-10, Chi3I3 (Ym1). *In vitro*, microglia can be driven to adopt M1 and M2 phenotypes, with M1 believed to drive inflammation and M2 to drive phagocytosis of debris. Given VIP's ability to skew T lymphocytes and macrophages towards an anti-inflammatory phenotype, there is a potential role for VIP in skewing microglia towards an M2 phenotype. An M2 phenotype would be likely in the presence of IL-4; this cytokine can activate microglia to release pro-

neurogenic mediators such as BDNF and IGF-1 (Butovsky et al., 2006, Derecki et al., 2010). BDNF, a well-documented neurogenic factor, promotes differentiation and maturation of adult born neurons through GABAergic transmission (Waterhouse et al., 2012). It may also be involved in regulating hippocampal cell proliferation; mice with hippocampal neural progenitor cells lacking the BDNF receptor TrkB have impaired proliferation and neurogenesis (Li et al., 2008, Bergami et al., 2008). Interestingly, BDNF levels are significantly reduced in mice deficient of T lymphocytes (Ziv et al., 2006). Understanding T lymphocytes involvement in microglial phenotyping remains to be fully elucidated and is central to the mechanisms of neurogenic regulation.

5.1.5: Aims and objectives

Understanding the exact mechanism by which T lymphocytes interact with microglia in neuro-immune modulation remains a challenge. Our culture paradigm allows the examination of the effects of T lymphocyte-releases cytokines on hippocampal cultures in the presence or absence of microglia. In addition, the generation of pure microglial cultures allows analysis of T lymphocyte-released cytokines on microglia. Another advantage of this paradigm is the ability to elucidate the role of VIP involvement in this model.

The aim of this chapter is threefold. Firstly, to determine the effects of VIP on T lymphocytes cytokine production, specifically investigating the role of IL-4. Secondly, to investigate the role of T lymphocytes-released IL-4 on microglia. Thirdly, to study the direct effect of T lymphocytes-derived cytokines on microglial phenotype and neurotrophic production.

5.2: Methods

Key cytokines modulating T lymphocyte-mediated proliferative and neurogenic effects on hippocampal cultures were investigated. Splenocyte cultures were generated under three experimental conditions: naive, activated with anti-CD3, activated with anti-CD3 and treated with 30nM VIP. Semi-quantitative PCR analysis was used to identify candidate Th2 cytokines. This was followed by pharmacological studies to further investigate cytokine modulation of hippocampal cells.

5.2.1: Generation of splenocyte cultures for RNA extraction

For each experiment, 4 spleens were used from adult mice to generate splenocyte cultures as detailed in *section 2.1.* Following a multi-step protocol as part of a $CD4^+$ T cell isolation kit, viable cells were plated at a density of 1, 000, 000 cells/mL directly on to poly-L-lysine coated 6 well plates. 1µg/mL of anti-CD3 was added at plating to activate cells. For VIP activation, T lymphocytes were treated with 30nM VIP at plating simultaneously during the addition of anti-CD3. Cells were grown in standard culture medium (NBA/B-27/glutamine) supplemented with antibiotic/antimycotic (5% CO_2/9% O_2/ 37°C incubator conditions). Cells were collected at 2 hours for RNA extraction and cDNA synthesis.

5.2.2: RNA extraction and cDNA synthesis

At the given time points, cells were washed with PBS and collected in TRizol® reagent (Invitrogen) to extract RNA and convert to cDNA as detailed in *section 2.9*. PCR was carried out on single-stranded cDNA using a one step real-time PCR kit (Primer Design Ltd, Southampton) in a PCR thermocycler (Rotor Gene 6000). All PCR reactions were performed according to manufacturer's instructions for 50 cycles. For IL-4 and the housekeeping gene GAPDH mRNAs, primers were designed by Primer Design Ltd (Southampton). Forward and reverse primers, sequence, positions on the gene, melting temperatures and expected product lengths are detailed in Table 3 *(section 2.9)*.

5.2.3: Investigating IL-4 mediation of hippocampal proliferation

This unique study model has the advantage of studying species-specific cytokine mediation of hippocampal neurogenesis since the supernatant is from mouse while

the hippocampal cultures are from rat. To investigate the role of mouse IL-4 (from T lymphocytes), a mouse-specific anti-IL-4 antibody was used. Similarly, in a separate set of experiments, the role of rat IL-4 (from endogenous cells including rat microglia) was investigated using a rat-specific anti-IL-4 antibody. For both anti-mouse and anti-rat IL-4, 10mg/mL of the anti-IL-4 antagonist (R&D systems) was used to neutralize IL-4 activity in hippocampal cultures. Primary rat hippocampal cultures were generated as detailed in *section 2.1*. At 2DIV, experimental conditions and BrdU were added to hippocampal cultures for the terminal 6 hours before being fixed in 4% PFA for 30 minutes at 4°C. Here the experimental conditions were standard control conditions, 5% activated supernatant, 30nM VIP added directly to cultures, 30nM VIP pre-treated activated supernatant, standard control conditions with anti-IL-4, 5% activated supernatant with anti-IL-4, 30nM VIP added directly to cultures with anti-IL-4, 30nM VIP pre-treated activated supernatant with anti-IL-4. Cells were then processed for BrdU incorporation and nestin expression.

5.2.4: Confirming specificity of antibodies using isotype controls

To confirm IL-4 antibody specificity, isotype controls were used. For anti-mouse IL-4, 10μg/mL rat IgG_1 isotype control was used. For anti-rat IL-4, 10μg/mL rat IgG2a isotype control was used. Primary hippocampal cultures were generated for 3DIV under standard control conditions and treated with BrdU and experimental conditions for the terminal 6 hours. Cells were fixed in 4% PFA for 30 minutes at 4°C. The experimental conditions for each isotype experiment were standard control conditions, 5% activated supernatant, 30nM VIP added directly to cultures, 30nM VIP pre-treated activated supernatant, standard control conditions with isotype (R&D systems), 5% activated supernatant with isotype, 30nM VIP added directly to cultures with isotype, 30nM VIP pre-treated activated supernatant with isotype. Cells were then processed for BrdU incorporation and nestin expression.

5.2.5: Examining the role of microglia in splenocyte modulated hippocampal neurogenesis

To deplete microglial cells from hippocampal cultures, rat-Mac-1-SAP (Advanced targeting systems) was used. The Mac-1-SAP antibody specifically binds to CD11b receptors on microglia; the antibody is conjugated to the ribosome-inactivating

protein saporin. Once the antibody binds to microglia, saporin is internalized and breaks away from the antibody, inactivating the ribosome. This in turn leads to protein inhibition and ultimately kills microglia. Primary rat hippocampal cultures were grown under standard control conditions for 2DIV. At 2 DIV, half the cultures were treated with Mac-1-SAP to deplete microglial cell populations (as detailed in *section 2.7.1*) while the other half were replaced with standard control medium.

At 3 DIV, cells were washed in fresh culture medium before being treated with BrdU and experimental conditions for the terminal 6 hours before fixation in 4% PFA for 30 minutes at 4°C. Specifically, experimental conditions were standard control conditions, 5% activated supernatant, 30nM VIP added directly to cultures, 30nM VIP pre-treated activated supernatant, control conditions in Mac-1-SAP treated cultures, 5% activated supernatant in Mac-1-SAP treated cultures, 30nM VIP added directly in Mac-1-SAP treated cultures, 30nM VIP pre-treated activated supernatant in Mac-1-SAP treated cultures. Cells were processed for BrdU incorporation and nestin expression,

5.2.6: Examining the relationship between IL-4 and microglia in the modulation of hippocampal neurogenesis

Hippocampal cultures were grown under standard control conditions for 2DIV. At 2DIV, cultures were either treated with Mac-1-SAP or replaced with fresh culture medium to deplete microglial cell populations (as detailed in *section 2.7.1*). At 3DIV, cells were washed in fresh culture medium before being treated with BrdU and experimental conditions (with anti-mouse IL-4) for the terminal 6 hours before fixation in 4% PFA for 30 minutes at 4°C. Specifically, experimental conditions were standard control conditions, 5% activated supernatant, 30nM VIP added directly to cultures, 30nM VIP pre-treated activated supernatant, control condition in Mac-1-SAP treated cultures, 5% activated supernatant in Mac-1-SAP treated cultures, 30nM VIP added directly to Mac-1-SAP treated cultures, 30nM VIP pre-treated activated supernatant in Mac-1-SAP treated cultures, control conditions in Mac-1-SAP treated cultures with anti-mouse IL-4, 5% activated supernatant in Mac-1-SAP treated culutres with anti-mouse IL-4, 30nM VIP added directly to Mac-1-SAP treated cultures with anti-mouse IL-4, 30nM VIP pre-treated activated supernatant

in Mac-1-SAP treated cultures with anti-mouse IL-4. Cells were processed for BrdU incorporation and nestin expression.

5.2.7: Generating pure microglial cultures

To investigate the effect of supernatant on microglia, pure microglial cultures were generated as detailed in *section 2.7.2.* Primary rat hippocampal cultures were generated from postnatal Sprague-Dawley rats (p7-10) as detailed in *section 2.1.* Cells were plated at a density of 500, 000 cells/mL in poly-L-lysine coated 6 well plates. At 2 hours post-plating, cultures were replenished with fresh culture medium (NBA/B-27/glutamine) supplemented with antibiotic/antimycotic and 10% FBS. Cultures were grown for 1 week without medium change (5% CO2/ 9% O2/ 37°C incubator conditions). At 7DIV, cultures were placed on a plate shaker at 1200rpm for 10 minutes at 37°C. Cells were collected and plated on 6 well plates for an hour and replaced with experimental conditions for 2 hours. Experimental conditions were standard control conditions, 5% activated supernatant, 30nM VIP added directly to cultures, 30nM VIP pre-treated activated supernatant. At the given time points, cells were collected in TRizol reagent.

5.2.8: RNA extraction and cDNA synthesis of microglial cells

At the given time points, cells were washed with PBS and collected in TRizol reagent to extract RNA and convert to cDNA as detailed in *section 2.9*. PCR was carried out on single-stranded cDNA using a one step real-time PCR kit (Primer Design Ltd, Southampton) in a PCR thermocycle (Rotor Gene 6000). All PCR reactions were performed according to the manufacturer's instructions for 50 cycles. For BDNF, TNFα, IL-10, NOS2, BDNF, CHi3I3 and the housekeeping gene GAPDH mRNAs, primers were designed by Primer Design Ltd (Southampton). Forward and reverse primers, sequence, positions on the gene, melting temperatures and expected product lengths are detailed in Table 3 *(section 2.9)*.

5.2.9: Imaging and statistical analysis

Images were taken on a DM RBE microscope (Leica Microsystems Limited) at 20x magnification. Six systemically randomized fields per well were taken using the Leica Application Suite image-capturing system version 3.8.0. Data was averaged

per well and expressed in cells/mm^2 or as a percentage, based on a sample of 4 wells per condition per experiment. All experiments were repeated a minimum of three times. Graph Pad prism data analysis software (GraphPad Inc, San Diego, CA, USA) was used to plot data points. For statistical comparisons a one-way ANOVA was used with Bonferroni correction for multiple comparisons ($p < 0.05$ considered significant).

5.3: Results

5.3.1: VIP treatment of activated splenocytes significantly upregulates IL-4 mRNA expression

An array of cytokines have been investigated in the lab under treatment conditions with VIP (Appendix II). The Th2 cytokine IL-4 has been studied to determine the effects of VIP on activated T lymphocytes. T lymphocytes cultures were generated and treated with experimental conditions for 2 hours. T cells were collected in TRizol and converted to cDNA for PCR analysis. Using the comparative Ct method, the increase in folds of expression in splenocytes were examined under treatment with VIP. Consistent with previous findings in the lab (Appendix II), there was a 6 fold increase in the expression of VIP-treated activated splenocytes compared to control **(Figure 41)**.

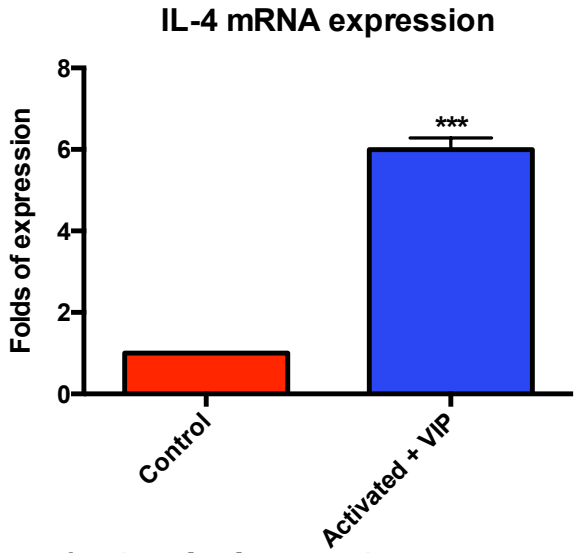

Figure 41: VIP treatment of activated splenocytes increases mRNA expression. Splenocytes were generated using the $CD4^+$ isolation kit and treated with anti-CD3 and 30nM VIP for 2 hours. Cells were then collected in trizol and converted to cDNA for PCR analysis. Data is from 2 different experiments. Comparisons between control and treatment conditions are a one-way ANOV A with Bonferroni correction for multiple comparisons (*, $p < 0.05$, **, $p < 0.01$, ***, $p < 0.001$)

5.3.2: IL-4 mediates T lymphocytes proliferative effects on hippocampal cells

Given the results from PCR analysis, IL-4 was further investigated for its role in modulating hippocampal neurogenesis. A mouse-specific IL-4 antagonist was used to neutralize T cell-released IL-4 activity. This antibody does not react with rat IL-4 and therefore allowed us to investigate the effect of specifically blocking IL-4 in the supernatant generated from mouse cultures. Hippocampal cultures were generated for 3DIV and treated with experimental conditions for the terminal 6 hours before

fixation. Experimental conditions were standard control conditions, 5% activated supernatant, 30nM VIP added directly to cultures, 5% VIP pre-treated activated supernatant, control conditions with anti-mouse IL-4, 5% activated supernatant with anti-mouse IL-4, 30nM VIP added directly to cultures with anti-mouse IL-4, 5% VIP pre-treated activated supernatant with anti-mouse IL-4. Cultures were immunostained for BrdU incorporation and nestin expression. There was a change in the mitotic index across experimental groups ($f(7,88)=1.3$) **(Figure 42 B)**. There was a significant increase in the mitotic index under treatment with 5% supernatant compared to control (0.18 ± 0.005 vs. 0.12 ± 0.003; $p < 0.001$). There was also an increase in the mitotic index under treatment with 5% supernatant pre-treated with VIP compared to control (0.25 ± 0.007 vs. 0.12 ± 0.003; $p < 0.001$). The increase under treatment with 5% supernatant pre-treated with VIP was significantly enhanced compared to treatment with 5% supernatant alone (0.25 ± 0.007 vs. 0.18 ± 0.005; $p < 0.001$). Treatment with 30nM VIP alone did not increase the mitotic index compared to control (0.12 ± 0.004 vs. 0.12 ± 0.003; p = n.s.). The addition of anti-mouse IL-4 to control conditions and VIP treated cultures did not changed the mitotic index compared to control (0.12 ± 0.005 vs. 0.12 ± 0.003 and 0.13 ± 0.004 vs. 0.12 ± 0.003; p = n.s., respectively). However, the addition of anti-mouse IL-4 to 5% supernatant treated cultures reduced the mitotic index to control levels (0.18 ± 0.005 vs. 0.12 ± 0.003; $p < 0.001$). There was also a reduction in the mitotic index following the addition of anti-mouse IL-4 to cultures treated with 5% supernatant pre-treated with VIP down to control levels (0.13 ± 0.006 vs. 0.12 ± 0.003; $p < 0.001$). There was no change in the total number of cells across experimental conditions ($f(7,88)=1.13$) **(Figure 42 A)**. These results suggest IL-4 mediates supernatant proliferative effects.

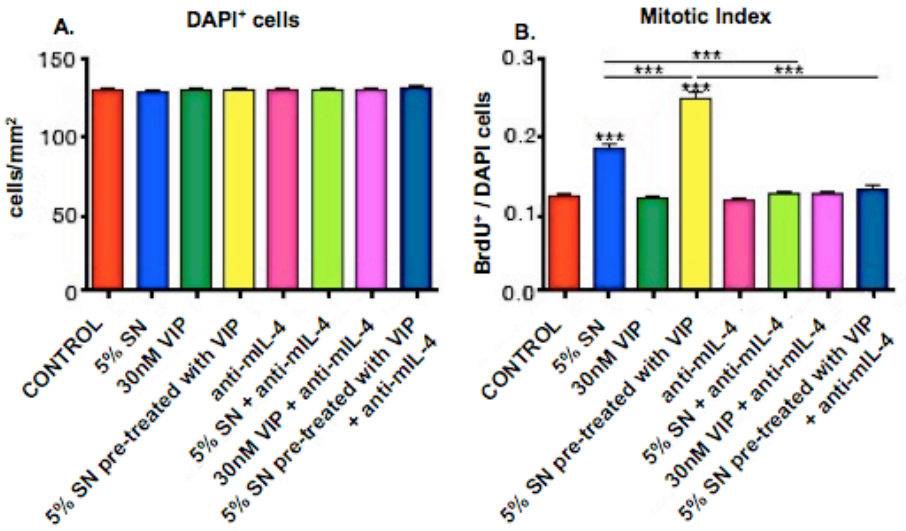

Figure 42: IL-4 mediates supernatant proliferative effects on mitotic index. Hippocampal cells were generated under control conditions for 3DIV. BrdU and treatment conditions were added for the terminal 6 hours before fixation. Cells were immunostained for BrdU incorporation. **A.** Total cell counts as measured by the number of DAPI positive cells. **B.** Proportion of BrdU incorporating cells, with respect to total number of cells. Data represents mean ± SE based on a sample that represents 12 wells per condition from 3 different experiments. Comparisons between control and treatment conditions are a one- way ANOVA with Bonferroni correction for multiple comparisons (*, $p < 0.05$, **, $p < 0.01$,***, $p < 0.001$)

Consistent with previous experiments, there was a change in the proportion of BrdU incorporating cells expressing nestin across experimental conditions ($f(7,88)=1.6$) **(Figure 43 B)**. There was an increase under treatment with 5% supernatant compared to control (0.23 ± 0.02 vs. 0.15 ± 0.007; $p < 0.001$). There was also an increase under treatment with 5% supernatant pre-treated with VIP compared to control (0.39 ± 0.007 vs. 0.15 ± 0.007; $p < 0.001$). The increase compared to cultures treated with 5% supernatant pre-treated with VIP was enhanced compared to 5% supernatant alone (0.39 ± 0.007 vs. 0.23 ± 0.02; $p < 0.001$). Addition of anti-mouse IL-4 to control cultures or cultures treated with VIP did not change the number of BrdU incorporating cells expressing nestin, with respect to total cell numbers (0.15 ± 0.009 vs. 0.15 ± 0.007 and 0.15 ± 0.005 vs. 0.15 ± 0.007, respectively; p = n.s.). Addition of anti-mouse IL-4 abolished supernatant effects (0.15 ± 0.005 vs. 0.23 ± 0.02; $p < 0.001$), reducing levels down to control (0.15 ± 0.005 vs. 0.15 ± 0.007; $p < 0.001$). Addition of anti-mouse IL-4 also abolished VIP mediated supernatant effects (0.17 ± 0.01 vs. 0.39 ± 0.007; $p < 0.001$), again reducing down to control levels (0.17 ± 0.01 vs. 0.15 ± 0.007; $p < 0.001$). There was no change in the total number of nestin positive cells across experimental conditions ($f(7,88)=0.9$) **(Figure 43 A)**.

These results show IL-4 mediates the supernatant proliferative effect of nestin-expressing hippocampal cells.

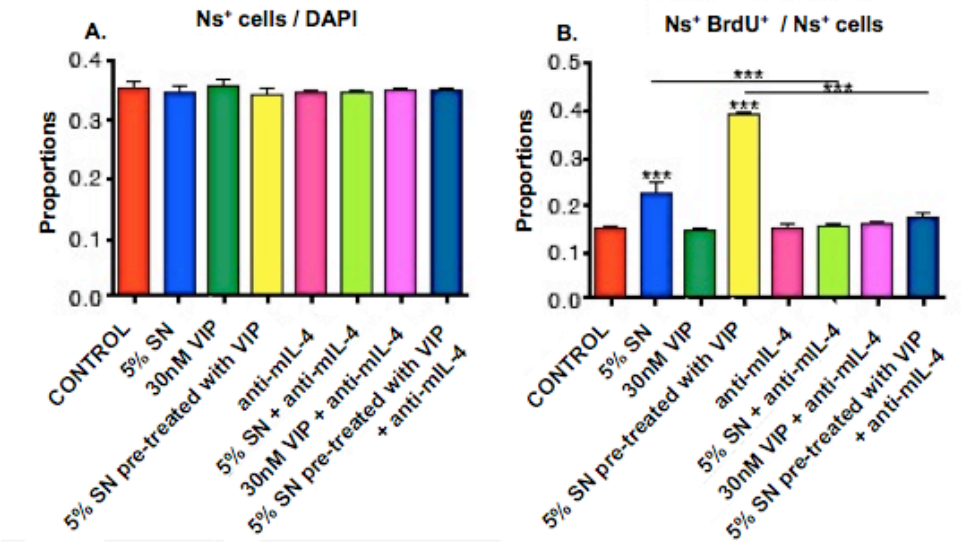

Figure 43: IL-4 mediates supernatant proliferative effects on nestin-expressing cells. Hippocampal cells were generated under control conditions for 3DIV. BrdU and treatment conditions were added for the terminal 6 hours before fixation. Cells were immunostained for nestin expression and BrdU incorporation. **A.** Total cell counts as measured by the number of nestin positive cells. **B.** Proportion of nestin-expressing cell incorporating BrdU, with respect to total number of nestin positive cells. Data represents mean ± SE based on a sample that represents 12 wells per condition from 3 different experiments. Comparisons between control and treatment conditions are a one-way ANOVA with Bonferroni correction for multiple comparisons (*, $p < 0.05$, **, $p < 0.01$, ***, $p < 0.001$)

To confirm the specificity of the IL-4 antibody and eliminate the possibility of non-specific binding, an isotype control antibody was used. The isotype antibody does not have specificity for a target cell but retains non-specific characteristics of the antibody. Cultures were generated for 3DIV under control conditions and treated with experimental conditions for the terminal 6 hours before fixation. Experimental conditions were standard control conditions, 5% activated supernatant, 30nM VIP added directly to cultures, 5% VIP pre-treated activated supernatant, control conditions with IgG_1 isotype, 5% activated supernatant with IgG_1 isotype, 30nM VIP added directly to cultures with IgG_1 isotype, 5% VIP pre-treated activated supernatant with IgG_1 isotype. Cultures were processed for BrdU incorporation and nestin expression.

There was a change in the mitotic index across experimental conditions ($f(7,88)=2.2$) **(Figure 44 B)**. As before, there was an increase under treatment with 5% activated supernatant pre-treated with VIP compared to control (0.22 ± 0.005

vs. 0.14 ± 0.003; $p < 0.001$). There was also an increase under 5% supernatant compared to control (0.19 ± 0.004 vs. 0.14 ± 0.003; $p < 0.001$). The increase under supernatant pre-treated with VIP was enhanced compared to treatment with supernatant alone (0.22 ± 0.005 vs. 0.19 ± 0.004; $p < 0.001$). There was no change under treatment with VIP compared to control (0.15 ± 0.002 vs. 0.14 ± 0.003; p = n.s.). The same trend was observed under treatment with 5% supernatant pre-treated with VIP in the presence of IgG_1 isotype, whereby there was an increase in the mitotic index compared to control (0.23 ± 0.004 vs. 0.14 ± 0.003; $p < 0.001$). This was comparable to treatment with 5% supernatant pre-treated with VIP (0.23 ± 0.004 vs. 0.22 ± 0.005; p = n.s.). There was also an increase under treatment with 5% supernatant in the presence of IgG_1 isotype compared to control (018 ± 0.003 vs. 0.14 ± 0.003; $p < 0.001$). Again, this increase was comparable to treatment with 5% supernatant (0.18 ± 0.003 vs. 0.19 ± 0.004; p = n.s.). There was no change under treatment with VIP in the presence of IgG_1 isotype compared to control, or indeed compared to VIP treatment alone (0.14 ± 0.002 vs. 0.14 ± 0.003 and 0.14 ± 0.002 vs 0.15 ± 0.002, respectively; p = n.s.). There was no change observed in the total cell numbers across experimental conditions ($f(7,88)=0.59$) **(Figure 44 A)**. This data shows the IgG_1 isotype does not change the mitotic index results observed under treatment conditions.

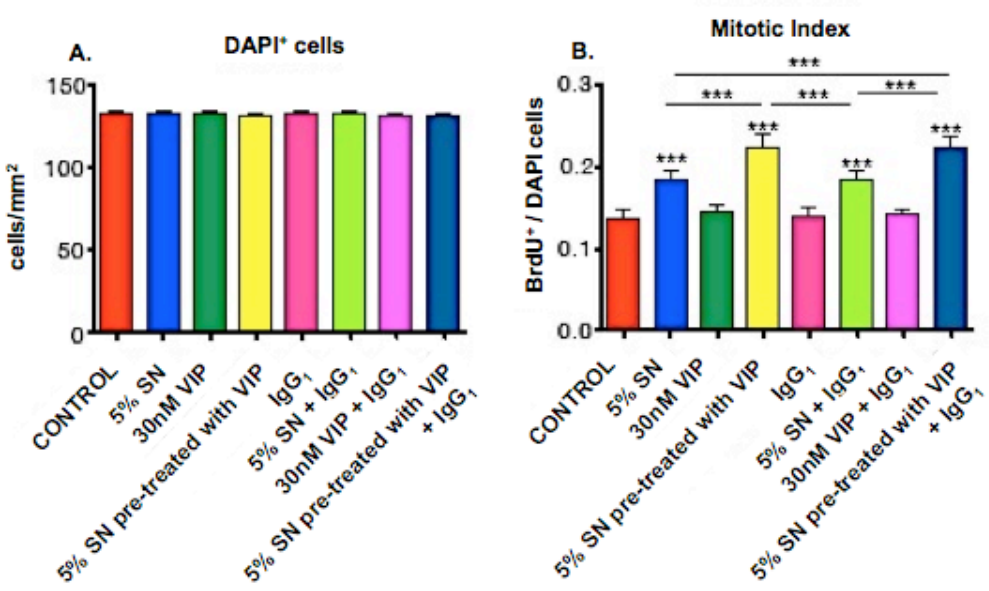

Figure 44: IgG_1 isotype antibody confirms anti-mouse IL-4 antibody binds specifically to mouse IL-4 and does not alter the mitotic index. Hippocampal cells were generated under control conditions for 3DIV. BrdU and treatment conditions were added for the terminal 6 hours before fixation. Cells were immunostained for BrdU incorporation and counterstained with DAPI. **A.** Total cell counts as measured by the number of DAPI positive cells. **B.** Proportion of BrdU incorporating cells, with respect to total number of cells. Data represents mean ± SE based on a sample that represents 12 wells per condition from 3 different experiments. Comparisons between control and treatment conditions are a one- way ANOVA with Bonferroni correction for multiple comparisons (*, $p < 0.05$, **, $p < 0.01$, ***, $p < 0.001$)

There was a change in the poportion of nestin-expressing cells incorporating BrdU, with respect to the total number of nestin positive cells, across experimental conditions ($f(7,88)=2.1$) **(Figure 45 B)**. As before, there was an increase under treatment with 5% supernatant pre-treated with VIP compared to control (0.23 ± 0.003 vs.0.12 ± 0.005; $p < 0.001$). There was also an increase under 5% supernatant compared to control (0.18 ± 0.006 vs. 0.12 ± 0.005; $p < 0.001$). The increase under supernatant pre-treated with VIP was enhanced compared to treatment with supernatant alone (0.23 ± 0.003 vs. 0.18 ± 0.006; $p < 0.001$). There was no change under treatment with VIP compared to control (0.13 ± 0.005 vs. 0.12 ± 0.005; p = n.s.). The same trend was observed under treatment with 5% supernatant pre-treated with VIP in the presence of IgG_1 isotype, whereby there was an increase in the proportion compared to control (0.22 ± 0.005 vs. 0.12 ± 0.005; $p < 0.001$). This was comparable to treatment with 5% supernatant pre-treated with VIP (0.22 ± 0.005 vs. 0.23 ± 0.003; p = n.s.). There was also an increase under treatment with 5% supernatant in the presence of IgG_1 isotype compared to control (0.19 ± 0.007 vs. 0.12 ± 0.005; $p < 0.001$). Again, this increase was comparable to treatment with 5% supernatant (0.18 ± 0.006 vs. 0.19 ± 0.007). There was no change under

treatment with VIP in the presence of IgG_1 isotype compared to control, or indeed compared to VIP treatment alone (0.13 ± 0.004 vs. 0.12 ± 0.005 and 0.13 ± 0.004 vs. 0.13 ± 0.005, respectively; p = n.s.). There was no change observed in the total number of nestin-expressing cells across experimental conditions (f(7,88)=0.69) **(Figure 45 A)**. This data shows the IgG_1 isotype does not change the results observed under treatment conditions without IgG_1 isotype. Taken together, the data confirms specificity of the anti-mouse IL-4 antibody.

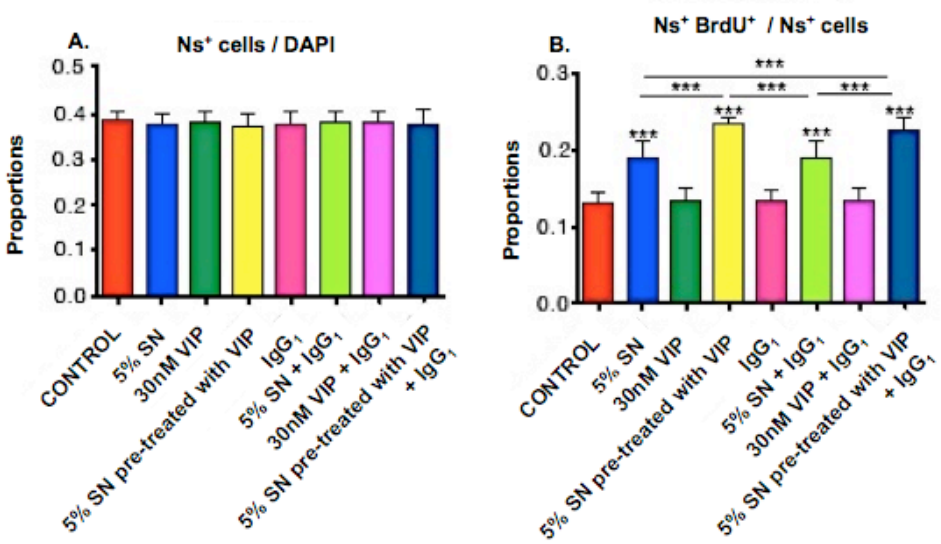

Figure 45: IgG_1 isotype antibody confirms anti-mouse IL-4 antibody binds specifically to mouse IL-4 and does not change the proportion of nestin-expressing cells incorporating BrdU. Hippocampal cells were generated under control conditions for 3DIV. BrdU and treatment conditions were added for the terminal 6 hours before fixation. Cells were immunostained for nestin expression and BrdU incorporation. **A.** Total cell counts as measured by the number of nestin positive cells. **B.** Proportion of nestin expressing cells incorporating BrdU, with respect to total number of nestin positive cells. Data represents mean ± SE based on a sample that represents 12 wells per condition from 3 different experiments. Comparisons between control and treatment conditions are a one-way ANOVA with Bonferroni correction for multiple comparisons (*,p< 0.05, **, p < 0.01, ***, p < 0.001)

5.3.3: IL-4 mediated effects are specifically from supernatant

Splenocyte cultures were generated from adult mice whilst hippocampal cultures were from postnatal rats (P7-10). Therefore, to determine the contribution of IL-4 generated from hippocampal cultures, a rat-specific anti-IL-4 antibody was used. Rat hippocampal cultures were generated for 2DIV under standard control conditions and treated with experimental conditions for the terminal 6 hours before fixation. Experimental conditions were standard control conditions, 5% activated supernatant, 30nM VIP added directly to cultures, 5% VIP pre-treated activated supernatant, control conditions with anti-rat IL-4, 5% activated supernatant with

anti-rat IL-4, 30nM VIP added directly to cultures with anti-rat IL-4, 5% VIP pre-treated activated supernatant with anti-rat IL-4. Cultures were processed for BrdU incorporation and nestin expression.

There was a change in the mitotic index across experimental conditions ($f(7,88)=3.4$) **(Figure 46 B)**. Consistent with previous data, there was an increase in the mitotic index under treatment with 5% supernatant pre-treated with VIP compared to control (0.22 ± 0.004 vs. 0.14 ± 0.003; $p < 0.001$). There was also an increase under treatment with 5% supernatant compared to control (0.19 ± 0.003 vs. 0.14 ± 0.003; $p < 0.001$). The increase under 5% supernatant pre-treated with VIP was enhanced compared to treatment with 5% supernatant alone ($0.22 \pm 0.00.4$ vs. 0.19 ± 0.003; $p < 0.001$). There was no change under treatment with VIP compared to control (0.14 ± 0.002 vs. 0.14 ± 0.003; p = n.s.). The same trend was observed under treatment with 5% supernatant pre-treated with VIP in the presence of anti-rat IL--4, whereby there was an increase in the mitotic index compared to control (0.23 ± 0.0005 vs. 0.14 ± 0.003; $p < 0.001$). This was comparable to treatment with 5% supernatant pre-treated with VIP (0.23 ± 0.005 vs. 0.22 ± 0.004; p = n.s.). There was also an increase under treatment with 5% supernatant in the presence of anti-rat IL-4 compared to control (0.18 ± 0.004 vs. 0.14 ± 0.003; $p < 0.001$). Again, this increase was comparable to treatment with 5% supernatant (0.18 ± 0.004 vs. 0.19 ± 0.003; p = n.s.). There was no change under treatment with VIP in the presence of anti-rat IL-4 compared to control, or indeed compared to VIP treatment alone (0.15 ± 0.002 vs. 0.14 ± 0.004 and 0.15 ± 0.002 vs. 0.14 ± 0.002; p = n.s.). There was no change observed in the total cell numbers across experimental conditions ($f(7,88)=1.6$) **(Figure 46 A)**. This data shows anti-rat IL-4 does not change the mitotic index of supernatant treated cultures.

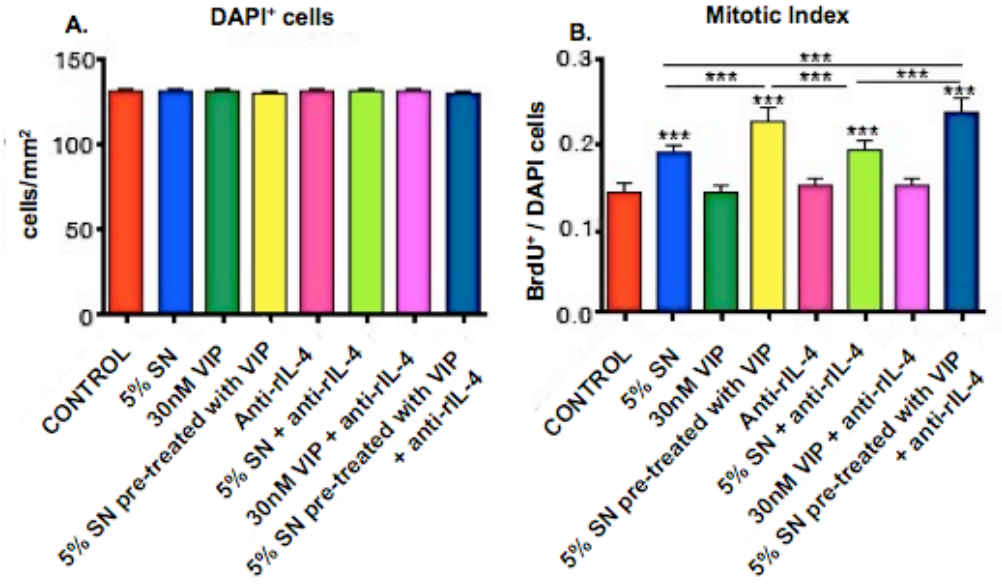

Figure 46: anti-rat IL-4 does not mediate supernatant proliferative effects on the mitotic index. Hippocampal cells were generated under control conditions for 3DIV. BrdU and treatment conditions were added for the terminal 6 hours before fixation. Cells were immunostained for BrdU incorporation and counterstained with DAPI. **A.** Total cell counts as measured by the number of DAPI positive cells. **B.** Proportion of BrdU incorporating cells, with respect to total number of cells. Data represents mean ± SE based on a sample that represents 12 wells per condition from 3 different experiments. Comparisons between control and treatment conditions are a one-way ANOVA with Bonferroni correction for multiple comparisons (*, $p < 0.05$, **, $p < 0.01$, ***, $p < 0.001$)

There was a change in the proportion of nestin-expressing cells incorporating BrdU, with respect to the total number of nestin-positive cells, across experimental conditions ($f(7,88)=1.1$) **(Figure 47 B)**. Consistent with previous data, there was an increase in the proportion under treatment with 5% supernatant pre-treated with VIP compared to control (0.23 ± 0.002 vs. 0.13 ± 0.003; $p < 0.001$). There was also an increase under treatment with 5% supernatant compared to control (0.18 ± 0.004 vs. 0.13 ± 0.003; $p < 0.001$). The increase under 5% supernatant pre-treated with VIP was enhanced compared to treatment with 5% supernatant alone (0.23 ± 0.002 vs. 0.18 ± 0.004; $p < 0.001$). There was no change under treatment with VIP compared to control (0.13 ± 004 vs. 0.13 ± 0.003; p = n.s.). The same trend was observed under treatment with 5% supernatant pre-treated with VIP in the presence of anti-rat IL-4, whereby there was an increase in the proportion compared to control (0.23 ± 0.003 vs. 0.13 ± 0.003; $p < 0.001$). This was comparable to treatment with 5% supernatant pre-treated with VIP (0.23 ± 0.003 vs. 0.23 ± 0.002; p = n.s.). There was an increase under treatment with 5% supernatant in the presence of anti-rat IL-4 compared to control (0.18 ± 0.003 vs. 0.13 ± 0.003; p <

0.001). Again, this increase was comparable to treatment with 5% supernatant (0.18 ± 0.004 vs. 0.18 ± 0.003; p = n.s.). There was no change under treatment with VIP in the presence of anti-rat IL-4 compared to control, or indeed compared to VIP treatment alone (0.13 ± 0.005 vs. 0.13 ± 0.003 and 0.13 ± 0.005 vs. 0.12 ± 0.004, respectively; p = n.s.). There was no change observed in the total number of nestin positive cells across experimental conditions (f(7,88)=0.43) **(Figure 47 A)**. This data shows anti-rat IL-4 does not change the proportion of nestin-expressing cells incorporating BrdU in supernatant treated cultures. This suggests rat IL-4 does not mediate the proliferative effects; increased proliferation is via splenocytes released IL-4.

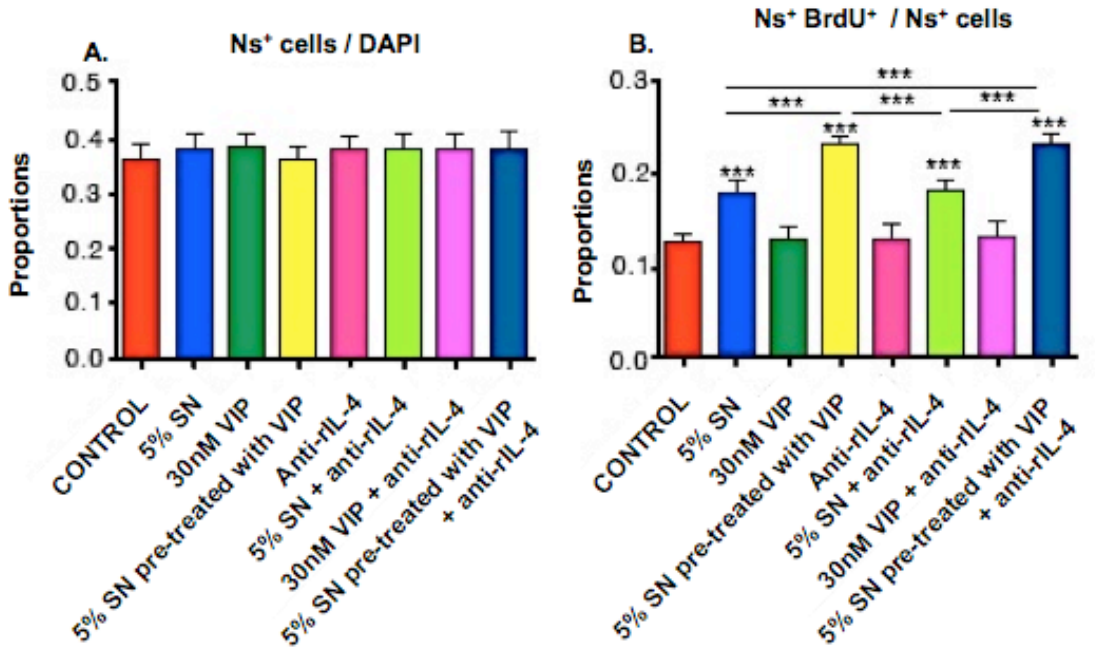

Figure 47: anti-rat IL-4 does not change supernatant proliferative effects on proportion of nestin-expressing cells incorporating BrdU. Hippocampal cells were generated under control conditions for 3DIV. BrdU and treatment conditions were added for the terminal 6 hours before fixation. Cells were immunostained for nestin expression and BrdU incorporation. **A.** Total cell counts as measured by the number of nestin positive cells. **B.** Proportion of nestin expressing cells incorporating BrdU, with respect to total number of nestin positive cells. Data represents mean ± SE based on a sample that represents 12 wells per condition, from 3 different experiments. Comparisons between control and treatment conditions are a one-way ANOVA with Bonferroni correction for multiple comparisons (*, $p < 0.05$, **, $p < 0.01$, ***, $p < 0.001$)

An isotype antibody was used. Cultures were generated for 3DIV under control conditions and treated with experimental conditions for the terminal 6 hours before fixation. Experimental conditions were standard control conditions, 5% activated supernatant, 30nM VIP added directly to cultures, 30nM VIP pre-treated activated

supernatant, control conditions with IgG2a isotype, 5% activated supernatant with IgG2a isotype, 30nM VIP added directly to cultures with IgG2a isotype, 30nM VIP pre-treated activated supernatant with IgG2a isotype. Cultures were processed for BrdU incorporation and nestin expression.

There was a change in the mitotic index across experimental conditions ($f(7,88)=2.4$) **(Figure 48 B)**. As before, there was an increase under treatment with 5% supernatant pre-treated with VIP compared to control (0.22 ± 0.004 vs. 0.14 ± 0.004; $p < 0.001$). There was also an increase under 5% supernatant compared to control (0.19 ± 0.003 vs. 0.14 ± 0.004; $p < 0.001$). The increase under supernatant pre-treated with VIP was enhanced compared to treatment with supernatant alone (0.22 ± 0.004 vs. 0.19 ± 0.003; $p < 0.001$). There was no change under treatment with VIP compared to control (0.14 ± 0.002 vs. 0.14 ± 0.004; p = n.s.). The same trend was observed under treatment with 5% supernatant pre-treated with VIP in the presence of IgG2a isotype, whereby there was an increase in the mitotic index compared to control (0.23 ± 0.002 vs. 0.14 ± 0.004; $p < 0.001$). This was comparable to treatment with 5% supernatant pre-treated with VIP (0.23 ± 0.002 vs. 0.22 ± 0.004; p = n.s.). There was also an increase under treatment with 5% supernatant in the presence of IgG2a isotype compared to control (0.18 ± 0.006 vs. 0.14 ± 0.004; $p < 0.001$). Again, this increase was comparable to treatment with 5% supernatant (0.18 ± 0.006 vs. 0.19 ± 0.003; p = n.s.). There was no change under treatment with VIP in the presence of IgG2a isotype compared to control, or indeed compared to VIP treatment alone (0.12 ± 0.003 vs. 0.14 ± 0.004 and 0.12 ± 0.003 vs 0.14 ± 0.002, respectively; p = n.s.). There was no change observed in the total cell number across experimental conditions ($f(7,88)=1.5$) **(Figure 48 A)**. This data shows the IgG2a isotype does not change the mitotic index results observed under treatment conditions.

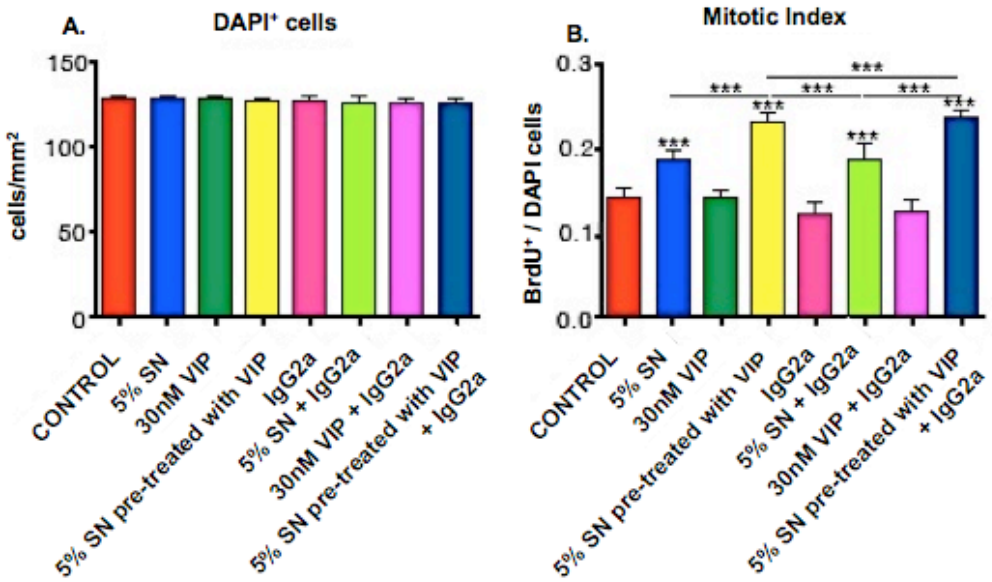

Figure 48: IgG2a isotype control antibody for anti-rat IL-4 activity does not change the mitotic index. Hippocampal cells were generated under control conditions for 3DIV. BrdU and treatment conditions were added for the terminal 6 hours before fixation. Cells were immunostained for BrdU incorporation and counterstained with DAPI. **A.** Total cell counts as measured by the number of DAPI positive cells. **B.** Proportion of BrdU incorporating cells, with respect to total number of cells. Data represents mean ± SE based on a sample that represents 12 wells per condition from 3 different experiments. Comparisons between control and treatment conditions are a one- way ANOV A with Bonferroni correction for multiple comparisons (*, $p < 0.05$, **, $p < 0.01$,***, $p < 0.001$)

There was a change in the proportion of nestin-expressing cells incorporating BrdU, with respect to the total number of nestin positive cells, across experimental conditions ($f(7,88)=1.2$) **(Figure 49 B)**. As before, there was an increase under treatment with 5% supernatant pre-treated with VIP compared to control (0.23 ± 0.002 vs. 0.13 ± 0.003; $p < 0.001$). There was also an increase under 5% supernatant compared to control (0.18 ± 0.004 vs. 0.13 ± 0.003; $p < 0.001$). The increase under supernatant pre-treated with VIP was enhanced compared to treatment with supernatant alone (0.23 ± 0.002 vs. 0.18 ± 0.004; $p < 0.001$). There was no change under treatment with VIP compared to control (0.13 ± 0.004 vs. 0.13 ± 0.003; p = n.s.). The same trend was observed under treatment with 5% supernatant pre-treated with VIP in the presence of IgG2a isotype, whereby there was an increase in the proportion compared to control (0.23 ± 0.003 vs. 0.13 ± 0.003; $p < 0.001$). This was comparable to treatment with 5% supernatant pre-treated with VIP (0.23 ± 0.003 vs. 0.23 ± 0.002; p = n.s.). There was also an increase under treatment with 5% supernatant in the presence of IgG2a isotype compared to control (0.19 ± 0.003 vs. 0.13 ± 0.003; $p < 0.001$). Again, this increase was comparable to treatment with 5% supernatant (0.19 ± 0.003 vs. 0.18 ± 0.004; p = n.s.). There was no change under

treatment with VIP in the presence of IgG2a isotype compared to control, or indeed compared to VIP treatment alone (0.15 ± 0.005 vs. 0.13 ± 0.003 and 0.15 ± 0.005 vs 0.13 ± 0.004, respectively; p = n.s.). There was no change observed on the total number of nestin-expressing cells across experimental conditions (f(7,88)=0.18) **(Figure 49 A)**. This data shows the IgG2a isotype does not change the results observed under treatment conditions without IgG2a isotype.

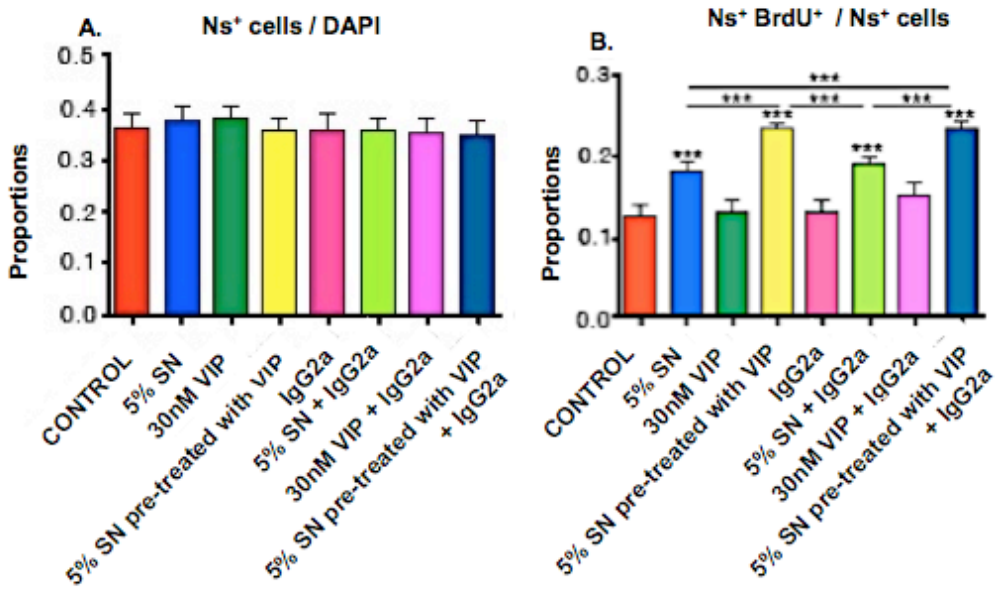

Figure 49: IgG2a isotype control antibody for anti-rat IL-4 does not change the proportion of nestin-expressing cells incorporating BrdU. Hippocampal cells were generated under control conditions for 3DIV. BrdU and treatment conditions were added for the terminal 6 hours before fixation. Cells were immunostained for nestin expression and BrdU incorporation. **A.** Total number of nestin positive cells. **B.** Proportion of nestin expressing cells incorporating BrdU, with respect to total nestin numbers. Data represents mean ± SE based on a sample that represents 12 wells per condition from 3 different experiments. Comparisons between control and treatment conditions are a one-way ANOVA with Bonferroni correction for multiple comparisons (*, $p < 0.05$, **, $p < 0.01$, ***, $p < 0.001$)

5.3.4: Abolishing microglia from hippocampal cultures significantly reduces supernatant proliferative effects on hippocampal cells

We sought to investigate whether supernatant IL-4 mediates proliferative effects by acting directly on neural precursor cells or indirectly via other cell types such as microglia. Microglial cell populations were depleted from hippocampal cultures by the addition of Mac-1-SAP, an antibody conjugated to a ribosome-inactivating protein (Saporin), that selectively targets CD11b-expressing cells in the brain.

CD11b expression is restricted to microglia (Heppner et al., 2005, Block et al., 2007). Once the antibody binds to microglia, saporin is internalized and breaks away from the antibody, inactivating the ribosome. This inactivates and then kills microglia. Hippocampal cultures were generated for 2DIV. At 2DIV, half the cultures were treated with Mac-1-SAP and the other half were replaced with fresh culture medium. At 3DIV, cultures were washed with fresh culture medium and treated with experimental conditions for the terminal 6 hours before fixation. Specifically the experimental conditions were standard control conditions, 5% activated supernatant, 30nM VIP added directly to cultures, 5% VIP pre-treated activated supernatant, control culture medium in Mac-1-SAP treated cultures, 5% activated supernatant in Mac-1-SAP treated cultures, 30nM VIP added directly to Mac-1-SAP treated cultures, 5% VIP pre-treated activated supernatant in Mac-1-SAP treated cultures. This allowed comparisons between cultures with and without microglia. Cells were processed for BrdU incorporation and nestin expression.

There was a change in the mitotic index across experimental groups ($f(7,88)=2.4$) **(Figure 50 B)**. Consistent with previous results, there was an increase in the mitotic index under treatment with 5% supernatant pre-treated with VIP compared to control (0.25 ± 0.007 vs. 0.12 ± 0.003; $p < 0.001$). There was also an increase under treatment with 5% supernatant compared to control (0.18 ± 0.006 vs. 0.12 ± 0.003; $p < 0.001$). The increase under 5% supernatant pre-treated with VIP was enhanced compared to 5% supernatant alone (0.25 ± 0.007 vs. 0.18 ± 0.006; $p < 0.001$). There was no change under treatment with VIP compared to control (0.12 ± 0.004 vs. 0.12 ± 0.003; p = n.s.). Addition of Mac-1-SAP to control conditions reduced the mitotic index compared to control (0.07 ± 0.003 vs. 0.12 ± 0.003; $p < 0.001$). Indeed, this is also the case for cultures treated with VIP and Mac-1-SAP compared to control (0.008 ± 0.005 vs. 0.12 ± 0.003; $p < 0.001$). There was a decrease in the mitotic index under treatment with 5% supernatant and Mac-1-SAP compared to 5% supernatant (0.11 ± 0.003 vs. 0.18 ± 0.006; $p < 0.001$). However, it was not reduced to levels of control cultures treated with Mac-1-SAP (0.11 ± 0.003 vs. 0.007 ± 0.003; $p < 0.001$). There was also a decrease in the mitotic index under treatment with 5% supernatant pre-treated with VIP and Mac-1-SAP compared to 5% supernatant pre-treated with VIP (0.13 ± 0.004 vs. 0.25 ± 0.007; $p < 0.001$). Again, this was not

reduced to levels of control cultures treated with Mac-1-SAP (0.13 ± 0.004 vs. 0.07 ± 0.003; $p < 0.001$). There was no change in total cell numbers across experimental conditions ($f(7,88)=0.12$) **(Figure 50 A)**. Taken together, these results suggest abolishing microglia from cultures significantly reduces the mitotic index and furthermore, that supernatant from splenocyte cultures acts predominantly via microglia. However, the results are also consistent with a small direct action of supernatant on neural progenitor cells to increase the mitotic index, since supernatant still had a proliferative effect.

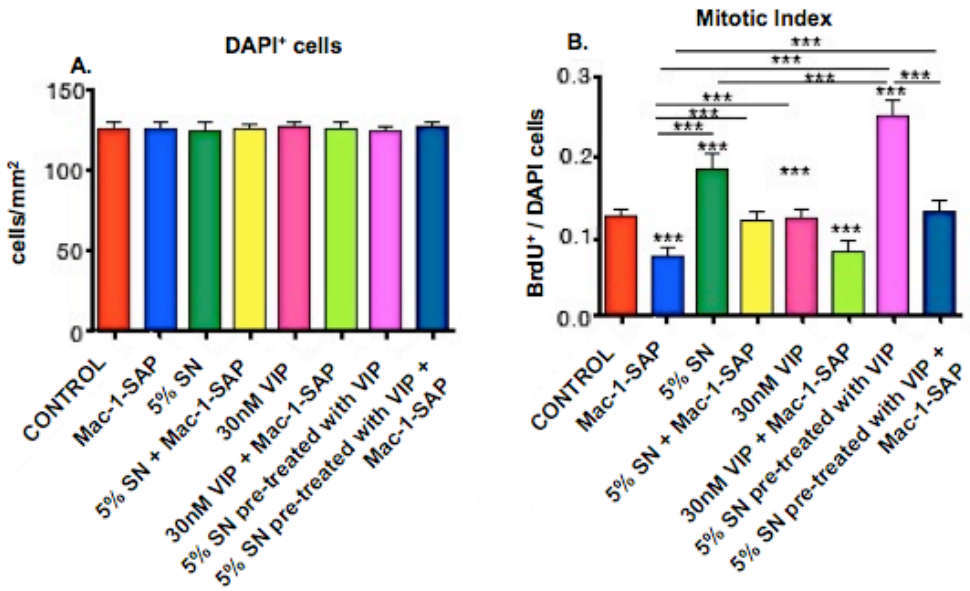

Figure 50: Microglia mediate proliferative effects. Hippocampal cells were generated under control conditions for 2DIV. At 2DIV, half the cultures were treated with Mac-1-SAP ad the other half replenished with fresh culture medium for 24 hours. After 24 hours, BrdU and experimental conditions were added for the terminal 6 hours before fixation. Cells were immunostained for BrdU incorporation and counterstained with DAPI. **A.** Total cell counts as measured by the number of DAPI positive cells. **B.** Proportion of BrdU incorporating cells, with respect to total cell numbers. Data represents mean± SE based on a sample that represents 12 wells per condition from 3 different experiments. Comparisons between control and treatment conditions are a one-way ANOV A with Bonferroni correction for multiple comparisons (*, $p < 0.05$, **, $p < 0.01$, ***, $p < 0.001$)

There was a change in the proportion of nestin-expressing cells incorporating BrdU, with respect to the total number of nestin positive cells, across experimental groups ($f(7,88)=2.1$) **(Figure 51 B)**. Consistent with previous results, treatment with 5% supernatant pre-treated with VIP increases the proportion compared to control (0.23 ± 0.003 vs. 0.13 ± 0.005; $p < 0.001$). The increase under 5% supernatant pre-treated with VIP is enhanced compared to 5% supernatant alone (0.23 ± 0.003 vs. 0.19 ± 0.003; $p < 0.001$). There was no change under treatment with VIP compared

to control (0.15 ± 0.005 vs. 0.13 ± 0.005; p = n.s.). Addition of MAC-1-SAP to control conditions reduced the proportion compared to control (0.08 ± 0.005 vs. 0.13 ± 0.005; $p < 0.001$). Indeed, this is also the case for cultures treated with VIP and MAC-1-SAP compared to control (0.008 ± 0.006 vs. 0.13 ± 0.005; $p < 0.001$). There was a decrease under treatment with 5% supernatant and Mac-1-SAP compared to 5% supernatant alone (0.13 ± 0.005 vs. 0.19 ± 0.003; $p < 0.001$). However, it was not reduced to levels of control cultures treated with Mac-1-SAP (0.13 ± 0,005 vs. 0.08 ± 0.005; $p < 0.001$). There was also a decrease in the proportion under treatment with 5% supernatant pre-treated with VIP and Mac-1-SAP compared to 5% supernatant pre-treated with VIP (0.14 ± 0.007 vs. 0.23 ± 0.003; $p < 0.001$). Again, this was not reduced to levels of control cultures treated with Mac-1-SAP (0.14 ± 0.007 vs. 0.008 ± 0.005; $p < 0.001$). There was no change in the total number of nestin positive cells across experimental conditions ($f(7,88)=1.2$) **(Figure 51 A)**. These results suggest microglia predominantly mediate the proliferative effects of supernatant on nestin-expressing hippocampal cells.

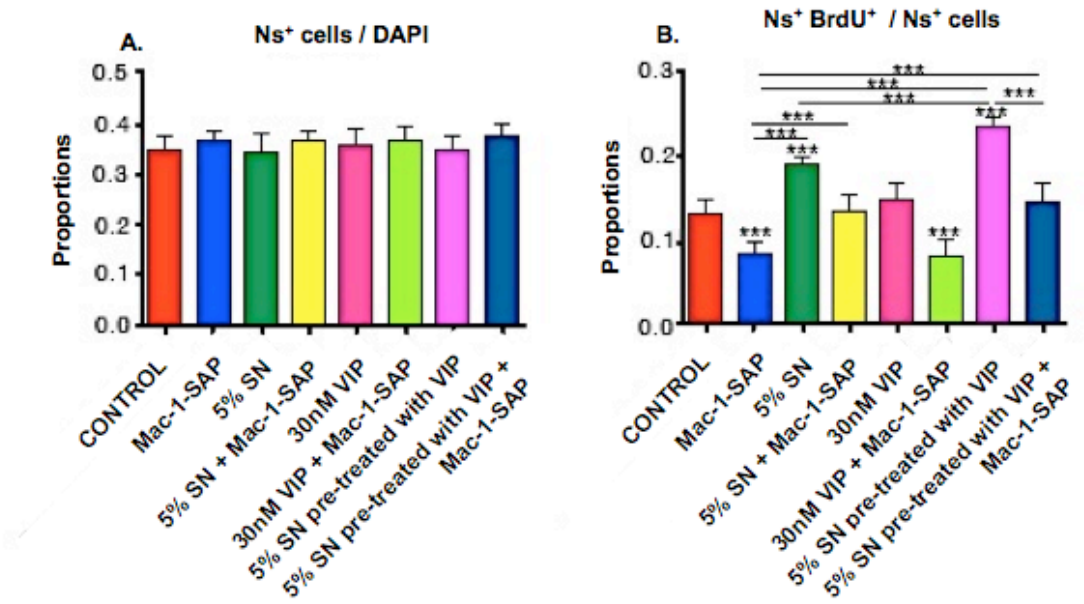

Figure 51: Microglia predominantly mediate the proliferative effects of supernatant on nestin-expressing cells incorporating BrdU. Hippocampal cells were generated under control conditions for 2DIV. At 2DIV, half the cultures were treated with Mac-1-SAP ad the other half replenished with fresh culture medium for 24 hours. After 24 hours, BrdU and experimental conditions were added for the terminal 6 hours before fixation. Cells were immunostained for nestin expression and BrdU incorporation. **A.** Total cell counts as measured by the number of nestin positive cells. **B.** Proportion of nestin expressing cells incorporating BrdU, with respect to total number of nestin cells. Data represents mean± SE based on a sample that represents 12 wells per condition from 3 different experiments. Comparisons between control and treatment conditions are a one-way ANOVA with Bonferroni correction for multiple comparisons (*, $p < 0.05$, **, $p < 0.01$, ***, $p < 0.001$)

5.3.5: IL-4 acts directly on progenitor cells and also via microglia to increase proliferation of hippocampal cells

Given that anti-mouse IL-4 abolishes supernatant effects, coupled with the partial microglial mediation of hippocampal proliferation, suggests the potential for IL-4 acting both directly and indirectly (via microglia) on hippocampal progenitor cells. To investigate this, anti-mouse IL-4 was given in combination with Mac-1-SAP treated cultures. Hippocampal cultures were generated under standard control conditions for 2DIV. At 2DIV, cultures were either treated with Mac-1-SAP or replaced with standard control conditions. At 3DIV, cultures were washed with fresh culture medium and treated with experimental conditions as before. However, this time with the addition of anti-mouse IL-4. Specifically the experimental conditions were standard control conditions, 5% activated supernatant, 30nM VIP added directly to cultures, 5% VIP pre-treated activated supernatant, control culture medium in Mac-1-SAP treated cultures, 5% activated supernatant in Mac-1-

SAP treated cultures, 30nM VIP added directly to Mac-1-SAP treated cultures, 5% VIP pre-treated activated supernatant in Mac-1-SAP treated cultures, control culture medium in Mac-1-SAP treated cultures with anti-mouse IL-4, 5% activated supernatant in Mac-1-SAP treated cultures with anti-mouse IL-4, 30nM VIP added directly to Mac-1-SAP treated cultures with anti-mouse IL-4, 5% VIP pre-treated activated supernatant in Mac-1-SAP treated cultures with anti-mouse IL-4. This was added for the terminal 6 hours before fixation. Cells were processed for BrdU incorporation and nestin expression.

There was a change in the mitotic index across experimental groups ($f(11,132)=0.68$) **(Figure 52 B)**. Consistent with previous results, there was an increase in the mitotic index in cultures treated with 5% supernatant pre-treated with VIP compared to control (0.24 ± 0.003 vs. 0.13 ± 0.003; $p < 0.001$). There was also an increase under treatment with 5% supernatant compared to control (0.18 ± 0.005 vs. 0.13 ± 0.003; $p < 0.001$). The increase under treatment with 5% supernatant pre-treated with VIP was enhanced compared to treatment with 5% supernatant (0.24 ± 0.003 vs. 0.18 ± 0.005; $p < 0.001$). There was no change under treatment with VIP compared to control (0.12 ± 0.005 vs. 0.13 ± 0.003; p = n.s.). Again, consistent with previous results, addition of Mac-1-SAP to control conditions reduced the mitotic index compared to control (0.08 ± 0.003 vs. 0.13 ± 0.003; $p < 0.001$). Indeed, this is also the case for cultures with VIP and Mac-1-SAP compared to control (0.08 ± 0.003 vs. 0.13 ± 0.003; $p < 0.001$). There was a decrease in the mitotic index under treatment with 5% supernatant and Mac-1-SAP compared to 5% supernatant (0.13 ± 0.003 vs. 0.18 ± 0.005; $p < 0.001$). This was reduced down to control levels (0.13 ± 0.003 vs. 0.13 ± 0.003; p = n.s.). However, it was not reduced to levels of control cultures treated with Mac-1-SAP (0.13 ± 0.003 vs. 0.18 ± 0.005; $p < 0.001$). There was also a decrease in the mitotic index under treatment with 5% supernatant pre-treated with VIP and Mac-1-SAP compared to 5% supernatant pre-treated with VIP (0.13 ± 0.003 vs, 0.24 ± 0.003; $p < 0.001$). Again, this was reduced to control levels (0.13 ± 0.003 vs. 0.13 ± 0.003; p = n.s.) but not reduced to levels of control cultures treated with Mac-1-SAP (0.13 ± 0.003 vs. 0.08 ± 0.005; $p < 0.001$).

Interestingly, the addition of anti-mouse IL-4 in Mac-1-SAP treated cultures with 5% supernatant reduced the mitotic index to levels of control conditions treated with Mac-1-SAP (0.07 ± 0.003 vs. 0.08 ± 0.003; p = n.s.). The addition of anti-mouse IL-4 in Mac-1-SAP treated cultures with 5% supernatant pre-treated with VIP reduced the mitotic index to the level of control cultures treated with Mac-1-SAP (0.07 ± 0.003 vs. 0.08 ± 0.003; p = n.s.). Anti-mouse IL-4 did not further reduce control conditions treated with Mac-1-SAP or VIP treated cultures with Mac-1-SAP (0.07 ± 0.003 vs. 0.08 ± 0.003 and 0.007 ± 0.003 vs. 0.08 ± 0.003, respectively; p = n.s.). There was no change in total cell numbers across experimental conditions (f(11,132)=1.9) **(Figure 52 A)**. These results show that addition of anti-mouse IL-4 reduces the mitotic index of Mac-1-SAP treated cultures with supernatant down to the level of Mac-1-SAP treatment. Therefore, these results suggest mouse IL-4 acts predominantly on microglia to increase the mitotic index in hippocampal cells. However, IL-4 also acts directly on neural progenitor cells.

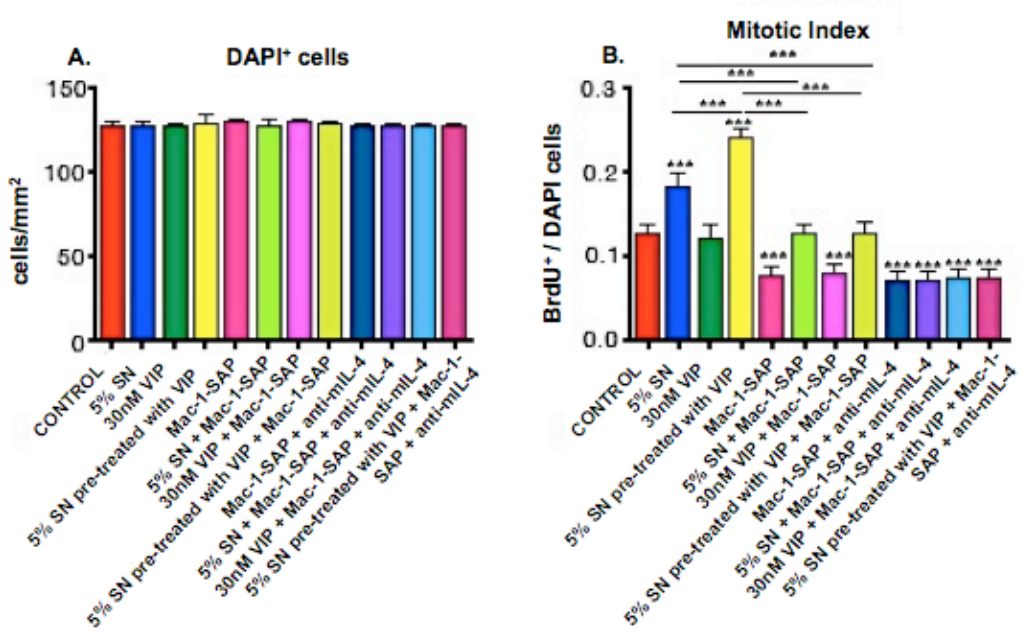

Figure 52: Addition of anti-mouse IL-4 in microglia-depleted cultures completely abolishes supernatant effects. Hippocampal cells were generated under control conditions for 2DIV. At 2DIV, half the cultures were treated with Mac-1-SAP ad the other half replenished with fresh culture medium for 24 hours. After 24 hours, BrdU and experimental conditions were added for the terminal 6 hours before fixation. Cells were immunostained for BrdU incorporation and counterstained wit h DAPI. **A.** Total cell counts as measured by the number of DAPI positive cells **B.** Proportion of BrdU incorporating cells, with respect to total cell numbers. Data represents mean ± SE based on a sample that represents 12 wells per condition from 3 different experiments. Comparisons between control and treatment conditions are a one-way ANOVA with Bonferroni correction for multiple comparisons (*, $p < 0.05$, **, $p < 0.01$, ***, $p < 0.001$)

There was a change in the proportion of nestin-expressing cells incorporating BrdU, with respect to total nestin numbers, across experimental groups ($f(11,132)=1.0$) **(Figure 53 B)**. Consistent with previous results, there was an increase in the proportion under treatment with 5% supernatant pretreated with VIP compared to control (0.24 ± 0.003 vs. 0.14 ± 0.006; $p < 0.001$). There was also an increase under treatment with 5% supernatant compared to control (0.20 ± 0.004 vs. 0.14 ± 0.006; $p < 0.001$). There was no change under VIP treatment alone compared to control (0.15 ± 0.007 vs. 0.14 ± 0.006; p = n.s.). Again, consistent with previous results, the addition of Mac-1-SAP to control conditions reduced the proportion compared to control (0.08 ± 0.003 vs. 0.14 ± 0.006; $p < 0.001$). Indeed, this is also the case for cultures treated with VIP and Mac-1-SAP compared to control (0.08 ± 0.005 vs. 0.14 ± 0.006; $p < 0.001$). There was a decrease in the proportion under treatment with 5% supernatant and Mac-1-SAP compared to 5% supernatant (0.13 ± 0.003 vs. 0.20 ± 0.004; $p < 0.001$). This was reduced down to control levels (0.13 ± 0.03 vs. 0.14 ± 0.006; p = n.s.). However it was not reduced to levels of control cultures treated with MAC-1-SAP (0.13 ± 0.003 vs, 0.08 ± 0.003; $p < 0.001$). There was also a decrease in the mitotic index under treatment with 5% supernatant pre-treated with VIP and MAC-1-SAP compared to 5% supernatant pre-treated with VIP (0.14 ± 0.004 vs. 0.24 ± 0.003; $p < 0.001$). Again, this was only reduced to control (0.13 ± 0.004 vs, 0.14 ± 0.006; p = n.s.) and not to levels of control cultures treated with Mac-1-SAP (0.13 ± 0.004 vs. 0.08 ± 0.003; $p < 0.001$).

The addition of anti-mouse IL-4 in Mac-1-SAP treated cultures with 5% supernatant reduced the proportion to levels of control conditions treated with Mac-1-SAP (0.07 ± 0.003 vs. 0.08 ± 0.003; p = n.s.). The addition of anti-mouse IL-4 in Mac-1-SAP treated cultures with 5% supernatant pre-treated with VIP reduced the proportion to levels of control cultures treated with Mac-1-SAP (0.07 ± 0.004 vs. 0.08 ± 0.003; p = n.s.). Anti-mouse IL-4 did not further reduce control conditions treated with Mac-1-SAP or VIP treated cultures with Mac-1-SAP (0.07 ± 0.004 vs. 0.08 ± 0.003 and 0.07 ± 0.004 vs. 0.08 ± 0.003, respectively; p = n.s.). There was no change in the total number of nestin-expressing cells across experimental conditions ($f(11,132)=2.0$) **(Figure 53 A)**. Taken together, these results suggest supernatant IL-4 acts

predominantly via microglia and also directly on hippocampal progenitor cells to increase the proportion of nestin-expressing cells incorporating BrdU.

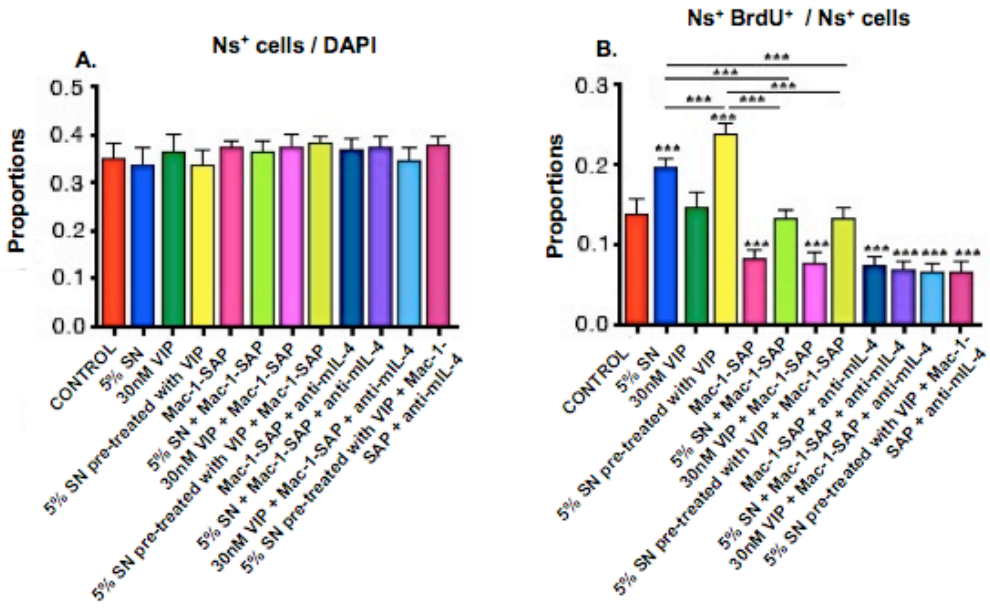

Figure 53: Addition of anti-mouse IL-4 in microglia-depleted cultures completely abolishes supernatant effects on the proportion of nestin-expressing cells incorporating BrdU. Hippocampal cells were generated under control conditions for 2DIV. At 2DIV, half the cultures were treated with Mac-1-SAP ad the other half replenished with fresh culture medium for 24 hours. After 24 hours, BrdU and experimental conditions were added for the terminal6 hours. before fixation. Cells were immunostained for nestin expression and BrdU incorporation. **A.** Total number of nestin positive cells. **B.** Proportion of nestin expressing cells incorporating BrdU, with respect to total number of nestin cells. Data represents mean ± SE based on a sample that represents 12 wells per condition from 3 different experiments. Comparisons between control and treatment conditions are a one-way ANOVA with Bonferroni correction for multiple comparisons (*, $p < 0.05$, **, $p < 0.01$, ***, $p < 0.001$)

5.3.6: Supernatant acts on microglia to significantly increase BDNF mRNA expression

T lymphocytes-released IL-4 is known to drive microglia to produce pro-neurogenic factors such as BDNF (Derecki et al., 2010). Therefore we investigated a potential role for BDNF in our study paradigm. Pure microglial cultures were generated from post-natal rat hippocampal cultures and treated with experimental conditions for 2 hours. Experimental conditions were standard control conditions, 5% activated supernatant, 30nM VIP added directly to cultures, 30nM VIP pre-treated activated supernatant. Cells were collected in TRizol and converted to cDNA for PCR analysis. There was an approximate four fold increase in BDNF mRNA expression in microglial cells under treatment with 5% activated supernatant **(Figure 54)**. Treatment with 5% supernatant pre-treated with 30nM VIP increased BDNF mRNA

expression in microglial cells by approximately eight fold. This was a significantly enhanced effect compared to treatment with 5% supernatant alone. There was two fold increase under treatment with 30nM VIP, but this was not significant. These results suggest a potential role for microglia-released BDNF in increasing hippocampal cultures following treatment with supernatant; an effect enhanced by VIP pre-treatment.

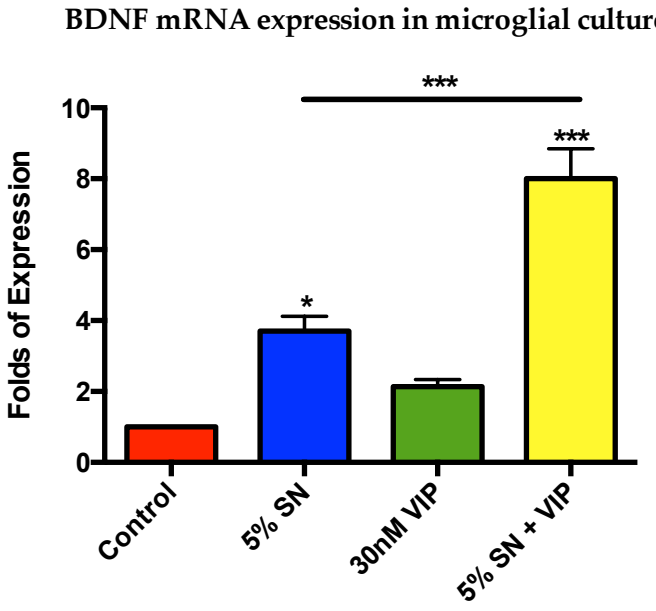

Figure 54: Supernatant increases BDNF mRNA expression. Pure rat microglial cultures were generated and treated with experimental conditions for 2 hours. Cells were then collected in trizol and converted to cDNA for PCR analysis. Data is from 2 different experiments. Comparisons between control and treatment conditions are a one-way ANOV A with Bonferroni correction for multiple comparisons (*, $p < 0.05$, **, $p < 0.01$, ***, $p < 0.001$)

5.3.7: Supernatant upregulates M1 and M2 microglial markers

The phenotype of microglia following treatment with T lymphocytes supernatant was investigated. Pure microglial cultures were generated from post-natal rat hippocampal cultures and treated with experimental conditions for 2 hours. Cells were collected in TRizol and converted to cDNA for PCR analysis. TNFα and NOS2 were used as M1 phenotype markers. IL-10 and Chi3I3 (Ym1) were used as M2 phenotype markers.

The M2 marker IL-10 was significantly upregulated in microglial cells **(Figure 55)**. There was a 24 fold increase in mRNA expression under treatment with

supernatant pre-treated with VIP. There was a 4 fold increase in mRNA under treatment with 5% supernatant, but this was not statistically significant. There was also a 2.5 increase in folds of expression under treatment with 30nM VIP, however this was not statistically significant either.

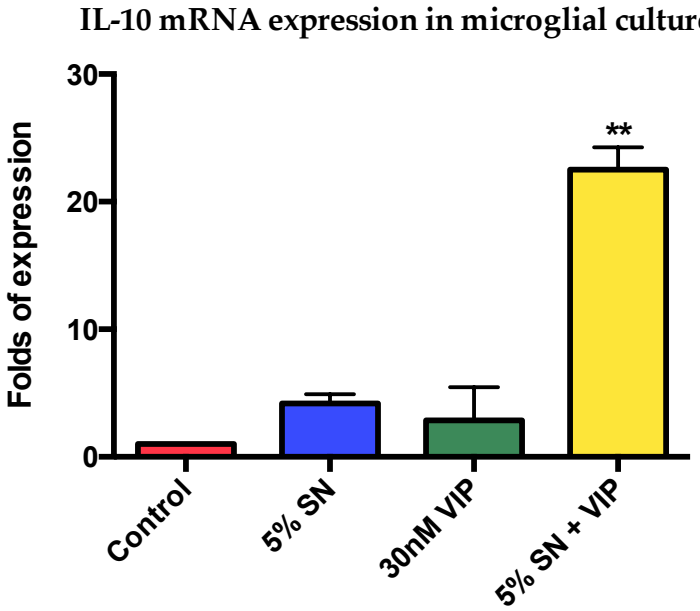

Figure 55: Supernatant increases IL-10 mRNA expression. Pure rat microglial cultures were generated and treated with experimental conditions for 2 hours. Cells were then collected in trizol and converted to cDNA for PCR analysis. Data is from 2 different experiments. Comparisons between control and treatment conditions are a one-way ANOV A with Bonferroni correction for multiple comparisons (*, $p < 0.05$, **, $p < 0.01$, ***, $p < 0.001$)

mRNA expression of the M2 marker Chi3I3 did not significantly change in microglial cells **(Figure 56)**. There was a 1.5 fold increase in mRNA under treatment with supernatant which was not significant. There was also a 2 fold increase under treatment with 5% supernatant pre-treated with VIP, but again this was not statistically significant.

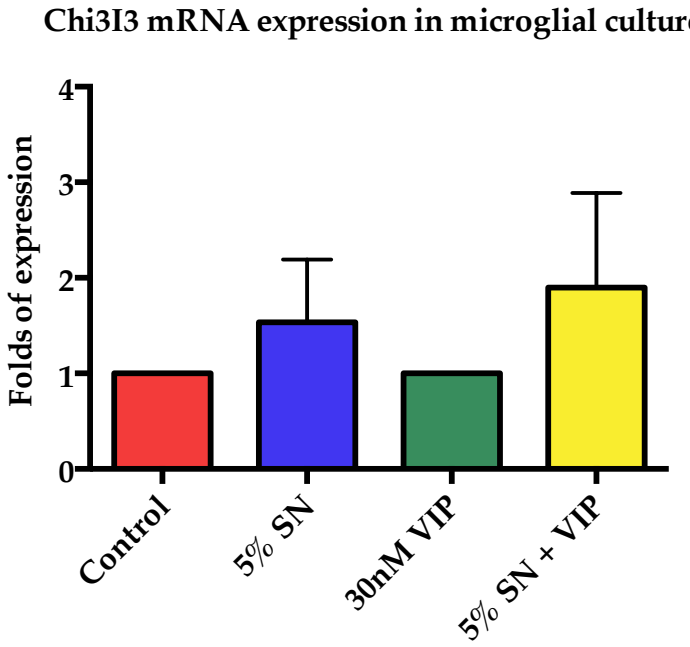

Figure 56: Supernatant does not alter Chi3I3 mRNA expression. Pure rat microglial cultures were generated and treated with experimental conditions for 2 hours. Cells were then collected in trizol and converted to cDNA for PCR analysis. Data is from 2 different experiments. Comparisons between control and treatment conditions are a one-way ANOV A with Bonferroni correction for multiple comparisons (*, $p < 0.05$, **, $p < 0.01$, ***, $p < 0.001$)

The M1 marker TNFα was significantly upregulated in microglial cells under treatment with supernatant pre-treated with VIP **(Figure 57)**. There was a 16 fold increase in mRNA. There was also a 15 fold increase in mRNA under treatment with 30nM VIP. There was also a 3 fold increase under treatment with 5% supernatant, however this was not statistically significant. These results suggest the effect on TNFα mRNA upregulation is due to the addition of VIP rather than the supernatant.

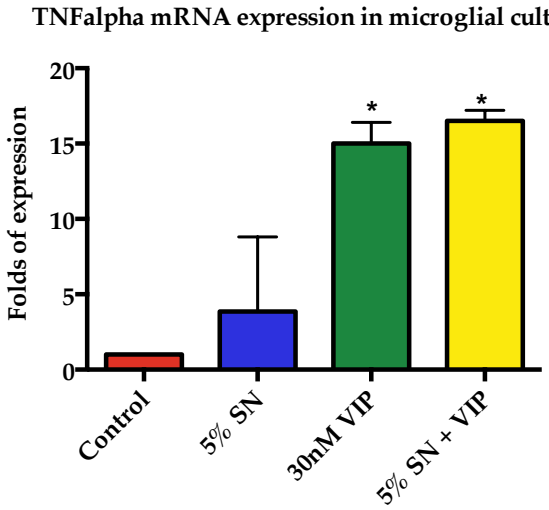

Figure 57: VIP increases TNF alpha mRNA expression. Pure rat microglial cultures were generated and treated with experimental conditions for 2 hours. Cells were then collected in trizol and converted to cDNA for PCR analysis. Data is from 2 different experiments. Comparisons between control and treatment conditions are a one-way ANOV A with Bonferroni correction for multiple comparisons (*, $p < 0.05$, **, $p < 0.01$, ***, $p < 0.001$)

The M1 marker iNOS did not significantly change its expression of mRNA in microglial cultures **(Figure 58)**. There was a down-regulation under treatment with 5% supernatant but this was not statistically significant. There was also a down-regulation in microglial cells under treatment with supernatant pre-treated with VIP. However this was not statistically significant either.

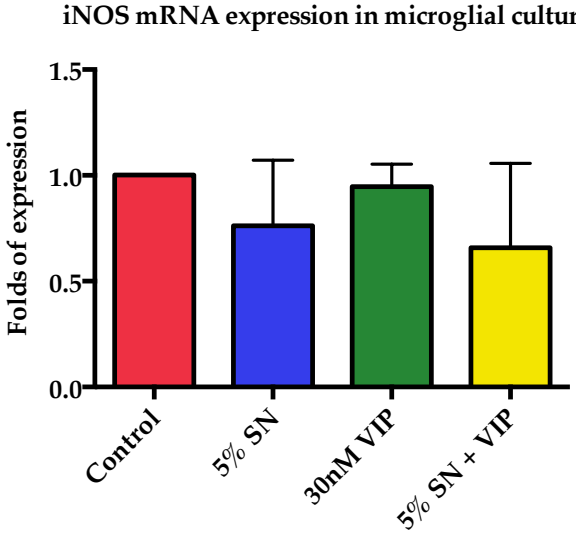

Figure 58: VIP increases TNF alpha mRNA expression. Pure rat microglial cultures were generated and treated with experimental conditions for 2 hours. Cells were then collected in trizol and converted to cDNA for PCR analysis. Data is from 2 different experiments. Comparisons between control and treatment conditions are a one-way ANOV A with Bonferroni correction for multiple comparisons (*, $p < 0.05$, **, $p < 0.01$, ***, $p < 0.001$)

5.4: Discussion

5.4.1: IL-4 mediates supernatant proliferative effects on hippocampal progenitor cells

The anti-inflammatory cytokine IL-4 has been implicated in positively regulating neurogenesis, with increased accumulation of IL-4 producing $CD4^+$ T lymphocytes within the meninges of mice following learning (Derecki et al., 2010). Furthermore, cognitive defects are exhibited in IL-4 knockout mice (Derecki et al., 2010). Investigating the role of IL-4 in this culture paradigm showed an increase of six fold mRNA expression following CD3 activation with the addition of 30nM VIP. Given this significant increase coupled with the aforementioned findings in literature, an anti-mouse IL-4 antibody was used to neutralise the effects of the cytokine. Addition of anti-mouse IL-4 abolished the proliferative effect of supernatant and supernatant pre-treated with VIP on hippocampal progenitor cells. This suggests the proliferative effect of supernatant is mediated via IL-4 activity. To determine whether the effect was purely via mouse IL-4 and/or also endogenous rat IL-4, an anti-rat IL-4 antibody was used to neutralize rat IL-4 activity. The addition of anti-rat IL-4 did not alter the proliferative effect of supernatant or supernatant pre-treated with VIP on hippocampal progenitor cells. This suggests IL4-mediated proliferative effects on hippocampal cells are from T lymphocytes-released IL-4.

5.4.2: Microglia are essential for supernatant-mediated effect on hippocampal progenitor cells

It is suggested that microglia are key components of the mechanism regulating hippocampal neurogenesis and that an “intact immune system” is essential for neurogenic maintenance (Ziv et al., 2006). Indeed, microglia are important for hippocampal neurogenesis and blocking their activity has shown reduced proliferation of newly generated neurons (Ziv et al., 2006). Microglia act via release of inflammatory agents or neurotrophic factors to regulate neurogenesis, neuronal survival and function (Battista et al., 2006, Butovsky et al., 2006, Ekdahl et al., 2006). Our results showed abolishing microglia from rat hippocampal cultures reduced proliferation below control levels. Cultures treated with supernatant (with and without VIP) in the absence of microglia had significantly reduced proliferation compared to treatment in the presence of microglia. This suggests that supernatant

acts primarily via microglia to increase proliferation. However, since the rate of proliferation was still higher in cultures treated with supernatant in the presence of microglia compared to untreated cultures that were absent of microglia, suggests supernatant comprises of mediators that act directly on neural progenitor cells. Given that IL-4 mediates supernatant proliferative effects, a mouse anti-IL-4 antibody was used in cultures absent of microglia to determine whether the higher levels of proliferation in supernatant treated cultures (-microglia) compared to control (-microglia) could be attributed to microglia-independent action of IL-4 on hippocampal cells. Results showed the addition of anti-mouse IL-4 to cultures treated with supernatant, in the absence of microglia, reduced proliferation to levels of control in the absence of microglia. Indeed, this suggests supernatant IL-4 acts in two ways: directly on hippocampal cells and indirectly via microglia, the latter of which is the predominant mechanism.

5.4.3: VIP pre-treated splenocytes enhance BDNF mRNA expression in microglia

$CD4^+$ T lymphocytes are suggested to "program" microglia to release factors such as BDNF (Derecki et al., 2010). BDNF is implicated in the regulation of hippocampal neurogenesis (Lee et al., 2002). BDNF increases proliferation in the hippocampus and promotes neuronal differentiation and maturation (Scharfman et al., 2005, Waterhouse et al., 2012). To address the involvement of BDNF, 5% supernatant (with and without VIP) were added to pure microglial cultures. Results showed a four fold increase in BDNF mRNA expression under treatment with 5% supernatant and an eight fold increase under treatment with 5% supernatant pre-treated with VIP. These results suggest supernatant "programs" microglia to upregulate BDNF; a potential factor in mediating microglial-T lymphocytes interaction in increasing hippocampal proliferation. This effect is enhanced under VIP treatment.

5.4.4: Splenocytes may skew microglia towards a Th2 phenotype

VIP is able to induce a Th2 phenotype and is associated with anti-inflammatory activities (Delgado et al., 1999a, Delagado et al., 1999b, Gomariz et al., 2000). Like T lymphocytes, microglia are also associated with pro- and anti-inflammatory phenotypes subcategorized primarily as M1 and M2, respectively (crain et al.,

2013). To determine whether supernatant pre-treated with VIP drives a particular phenotype, M1 and M2 markers were used on treated pure microglial cultures. Interestingly there was an upregulation of mRNA expression of the M1 marker TNFα and the M2 marker IL-10. However, the increased upregulation of TNFα is a result of the addition of VIP, given that the increase is of the same magnitude as that under treatment with 5% supernatant pre-treated with VIP. It is therefore possible to speculate that T lymphocytes drive an M2 microglia phenotype based on these findings. Given the massive increase in IL-10 expression and the dual role of TNFα as an anti-inflammatory cytokine, coupled with the increase of the pro-neurogenic neurotrophic factor BDNF mRNA, suggests VIP pre-treated supernatant may skew microglia towards an M2 phenotype. This supports previous findings whereby IL-4 drives microglia towards an M2 phenotype (Fenn et al., 2012). This is consistent with the enhanced proliferative effect of supernatant in the presence of microglia in hippocampal cultures.

5.4.5: Chapter summary

The results presented in this chapter have identified IL-4 as a key cytokine in mediating the effects of supernatant in the modulation of hippocampal neurogenesis. IL-4 mRNA expression has been shown to be up-regulated under VIP treatment, which is consistent with VIP's anti-inflammatory role in neuromodulation. Furthermore, IL-4 activity is both direct on neural progenitor cells and also via microglial interactions.

The data shows microglia are essential for maintaining proliferative effects in this culture system, which is consistent with the concept of "intact immune system" regulation. Furthermore, microglia are necessary to elicit the full effects of supernatant. Supernatant IL-4 may skew microglia towards an M2 phenotype, which is associated with anti-inflammatory and pro-neurogenic phenotype as concluded by the mRNA upregulation of M2 marker IL-10. Supernatant IL-4 $CD4^+$ T lymphocytes modulate hippocampal neurogenesis via IL-4 release, acting primarily via microglia but also directly on neural progenitor cells. Microglia are driven towards a Th2 phenotype and could potentially act via release of key mediators such as BDNF. VIP enhances this effect significantly.

Chapter 6

General Discussion

6. General discussion

6.1: Summary of major findings

Our results can be summarized in three broad sections. Firstly, in agreement with literature (Delgado et al., 2004), we established that T lymphocytes need to be activated by an antigen (anti-CD3) to regulate hippocampal neurogenesis. Activated supernatant increases the mitotic index and does not affect cell survival. By increasing the labelling index and not altering the growth fraction, these results suggest activated T lymphocytes increases the speed of the cell cycle. Activated supernatant increases the proliferation of nestin-expressing and TuJ1-expressing hippocampal cells, suggesting supernatant is neuroproliferative for hippocampal precursor cells. Activated supernatant increases the proportion of nestin positive, TuJ1 positive and nestin^{+}TuJ1^{+} cells, suggesting it is neurogenic as well as proliferative. There was an increase in the total number and proportion of Prox1 cells and the proportion of TuJ1^{+}Prox1^{+} cells indicating the increase in the number of newly generated neurons is granule cell specific. We also showed that using a CD4^{+} isolation column system to isolate CD4^{+} T lymphocytes was a viable alternative to generating pure CD4^{+} T lymphocytes cultures using flow cytometry.

Secondly, we showed that VIP pre-treatment of activated T lymphocytes enhances activated T lymphocyte supernatant proliferative effects on postnatal hippocampal cells. VIP pre-treated T lymphocytes supernatant enhances the mitotic index and labelling index, without altering the growth fraction. This suggests VIP pre-treated T lymphocytes supernatant increases the speed of the cell cycle. VIP pre-treated T lymphocytes supernatant enhances the proliferation of nestin-expressing and TuJ1-expressing cells, suggesting an enhanced neuroproliferative effect. VIP pre-treated T lymphocytes supernatant enhances the proportion of nestin positive, TuJ1 positive and nestin^{+}TuJ1^{+} cells, suggesting it is neurogenic. There was also an enhanced increase in the total number and proportion of Prox1 cells and the proportion of TuJ1^{+}Prox1^{+} cells indicating the increase in the number of newly generated neurons is granule cell specific. Using a VPAC1 specific agonist, we showed VPAC1 receptor on T lymphocytes mediate VIP proliferative effects on postnatal hippocampal cells. VPAC1 agonist pre-treated T lymphocytes supernatant increased the mitotic index and proliferation of nestin-expressing cells to the same magnitude as VIP pre-

treated T lymphocytes supernatant. Addition of VPAC1 agonist directly to hippocampal cells did not alter the mitotic index or proliferation of nestin-expressing cells, suggesting the VPAC1-mediated effect was specific to T lymphocytes and that residual VPAC1 agonist was not accountable for the proliferative effects. Using a VPAC1 specific antagonist, we confirmed VPAC1 receptor mediation. VPAC1 antagonist/VIP pre-treated T lymphocytes supernatant abolished the enhanced effects on mitotic index and proliferation of nestin-expressing cells. Addition of VPAC1 antagonist directly into control hippocampal cultures did not alter the mitotic index or the proliferation of nestin-expressing hippocampal cells, suggesting that the effects of the VPAC1 antagonist were specific to T lymphocytes.

Thirdly, we demonstrated that IL-4 is the major cytokine involved in VIP-T lymphocyte mediation of hippocampal neurogenesis via interaction with microglia. IL-4 mRNA is significantly upregulated in T lymphocyte cultures under treatment with VIP. Using a mouse-specific anti-IL-4 antibody, we showed that blocking IL-4 abolished supernatant effects. There was no change under treatment with rat-specific anti-IL-4, implying that rat IL-4 was not responsible for IL-4–mediated proliferative effects. Using specific isotypes, we confirmed the specificity of the antibodies. Ablation of microglial cells significantly reduced T lymphocyte supernatant proliferative effects but did not reduce them to levels of control conditions without microglia. Addition of anti-mouse IL-4 to cultures treated with T lymphocytes supernatant in the absence of microglia completely abolished the effect, showing that IL-4 acts via a dual mechanism: indirectly via microglia (predominantly) and directly on hippocampal precursor cells. VIP pre-treated T lymphocytes increase BDNF mRNA expression and significantly upregulate M2 anti-inflammatory IL-10 and BDNF, suggesting a drive towards an M2 phenotype of supernatant-treated microglia.

Taken together, we suggest VIP acts via VPAC1 receptors on activated $CD4^+$ T lymphocytes to regulate hippocampal neurogenesis via proliferative mechanisms. Activated T lymphocytes release IL-4, which act both indirectly via microglia and directly on neural progenitor cells. Activated T lymphocytes supernatant

significantly upregulates microglial cytokine expression. Given the increase of BDNF and IL-10 mRNA suggests these may mediate the effect of microglia on neural stem cells. Indeed, BDNF is both proliferative and trophic (Katoh-Sehmba et al., 2002; Lee et al., 2002). IL-10 enhances neurogenesis and restores cognition in models of Alzheimers (Kiyota et al., 2012). However, this requires further investigation.

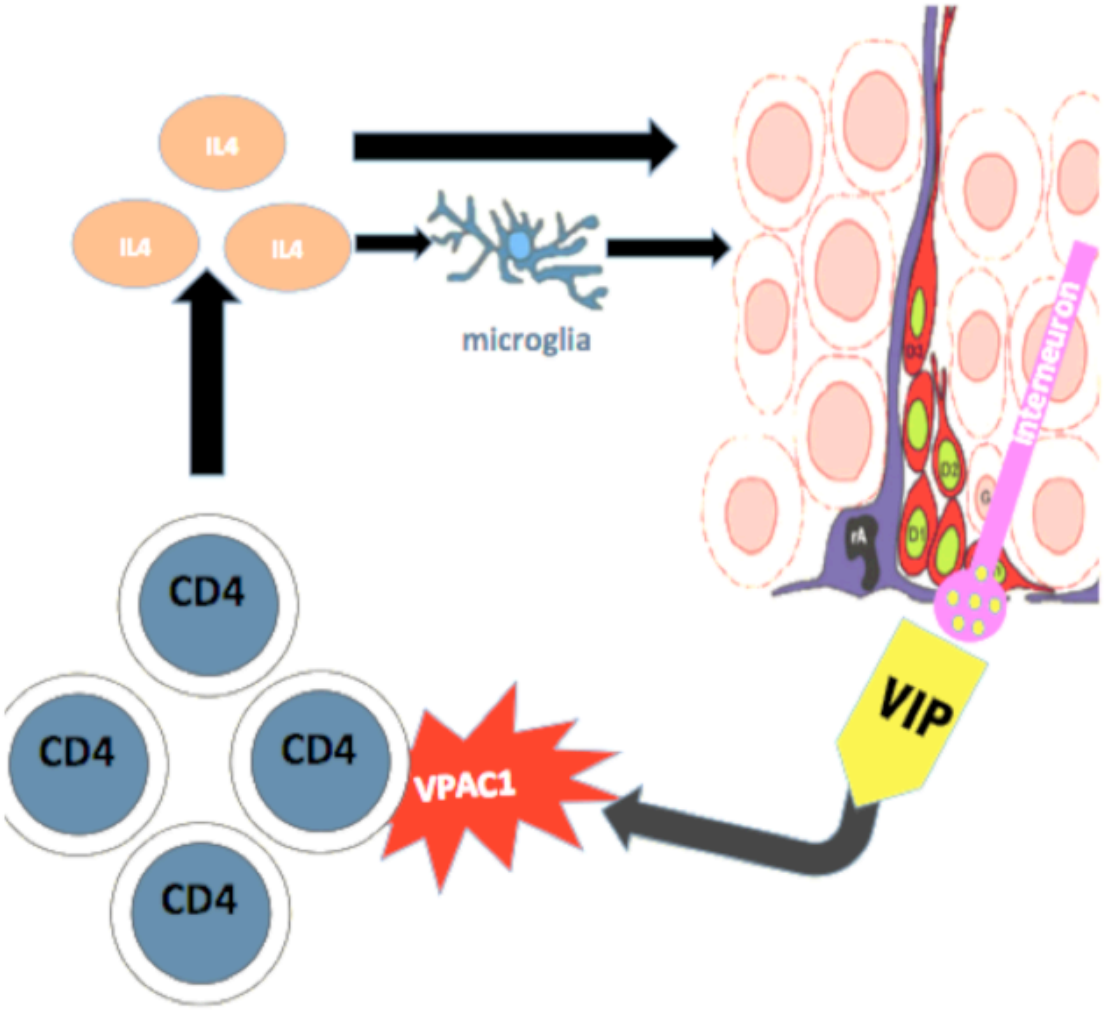

Figure 59: Schematic of mechanism underlying VIP-mediated T lymphocyte modulation of hippocampal neurogenesis. VIP released from interneurons act on VPAC1 receptor on activated $CD4^+$ T lymphocytes to release IL-4. IL-4 acts primarily on microglia to release mediators to increase hippocampal neurogenesis via proliferative mechanisms. IL-4 also acts directly on hippocampal cells. (D1, D2, D3 cells represent varying stages of cell differentiation, with D3 representing granule neurons).

Table 5: Overview of main findings

Key findings	Figures
$CD4^+$ column kits are a viable alternative to flow cytometric cell sorting for generation of T lymphocytes cultures	28, 32
CD3-activated supernatant increases proliferation of nestin expressing hippocampal cells	18
VIP enhances the effects observed following treatment with activated supernatant	30, 31
VIP enhances the rate of cell proliferation	34
VIP acts via the VPAC1 receptor on $CD4^+$ T lymphocytes	37 - 40
VIP upregulates IL-4 mRNA expression	41, 42
IL-4 abolishes VIP mediated effects	43 - 45
Supernatant IL-4 acts predominantly via microglia to increase proliferation	50 , 51
Supernatant IL-4 also acts directly on neural progenitor cells	52, 53
There is an overall neurogenic effect of supernatant	24, 35, 36

6.2: Overview of literature

Neuroimmunomodulation is a complex area of study that is in its infancy. There are many challenges in this research area, which are being overcome with the advancement of technology. It is only in the last twenty odd years that hippocampal neurogenesis has been recognised as a lifelong process that generates functional neurons in the adult brain, albeit in two defined microenvironments (Reynolds and Weiss, 1992, Eriksson et al., 1998, Gage, 2000, Riquelme et al., 2008). The subgranular zone of the hippocampal dentate gyrus has spurred great interest due to its implication in cognition and further still in its role in pathological states (Gould et al., 1999, Kempermann et al., 2004, Jessberger et al., 2007, Cao et al., 2004, Barkas et al., 2012, Ekdahl et al., 2003, Hattiangady et al., 2004, Kuruba et al., 2009). The unique microenvironment within which neurogenesis occurs is regulated by an array of intrinsic and external factors, in a complex relationship that remains to be fully understood (Favaro et al., 2009, Karalay et al., 2011, van Praag et al., 1999, Villeda et al., 2011).

The immune system has emerged as an important modulator of hippocampal neurogenesis since the turn of the millennium. Until recently, it was considered an "immune-privileged" site devoid of immunological regulation, except under pathological conditions (Shrestha et al., 2013). However, the immune system combines innate and adaptive components of immunity to orchestrate a delicate balance in the maintenance of homeostatic regulation (Butovsky et al., 2006, Ziv et al., 2006). Recent findings attribute a key role for $CD4^+$ T lymphocytes in the regulation of neurogenesis by a poorly understood mechanism (Ziv et al., 2006, Wolf et al., 2009). IL-4 has been implicated with an important role, however cross-talks between the brain and T lymphocytes remains largely elusive (Derecki et al., 2010). One of the major hurdles of this research is the ability for T lymphocytes to elicit pro-neurogenic effects without infiltrating the brain. It is generally accepted that T lymphocytes only penetrate the brain parenchyma under pathological conditions. Under physiological conditions, it is postulated that T lymphocytes mediate neurogenesis from within the meningeal spaces in which they reside (Derecki et al., 2010). $CD4^+$ T lymphocytes are found within CSF and this flows within the subarachnoid space of the meninges (Ransohoff et al., 2003, Svenningsson et al., 1995, Carrithers et al., 2000). This ideal positioning raises the possibility for intermediary cells or neurotransmitters as messengers that can relay communication between the niche and the adaptive immune system.

The 28 amino acid neuropeptide, vasoactive intestinal peptide, is an extensively studied neuropeptide that has pleiotropic effects (Said and Mutt, 1970, Bryant et al., 1976). VIP is involved in neurogenesis from the embryonic stage and throughout adulthood (Zupan et al., 2000, Scharf et al., 2008). VIP Is fired by interneurons from the dentate gyrus into the surrounding microenvironment. VIP divides the pool of symmetrically diving progenitor cells in the hippocampal dentate gyrus and can direct these cells towards a neuronal lineage (Zaben et al., 2009). VIP also acts on T lymphocytes and is regarded as an anti-inflammatory agent. VIP drives T lymphocytes towards a Th2 anti-inflammatory phenotype, which is primarily associated with IL-4 cytokine production (Delgado et al., 1999, Delgado et al., 2004, Voice et al., 2001). There is, therefore, a potential role for VIP released from firing interneurons to act on T lymphocytes residing within the meninges to release

cytokines. These in turn can act either directly on neural progenitor cells or via intermediary cells such as microglia. Microglia are innate cells that scavenge the brain in their capacity as immune surveillance cells. Cytokine activation can program microglia towards an anti- or pro-inflammatory phenotype, depending on the cytokine and the environment (e.g. pathological or physiological conditions) (Chhor et al., 2013). These cells are therefore ideal candidates in an intermediary capacity to regulate T lymphocyte-mediated hippocampal neurogenesis.

The highest expression of VIP mRNA occurs during the postnatal period, peaking at P10 (Lopez-Tellez et al., 2004). This is also the time period within which more than half of the hippocampal dentate gyrus granule cell layer is formed, with almost all the neurons surviving into adulthood (Namba et al., 2005, Namba et al., 2007). Therefore we elected to utilise a postnatal rat hippocampal culture system to investigate the effect of T lymphocytes on neurogenesis. Adult mice have fully functioning immune systems. By using adult mouse T lymphocytes, we were able to distinguish between the effects of cytokines generated from mice T lymphocytes compared to rat hippocampal cells. It also provides a potential to translate this work from *in vitro* cultures to *in vivo*, where immune studies are primarily conducted on mice. Given the mounting evidence for T lymphocyte modulation of neurogenesis without infiltration into the brain parenchyma, we used T lymphocytes supernatant instead of co-culturing hippocampal cells with T lymphocytes.

6.3: VIP mediates T lymphocyte interaction with microglia to enhance neurogenesis

Our results have shown that supernatant pure $CD4^{++}$T lymphocytes increase proliferation of nestin-expressing cells, while supernatant from splenocytes devoid of $CD4^{+}$ T lymphocytes did not. This is in agreement with other studies that have shown a VIP effects on $CD4^{+}$ T lymphocytes (Delgado et al., 1999b; Ganea et al., 2003). Differential T lymphocyte VIP receptor expression is observed in rodents and humans (Gomariz et al., 1994a; Delgado et al., 1996a; Pankhaniya et al., 1998). The VPAC1 receptor is expressed on $CD4^{+}$T lymphocytes and is the predominant receptor in the naïve state (Lara-Marques et al., 2001). In contrast to other studies which report VPAC2 mRNA expression is only induced after splenic T lymphocyte

activation, our studies have shown that VPAC2 expression remains undetected (Delagado et al., 1996b). This is further substantiated with our experiments using VPAC1-specific agonist/antagonist, which show that VPAC1 mediates VIP effects on T lymphocytes. This could be attributed to the fact that VPAC2 is expressed relatively late during activation (12 hours) and therefore VPAC1 is likely to be the major receptor type present during early culture period (Delgado et al., 2004). This is in line with our culture system, where VIP/VPAC1 agonist treated T lymphocytes are generated for 24 hours.

IL-4 is the predominant Th2 cytokine and VIP is shown to skew T lymphocytes towards the Th2 phenotype. VIP upregulates IL-4 production, whilst simultaneously reducing IFN-γ production and thereby inhibiting the Th1 phenotype (Delgado et al., 1999b). Eliminating VIP from stimulated T lymphocyte cultures using a VIPase antibody decreases the number of IL-4 producing $CD4^+$ T lymphocytes, decreases IL-4 and IL-10 production and increases IFN-γ production (Voice at al., 2003). *In vivo* studies in transgenic mice have identified endogenous VIP as key for bias towards a Th2 phenotype (Voice et al., 2001; Goetzel et al., 2001). Consistent with these findings, we have shown increased IL-4 mRNA production following VIP treatment of $CD4^+$ T lymphocytes. In addition, we have shown that T lymphocyte-released IL4 is the key mediator of the observed proliferative effects. This is consistent with the idea that $CD4^+$ T lymphocytes regulate hippocampal neurogenesis (Wolf et al., 2009) and could explain the learning deficits exhibited by IL-4 knockout mice, which have reduced $CD4^+$ T lymphocytes in the meninges (Derecki et al., 2009). Further to this, learning increases meningeal T lymphocyte production of IL-4 (Derecki et al., 2010). Following learning tasks, wild type mice have increased BDNF production in astrocytes, however these effects are absent in IL-4 knock-outs (Derecki et al., 2010). Given the importance of BDNF in neuronal growth and survival further implicates IL-4 in a beneficial regulatory role (Choy et al., 2008; Hall et al., 2000). While IL-4 induced BDNF production has been observed in astrocytes, our results show T lymphocyte released IL-4 increases BDNF mRNA expression in microglia. This has been observed by Butovksy et al. (2006). However, while IL-4 treated microglia are responsible for a proliferative and neurogenic effect, Butovsky et al. (2006) report a bias towards oligodendrogenesis. This could

be attributed to differences in culture protocols, where they co-cultured microglial cultures with dissociated neuronal progenitor cell neurospheres. Our results also showed increased expression of IL-10 and TNFα mRNA expression in microglia treated with T lymphocytes supernatant. Whilst IL-10 is an anti-inflammatory cytokine used as an M2 marker, TNF alpha is an M1 pro-inflammatory cytokine. Given that there was no significant difference in the expression of the other phenotyping markers (M1= iNOS, M2=Chi3I3), we cannot conclusively determine the classification of these microglia following activation. However, given that TNFα is also reported to have anti-inflammatory effects, in light of our enhanced neurogenic findings we can postulate a M2-role for this cytokine in our culture system (Masli and Turple, 2009; Zakharova and Ziegler, 2005). Of importance is the ever-increasing controversy surrounding microglial classification and overlap between cytokine markers. Another dynamic to investigating cytokine expression is the differences in expression relating to developmental stages (Crain et al., 2013). There is early postnatal expression (P3) of iNOS and TNFα but by P21 there is high expression of CD11b and TLR4 (Crain et al., 2013). In the healthy brain there is no bias towards M1 or M2 expression, which suggests a balance until otherwise instructed by environmental cues (learning, immune response etc.). Although findings are suggestive of a microglial population inclined towards anti-inflammatory/beneficial effects, further analysis is essential using more cytokine markers and morphological analysis. Regardless of the classification of microglia, our findings suggest they are essential for supernatant mediated effects. Ablating microglial cultures significantly reduces hippocampal proliferation, which is in agreement with *in vivo* studies (Ziv et al., 2006). Blocking microglial activity with minocycline significantly reduces proliferation of newly generated neurons in the dentate gyrus (Ziv et al., 2006). Increased microglial numbers in the dentate gyrus, simultaneous with increased proliferation of newly generated neurons following environmental enrichment, also highlights their importance.

6.4: Conclusions

We have identified a neuro-immune signalling pathway, with VIP as a candidate cytokine for communication between the stem cell niche and the adaptive immune system. Furthermore, microglia have been identified as essential for VIP-mediated T

lymphocyte effects. This constitutes a novel mechanism for neuro-immune modulation of hippocampal neurogenesis *in vitro* and requires validation through *in vivo* studies. This highlights candidates for therapeutic targets to restore cognitive function in mood disorders and temporal lobe epilepsy.

6.5: Future work

Our findings show VIP treated T lymphocytes supernatant significantly increases microglial BDNF mRNA. This, coupled with the significance of BDNF in the brain, dictates the importance of investigating the exact role of BDNF in this mechanism. For this, we suggest the use of a BDNF antagonist. BDNF antagonists have been reported extensively (Alhusban et al., 2013, Fanous et al., 2011, Zochodne and Cheng, 2000). By binding to the BDNF receptor TrkB, antagonists can block BDNF activity (Cazorla et al., 2011). This is of particular interest since it has been shown that hippocampal neural progenitor cells lacking TrkB receptors impair proliferation and neurogenesis (Li et al., 2008, Bergami et al., 2008).

It is also essential to translate these findings *in vivo*. For this, we suggest the use of VPAC1 receptor knockout mice (Yadav et al., 2011). As previously mentioned, nude mice (that are devoid of T lymphocytes) have reduced proliferation in the hippocampal dentate gyrus (Ziv et al., 2006). Studies have shown transfer of $CD4^+$ T lymphocytes into nude mice rescues the effect (Wolf et al., 2009). Flow cytometry could be used to generate pure $CD4^+$ T lymphocytes serum from VPAC1 knockout mice and transferred into nude mice, using a protocol adopted from Deprez et al. (2011) **(Figure 6.2)**. This can identify whether the VPAC1 receptor on T lymphocytes modulates VIP activity *in vivo*. It would also be interesting to determine the effect of ablating microglia within this specific *in vivo* model. These studies will help to fully elucidate the cellular mechanisms underlying T lymphocyte modulation of hippocampal neurogenesis, identifying targets for treatment of conditions such as epilepsy and mood disorders.

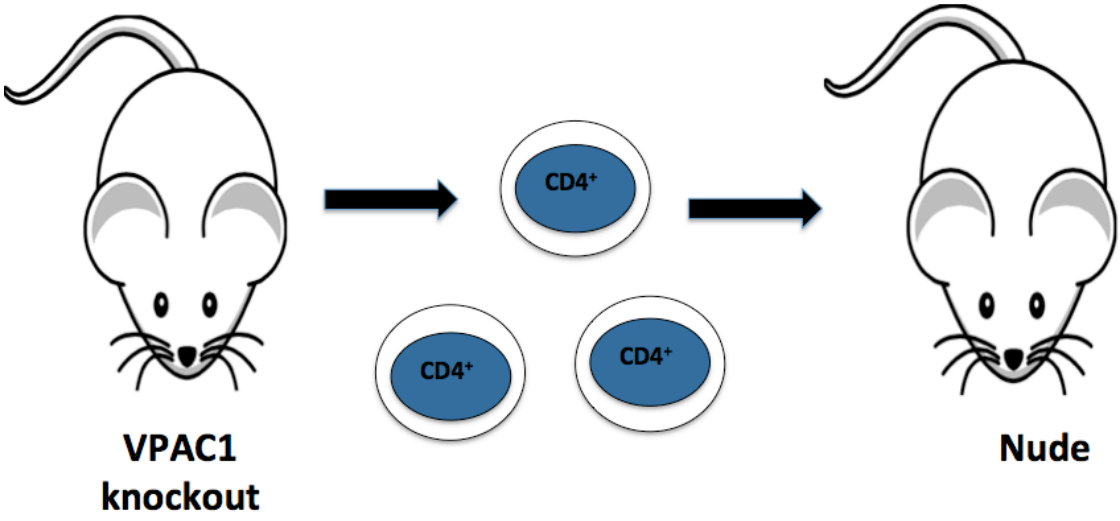

Figure 60: *In vivo* model. $CD4^+$ T lymphocytes from VPAC1 knock-out mice can be adoptively transferred into nude mice.

References

ABROUS, D. N., KOEHL, M. & LE MOAL, M. 2005. Adult neurogenesis: from precursors to network and physiology. *Physiol Rev,* 85**,** 523-69.

ACSADY, L., ARABADZISZ, D. & FREUND, T. F. 1996. Correlated morphological and neurochemical features identify different subsets of vasoactive intestinal polypeptide-immunoreactive interneurons in rat hippocampus. *Neuroscience,* 73**,** 299-315.

AJMONE-CAT, M. A., NICOLINI, A. & MINGHETTI, L. 2003. Prolonged exposure of microglia to lipopolysaccharide modifies the intracellular signaling pathways and selectively promotes prostaglandin E2 synthesis. *J Neurochem,* 87**,** 1193-203.

ALHUSBAN, A., KOZAK, A., ERGUL, A. & FAGAN, S. C. 2013. AT1 receptor antagonism is proangiogenic in the brain: BDNF a novel mediator. *J Pharmacol Exp Ther,* 344**,** 348-59.

ALOISI, F., DE SIMONE, R., COLUMBA-CABEZAS, S., PENNA, G. & ADORINI, L. 2000. Functional maturation of adult mouse resting microglia into an APC is promoted by granulocyte-macrophage colony-stimulating factor and interaction with Th1 cells. *J Immunol,* 164**,** 1705-12.

ALTMAN, J. & DAS, G. D. 1965. Autoradiographic and histological evidence of postnatal hippocampal neurogenesis in rats. *J Comp Neurol,* 124**,** 319-35.

ASHTON, R. S., CONWAY, A., PANGARKAR, C., BERGEN, J., LIM, K. I., SHAH, P., BISSELL, M. & SCHAFFER, D. V. 2012. Astrocytes regulate adult hippocampal neurogenesis through ephrin-B signaling. *Nat Neurosci,* 15**,** 1399-406.

BANGASSER, D. A., WAXLER, D. E., SANTOLLO, J. & SHORS, T. J. 2006. Trace conditioning and the hippocampus: the importance of contiguity. *J Neurosci,* 26**,** 8702-6.

BARAN, J., KOWALCZYK, D., OZOG, M. & ZEMBALA, M. 2001. Three-color flow cytometry detection of intracellular cytokines in peripheral blood mononuclear cells: comparative analysis of phorbol myristate acetate-ionomycin and phytohemagglutinin stimulation. *Clinical & Diagnostic Laboratory Immunology,* 8**,** 303-13.

BARKAS, L., REDHEAD, E., TAYLOR, M., SHTAYA, A., HAMILTON, D. A. & GRAY, W. P. 2012. Fluoxetine restores spatial learning but not accelerated forgetting in mesial temporal lobe epilepsy. *Brain,* 135**,** 2358-74.

BARKHO, B. Z., SONG, H., AIMONE, J. B., SMRT, R. D., KUWABARA, T., NAKASHIMA, K., GAGE, F. H. & ZHAO, X. 2006. Identification of astrocyte-expressed factors that modulate neural stem/progenitor cell differentiation. *Stem Cells Dev,* 15**,** 407-21.

BARTHOLOMAUS, I., KAWAKAMI, N., ODOARDI, F., SCHLAGER, C., MILJKOVIC, D., ELLWART, J. W., KLINKERT, W. E., FLUGEL-KOCH, C., ISSEKUTZ, T. B., WEKERLE, H. & FLUGEL, A. 2009. Effector T cell interactions with meningeal vascular structures in nascent autoimmune CNS lesions. *Nature,* 462**,** 94-8.

BASILLE, M., VAUDRY, D., COULOUARN, Y., JEGOU, S., LIHRMANN, I., FOURNIER, A., VAUDRY, H. & GONZALEZ, B. 2000. Comparative distribution of pituitary adenylate cyclase-activating polypeptide (PACAP) binding sites and PACAP receptor mRNAs in the rat brain during development. *J Comp Neurol,* 425**,** 495-509.

BELLINGER, D. L., LORTON, D., BROUXHON, S., FELTEN, S. & FELTEN, D. L. 1996. The significance of vasoactive intestinal polypeptide (VIP) in immunomodulation. *Adv Neuroimmunol,* 6**,** 5-27.
BENGZON, J., KOKAIA, Z., ELMER, E., NANOBASHVILI, A., KOKAIA, M. & LINDVALL, O. 1997. Apoptosis and proliferation of dentate gyrus neurons after single and intermittent limbic seizures. *Proc Natl Acad Sci U S A,* 94**,** 10432-7.
BERGAMI, M., RIMONDINI, R., SANTI, S., BLUM, R., GOTZ, M. & CANOSSA, M. 2008. Deletion of TrkB in adult progenitors alters newborn neuron integration into hippocampal circuits and increases anxiety-like behavior. *Proc Natl Acad Sci U S A,* 105**,** 15570-5.
BERGMANN, O., LIEBL, J., BERNARD, S., ALKASS, K., YEUNG, M. S., STEIER, P., KUTSCHERA, W., JOHNSON, L., LANDEN, M., DRUID, H., SPALDING, K. L. & FRISEN, J. 2012. The age of olfactory bulb neurons in humans. *Neuron,* 74**,** 634-9.
BLUMCKE, I., SCHEWE, J. C., NORMANN, S., BRUSTLE, O., SCHRAMM, J., ELGER, C. E. & WIESTLER, O. D. 2001. Increase of nestin-immunoreactive neural precursor cells in the dentate gyrus of pediatric patients with early-onset temporal lobe epilepsy. *Hippocampus,* 11**,** 311-21.
BONDY, C. A. & CHENG, C. M. 2004. Signaling by insulin-like growth factor 1 in brain. *Eur J Pharmacol,* 490**,** 25-31.
BRENNEMAN, D. E., GLAZNER, G., HILL, J. M., HAUSER, J., DAVIDSON, A. & GOZES, I. 1998. VIP neurotrophism in the central nervous system: multiple effectors and identification of a femtomolar-acting neuroprotective peptide. *Ann N Y Acad Sci,* 865**,** 207-12.
BRENNEMAN, D. E., PHILLIPS, T. M., HAUSER, J., HILL, J. M., SPONG, C. Y. & GOZES, I. 2003. Complex array of cytokines released by vasoactive intestinal peptide. *Neuropeptides,* 37**,** 111-9.
BRYANT, M. G., POLAK, M. M., MODLIN, I., BLOOM, S. R., ALBUQUERQUE, R. H. & PEARSE, A. G. 1976. Possible dual role for vasoactive intestinal peptide as gastrointestinal hormone and neurotransmitter substance. *Lancet,* 1**,** 991-3.
BRYNSKIKH, A., WARREN, T., ZHU, J. & KIPNIS, J. 2008. Adaptive immunity affects learning behavior in mice. *Brain Behav Immun,* 22**,** 861-9.
BSIBSI, M., RAVID, R., GVERIC, D. & VAN NOORT, J. M. 2002. Broad expression of Toll-like receptors in the human central nervous system. *J Neuropathol Exp Neurol,* 61**,** 1013-21.
BUTOVSKY, O., ZIV, Y., SCHWARTZ, A., LANDA, G., TALPALAR, A. E., PLUCHINO, S., MARTINO, G. & SCHWARTZ, M. 2006. Microglia activated by IL-4 or IFN-gamma differentially induce neurogenesis and oligodendrogenesis from adult stem/progenitor cells. *Mol Cell Neurosci,* 31**,** 149-60.
CACCI, E., CLAASEN, J. H. & KOKAIA, Z. 2005. Microglia-derived tumor necrosis factor-alpha exaggerates death of newborn hippocampal progenitor cells *in vitro*. *J Neurosci Res,* 80**,** 789-97.
CAMERON, H. A. & GOULD, E. 1994. Adult neurogenesis is regulated by adrenal steroids in the dentate gyrus. *Neuroscience,* 61**,** 203-9.
CAMERON, H. A. & MCKAY, R. 1998. Stem cells and neurogenesis in the adult brain. *Curr Opin Neurobiol,* 8**,** 677-80.

CAO, C., ARENDASH, G. W., DICKSON, A., MAMCARZ, M. B., LIN, X. & ETHELL, D. W. 2009. Abeta-specific Th2 cells provide cognitive and pathological benefits to Alzheimer's mice without infiltrating the CNS. *Neurobiol Dis,* 34**,** 63-70.

CAO, L., JIAO, X., ZUZGA, D. S., LIU, Y., FONG, D. M., YOUNG, D. & DURING, M. J. 2004. VEGF links hippocampal activity with neurogenesis, learning and memory. *Nat Genet,* 36**,** 827-35.

CARDOSO, A., LUKOYANOVA, E. A., MADEIRA, M. D. & LUKOYANOV, N. V. 2011. Seizure-induced structural and functional changes in the rat hippocampal formation: comparison between brief seizures and status epilepticus. *Behav Brain Res,* 225**,** 538-46.

CARLEN, M., CASSIDY, R. M., BRISMAR, H., SMITH, G. A., ENQUIST, L. W. & FRISEN, J. 2002. Functional integration of adult-born neurons. *Curr Biol,* 12**,** 606-8.

CARRITHERS, M. D., VISINTIN, I., KANG, S. J. & JANEWAY, C. A., JR. 2000. Differential adhesion molecule requirements for immune surveillance and inflammatory recruitment. *Brain,* 123 (Pt 6)**,** 1092-101.

CAZORLA, M., PREMONT, J., MANN, A., GIRARD, N., KELLENDONK, C. & ROGNAN, D. 2011. Identification of a low-molecular weight TrkB antagonist with anxiolytic and antidepressant activity in mice. *J Clin Invest,* 121**,** 1846-57.

CHHOR, V., LE CHARPENTIER, T., LEBON, S., ORE, M. V., CELADOR, I. L., JOSSERAND, J., DEGOS, V., JACOTOT, E., HAGBERG, H., SAVMAN, K., MALLARD, C., GRESSENS, P. & FLEISS, B. 2013. Characterization of phenotype markers and neuronotoxic potential of polarised primary microglia *in vitro*. *Brain Behav Immun,* 32**,** 70-85.

CROLL, S. D., GOODMAN, J. H. & SCHARFMAN, H. E. 2004. Vascular endothelial growth factor (VEGF) in seizures: a double-edged sword. *Adv Exp Med Biol,* 548**,** 57-68.

CZEH, B., MICHAELIS, T., WATANABE, T., FRAHM, J., DE BIURRUN, G., VAN KAMPEN, M., BARTOLOMUCCI, A. & FUCHS, E. 2001. Stress-induced changes in cerebral metabolites, hippocampal volume, and cell proliferation are prevented by antidepressant treatment with tianeptine. *Proc Natl Acad Sci U S A,* 98**,** 12796-801.

DE SIMONI, M. G., PEREGO, C., RAVIZZA, T., MONETA, D., CONTI, M., MARCHESI, F., DE LUIGI, A., GARATTINI, S. & VEZZANI, A. 2000. Inflammatory cytokines and related genes are induced in the rat hippocampus by limbic status epilepticus. *Eur J Neurosci,* 12**,** 2623-33.

DEISSEROTH, K., SINGLA, S., TODA, H., MONJE, M., PALMER, T. D. & MALENKA, R. C. 2004. Excitation-neurogenesis coupling in adult neural stem/progenitor cells. *Neuron,* 42**,** 535-52.

DELGADO, M. & GANEA, D. 2000a. Vasoactive intestinal peptide and pituitary adenylate cyclase activating polypeptide inhibit the MEKK1/MEK4/JNK signaling pathway in LPS-stimulated macrophages. *J Neuroimmunol,* 110**,** 97-105.

DELGADO, M. & GANEA, D. 2000b. Vasoactive intestinal peptide and pituitary adenylate cyclase-activating polypeptide inhibit T cell-mediated cytotoxicity by inhibiting Fas ligand expression. *J Immunol,* 165**,** 114-23.

DELGADO, M. & GANEA, D. 2001a. Cutting edge: is vasoactive intestinal peptide a type 2 cytokine? *J Immunol,* 166**,** 2907-12.

DELGADO, M. & GANEA, D. 2001b. Vasoactive intestinal peptide and pituitary adenylate cyclase-activating polypeptide inhibit expression of Fas ligand in activated T lymphocytes by regulating c-Myc, NF-kappa B, NF-AT, and early growth factors 2/3. *J Immunol,* 166**,** 1028-40.
DELGADO, M., GONZALEZ-REY, E. & GANEA, D. 2004a. VIP/PACAP preferentially attract Th2 effectors through differential regulation of chemokine production by dendritic cells. *FASEB J,* 18**,** 1453-5.
DELGADO, M., LECETA, J. & GANEA, D. 2002. Vasoactive intestinal peptide and pituitary adenylate cyclase-activating polypeptide promote *in vivo* generation of memory Th2 cells. *FASEB J,* 16**,** 1844-6.
DELGADO, M., LECETA, J., GOMARIZ, R. P. & GANEA, D. 1999a. Vasoactive intestinal peptide and pituitary adenylate cyclase-activating polypeptide stimulate the induction of Th2 responses by up-regulating B7.2 expression. *J Immunol,* 163**,** 3629-35.
DELGADO, M., MARTINEZ, C., JOHNSON, M. C., GOMARIZ, R. P. & GANEA, D. 1996a. Differential expression of vasoactive intestinal peptide receptors 1 and 2 (VIP-R1 and VIP-R2) mRNA in murine lymphocytes. *J Neuroimmunol,* 68**,** 27-38.
DELGADO, M., MUNOZ-ELIAS, E. J., GOMARIZ, R. P. & GANEA, D. 1999b. VIP and PACAP inhibit IL-12 production in LPS-stimulated macrophages. Subsequent effect on IFNgamma synthesis by T cells. *J Neuroimmunol,* 96**,** 167-81.
DELGADO, M., POZO, D. & GANEA, D. 2004b. The significance of vasoactive intestinal peptide in immunomodulation. *Pharmacol Rev,* 56**,** 249-90.
DELGADO, M., POZO, D., MARTINEZ, C., GARRIDO, E., LECETA, J., CALVO, J. R. & GOMARIZ, R. P. 1996b. Characterization of gene expression of VIP and VIP1-receptor in rat peritoneal lymphocytes and macrophages. *Regul Pept,* 62**,** 161-6.
DELGADO, M., POZO, D., MARTINEZ, C., LECETA, J., CALVO, J. R., GANEA, D. & GOMARIZ, R. P. 1999c. Vasoactive intestinal peptide and pituitary adenylate cyclase-activating polypeptide inhibit endotoxin-induced TNF-alpha production by macrophages: *in vitro* and *in vivo* studies. *J Immunol,* 162**,** 2358-67.
DELGADO, M., REDUTA, A., SHARMA, V. & GANEA, D. 2004c. VIP/PACAP oppositely affects immature and mature dendritic cell expression of CD80/CD86 and the stimulatory activity for CD4(+) T cells. *Journal of Leukocyte Biology,* 75**,** 1122-30.
DEPREZ, F., ZATTONI, M., MURA, M. L., FREI, K. & FRITSCHY, J. M. 2011. Adoptive transfer of T lymphocytes in immunodeficient mice influences epileptogenesis and neurodegeneration in a model of temporal lobe epilepsy. *Neurobiol Dis,* 44**,** 174-84.
DERECKI, N. C., CARDANI, A. N., YANG, C. H., QUINNIES, K. M., CRIHFIELD, A., LYNCH, K. R. & KIPNIS, J. 2010. Regulation of learning and memory by meningeal immunity: a key role for IL-4. *J Exp Med,* 207**,** 1067-80.
DICICCO-BLOOM, E. 1996. Region-specific regulation of neurogenesis by VIP and PACAP: direct and indirect modes of action. *Ann N Y Acad Sci,* 805**,** 244-56; discussion 256-8.
DIETL, M. M., HOF, P. R., MARTIN, J. L., MAGISTRETTI, P. J. & PALACIOS, J. M. 1990. Autoradiographic analysis of the distribution of vasoactive

intestinal peptide binding sites in the vertebrate central nervous system: a phylogenetic study. *Brain Res,* 520**,** 14-26.
DOETSCH, F. 2003. The glial identity of neural stem cells. *Nat Neurosci,* 6**,** 1127-34.
DOGRUKOL-AK, D., BANKS, W. A., TUNCEL, N. & TUNCEL, M. 2003. Passage of vasoactive intestinal peptide across the blood-brain barrier. *Peptides,* 24**,** 437-44.
EHM, O., GORITZ, C., COVIC, M., SCHAFFNER, I., SCHWARZ, T. J., KARACA, E., KEMPKES, B., KREMMER, E., PFRIEGER, F. W., ESPINOSA, L., BIGAS, A., GIACHINO, C., TAYLOR, V., FRISEN, J. & LIE, D. C. 2010. RBPJkappa-dependent signaling is essential for long-term maintenance of neural stem cells in the adult hippocampus. *J Neurosci,* 30**,** 13794-807.
EISCH, A. J. & PETRIK, D. 2012. Depression and hippocampal neurogenesis: a road to remission? *Science,* 338**,** 72-5.
EKDAHL, C. T., CLAASEN, J. H., BONDE, S., KOKAIA, Z. & LINDVALL, O. 2003. Inflammation is detrimental for neurogenesis in adult brain. *Proc Natl Acad Sci U S A,* 100**,** 13632-7.
EKDAHL, C. T., KOKAIA, Z. & LINDVALL, O. 2009. Brain inflammation and adult neurogenesis: the dual role of microglia. *Neuroscience,* 158**,** 1021-9.
ENCINAS, J. M., VAAHTOKARI, A. & ENIKOLOPOV, G. 2006. Fluoxetine targets early progenitor cells in the adult brain. *Proc Natl Acad Sci U S A,* 103**,** 8233-8.
ENGEL, J., JR. 2001. Intractable epilepsy: definition and neurobiology. *Epilepsia,* 42 Suppl 6**,** 3.
ENGELHARDT, B. & COISNE, C. 2011. Fluids and barriers of the CNS establish immune privilege by confining immune surveillance to a two-walled castle moat surrounding the CNS castle. *Fluids Barriers CNS,* 8**,** 4.
ERIKSSON, P. S., PERFILIEVA, E., BJORK-ERIKSSON, T., ALBORN, A. M., NORDBORG, C., PETERSON, D. A. & GAGE, F. H. 1998. Neurogenesis in the adult human hippocampus. *Nat Med,* 4**,** 1313-7.
ERNST, C. & CHRISTIE, B. R. 2006. The putative neural stem cell marker, nestin, is expressed in heterogeneous cell types in the adult rat neocortex. *Neuroscience,* 138**,** 183-8.
ETTINGER, A. B., WEISBROT, D. M., NOLAN, E. E., GADOW, K. D., VITALE, S. A., ANDRIOLA, M. R., LENN, N. J., NOVAK, G. P. & HERMANN, B. P. 1998. Symptoms of depression and anxiety in pediatric epilepsy patients. *Epilepsia,* 39**,** 595-9.
FANOUS, S., LACAGNINA, M. J., NIKULINA, E. M. & HAMMER, R. P., JR. 2011. Sensitized activation of Fos and brain-derived neurotrophic factor in the medial prefrontal cortex and ventral tegmental area accompanies behavioral sensitization to amphetamine. *Neuropharmacology,* 61**,** 558-64.
FAVARO, R., VALOTTA, M., FERRI, A. L., LATORRE, E., MARIANI, J., GIACHINO, C., LANCINI, C., TOSETTI, V., OTTOLENGHI, S., TAYLOR, V. & NICOLIS, S. K. 2009. Hippocampal development and neural stem cell maintenance require Sox2-dependent regulation of Shh. *Nat Neurosci,* 12**,** 1248-56.
FLAMAND, V., ABRAMOWICZ, D., GOLDMAN, M., BIERNAUX, C., HUEZ, G., URBAIN, J., MOSER, M. & LEO, O. 1990. Anti-CD3 antibodies induce T cells

from unprimed animals to secrete IL-4 both *in vitro* and *in vivo*. *Journal of Immunology,* 144**,** 2875-82.
FOTUHI, M., DO, D. & JACK, C. 2012. Modifiable factors that alter the size of the hippocampus with ageing. *Nat Rev Neurol,* 8**,** 189-202.
FREIDIN, M., BENNETT, M. V. & KESSLER, J. A. 1992. Cultured sympathetic neurons synthesize and release the cytokine interleukin 1 beta. *Proc Natl Acad Sci U S A,* 89**,** 10440-3.
FUKUDA, S., KATO, F., TOZUKA, Y., YAMAGUCHI, M., MIYAMOTO, Y. & HISATSUNE, T. 2003. Two distinct subpopulations of nestin-positive cells in adult mouse dentate gyrus. *J Neurosci,* 23**,** 9357-66.
GAGE, F. H. 2000. Mammalian neural stem cells. *Science,* 287**,** 1433-8.
GAGE, F. H., COATES, P. W., PALMER, T. D., KUHN, H. G., FISHER, L. J., SUHONEN, J. O., PETERSON, D. A., SUHR, S. T. & RAY, J. 1995. Survival and differentiation of adult neuronal progenitor cells transplanted to the adult brain. *Proc Natl Acad Sci U S A,* 92**,** 11879-83.
GAN, Q., LEE, A., SUZUKI, R., YAMAGAMI, T., STOKES, A., NGUYEN, B. C., PLEASURE, D., WANG, J., CHEN, H. W. & ZHOU, C. J. 2014. Pax6 mediates ss-catenin signaling for self-renewal and neurogenesis by neocortical radial glial stem cells. *Stem Cells,* 32**,** 45-58.
GANEA, D. 1996. Regulatory effects of vasoactive intestinal peptide on cytokine production in central and peripheral lymphoid organs. *Advances in Neuroimmunology,* 6**,** 61-74.
GANEA, D., RODRIGUEZ, R. & DELGADO, M. 2003. Vasoactive intestinal peptide and pituitary adenylate cyclase-activating polypeptide: players in innate and adaptive immunity. *Cell Mol Biol (Noisy-le-grand),* 49**,** 127-42.
GAO, Z., URE, K., ABLES, J. L., LAGACE, D. C., NAVE, K. A., GOEBBELS, S., EISCH, A. J. & HSIEH, J. 2009. Neurod1 is essential for the survival and maturation of adult-born neurons. *Nat Neurosci,* 12**,** 1090-2.
GE, S., GOH, E. L., SAILOR, K. A., KITABATAKE, Y., MING, G. L. & SONG, H. 2006. GABA regulates synaptic integration of newly generated neurons in the adult brain. *Nature,* 439**,** 589-93.
GINHOUX, F., GRETER, M., LEBOEUF, M., NANDI, S., SEE, P., GOKHAN, S., MEHLER, M. F., CONWAY, S. J., NG, L. G., STANLEY, E. R., SAMOKHVALOV, I. M. & MERAD, M. 2010. Fate mapping analysis reveals that adult microglia derive from primitive macrophages. *Science,* 330**,** 841-5.
GLOWA, J. R., PANLILIO, L. V., BRENNEMAN, D. E., GOZES, I., FRIDKIN, M. & HILL, J. M. 1992. Learning impairment following intracerebral administration of the HIV envelope protein gp120 or a VIP antagonist. *Brain Res,* 570**,** 49-53.
GOLDMAN, S. A. & NOTTEBOHM, F. 1983. Neuronal production, migration, and differentiation in a vocal control nucleus of the adult female canary brain. *Proc Natl Acad Sci U S A,* 80**,** 2390-4.
GOMARIZ, R., LECETA, J., MARTINEZ, C., ABAD, C., GANEA, D. & DELGADO, M. 2000. Anti-inflammatory actions of VIP/PACAP. Role in endotoxemia. *Ann N Y Acad Sci,* 921**,** 284-8.
GOMARIZ, R. P., LECETA, J., GARRIDO, E., GARRIDO, T. & DELGADO, M. 1994. Vasoactive intestinal peptide (VIP) mRNA expression in rat T and B lymphocytes. *Regulatory Peptides,* 50**,** 177-84.

GOMEZ-PINILLA, F., VAN DER WAL, E. A. & COTMAN, C. W. 1995. Possible coordinated gene expressions for FGF receptor, FGF-5, and FGF-2 following seizures. *Exp Neurol,* 133**,** 164-74.
GOSHEN, I., KREISEL, T., BEN-MENACHEM-ZIDON, O., LICHT, T., WEIDENFELD, J., BEN-HUR, T. & YIRMIYA, R. 2008. Brain interleukin-1 mediates chronic stress-induced depression in mice via adrenocortical activation and hippocampal neurogenesis suppression. *Mol Psychiatry,* 13**,** 717-28.
GOULD, E., BEYLIN, A., TANAPAT, P., REEVES, A. & SHORS, T. J. 1999. Learning enhances adult neurogenesis in the hippocampal formation. *Nat Neurosci,* 2**,** 260-5.
GOULD, E., VAIL, N., WAGERS, M. & GROSS, C. G. 2001. Adult-generated hippocampal and neocortical neurons in macaques have a transient existence. *Proceedings of the National Academy of Sciences of the United States of America,* 98**,** 10910-7.
GOZES, I., BARDEA, A., RESHEF, A., ZAMOSTIANO, R., ZHUKOVSKY, S., RUBINRAUT, S., FRIDKIN, M. & BRENNEMAN, D. E. 1996. Neuroprotective strategy for Alzheimer disease: intranasal administration of a fatty neuropeptide. *Proc Natl Acad Sci U S A,* 93**,** 427-32.
GOZES, I., GLOWA, J., BRENNEMAN, D. E., MCCUNE, S. K., LEE, E. & WESTPHAL, H. 1993. Learning and sexual deficiencies in transgenic mice carrying a chimeric vasoactive intestinal peptide gene. *J Mol Neurosci,* 4**,** 185-93.
GOZES, I., PERL, O., GILADI, E., DAVIDSON, A., ASHUR-FABIAN, O., RUBINRAUT, S. & FRIDKIN, M. 1999. Mapping the active site in vasoactive intestinal peptide to a core of four amino acids: neuroprotective drug design. *Proc Natl Acad Sci U S A,* 96**,** 4143-8.
GRESSENS, P., HILL, J. M., PAINDAVEINE, B., GOZES, I., FRIDKIN, M. & BRENNEMAN, D. E. 1994. Severe microcephaly induced by blockade of vasoactive intestinal peptide function in the primitive neuroepithelium of the mouse. *J Clin Invest,* 94**,** 2020-7.
GRONBERG, N. V., JOHANSEN, F. F., KRISTIANSEN, U. & HASSELDAM, H. 2013. Leukocyte infiltration in experimental stroke. *J Neuroinflammation,* 10**,** 115.
HATTIANGADY, B., RAO, M. S. & SHETTY, A. K. 2004. Chronic temporal lobe epilepsy is associated with severely declined dentate neurogenesis in the adult hippocampus. *Neurobiol Dis,* 17**,** 473-90.
HATTORI, K., LEE, H., HURN, P. D., CRAIN, B. J., TRAYSTMAN, R. J. & DEVRIES, A. C. 2000. Cognitive deficits after focal cerebral ischemia in mice. *Stroke,* 31**,** 1939-44.
HENNING, R. J. & SAWMILLER, D. R. 2001. Vasoactive intestinal peptide: cardiovascular effects. *Cardiovascular Research,* 49**,** 27-37.
HERNANDEZ, E. J., WILLIAMS, P. A. & DUDEK, F. E. 2002. Effects of fluoxetine and TFMPP on spontaneous seizures in rats with pilocarpine-induced epilepsy. *Epilepsia,* 43**,** 1337-45.
HILL, J. M., CUASAY, K. & ABEBE, D. T. 2007. Vasoactive intestinal peptide antagonist treatment during mouse embryogenesis impairs social behavior and cognitive function of adult male offspring. *Exp Neurol,* 206**,** 101-13.

HOWARD, C. E., ANDRES, P., BROKS, P., NOAD, R., SADLER, M., COKER, D. & MAZZONI, G. 2010. Memory, metamemory and their dissociation in temporal lobe epilepsy. *Neuropsychologia,* 48**,** 921-32.
HSIEH, J. 2012. Orchestrating transcriptional control of adult neurogenesis. *Genes Dev,* 26**,** 1010-21.
INOSTROZA, M., CID, E., BROTONS-MAS, J., GAL, B., AIVAR, P., UZCATEGUI, Y. G., SANDI, C. & MENENDEZ DE LA PRIDA, L. 2011. Hippocampal-dependent spatial memory in the water maze is preserved in an experimental model of temporal lobe epilepsy in rats. *PLoS One,* 6**,** e22372.
ITOH, S., TAKASHIMA, A. & MORIMOTO, T. 1994. Impaired spatial learning by vasoactive intestinal peptide in Morris water maze task in the rat. *Can J Physiol Pharmacol,* 72**,** 25-9.
ITRI, J. & COLWELL, C. S. 2003. Regulation of inhibitory synaptic transmission by vasoactive intestinal peptide (VIP) in the mouse suprachiasmatic nucleus. *J Neurophysiol,* 90**,** 1589-97.
IWANO, T., MASUDA, A., KIYONARI, H., ENOMOTO, H. & MATSUZAKI, F. 2012. Prox1 postmitotically defines dentate gyrus cells by specifying granule cell identity over CA3 pyramidal cell fate in the hippocampus. *Development,* 139**,** 3051-62.
JAYATISSA, M. N., HENNINGSEN, K., NIKOLAJSEN, G., WEST, M. J. & WIBORG, O. 2010. A reduced number of hippocampal granule cells does not associate with an anhedonia-like phenotype in a rat chronic mild stress model of depression. *Stress,* 13**,** 95-105.
JESSBERGER, S. & KEMPERMANN, G. 2003. Adult-born hippocampal neurons mature into activity-dependent responsiveness. *Eur J Neurosci,* 18**,** 2707-12.
JESSBERGER, S., NAKASHIMA, K., CLEMENSON, G. D., JR., MEJIA, E., MATHEWS, E., URE, K., OGAWA, S., SINTON, C. M., GAGE, F. H. & HSIEH, J. 2007. Epigenetic modulation of seizure-induced neurogenesis and cognitive decline. *J Neurosci,* 27**,** 5967-75.
JESSBERGER, S., TONI, N., CLEMENSON, G. D., JR., RAY, J. & GAGE, F. H. 2008. Directed differentiation of hippocampal stem/progenitor cells in the adult brain. *Nat Neurosci,* 11**,** 888-93.
JIANG, X., WANG, H. Y., YU, J. & GANEA, D. 1998. VIP1 and VIP2 receptors but not PVR1 mediate the effect of VIP/PACAP on cytokine production in T lymphocytes. *Ann N Y Acad Sci,* 865**,** 397-407.
JIMENO, R., GOMARIZ, R. P., GUTIERREZ-CANAS, I., MARTINEZ, C., JUARRANZ, Y. & LECETA, J. 2010. New insights into the role of VIP on the ratio of T-cell subsets during the development of autoimmune diabetes. *Immunol Cell Biol,* 88**,** 734-45.
JIN, K., MINAMI, M., LAN, J. Q., MAO, X. O., BATTEUR, S., SIMON, R. P. & GREENBERG, D. A. 2001. Neurogenesis in dentate subgranular zone and rostral subventricular zone after focal cerebral ischemia in the rat. *Proc Natl Acad Sci U S A,* 98**,** 4710-5.
JOBE, P. C. & BROWNING, R. A. 2005. The serotonergic and noradrenergic effects of antidepressant drugs are anticonvulsant, not proconvulsant. *Epilepsy Behav,* 7**,** 602-19.
JUNE, C. H., BLUESTONE, J. A., NADLER, L. M. & THOMPSON, C. B. 1994. The B7 and CD28 receptor families. *Immunol Today,* 15**,** 321-31.

KANNER, A. M. 2003. Depression in epilepsy: prevalence, clinical semiology, pathogenic mechanisms, and treatment. *Biol Psychiatry,* 54**,** 388-98.
KAPLAN, M. S. & HINDS, J. W. 1977. Neurogenesis in the adult rat: electron microscopic analysis of light radioautographs. *Science,* 197**,** 1092-4.
KARALAY, O., DOBERAUER, K., VADODARIA, K. C., KNOBLOCH, M., BERTI, L., MIQUELAJAUREGUI, A., SCHWARK, M., JAGASIA, R., TAKETO, M. M., TARABYKIN, V., LIE, D. C. & JESSBERGER, S. 2011. Prospero-related homeobox 1 gene (Prox1) is regulated by canonical Wnt signaling and has a stage-specific role in adult hippocampal neurogenesis. *Proc Natl Acad Sci U S A,* 108**,** 5807-12.
KARMAN, J., LING, C., SANDOR, M. & FABRY, Z. 2004. Dendritic cells in the initiation of immune responses against central nervous system-derived antigens. *Immunol Lett,* 92**,** 107-15.
KEE, N. J., PRESTON, E. & WOJTOWICZ, J. M. 2001. Enhanced neurogenesis after transient global ischemia in the dentate gyrus of the rat. *Exp Brain Res,* 136**,** 313-20.
KEMPERMANN, G. & GAGE, F. H. 2002. Genetic determinants of adult hippocampal neurogenesis correlate with acquisition, but not probe trial performance, in the water maze task. *Eur J Neurosci,* 16**,** 129-36.
KEMPERMANN, G., KUHN, H. G. & GAGE, F. H. 1997. More hippocampal neurons in adult mice living in an enriched environment. *Nature,* 386**,** 493-5.
KEMPERMANN, G., WISKOTT, L. & GAGE, F. H. 2004. Functional significance of adult neurogenesis. *Curr Opin Neurobiol,* 14**,** 186-91.
KIGERL, K. A., GENSEL, J. C., ANKENY, D. P., ALEXANDER, J. K., DONNELLY, D. J. & POPOVICH, P. G. 2009. Identification of two distinct macrophage subsets with divergent effects causing either neurotoxicity or regeneration in the injured mouse spinal cord. *J Neurosci,* 29**,** 13435-44.
KIPNIS, J., COHEN, H., CARDON, M., ZIV, Y. & SCHWARTZ, M. 2004. T cell deficiency leads to cognitive dysfunction: implications for therapeutic vaccination for schizophrenia and other psychiatric conditions. *Proc Natl Acad Sci U S A,* 101**,** 8180-5.
KITAJIMA, H., YOSHIMURA, S., KOKUZAWA, J., KATO, M., IWAMA, T., MOTOHASHI, T., KUNISADA, T. & SAKAI, N. 2005. Culture method for the induction of neurospheres from mouse embryonic stem cells by coculture with PA6 stromal cells. *J Neurosci Res,* 80**,** 467-74.
KIVISAKK, P., LIU, Z., TREBST, C., TUCKY, B., WU, L., STINE, J., MACK, M., RUDICK, R. A., CAMPBELL, J. J. & RANSOHOFF, R. M. 2003a. Flow cytometric analysis of chemokine receptor expression on cerebrospinal fluid leukocytes. *Methods,* 29**,** 319-25.
KIVISAKK, P., MAHAD, D. J., CALLAHAN, M. K., TREBST, C., TUCKY, B., WEI, T., WU, L., BAEKKEVOLD, E. S., LASSMANN, H., STAUGAITIS, S. M., CAMPBELL, J. J. & RANSOHOFF, R. M. 2003b. Human cerebrospinal fluid central memory CD4+ T cells: evidence for trafficking through choroid plexus and meninges via P-selectin. *Proc Natl Acad Sci U S A,* 100**,** 8389-94.
KNOTH, R., SINGEC, I., DITTER, M., PANTAZIS, G., CAPETIAN, P., MEYER, R. P., HORVAT, V., VOLK, B. & KEMPERMANN, G. 2010. Murine features of neurogenesis in the human hippocampus across the lifespan from 0 to 100 years. *PLoS One,* 5**,** e8809.

KOCHENDERFER, J. N., WILSON, W. H., JANIK, J. E., DUDLEY, M. E., STETLER-STEVENSON, M., FELDMAN, S. A., MARIC, I., RAFFELD, M., NATHAN, D. A., LANIER, B. J., MORGAN, R. A. & ROSENBERG, S. A. 2010. Eradication of B-lineage cells and regression of lymphoma in a patient treated with autologous T cells genetically engineered to recognize CD19. *Blood,* 116**,** 4099-102.

KOMITOVA, M. & ERIKSSON, P. S. 2004. Sox-2 is expressed by neural progenitors and astroglia in the adult rat brain. *Neurosci Lett,* 369**,** 24-7.

KRADY, J. K., BASU, A., ALLEN, C. M., XU, Y., LANOUE, K. F., GARDNER, T. W. & LEVISON, S. W. 2005. Minocycline reduces proinflammatory cytokine expression, microglial activation, and caspase-3 activation in a rodent model of diabetic retinopathy. *Diabetes,* 54**,** 1559-65.

KRONFOL, Z. & REMICK, D. G. 2000. Cytokines and the brain: implications for clinical psychiatry. *Am J Psychiatry,* 157**,** 683-94.

KURUBA, R., HATTIANGADY, B. & SHETTY, A. K. 2009. Hippocampal neurogenesis and neural stem cells in temporal lobe epilepsy. *Epilepsy Behav,* 14 Suppl 1**,** 65-73.

KUWABARA, T., HSIEH, J., MUOTRI, A., YEO, G., WARASHINA, M., LIE, D. C., MOORE, L., NAKASHIMA, K., ASASHIMA, M. & GAGE, F. H. 2009. Wnt-mediated activation of NeuroD1 and retro-elements during adult neurogenesis. *Nat Neurosci,* 12**,** 1097-105.

LADEBY, R., WIRENFELDT, M., GARCIA-OVEJERO, D., FENGER, C., DISSING-OLESEN, L., DALMAU, I. & FINSEN, B. 2005. Microglial cell population dynamics in the injured adult central nervous system. *Brain Res Brain Res Rev,* 48**,** 196-206.

LAGACE, D. C., DONOVAN, M. H., DECAROLIS, N. A., FARNBAUCH, L. A., MALHOTRA, S., BERTON, O., NESTLER, E. J., KRISHNAN, V. & EISCH, A. J. 2010. Adult hippocampal neurogenesis is functionally important for stress-induced social avoidance. *Proc Natl Acad Sci U S A,* 107**,** 4436-41.

LARA-MARQUEZ, M., O'DORISIO, M., O'DORISIO, T., SHAH, M. & KARACAY, B. 2001. Selective gene expression and activation-dependent regulation of vasoactive intestinal peptide receptor type 1 and type 2 in human T cells. *J Immunol,* 166**,** 2522-30.

LARSSON, L. I., FAHRENKRUG, J., SCHAFFALITZKY DE MUCKADELL, O., SUNDLER, F., HAKANSON, R. & REHFELD, J. R. 1976. Localization of vasoactive intestinal polypeptide (VIP) to central and peripheral neurons. *Proc Natl Acad Sci U S A,* 73**,** 3197-200.

LAVADO, A., LAGUTIN, O. V., CHOW, L. M., BAKER, S. J. & OLIVER, G. 2010. Prox1 is required for granule cell maturation and intermediate progenitor maintenance during brain neurogenesis. *PLoS Biol,* 8.

LAWSON, L. J., PERRY, V. H., DRI, P. & GORDON, S. 1990. Heterogeneity in the distribution and morphology of microglia in the normal adult mouse brain. *Neuroscience,* 39**,** 151-70.

LECOEUR, H. 2002. Nuclear apoptosis detection by flow cytometry: influence of endogenous endonucleases. *Experimental Cell Research,* 277**,** 1-14.

LEFEBVRE, V., DUMITRIU, B., PENZO-MENDEZ, A., HAN, Y. & PALLAVI, B. 2007. Control of cell fate and differentiation by Sry-related high-mobility-group box (Sox) transcription factors. *Int J Biochem Cell Biol,* 39**,** 2195-214.

LEHTIMAKI, K. A., KERANEN, T., PALMIO, J., MAKINEN, R., HURME, M., HONKANIEMI, J. & PELTOLA, J. 2007. Increased plasma levels of cytokines after seizures in localization-related epilepsy. *Acta Neurol Scand,* 116**,** 226-30.

LI, Y. & KURLANDER, R. J. 2010. Comparison of anti-CD3 and anti-CD28-coated beads with soluble anti-CD3 for expanding human T cells: differing impact on CD8 T cell phenotype and responsiveness to restimulation. *Journal of Translational Medicine,* 8**,** 104.

LI, Y., LUIKART, B. W., BIRNBAUM, S., CHEN, J., KWON, C. H., KERNIE, S. G., BASSEL-DUBY, R. & PARADA, L. F. 2008. TrkB regulates hippocampal neurogenesis and governs sensitivity to antidepressive treatment. *Neuron,* 59**,** 399-412.

LICINIO, J., KLING, M. A. & HAUSER, P. 1998. Cytokines and brain function: relevance to interferon-alpha-induced mood and cognitive changes. *Semin Oncol,* 25**,** 30-8.

LIGHTMAN, S. & GREENWOOD, J. 1992. Effect of lymphocytic infiltration on the blood-retinal barrier in experimental autoimmune uveoretinitis. *Clin Exp Immunol,* 88**,** 473-7.

LIU, J., SOLWAY, K., MESSING, R. O. & SHARP, F. R. 1998. Increased neurogenesis in the dentate gyrus after transient global ischemia in gerbils. *J Neurosci,* 18**,** 7768-78.

LOPEZ-TELLEZ, J. F., VELA, J., DEL RIO, J. C., RAMOS, B., BAGLIETTO-VARGAS, D., SANTA-MARIA, C., RUANO, D., GUTIERREZ, A. & VITORICA, J. 2004. Postnatal development of the alpha1 containing GABAA receptor subunit in rat hippocampus. *Brain Res Dev Brain Res,* 148**,** 129-41.

LU, N., BLACK, I. B. & DICICCO-BLOOM, E. 1996. A paradigm for distinguishing the roles of mitogenesis and trophism in neuronal precursor proliferation. *Brain Res Dev Brain Res,* 94**,** 31-6.

LUGERT, S., BASAK, O., KNUCKLES, P., HAUSSLER, U., FABEL, K., GOTZ, M., HAAS, C. A., KEMPERMANN, G., TAYLOR, V. & GIACHINO, C. 2010. Quiescent and active hippocampal neural stem cells with distinct morphologies respond selectively to physiological and pathological stimuli and aging. *Cell Stem Cell,* 6**,** 445-56.

MAEKAWA, M., TAKASHIMA, N., ARAI, Y., NOMURA, T., INOKUCHI, K., YUASA, S. & OSUMI, N. 2005. Pax6 is required for production and maintenance of progenitor cells in postnatal hippocampal neurogenesis. *Genes Cells,* 10**,** 1001-14.

MALBERG, J. E., EISCH, A. J., NESTLER, E. J. & DUMAN, R. S. 2000. Chronic antidepressant treatment increases neurogenesis in adult rat hippocampus. *J Neurosci,* 20**,** 9104-10.

MARTINEZ, C., DELGADO, M., ABAD, C., GOMARIZ, R. P., GANEA, D. & LECETA, J. 1999. Regulation of VIP production and secretion by murine lymphocytes. *Journal of Neuroimmunology,* 93**,** 126-38.

MAZARATI, A. M., SHIN, D., KWON, Y. S., BRAGIN, A., PINEDA, E., TIO, D., TAYLOR, A. N. & SANKAR, R. 2009. Elevated plasma corticosterone level and depressive behavior in experimental temporal lobe epilepsy. *Neurobiol Dis,* 34**,** 457-61.

MCHUGH, T. J., JONES, M. W., QUINN, J. J., BALTHASAR, N., COPPARI, R., ELMQUIST, J. K., LOWELL, B. B., FANSELOW, M. S., WILSON, M. A. &

TONEGAWA, S. 2007. Dentate gyrus NMDA receptors mediate rapid pattern separation in the hippocampal network. *Science,* 317**,** 94-9.
MCMENAMIN, P. G., WEALTHALL, R. J., DEVERALL, M., COOPER, S. J. & GRIFFIN, B. 2003. Macrophages and dendritic cells in the rat meninges and choroid plexus: three-dimensional localisation by environmental scanning electron microscopy and confocal microscopy. *Cell & Tissue Research,* 313**,** 259-69.
MENEZES, J. R. & LUSKIN, M. B. 1994. Expression of neuron-specific tubulin defines a novel population in the proliferative layers of the developing telencephalon. *Journal of Neuroscience,* 14**,** 5399-416.
MESHI, D., DREW, M. R., SAXE, M., ANSORGE, M. S., DAVID, D., SANTARELLI, L., MALAPANI, C., MOORE, H. & HEN, R. 2006. Hippocampal neurogenesis is not required for behavioral effects of environmental enrichment. *Nat Neurosci,* 9**,** 729-31.
METWALI, A., BLUM, A. M., ELLIOTT, D. E. & WEINSTOCK, J. V. 2002. IL-4 inhibits vasoactive intestinal peptide production by macrophages. *Am J Physiol Gastrointest Liver Physiol,* 283**,** G115-21.
METWALI, A., BLUM, A. M., LI, J., ELLIOTT, D. E. & WEINSTOCK, J. V. 2000. IL-4 regulates VIP receptor subtype 2 mRNA (VPAC2) expression in T cells in murine schistosomiasis. *FASEB J,* 14**,** 948-54.
MOALEM, G., LEIBOWITZ-AMIT, R., YOLES, E., MOR, F., COHEN, I. R. & SCHWARTZ, M. 1999. Autoimmune T cells protect neurons from secondary degeneration after central nervous system axotomy. *Nat Med,* 5**,** 49-55.
MONJE, M. L., TODA, H. & PALMER, T. D. 2003. Inflammatory blockade restores adult hippocampal neurogenesis. *Science,* 302**,** 1760-5.
MONTARON, M. F., PETRY, K. G., RODRIGUEZ, J. J., MARINELLI, M., AUROUSSEAU, C., ROUGON, G., LE MOAL, M. & ABROUS, D. N. 1999. Adrenalectomy increases neurogenesis but not PSA-NCAM expression in aged dentate gyrus. *Eur J Neurosci,* 11**,** 1479-85.
MOODY, T. W., HILL, J. M. & JENSEN, R. T. 2003. VIP as a trophic factor in the CNS and cancer cells. *Peptides,* 24**,** 163-77.
MORRIS, R. G., GARRUD, P., RAWLINS, J. N. & O'KEEFE, J. 1982. Place navigation impaired in rats with hippocampal lesions. *Nature,* 297**,** 681-3.
MORSTYN, G., PYKE, K., GARDNER, J., ASHCROFT, R., DE FAZIO, A. & BHATHAL, P. 1986. Immunohistochemical identification of proliferating cells in organ culture using bromodeoxyuridine and a monoclonal antibody. *J Histochem Cytochem,* 34**,** 697-701.
MOSMANN, T. R., CHERWINSKI, H., BOND, M. W., GIEDLIN, M. A. & COFFMAN, R. L. 1986a. Two types of murine helper T cell clone. I. Definition according to profiles of lymphokine activities and secreted proteins. *J Immunol,* 136**,** 2348-57.
MOSMANN, T. R., CHERWINSKI, H., BOND, M. W., GIEDLIN, M. A. & COFFMAN, R. L. 1986b. Two types of murine helper T cell clone. I. Definition according to profiles of lymphokine activities and secreted proteins. *Journal of Immunology,* 136**,** 2348-57.
MURPHY, G. G. 2013. Spatial Learning and Memory-What's TLE Got To Do With It? *Epilepsy Curr,* 13**,** 26-9.
NADEL, L. & HARDT, O. 2004. The spatial brain. *Neuropsychology,* 18**,** 473-6.

NAMBA, T., MOCHIZUKI, H., ONODERA, M., MIZUNO, Y., NAMIKI, H. & SEKI, T. 2005. The fate of neural progenitor cells expressing astrocytic and radial glial markers in the postnatal rat dentate gyrus. *Eur J Neurosci,* 22**,** 1928-41.

NAMBA, T., MOCHIZUKI, H., ONODERA, M., NAMIKI, H. & SEKI, T. 2007. Postnatal neurogenesis in hippocampal slice cultures: early *in vitro* labeling of neural precursor cells leads to efficient neuronal production. *J Neurosci Res,* 85**,** 1704-12.

NILSSON, M., PERFILIEVA, E., JOHANSSON, U., ORWAR, O. & ERIKSSON, P. S. 1999. Enriched environment increases neurogenesis in the adult rat dentate gyrus and improves spatial memory. *J Neurobiol,* 39**,** 569-78.

NUNN, J. & HODGES, H. 1994. Cognitive deficits induced by global cerebral ischaemia: relationship to brain damage and reversal by transplants. *Behav Brain Res,* 65**,** 1-31.

O'GARRA, A. 1998. Cytokines induce the development of functionally heterogeneous T helper cell subsets. *Immunity,* 8**,** 275-83.

PALMER, T. D., WILLHOITE, A. R. & GAGE, F. H. 2000. Vascular niche for adult hippocampal neurogenesis. *J Comp Neurol,* 425**,** 479-94.

PARENT, J. M., JANUMPALLI, S., MCNAMARA, J. O. & LOWENSTEIN, D. H. 1998. Increased dentate granule cell neurogenesis following amygdala kindling in the adult rat. *Neurosci Lett,* 247**,** 9-12.

PARENT, J. M., YU, T. W., LEIBOWITZ, R. T., GESCHWIND, D. H., SLOVITER, R. S. & LOWENSTEIN, D. H. 1997. Dentate granule cell neurogenesis is increased by seizures and contributes to aberrant network reorganization in the adult rat hippocampus. *J Neurosci,* 17**,** 3727-38.

PEREIRA, A. C., HUDDLESTON, D. E., BRICKMAN, A. M., SOSUNOV, A. A., HEN, R., MCKHANN, G. M., SLOAN, R., GAGE, F. H., BROWN, T. R. & SMALL, S. A. 2007. An *in vivo* correlate of exercise-induced neurogenesis in the adult dentate gyrus. *Proc Natl Acad Sci U S A,* 104**,** 5638-43.

PERERA, T. D., COPLAN, J. D., LISANBY, S. H., LIPIRA, C. M., ARIF, M., CARPIO, C., SPITZER, G., SANTARELLI, L., SCHARF, B., HEN, R., ROSOKLIJA, G., SACKEIM, H. A. & DWORK, A. J. 2007. Antidepressant-induced neurogenesis in the hippocampus of adult nonhuman primates. *J Neurosci,* 27**,** 4894-901.

PETRIK, D., LAGACE, D. C. & EISCH, A. J. 2012. The neurogenesis hypothesis of affective and anxiety disorders: are we mistaking the scaffolding for the building? *Neuropharmacology,* 62**,** 21-34.

PORTER, D. L., LEVINE, B. L., KALOS, M., BAGG, A. & JUNE, C. H. 2011. Chimeric antigen receptor-modified T cells in chronic lymphoid leukemia. *N Engl J Med,* 365**,** 725-33.

POZO, D. & DELGADO, M. 2004. The many faces of VIP in neuroimmunology: a cytokine rather a neuropeptide? *FASEB Journal,* 18**,** 1325-34.

RANSOHOFF, R. M., KIVISAKK, P. & KIDD, G. 2003. Three or more routes for leukocyte migration into the central nervous system. *Nat Rev Immunol,* 3**,** 569-81.

REICHENSTEIN, M., REHAVI, M. & PINHASOV, A. 2008. Involvement of pituitary adenylate cyclase activating polypeptide (PACAP) and its receptors in the mechanism of antidepressant action. *J Mol Neurosci,* 36**,** 330-8.

REYNOLDS, B. A. & WEISS, S. 1992. Generation of neurons and astrocytes from isolated cells of the adult mammalian central nervous system. *Science,* 255**,** 1707-10.
REZNIKOV, K. Y. 1991. Cell proliferation and cytogenesis in the mouse hippocampus. *Adv Anat Embryol Cell Biol,* 122**,** 1-74.
RICHARDS, L. J., KILPATRICK, T. J. & BARTLETT, P. F. 1992. De novo generation of neuronal cells from the adult mouse brain. *Proc Natl Acad Sci U S A,* 89**,** 8591-5.
RIQUELME, P. A., DRAPEAU, E. & DOETSCH, F. 2008. Brain micro-ecologies: neural stem cell niches in the adult mammalian brain. *Philos Trans R Soc Lond B Biol Sci,* 363**,** 123-37.
RIZZI, M., PEREGO, C., ALIPRANDI, M., RICHICHI, C., RAVIZZA, T., COLELLA, D., VELISKOVA, J., MOSHE, S. L., DE SIMONI, M. G. & VEZZANI, A. 2003. Glia activation and cytokine increase in rat hippocampus by kainic acid-induced status epilepticus during postnatal development. *Neurobiol Dis,* 14**,** 494-503.
ROSENZWEIG, M. R. 1966. Environmental complexity, cerebral change, and behavior. *Am Psychol,* 21**,** 321-32.
RUSSO, I., BARLATI, S. & BOSETTI, F. 2011. Effects of neuroinflammation on the regenerative capacity of brain stem cells. *J Neurochem,* 116**,** 947-56.
SAID, S. I. & MUTT, V. 1970. Polypeptide with broad biological activity: isolation from small intestine. *Science,* 169**,** 1217-8.
SAID, S. I. & MUTT, V. 1972. Isolation from porcine-intestinal wall of a vasoactive octacosapeptide related to secretin and to glucagon. *Eur J Biochem,* 28**,** 199-204.
SAID, S. I. & ROSENBERG, R. N. 1976. Vasoactive intestinal polypeptide: abundant immunoreactivity in neural cell lines and normal nervous tissue. *Science,* 192**,** 907-8.
SANTARELLI, L., SAXE, M., GROSS, C., SURGET, A., BATTAGLIA, F., DULAWA, S., WEISSTAUB, N., LEE, J., DUMAN, R., ARANCIO, O., BELZUNG, C. & HEN, R. 2003. Requirement of hippocampal neurogenesis for the behavioral effects of antidepressants. *Science,* 301**,** 805-9.
SARTORI, A., MA, X., GRI, G., SHOWE, L., BENJAMIN, D. & TRINCHIERI, G. 1997. Interleukin-12: an immunoregulatory cytokine produced by B cells and antigen-presenting cells. *Methods (Duluth),* 11**,** 116-27.
SCHARF, E., MAY, V., BRAAS, K. M., SHUTZ, K. C. & MAO-DRAAYER, Y. 2008. Pituitary adenylate cyclase-activating polypeptide (PACAP) and vasoactive intestinal peptide (VIP) regulate murine neural progenitor cell survival, proliferation, and differentiation. *J Mol Neurosci,* 36**,** 79-88.
SCHWARTZ, M., BUTOVSKY, O., BRUCK, W. & HANISCH, U. K. 2006. Microglial phenotype: is the commitment reversible? *Trends Neurosci,* 29**,** 68-74.
SERI, B., GARCIA-VERDUGO, J. M., MCEWEN, B. S. & ALVAREZ-BUYLLA, A. 2001. Astrocytes give rise to new neurons in the adult mammalian hippocampus. *J Neurosci,* 21**,** 7153-60.
SERI, B., HERRERA, D. G., GRITTI, A., FERRON, S., COLLADO, L., VESCOVI, A., GARCIA-VERDUGO, J. M. & ALVAREZ-BUYLLA, A. 2006. Composition and organization of the SCZ: a large germinal layer containing neural stem cells in the adult mammalian brain. *Cereb Cortex,* 16 Suppl 1**,** i103-11.

SERVOSS, S. J., LEE, S. J., GIBNEY, G., GOZES, I., BRENNEMAN, D. E. & HILL, J. M. 2001. IGF-I as a mediator of VIP/activity-dependent neurotrophic factor-stimulated embryonic growth. *Endocrinology,* 142**,** 3348-53.

SHAPIRO, L. A., KORN, M. J. & RIBAK, C. E. 2005. Newly generated dentate granule cells from epileptic rats exhibit elongated hilar basal dendrites that align along GFAP-immunolabeled processes. *Neuroscience,* 136**,** 823-31.

SHAPIRO, L. A. & RIBAK, C. E. 2006. Newly born dentate granule neurons after pilocarpine-induced epilepsy have hilar basal dendrites with immature synapses. *Epilepsy Res,* 69**,** 53-66.

SHARMA, V., DELGADO, M. & GANEA, D. 2006. VIP protects Th2 cells by downregulating granzyme B expression. *Ann N Y Acad Sci,* 1070**,** 540-4.

SHECHTER, R., LONDON, A., VAROL, C., RAPOSO, C., CUSIMANO, M., YOVEL, G., ROLLS, A., MACK, M., PLUCHINO, S., MARTINO, G., JUNG, S. & SCHWARTZ, M. 2009. Infiltrating blood-derived macrophages are vital cells playing an anti-inflammatory role in recovery from spinal cord injury in mice. *PLoS Med,* 6**,** e1000113.

SHETTY, A. K., RAO, M. S., HATTIANGADY, B., ZAMAN, V. & SHETTY, G. A. 2004. Hippocampal neurotrophin levels after injury: Relationship to the age of the hippocampus at the time of injury. *J Neurosci Res,* 78**,** 520-32.

SHETTY, A. K., ZAMAN, V. & SHETTY, G. A. 2003. Hippocampal neurotrophin levels in a kainate model of temporal lobe epilepsy: a lack of correlation between brain-derived neurotrophic factor content and progression of aberrant dentate mossy fiber sprouting. *J Neurochem,* 87**,** 147-59.

SHEWARD, W. J., LUTZ, E. M. & HARMAR, A. J. 1995. The distribution of vasoactive intestinal peptide2 receptor messenger RNA in the rat brain and pituitary gland as assessed by in situ hybridization. *Neuroscience,* 67**,** 409-18.

SHIODA, S., OHTAKI, H., NAKAMACHI, T., DOHI, K., WATANABE, J., NAKAJO, S., ARATA, S., KITAMURA, S., OKUDA, H., TAKENOYA, F. & KITAMURA, Y. 2006. Pleiotropic functions of PACAP in the CNS: neuroprotection and neurodevelopment. *Ann N Y Acad Sci,* 1070**,** 550-60.

SHRESTHA, R., MILLINGTON, O., BREWER, J. & BUSHELL, T. 2013. Is central nervous system an immune-privileged site? *Kathmandu Univ Med J (KUMJ),* 11**,** 102-7.

SISTI, H. M., GLASS, A. L. & SHORS, T. J. 2007. Neurogenesis and the spacing effect: learning over time enhances memory and the survival of new neurons. *Learn Mem,* 14**,** 368-75.

SMALL, S. A., SCHOBEL, S. A., BUXTON, R. B., WITTER, M. P. & BARNES, C. A. 2011. A pathophysiological framework of hippocampal dysfunction in ageing and disease. *Nat Rev Neurosci,* 12**,** 585-601.

SONG, C. & WANG, H. 2011. Cytokines mediated inflammation and decreased neurogenesis in animal models of depression. *Prog Neuropsychopharmacol Biol Psychiatry,* 35**,** 760-8.

SONG, H., STEVENS, C. F. & GAGE, F. H. 2002. Astroglia induce neurogenesis from adult neural stem cells. *Nature,* 417**,** 39-44.

SPALDING, K. L., BERGMANN, O., ALKASS, K., BERNARD, S., SALEHPOUR, M., HUTTNER, H. B., BOSTROM, E., WESTERLUND, I., VIAL, C., BUCHHOLZ, B. A., POSSNERT, G., MASH, D. C., DRUID, H. & FRISEN, J. 2013. Dynamics of hippocampal neurogenesis in adult humans. *Cell,* 153**,** 1219-27.

SUN, G., YU, R. T., EVANS, R. M. & SHI, Y. 2007. Orphan nuclear receptor TLX recruits histone deacetylases to repress transcription and regulate neural stem cell proliferation. *Proc Natl Acad Sci U S A,* 104**,** 15282-7.
SUN, M. K. & ALKON, D. L. 2004. Induced depressive behavior impairs learning and memory in rats. *Neuroscience,* 129**,** 129-39.
SVENNINGSSON, A., ANDERSEN, O., EDSBAGGE, M. & STEMME, S. 1995. Lymphocyte phenotype and subset distribution in normal cerebrospinal fluid. *J Neuroimmunol,* 63**,** 39-46.
SZTAINBERG, Y. & CHEN, A. 2010. An environmental enrichment model for mice. *Nat Protoc,* 5**,** 1535-9.
TANAKA, R., YAMASHIRO, K., MOCHIZUKI, H., CHO, N., ONODERA, M., MIZUNO, Y. & URABE, T. 2004. Neurogenesis after transient global ischemia in the adult hippocampus visualized by improved retroviral vector. *Stroke,* 35**,** 1454-9.
TSAI, Y. W., YANG, Y. R., SUN, S. H., LIANG, K. C. & WANG, R. Y. 2013. Post ischemia intermittent hypoxia induces hippocampal neurogenesis and synaptic alterations and alleviates long-term memory impairment. *J Cereb Blood Flow Metab,* 33**,** 764-73.
TSOUKAS, C. D., LANDGRAF, B., BENTIN, J., VALENTINE, M., LOTZ, M., VAUGHAN, J. H. & CARSON, D. A. 1985. Activation of resting T lymphocytes by anti-CD3 (T3) antibodies in the absence of monocytes. *J Immunol,* 135**,** 1719-23.
VALLIERES, L., CAMPBELL, I. L., GAGE, F. H. & SAWCHENKO, P. E. 2002. Reduced hippocampal neurogenesis in adult transgenic mice with chronic astrocytic production of interleukin-6. *J Neurosci,* 22**,** 486-92.
VAN PRAAG, H., CHRISTIE, B. R., SEJNOWSKI, T. J. & GAGE, F. H. 1999. Running enhances neurogenesis, learning, and long-term potentiation in mice. *Proc Natl Acad Sci U S A,* 96**,** 13427-31.
VAN PRAAG, H., SCHINDER, A. F., CHRISTIE, B. R., TONI, N., PALMER, T. D. & GAGE, F. H. 2002. Functional neurogenesis in the adult hippocampus. *Nature,* 415**,** 1030-4.
VERTONGEN, P., SCHIFFMANN, S. N., GOURLET, P. & ROBBERECHT, P. 1997. Autoradiographic visualization of the receptor subclasses for vasoactive intestinal polypeptide (VIP) in rat brain. *Peptides,* 18**,** 1547-54.
VILLEDA, S. A., LUO, J., MOSHER, K. I., ZOU, B., BRITSCHGI, M., BIERI, G., STAN, T. M., FAINBERG, N., DING, Z., EGGEL, A., LUCIN, K. M., CZIRR, E., PARK, J. S., COUILLARD-DESPRES, S., AIGNER, L., LI, G., PESKIND, E. R., KAYE, J. A., QUINN, J. F., GALASKO, D. R., XIE, X. S., RANDO, T. A. & WYSS-CORAY, T. 2011. The ageing systemic milieu negatively regulates neurogenesis and cognitive function. *Nature,* 477**,** 90-4.
VOICE, J. K., DORSAM, G., LEE, H., KONG, Y. & GOETZL, E. J. 2001a. Allergic diathesis in transgenic mice with constitutive T cell expression of inducible vasoactive intestinal peptide receptor. *FASEB J,* 15**,** 2489-96.
VOICE, J. K., DORSAM, G., LEE, H., KONG, Y. & GOETZL, E. J. 2001b. Allergic diathesis in transgenic mice with constitutive T cell expression of inducible vasoactive intestinal peptide receptor. *FASEB Journal,* 15**,** 2489-96.
VOICE, J. K., GRINNINGER, C., KONG, Y., BANGALE, Y., PAUL, S. & GOETZL, E. J. 2003. Roles of vasoactive intestinal peptide (VIP) in the expression of

different immune phenotypes by wild-type mice and T cell-targeted type II VIP receptor transgenic mice. *J Immunol,* 170**,** 308-14.
WANG, H. Y., JIANG, X., GOZES, I., FRIDKIN, M., BRENNEMAN, D. E. & GANEA, D. 1999. Vasoactive intestinal peptide inhibits cytokine production in T lymphocytes through cAMP-dependent and cAMP-independent mechanisms. *Regul Pept,* 84**,** 55-67.
WANG, H. Y., JIANG, X. M. & GANEA, D. 2000. The neuropeptides VIP and PACAP inhibit IL-2 transcription by decreasing c-Jun and increasing JunB expression in T cells. *J Neuroimmunol,* 104**,** 68-78.
WEISS, S., DUNNE, C., HEWSON, J., WOHL, C., WHEATLEY, M., PETERSON, A. C. & REYNOLDS, B. A. 1996. Multipotent CNS stem cells are present in the adult mammalian spinal cord and ventricular neuroaxis. *J Neurosci,* 16**,** 7599-609.
WILSON, E. H., WENINGER, W. & HUNTER, C. A. 2010. Trafficking of immune cells in the central nervous system. *J Clin Invest,* 120**,** 1368-79.
WOLF, S. A., STEINER, B., AKPINARLI, A., KAMMERTOENS, T., NASSENSTEIN, C., BRAUN, A., BLANKENSTEIN, T. & KEMPERMANN, G. 2009. CD4-positive T lymphocytes provide a neuroimmunological link in the control of adult hippocampal neurogenesis. *J Immunol,* 182**,** 3979-84.
XI, G., HUI, J., ZHANG, Z., LIU, S., ZHANG, X., TENG, G., CHAN, K. C., WU, E. X., NIE, B., SHAN, B., LI, L. & REYNOLDS, G. P. 2011. Learning and memory alterations are associated with hippocampal N-acetylaspartate in a rat model of depression as measured by 1H-MRS. *PLoS One,* 6**,** e28686.
XIN, Z. & SRIRAM, S. 1998. Vasoactive intestinal peptide inhibits IL-12 and nitric oxide production in murine macrophages. *J Neuroimmunol,* 89**,** 206-12.
YADAV, M., HUANG, M. C. & GOETZL, E. J. 2011. VPAC1 (vasoactive intestinal peptide (VIP) receptor type 1) G protein-coupled receptor mediation of VIP enhancement of murine experimental colitis. *Cell Immunol,* 267**,** 124-32.
ZABEN, M., SHEWARD, W. J., SHTAYA, A., ABBOSH, C., HARMAR, A. J., PRINGLE, A. K. & GRAY, W. P. 2009. The neurotransmitter VIP expands the pool of symmetrically dividing postnatal dentate gyrus precursors via VPAC2 receptors or directs them toward a neuronal fate via VPAC1 receptors. *Stem Cells,* 27**,** 2539-51.
ZHU, J. & PAUL, W. E. 2008. CD4 T cells: fates, functions, and faults. *Blood,* 112**,** 1557-69.
ZIV, Y., RON, N., BUTOVSKY, O., LANDA, G., SUDAI, E., GREENBERG, N., COHEN, H., KIPNIS, J. & SCHWARTZ, M. 2006. Immune cells contribute to the maintenance of neurogenesis and spatial learning abilities in adulthood. *Nat Neurosci,* 9**,** 268-75.
ZOCHODNE, D. W. & CHENG, C. 2000. Neurotrophins and other growth factors in the regenerative milieu of proximal nerve stump tips. *J Anat,* 196 (Pt 2)**,** 279-83.
ZUPAN, V., NEHLIG, A., EVRARD, P. & GRESSENS, P. 2000. Prenatal blockade of vasoactive intestinal peptide alters cell death and synaptic equipment in the murine neocortex. *Pediatr Res,* 47**,** 53-63.

Appendix I

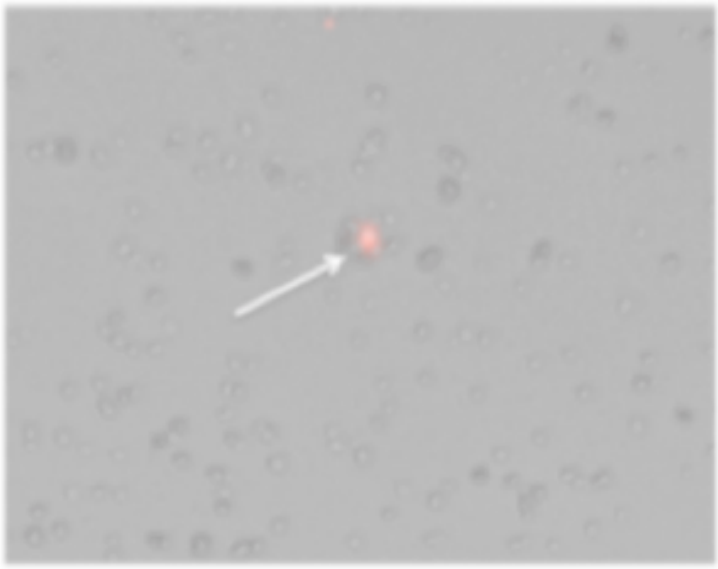

Figure 61: PI and TEM images of live T lymphocytes in cultures. T lymphocytes were grown in RPMI media or NBA/B-27/Glutamine media for 24 hours. Wells were treated with PI for 40 minutes at 37°C in the dark. Cells were washed and re-placed with fresh pre-warmed medium and then imaged. PI positive cells are red (arrowed). PI negative cells are viable in culture.

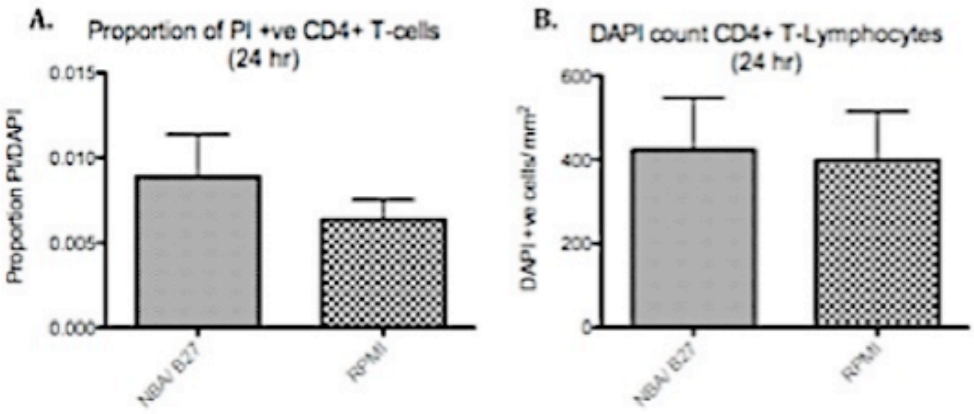

Figure 62: Studying cell death in two different media conditions. Total cells were counted as the number of cells visible under TEM light. PI positive cells were counted as the number of dead or dying cells. There was no difference in the proportion of PI positive cells between the two different media conditions **A.** The proportion of PI positive cells with respect to total cell numbers **B.** Total number of cultured cells. Data represents mean ± SE based on a sample that represent at least 6 wells per condition. Comparisons between control and different media conditions are one way ANOVA with Neuman-Keuls post-hoc test.

Appendix II

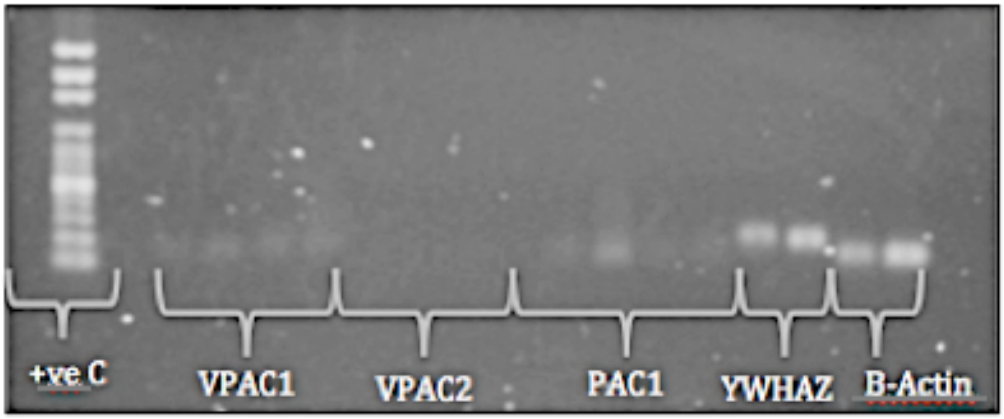

Figure 63: Expression of mRNAs for VPAC1, VPAC2 and PAC1 receptors in Adult Murine Naïve and Activated CD4⁺ T-lymphocytes in control and VIP treated conditions at 2 hours post treatment, as shown by 2% agarose gel electrophoresis. Universal mouse cDNA was used as a positive control. YWHAZ and β-actin were used as the housekeeping genes for naïve and activated T-lymphocytes, respectively.

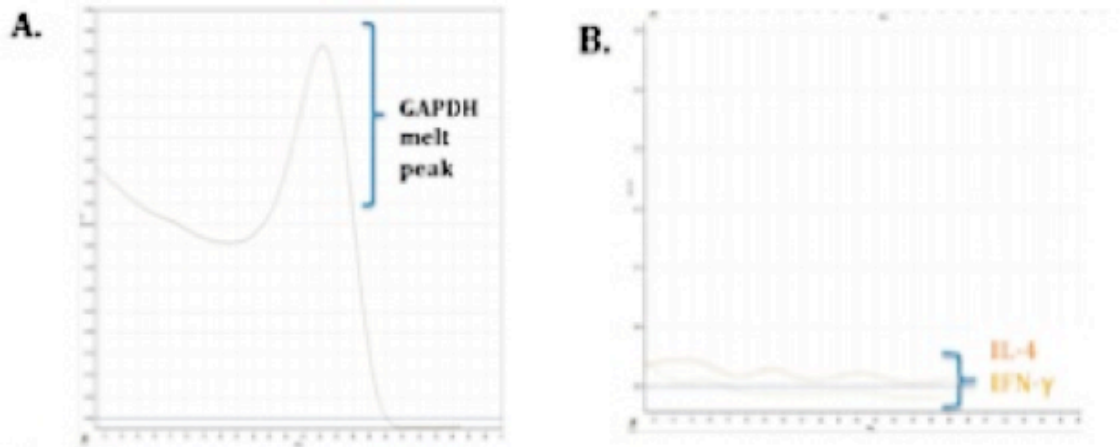

Figure 64: Naïve CD4+ T lymphocytes do not express IL-4 of IFN-γ under control or VIP treated conditions. A. The melt curve for GAPDH house-keeping gene **B.** IL-4, IFN-γ, as the uniqueness of the amplicons synthesised using each primer and amplification conditions were assessed by SYBR Green dye melting analysis. Ramping of the temperature from 65°C to 95°C did not produce a single unique DNA dissociation curve for IL-4 or IFN-γ, but produced a single melt curve for GAPDH. 3 samples of cDNA were analysed under each condition, extracted from three separate experiments. Quantitative PCR was repeated twice.

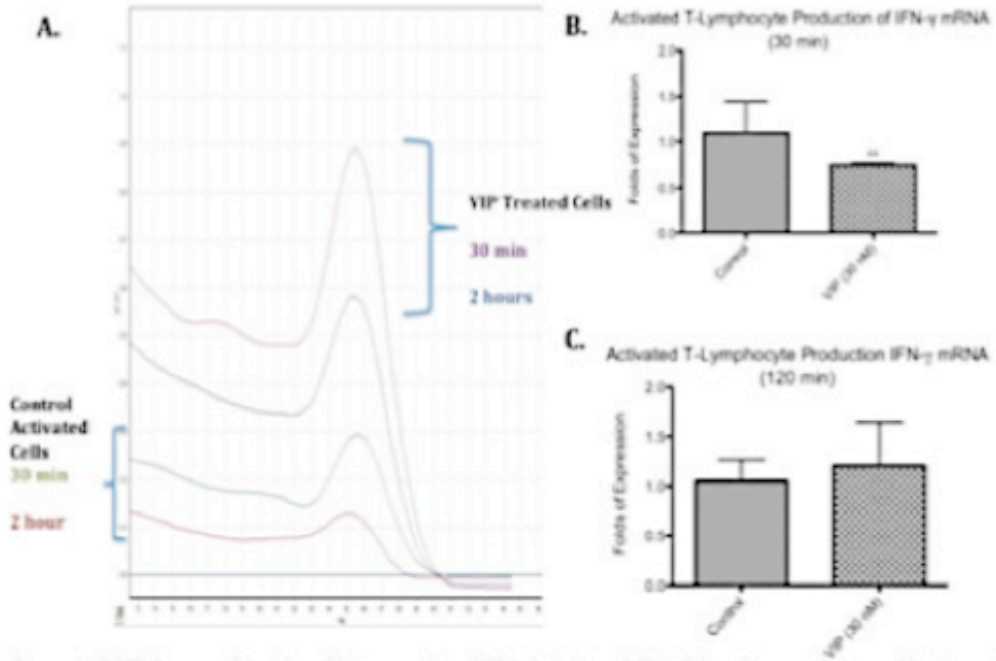

Figure 65: VIP downregulates mRNA expression of IFN-γ in activated CD4⁺ T lymphocytes at 30 minutes in culture. A. The melt curve for IFN-γ as the uniqueness of the amplicons synthesised using the IFN-Υ primer and amplification conditions assessed by SYBR Green dye melting analysis. Ramping of the temperature from 65°C to 95°C produced a single unique DNA dissociation curve in each case **B.** IFN-γ mRNA expression as measured by real-time PCR at 30 minutes post-treatment **C.** and 2 hours post-treatment. Data represents mean ± SE for folds of expression as calculated by the comparative Ct method. Comparisons between control and VIP conditions are Student's t test (*, $p < 0.05$, **, $p < 0.01$)

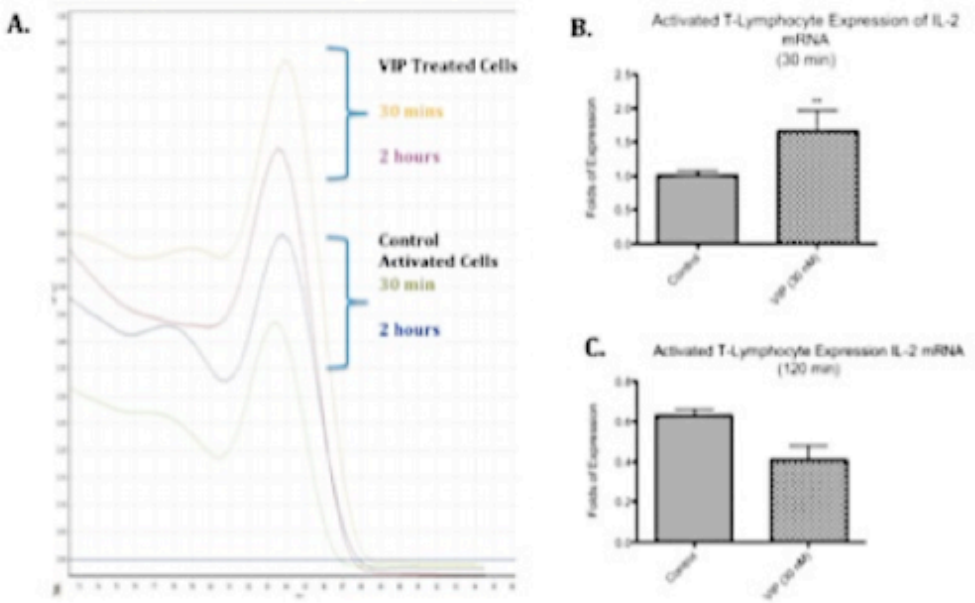

Figure 66: VIP downregulates mRNA expression of IL-2 in activated CD4⁺ T lymphocytes at 30 minutes in culture. A. The melt curve for IL-2 as the uniqueness of the amplicons synthesised using the IL-2 primer and amplification conditions assessed by SYBR Green dye melting analysis. Ramping of the temperature from 65°C to 95°C produced a single unique DNA dissociation curve in each case **B.** IL-2mRNA expression as measured by real-time PCR at 30 minutes post-treatment **C.** and 2 hours post-treatment. Data represents mean ± SE for folds of expression as calculated by the comparative Ct method. Comparisons between control and VIP conditions are Student's t test (*, $p < 0.05$, **, $p < 0.01$)

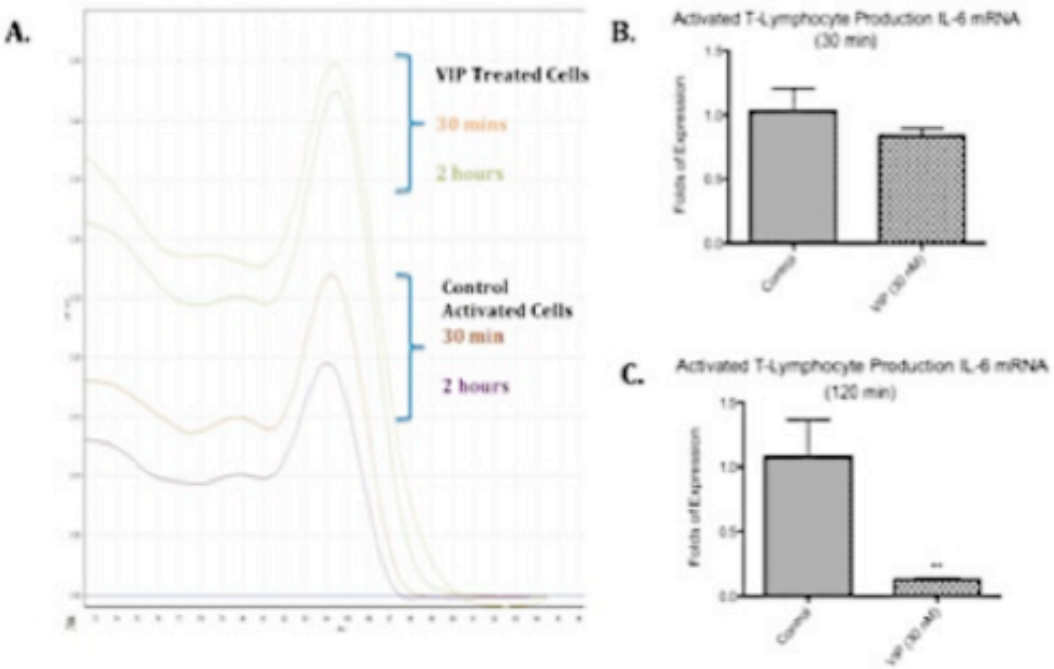

Figure 67: VIP downregulates mRNA expression of IL-6 in activated CD4⁺ T lymphocytes at 120 minutes in culture. A. The melt curve for IL-6 as the uniqueness of the amplicons synthesised using the IL-2 primer and amplification conditions assessed by SYBR Green dye melting analysis. Ramping of the temperature from 65°C to 95°C produced a single unique DNA dissociation curve in each case **B.** IL-2 mRNA expression as measured by real-time PCR at 30 minutes post-treatment **C.** and 2 hours post-treatment. Data represents mean ± SE for folds of expression as calculated by the comparative Ct method. Comparisons between control and VIP conditions are Student's t test (*, $p < 0.05$, **, $p < 0.01$)

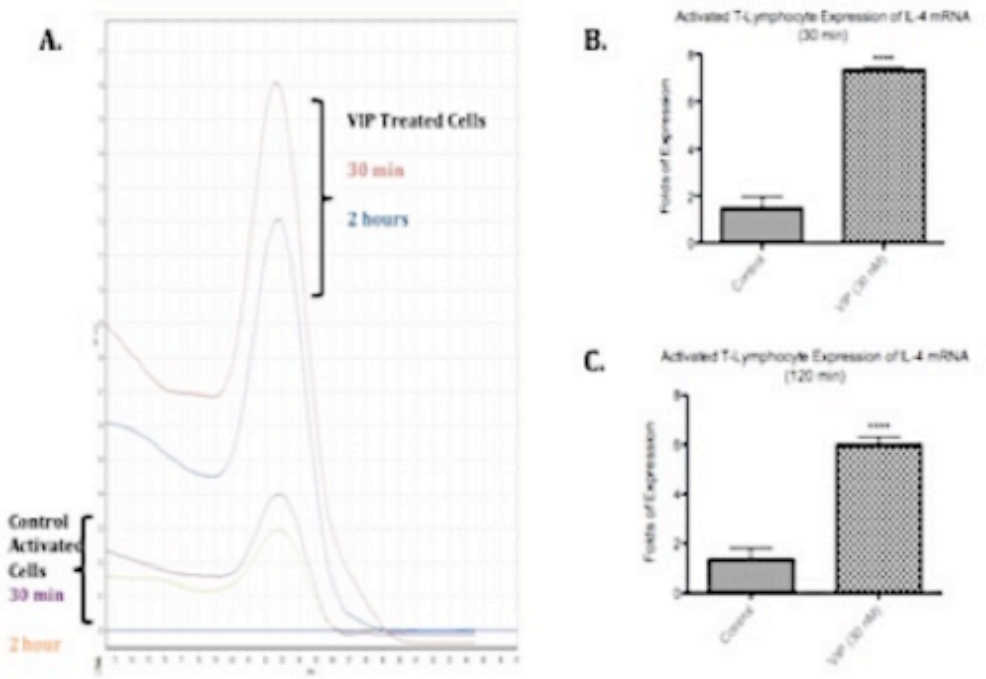

Figure 68: VIP upregulates mRNA expression of IL-4 in activated CD4⁺ T lymphocytes in culture. A. The melt curve for IL-4 as the uniqueness of the amplicons synthesised using the IL-4 primer and amplification conditions assessed by SYBR Green dye melting analysis. Ramping of the temperature from 65°C to 95°C produced a single unique DNA dissociation curve in each case **B.** IL-4 mRNA expression as measured by real-time PCR at 30 minutes post-treatment **C.** and 2 hours post-treatment. Data represents mean ± SE for folds of expression as calculated by the comparative Ct method. Comparisons between control and VIP conditions are Student's t test (*, $p < 0.05$, **, $p < 0.01$)